ZooKeys 754: 1–21 (2018)
doi: 10.3897/zookeys.754.24276
http://zookeys.pensoft.net

RESEARCH ARTICLE

A peer-reviewed open-access journal
ZooKeys
Launched to accelerate biodiversity research

Three new species of *Grouvellinus* Champion, 1923 from Maliau Basin, Sabah, Borneo, discovered by citizen scientists during the first Taxon Expedition (Insecta, Coleoptera, Elmidae)

Hendrik Freitag[1,2], Clister V. Pangantihon[1,2], Iva Njunjić[2,3]

1 *Ateneo de Manila University, Department of Biology, School of Science & Engineering, Loyola Heights, Quezon City 1101, Philippines* **2** *Taxon Expeditions, Rembrandtstraat 20, 2311 VW, Leiden, Netherlands* **3** *Naturalis Biodiversity Center, Vondellaan 55, 2332 AA, Leiden, Netherlands*

Corresponding author: *Hendrik Freitag* (hfreitag@ateneo.edu)

Academic editor: *M. Michat* | Received 7 February 2018 | Accepted 22 March 2018 | Published 30 April 2018

http://zoobank.org/66CB2B85-CA72-400B-AB9C-9CEEAB8EE9F3

Citation: Freitag H, Pangantihon CV, Njunjić I (2018) Three new species of *Grouvellinus* Champion, 1923 from Maliau Basin, Sabah, Borneo, discovered by citizen scientists during the first Taxon Expedition (Insecta, Coleoptera, Elmidae). ZooKeys 754: 1–21. https://doi.org/10.3897/zookeys.754.24276

Abstract

Further results are presented of the first field course at Maliau Basin, Malaysian Borneo organized by Taxon Expeditions, an organization which enables citizen scientists to be directly involved in taxonomic discoveries. Three new species of the aquatic beetle genus *Grouvellinus* Champion, 1923, namely *G. leonardodicaprioi* **sp. n.**, G. *andrekuipersi* **sp. n.**, and *G. quest* **sp. n.** were collected jointly by the citizen scientists and taxonomists during the fieldwork in Maliau Basin. Material was mainly sampled from sandstone bottom rocks of blackwater streams at altitudes between 900 m and 1,000 m using fine-meshed handnets. The genus is widely distributed in the Oriental and Palearctic regions, but these are the first records from the island of Borneo.

Keywords

André Kuipers, Leonardo DiCaprio, new species, riffle beetle, taxon expeditions, taxonomy, Quest magazine

Introduction

During the first biodiversity discovery field course for citizen scientists, termed "taxon expedition" (Schilthuizen et al. 2017), participants collected six new species for science from Maliau Basin, Malaysian Borneo. Three of them, litter-dwelling Coleoptera, were recently described jointly by taxonomists and citizen scientists (Schilthuizen et al. 2017). The taxonomic treatments for the other three species, all belonging to the genus *Grouvellinus* (Elmidae), are provided here. Names of the new species were selected in two ways: during a naming ceremony in Maliau Basin by the course participants and staff of the Maliau Basin Studies Centre; and in an online public contest organized by the Dutch science program De Kennis van Nu (2017).

Citizen Science initiatives in biodiversity research have become increasingly popular with an estimated annual growth rate of 10% in number of projects launched (Theobald et al. 2015). They generate important scientific information, especially in terms of biodiversity monitoring (Chandler et al. 2017), planning and management of ecosystems and protected areas (e.g., Pollock and Whitelaw 2005), species distribution (e.g., Suprayitno et al. 2017), and conservation (McKinley et al. 2017), among other fields. Some of them run successfully already for decades and have involved thousands of citizens (e.g., Florida Lakewatch 2017, EarthWatch Institute 2018). However, it is rather rare that the results are published in peer-reviewed journals, which is considered, last but not least, an important quality control for scientific data. Theobald et al. (2015) concluded that only 12% of several hundred citizen science projects screened refer to peer-reviewed published results, although it is possible that more citizen scientist data were published, but not clearly indicated as such.

Conrad and Hilchey (2011) point out that "the nature of citizen science implies that in many cases, the work being undertaken is not documented in traditional journal articles, although there certainly are exceptions". Our taxon expeditions are in fact such an exception, as the ultimate goal is to publish the descriptions of the new species that have been discovered and tentatively named by our participating citizen scientists. We also encourage their direct involvement as co-authors in the process of the verbal species' descriptions and scientific illustration of diagnostic characters (although not embraced in this paper, but see Schilthuizen et al. 2017). The focus on publishing species discoveries by citizen scientists makes our initiative unique, since such approaches are only seen in student volunteer funded programs before (e.g., Opwall 2018).

Since basic research on invertebrates (including taxonomy and faunistics) is relatively infrequent and underfunded (Cardoso et al. 2011), the valued financial contribution of the participating citizen scientists enables taxonomic explorations in key biodiversity areas which are very unlikely being supported by any conventional science funding agency.

This paper deals with three new species of the genus *Grouvellinus* Champion, 1923. The genus, named in honour of the French coleopterologist Antoine Henri Grouvelle (1843–1917), comprises small to medium-sized riffle beetles (Elmidae) of dark (usually black), or rarely cupreous colour and is distributed in the Oriental and Palaearctic regions from Samos (Greece) in the west up to Japan in the East and Java (Indonesia)

Figure 1. A Citizen scientists on the first taxon expedition to Maliau Basin, Malaysian Borneo, performing microhabitat sampling **B** The first author (on the left) instructing journalist Paul Serail of QUEST magazine (on the right) on the identification of riffle beetles.

in the south (Jäch et al. 2016). It is also recorded from the neighbouring Philippines where several species await formal description (Freitag et al. 2016). Forty species are known to science (Jäch et al. 2016, Bian and Jäch 2018), of which seven are endemic

to Indonesia and one, *Grouvellinus bishopi* Jäch, 1984, to Peninsular Malaysia. Since there are no previously published records from the island of Borneo, our data extend the known distributional range of *Grouvellinus* to the largest Asian island. *Grouvellinus* species are sometimes hardly distinguishable by external morphological characters, but the differences in their aedeagi are diagnostic.

Materials and methods

The specimens were collected by taxon expedition participants and instructors using small-meshed hand-nets and preserved in 96% ethanol. After return to the field station, participants sorted the collected specimens to genus level under a Nikon SMZ445 stereomicroscope with 20 × oculars (allowing magnification up to 70 ×) and with the help of provided taxonomic literature. Microforceps, insect pins, and the same optical equipment were subsequently used for the dissection of specimens and the detailed material examination. This step was carried out by the participants only for morpho-species of which larger series were available, while the instructors handled single records of new species to limit damage through unexperienced handling of potential holotypes. Diagnostic characters of the external habitus and the genitalia were briefly recorded by the participants.

Photographs of dissected parts were taken from temporary slides in lactic acid under an Olympus CX compound microscope. Preliminary photographs of the dorsal habitus of entire specimens (as used in the public species-naming contest) were obtained by the participants using a Canon EOS 500D with MP-E 65 mm lens attached to a Kaiser stand with vertical micro-adjustment drive. Series of vertical photographs series were taken and layers were subsequently stacked using CombineZP software.

After the actual field course, CorelDRAW Version 10.0 software was used by the authors to compile digital line drawings. Additional high-quality photographs were taken under a Zeiss Axio zoom V 16 microscope with Canon 5D SLR camera using diffuse LED lighting. Images were captured at various focus layers and subsequently stacked using the Zerene Stacker software.

Morphological terminology used herein mainly follows the Elmidae chapter of the Handbook of Zoology/Coleoptera (Kodada et al. 2016). Elytral striae (rows of punctures) and intervals are numbered as actually visible (from suture to lateral rim) ignoring presumable fusion of seventh and eighth striae (comp. Jäch 1984).

The following abbreviations were used:

a.s.l. above sea level (elevation)
CL calculated length (PL + EL)
EL elytral length, measured along the elytral suture from basis to apex
EW maximum elytral width
HW head width, including eyes
ID interocular distance
PW maximum pronotal width (at posterior portion)
PL pronotal length

All collected material is deposited at the Borneensis Coleoptera Collection (**BOR/COL**) of the Institute for Tropical Biology and Conservation, Universiti Malaysia Sabah, Kota Kinabalu. Previously undetermined specimens of the Coleoptera collections of the BOR/COL repository and the Natural History Museum Vienna, Austria (**NMW**) were checked by the first author for conspecific material which was designated as paratype material, in order to extend the type series and distributional knowledge. We additionally refer to some material from the Sabah Parks Museum, Kinabalu Park Headquarters, Malaysia (**SP**).

Taxonomy

Genus *Grouvellinus* Champion, 1923

***Grouvellinus leonardodicaprioi* sp. n.**
http://www.zoobank.org/F5E77C1D-1938-417E-A94D-D2624ECEAB3A
Figures 2, 5–6

Type locality. Malaysia, Sabah (Eastern Borneo Island), Maliau Basin, upstream Giluk Falls, ca. 4°44'49"N, 116°52'38"E, ca. 950 m a.s.l. (Fig. 12A)

Type material. Holotype ♂ (BOR/COL): "MALAYSIA: Sabah: Maliau Basin: \ upstr. Giluk Falls; bottom rock, run; \ ca. 4°44'49"N, 116°52'38"E, ca.950m a.s.l. \ 01.X.2017, leg. I. Njunjić, CV. Pangantihon, P. Serail (GilF3g)"; terminal parts of abdomen incl. aedeagus glued separately; right foreleg, left protarsus incl. parts of protibia and left antenna lacking; right elytral apex slightly damaged.

Etymology. The new species is named in honour of the actor Leonardo DiCaprio to acknowledge his inspiring work in promoting environmental awareness and bringing the problems of climate change and biodiversity loss into the spotlight. The species name was selected during a naming ceremony at Maliau Basin Studies Centre on 6 October 2017, in which expedition participants as well as a large number of field centre staff and porters took part.

Description. *Body* obovate, 2.97 mm long (CL), 1.60 mm wide (EW), 1.9 times as long as wide (CL/EW).

Dorsal colouration (Figs 2, 5A) black with slight metallic lustre; claws and antennae dark brown; pubescence yellow. Ventral side (Figs 5B, C) very dark brown. Plastron pubescence shiny golden.

Head 0.65 mm wide (HW); ID 0.27 mm; partly retractable; labrum with dense fringes of moderately long setae, punctures very small and dense; frons and clypeus moderately pubescent, setae moderately long, punctures small and moderately dense; intervals almost flat and glabrous. Frontoclypeal suture distinct, slightly concave. Eyes moderately protruding. Antennae genus-typical, slightly shorter than HW.

Pronotum (Fig. 5A) 0.85 mm long (PL), 1.12 mm wide (PW), distinctly wider than long (PL/MW), widest posterior 0.25, distinctly narrower than elytra, anteriorly distinctly attenuate; anterior margin convex; median carina absent, distinct sublateral

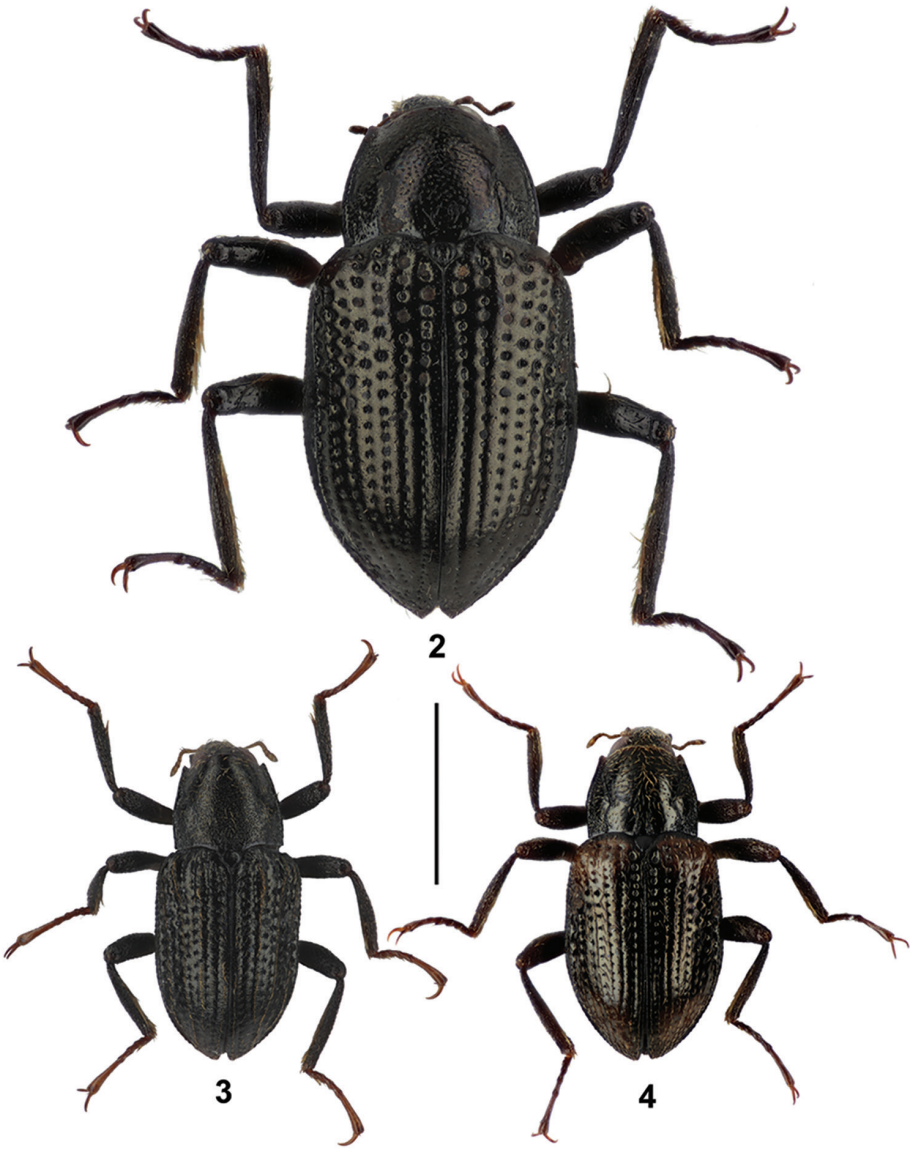

Figures 2–4. Habitus of the new *Grouvellinus* species collected from the Maliau Basin: **2** *G. leonardodicaprioi* sp. n. (image of holotype male partly complemented) **3** *G. quest* sp. n. (paratype male from 'NepC3g') **4** *G. andrekuipersi* sp. n. (paratype male from 'NepC3g'). Scale bar: 1 mm.

carinae present posterior 0–0.3; oblique impressions very shallow; laterobasal impression very shallow, indistinct; pronotal disc moderately vaulted, densely punctate; punctures moderately big and shallowly impressed; interstices glabrous and flat; setae comparably short; pronotal impressions appearing rugose by irregularly enlarged punctures. Hypomeron rugose, increasingly pubescent (plastron) ventrad.

Prosternum (Fig. 5B) very short, lateral portions with very dense, fine pubescence (plastron); median portion and process glabrous; prosternal process distinctly parti-

Figure 5. *Grouvellinus leonardodicaprioi* sp. n. (holotype male): **A** anterio-dorsal aspect with pronotum **B** anterio-ventral aspect with prosternum **C** posterio-ventral aspect with meso-, metaventrite, and ventrites 1–5.

tioned and elevated from remaining prosternum, short, distinctly wider than long, posteriorly broadly rounded; margins conspicuously fringed; sub-posteriolateral portion slightly impressed, rugose.

Scutellum (Fig. 5A) elongate sub-cordiform, posteriorly impressed, glabrous.

Elytra (Figs 2, 5A) roundly elongate, strongly convex dorsally, 2.31 mm long (EL), ca. 1.4 times as long as wide (EL/EW); apices separately conically pointed in posterior 0.05, with eight to nine (most lateral row partly divided anterior 0.3–0.7) longitudinal rows of punctures (striae); striae moderately (anterior portion) to inconspicuously (posterior portion) impressed; punctures of rows 2 and 3 dissolved beyond anterior 0.8; remaining punctures somewhat regularly arranged (except for most lateral row), but distinctly varying in size and degree of impression: much larger (2–6 times of intervals) and deeply impressed medio-basally, small (0.1–0.3 times of intervals) and shallowly impressed sub-apically; interstices glabrous; intervals 7 and 8 with finely crenulate carinae approx. from basal 0.1 to 0.9; carinate interval 8 extending as "shoulder crest" basad up to pronotal angle; intervals 1–3 slightly broadly elevated basal 0.1–0.2; at least intervals 1, 3, 5, 7, 8 with rows of scattered setae (most of them presumably broken off in the specimen examined); lateral elytral margin serrate and with row of setae.

Mesoventrite (Fig. 5C) with two pairs of moderately deeply impressed grooves, one sub-rectangular pair behind procoxae and another sub-trapezoidal pair medially behind prosternal process.

Metaventrite (Fig. 5C) disc glabrous, with longitudinal impression along median suture, medioanteriorly impressed; anterior angles (bordering mesocoxae) process-like elevated; lateral metaventrite portions with large irregular punctures or impressions; their interstices rugulose; most lateral portion (approx. between hind coxae and shoulder) with dense plastron pubescence.

Abdominal ventrites (Fig. 5C). Ventrite 1 with pair of longitudinal carinae between glabrous disc and densely pubescent lateral portions (plastron); broad lateral portions of ventrites 1–4 and almost entire ventrite 5 densely covered with plastron (Fig. 5C); median glabrous portions with sparse punctures and small setae.

Legs (Fig. 2) slightly shorter than body, hind leg longest; hind tibiae slightly broader than those of the other legs; tibia longer than tarsus and femur in all legs; parts of coxae, proximal femora and entire inner (ventral) face of tibiae and femora moderately densely covered with short adpressed setae; outer (dorsal) edge of femora and tibiae and inner (ventral) edge of tarsomeres 1–4 with fringes of long trichoid setae; remaining portions with scattered short setae; distal portion of tibiae and inner edge with longitudinal rows of robust setae; apex of tibiae additionally with pair of spines.

Aedeagus (Fig. 6A–C) ca. 840 µm long, ca. 180 µm wide. Phallobase slightly asymmetrical basally, reaching basal 0.41 of total aedeagus length. Median lobe almost four times as long as wide, distinctly overreaching parameres, evenly slightly conical towards round apex. Ventral sac large, apically inflated beyond apex (presumably more inflated than in regular position), internal surface entirely densely covered with moderately short and thin spines, outer surface also covered with such spines up to the level of the parameres (presumably because more inflated than in regular position). Parameres distinctly shorter than median lobe, apices evenly rounded (lateral view), conical from insertion to half-length and very slender in apical half in lateral view, with approx. 20 trichoid setae in apical fourth of ventrolateral margin; most apical setae distinctly longer than all others.

Male sternite IX ('spiculum gastrale') with posterior margin rounded and entirely fringed with a broad, distinctly sclerotized margin; paraprocts closely attached to posterior portion, sub-equally long, not reaching apical margin; median strut broken and not examined.

Female and larva. Unknown.

Differential diagnosis. By its unusually large size, *Grouvellinus leonardodicaprioi* sp. n. resembles *G. hercules* Jäch, 1984 from Nepal, which also shares some other characters with the new species (only 7th and 8th elytra interval crested, margins of prosternal process fringed, elytral apices pointed), but *G. leonardodicaprioi*, sp. n. can be distinguished by the slenderer elytra, the fully glabrous (in between punctures) and not elevated median pronotum, the shallower elytral striae, as well as by its conspicuously varying aedeagus with broad main piece which distinctly overreaches the evenly rounded paramere tips (vs. very slender main piece only slightly overreaching the conically tapered paramere tips in *G. hercules*). The large size and other characters mentioned above also allow clear distinction from the species described below and any known congeners from Malaysia and Indonesia.

Distribution. This species is only known from the type locality, the Giluk Falls of the upper Maliau Basin, Sabah (Figs 11, 12A).

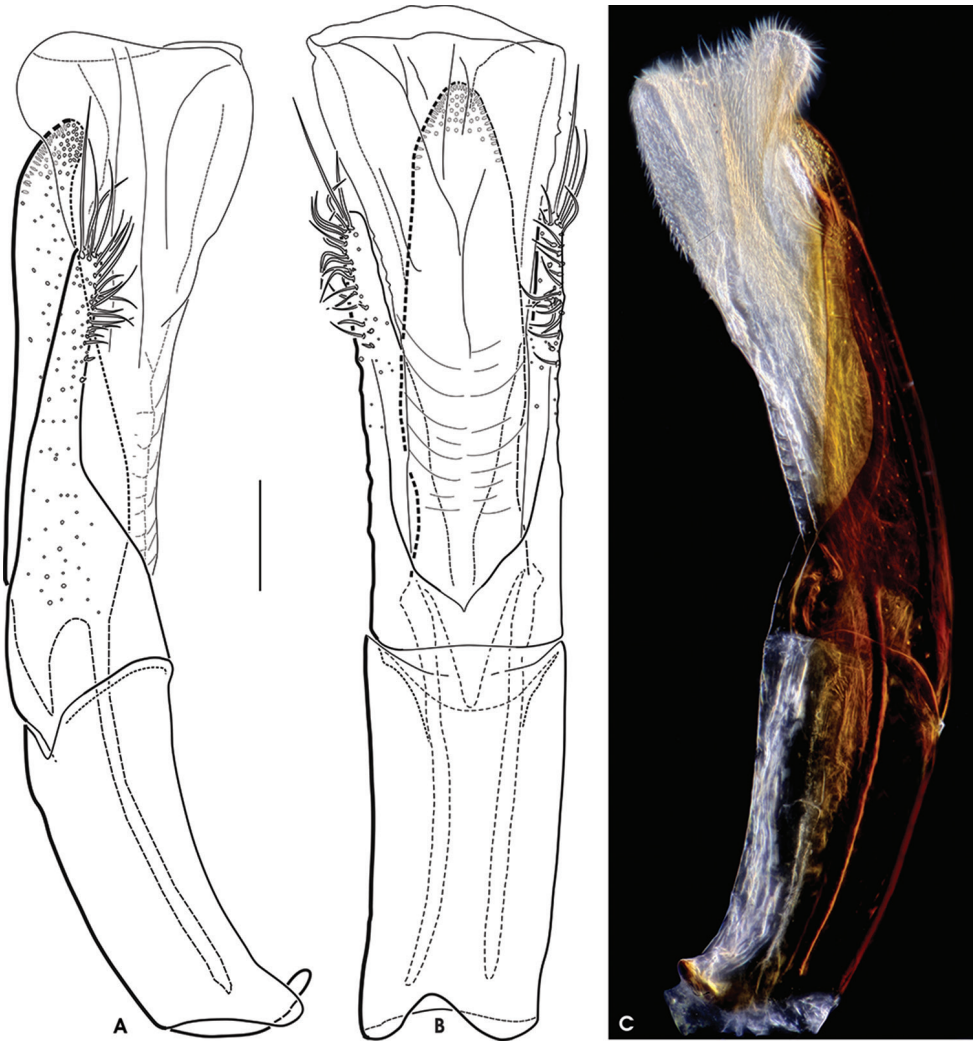

Figure 6. *Grouvellinus leonardodicaprioi* sp. n. (holotype male): **A** aedeagus in lateral view (spines of ventral sac omitted) **B** aedeagus in ventral view (spines of ventral sac omitted) **C** microscopic photograph of aedeagus in lateral view optically emphasizing the dense distribution of internal and external spines of the ventral sac. Scale bar: 0.1 mm.

***Grouvellinus quest* sp. n.**

http://www.zoobank.org/8998CB72-A2AD-4D43-AEA0-5382BD450D93

Figures 3, 7–8

Type locality. Malaysia, Sabah (Eastern Borneo Island), Maliau Basin, Creek east of 'Nepenthes Camp', ca. 4°44'57"N, 116°52'45"E, 1000 m a.s.l. (Fig. 12B).

Type material. Holotype ♂ (BOR/COL): "MALAYSIA: Sabah: Maliau Basin: \ Creek E Nepenthes Camp; bottom rock, \ run; ca. 4°43'57"N, 116°52'45"E, ca. 1000m a.s.l. \ 01.X.2017, leg. I. Njunjić, P. Serail, C. de Groot (NepC3g)"; terminal

parts of abdomen incl. aedeagus glued separately on entomological cards. **Paratypes:** 3 ♂, 4 ♀ (BOR/COL): same data as holotype; 3 ♂, 3 ♀ (BOR/COL) "MALAYSIA: Sabah: Maliau Basin: \ Giluk River; Cryptochorinae water plants, \ run; ca. 4°44'36"N, 116°52'21"E, ca. 980m a.s. \ l.01.X.2017, leg. I. Njunjić, H. Freitag, L. Seip, P. Piccoli (GilR2r)"; 1 ♂, 5 ♀, (BOR/COL) "MALAYSIA: Sabah: Maliau Basin: \ upstr. Giluk Falls; bottom rock, run; \ ca. 4°44'49"N, 116°52'38"E, ca. 950m a.s.l. \ 01.X.2017, leg. I. Njunjić, CV. Pangantihon, P. Serail (GilF3g)"; 1 ♂, 1 ♀ (NMW) "BRUNEI: Mt. Pagon \ 61 ARIF3 \ 4°20'35.8"N, 115°15'40.6"E \ 5.VI.2012 \ leg. K. Baker"; 5 ♂, 4 ♀ (NMW) "BRUNEI: Muara, Mukin Kilanas, \ Wasai Kendal Fall; sandy lowland creek; \ sec. forest; c.10m asl, c. 4°52'N, 114°53'E \ 15.6.1997 leg. Mendoza (3)".

Etymology. The species epithet refers to the English noun 'quest' (search, aspiration) in reference to the intense search for riffle beetles at Maliau Basin which was a big quest for the citizen scientists involved in the project. Additionally, the new species is named for the Dutch popular science magazine QUEST of which journalist Paul Serail joined the first taxon expedition. The word is used as a noun in apposition.

Description. *Body* elongate obovate, 1.5–1.8 mm long (CL), 0.73–0.85 mm wide (EW), 2.1 times as long as wide (CL/EW).

Dorsal colouration (Figs 3, 7A) predominantly black; tarsi, antennae, and maxillary palps reddish dark brown; pubescence yellow. Ventral side (Fig. 7B, C) reddish dark brown.

Head 0.35–0.37 mm wide (HW); ID 0.14–0.21 mm; partly retractable; frons, clypeus, and labrum sparsely pubescent, slightly denser laterally; punctures small and scattered; intervals flat, glabrous. Frontoclypeal suture almost straight. Eyes very slightly protruding. Antennae genus-typical, rarely exposed, usually semi-circularly folded around anterior eye margin.

Pronotum (Fig. 7A) 0.49–0.55 mm long (PL), 0.56–0.64 mm wide (PW), wider than long (PL/MW), widest posterior 0.25, distinctly narrower than elytra, anteriorly moderately attenuate; anterior margin distinctly convex; median carina absent, sublateral carinae present, but indistinct at posterior 0–0.2; oblique impression shallow, extending from mid lateral rim to posterior 0.2; laterobasal impression shallow; pronotal disc distinctly vaulted, very densely punctate; punctures small and shallowly impressed; setae moderately long, often broken off; anterior and anteriolateral portions sparsely punctate; interstices glabrous and flat; impressions and lateral margins rugose. Hypomeron rugose.

Prosternum (Fig. 7B) short; lateral portions with very dense, fine pubescence (plastron); median portion including process medially broadly impressed and glabrous; margins finely striate; prosternal process sub-pentagonal, much wider than long.

Scutellum (Fig. 7A) sub-cordiform, flat and glabrous.

Elytra (Figs 3, 7A) roundly elongate, strongly convex dorsally, 1.08–1.29 mm long (EL), ca. 1.4 times as long as wide (EL/EW), sub-parallel basal 0.1–0.5, apices separately rounded (in both sexes), with eight longitudinal, moderately to slightly impressed rows of punctures; punctures somewhat regularly arranged, much larger (1.5–2.5 times of intervals) and deeper impressed basally, very small (0.2–0.4 times of intervals) and more shallowly impressed apically; less regularly arranged in lateral rows; interstices rugose except for almost glabrous apical portion; intervals 3, 5, 7, 8 with

Figure 7. *Grouvellinus quest* sp. n. (paratype males from NepC3g): **A** anterio-dorsal aspect with pronotum **B** posterio-ventral aspect with ventrites 1–5 **C** anterio-ventral aspect with prosternum, meso- and metaventrite.

crenulate carinae approx. from basal 0.05 to 0.75, particularly on 2nd interval distinctly elevated basal 0.1–0.3; carinate intervals 5 and 7 convergent basal 0.05–0.15; all carinae with row of yellowish pubescence; lateral elytral margin serrate.

Mesoventrite (Fig. 7B) with deep subtrapezoidal grooves behind procoxae, medially with pair of oval impressions in males, the latter more indistinct or lacking in females.

Metaventrite (Fig. 7B) with irregular impressions, except for almost glabrous disc with longitudinally impression along median suture; interstices on marginal portions somewhat irregularly micro-striate to micro-reticulate.

Abdominal ventrites (Fig. 7C). Ventrite 1 with pair of longitudinal carinae bordering glabrous disc; ventrites 1–2 glabrous medially; lateral portions of ventrites 1–2 and almost entire ventrites 4–5 densely covered with plastron and scattered moderately long setae (Fig. 7C); apex and lateral margins of ventrite 5 more densely pubescent.

Legs (Fig. 3) slightly shorter than body; hind leg longest; tibia longer than tarsus and femur in all legs; coxae, femora, and tibiae moderately densely covered with short adpressed setae; inner (ventral) edge of distal tibia and tarsomeres 1–4 with fringe of long trichoid

setae and short spine-like setae; outer (dorsal) edge of all femora and tibiae with longitudinal row of spine-like setae (in both sexes); apex of tibiae with pair of apical spines (most conspicuous at hind tibia). Legs not conspicuously varying between male and female.

Aedeagus (Fig. 8A, B) 550–560 µm long, 130–150 µm wide. Phallobase slightly asymmetrical basally, reaching ca. basal 0.6 of total aedeagus length. Median lobe moderately slender, gradually tapered towards a sub-globularly expanded apex; sub-globular apex bent ventrad (lateral view). Ventral sac apically inflated internally densely stippled and with dense fringe of moderately short, thin and comparably delicate spines; few of those overreaching apical fringe. Parameres slightly shorter than median lobe, apically moderately truncate and slightly dilated ventrally (lateral view), moderately broad and evenly conical from insertion to apical 0.15 in lateral view, usually with more than 30 trichoid setae in apical half, most of them at inner face; most apical setae longest and inserted at outer surface.

Male sternite IX with median strut moderately long and almost rectangularly bent sub-distally; posterior portion entirely fringed with a broad, distinctly sclerotized margin; posterior margin rounded; paraprocts sub-equal in length, not reaching apical margin.

Ovipositor (Fig. 8C). Total length ca. 620 µm. Stylus ca. 45 µm long, slightly conical basad, very slightly bent outwards, with ca. six short sensilla. Coxite approx. half as long as entire ovipositor (ca. 300 µm), with scattered extremely short, acute setae (most densely near apex) and few apical, hook-like sensilla; distal portion medially very slender, 2.4 times as long as proximal portion, inner margin pubescent (rather inconspicuous). Valvifer almost as long as coxite (ca. 280 µm), caudal portion slightly sclerotized and with scattered, extremely short, acute setae; fibula almost straight.

Variability. The paratypes from Brunei are among the smallest specimens within the given measurement ranges and have a somewhat smoother elytral surface with less impressed punctures and less elevated carinae; the aedeagus agrees well in the distinctive features (shape, size and setation of parameres; shape and size of median lobe), but the phallobase is slightly longer (0.67 of total aedeagus length), slightly slenderer and more ventrally bent basally. In specimens from either locality, elytra and pronotum are commonly incrusted with deposits making proper examination of the surface structure hardly possible.

Larva. Unknown.

Differential diagnosis. *Grouvellinus quest* sp. n. superficially resembles the Indonesian species *G. aeneus* (Grouvelle, 1896), but it is slightly larger (CL: 1.5–1.8 mm vs. total length 1.5–1.7 mm), black (vs. brown), and the pronotal disc is flat between punctures (vs. shagreened). Based on the only available undamaged male material of *G. aeneus* (see Jäch 1984; NMW: "Bali Baturiti D. Limnol. Exp.") that was, however, not determined with absolute certainty, there are distinct differences in their aedeagi: larger (550–560 µm long), with longer phallobase (> half total length) and with subglobular, ventrally bent tip of the median lobe in *G. quest* sp. n. (vs. smaller (400 µm long), with shorter phallobase (< half total length) and regularly rounded tip of median lobe in *G. aeneus*). *G. quest* sp. n. and all other new species treated in here can easily be distinguished from the only know Malaysian species *G. bishopi* by the absence of a median pronotal carina.

Distribution. This species is known only from Borneo Island, namely the upper Maliau Basin in Sabah and two sites in Brunei (Fig. 11).

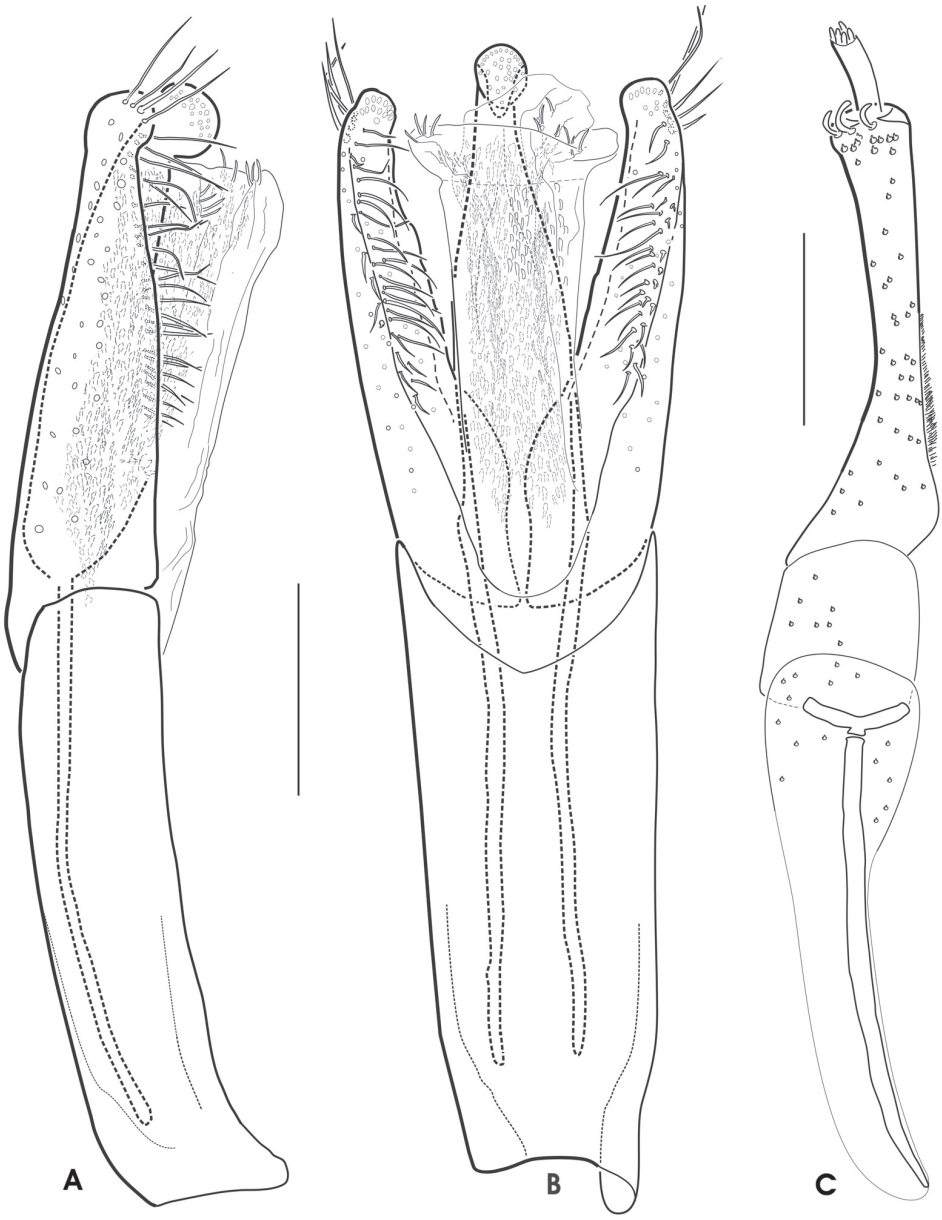

Figure 8. *Grouvellinus quest* sp. n. (paratype male & female from 'NepC3g'): **A** aedeagus in lateral view **B** aedeagus in ventral view **C** ovipositor in ventral view (right half). Scale bars: 0.1 mm.

***Grouvellinus andrekuipersi* sp. n.**

http://www.zoobank.org/1AF51771-C764-489E-9122-301C688D0EFA
Figures 4, 9–10

Type locality. Malaysia, Sabah (on Borneo Island), Maliau Basin, upstream Giluk Falls, ca. 4°44'49"N, 116°52'38"E, ca. 950 m a.s.l. (Fig. 12A).

Type material. Holotype ♂ (BOR/COL): "MALAYSIA: Sabah: Maliau Basin: \ upstr. Giluk Falls; bottom rock, run; \ ca. 4°44'49"N, 116°52'38"E, ca. 950m a.s.l. \ 01.X.2017, leg. I. Njunjić, CV. Pangantihon, P. Serail (GilF3g)", terminal parts of abdomen incl. aedeagus glued separately. **Paratypes:** 2♂, 2♀ (BOR/COL) same data as holotype; 5♂, 3♀ (BOR/COL) "MALAYSIA: Sabah: Maliau Basin: \ Creek E Nepenthes Camp; bottom rock, \ run; ca. 4°43'57"N, 116°52'45"E, ca. 1000m a.s.l. \ 01.X.2017, leg. I. Njunjić, P. Serail, C. de Groot (NepC3g)"; 1♂, 1♀ (BOR/COL) "MALAYSIA: Sabah: Maliau Basin: Creek W Nepenthes Camp; bottom rock, run; ca. 4°44'04"N, 116°52'41"E, 1000 m a.s.l.; 01.X.2017, leg. I. Njunjić & H. Freitag (NepC4g)"; 2 ♂, 2 ♀ (BOR/COL) "MALAYSIA: Sabah: Maliau Basin: \ Giluk River; Cryptochorinae water plants, \ run; ca. 4°44'36"N, 116°52'21"E, ca. 980m a.s. \ l.01.X.2017, leg. I. Njunjić, H. Freitag, L. Seip, P. Piccoli (GilR2r)"; 7♂, 7♀, 7exs. (NMW) "Malaysia, Sabah, Crocker \ Range, Rafflesia Centre, \ around km 61 of road Kota \ Kinabalu, Tambunan, \ 13-14.VI. 1996, 6 a"; 1♂ (NMW) "Malaysia, Sabah, ca. 7 km S \ Sapulut, Saupi riv. in primary \ forest, ca. 500m a.s.l.,J.F. Kočiam lgt."; 1♂, 4♀, (NMW) "Malaysia, Sabah, Crocker, \ Range, Sunsuron, 10.-11.VI. \ 1996, 8a, Sunsuron riv. flowing \ through deforested area"; 1♂, 1 ex. (NMW) "MAL., Sarawak 1993 \ Kelabit HL, Umg. Bario \ 26.2., ca 1000 m \ leg. M. Jäch (14)"; 1♂, 1 ♀, 1 ex. (NMW) "MAL., Sarawak 1993 \ Kelabit HL, 6km E Bario \ Pa Ukat, 27.2., ca 1000 m \ leg. M. Jäch (16)"; 1♂, 2exs. (SP) "MALAYSIA: Sabah: Tawau, Lucia River, 750 m a.s.l.".

Etymology. The new species is named after the Dutch astronaut André Kuipers in recognition of his engagement against the loss of the planet's natural resources and his ambassadorship for various entomological organizations. The name was elected in an online public contest organized by the science program De Kennis van Nu of the Dutch public broadcaster NTR.

Description. Body elongate obovate, 1.7–1.8 mm long (CL), 0.86–0.91 mm wide (EW), 2.0 times as long as wide (CL/EW).

Dorsal colouration (Fig. 4) predominantly dark brown; pronotum black; elytra darkest at disc; basal area between shoulder and sutural interval usually with a pair of more or less distinct and extended yellowish brown spot; commonly also sub-apical elytral areas with indistinct faint paler spots; legs dark brown increasingly paler distad; tarsi and antennae golden brown; maxillary and labial palps brown; pubescence shiny yellowish. Ventral side (Fig. 9B, C) reddish dark brown.

Head 0.35–0.39 mm wide (HW); ID 0.16–0.17 mm; partly retractable; frons, clypeus, and anterior and lateral areas of labrum moderately pubescent; punctures small; intervals medially flat and glabrous, laterally rugulose. Frontoclypeal suture straight, indistinct. Eyes slightly protruding. Antennae genus-typical, usually semi-circularly folded around anterio-lateral eye margin.

Pronotum (Fig. 9A) 0.52–0.55 mm long (PL), 0.62–0.64 mm wide (PW), wider than long (PL/MW), widest posterior 0–0.3, distinctly narrower than elytra, anteriorly attenuate; anterior margin slightly convex; median carina absent, but with a pair of short posterior-median rugose patches (anterior of the scutellum); sublateral carinae very indistinct and short; oblique impression moderately deep, narrow, extending

Figure 9. *Grouvellinus andrekuipersi* sp. n. (paratype males from 'NepC3g'): **A** anterio-dorsal aspect with pronotum **B** anterio-ventral aspect with prosternum, meso- and metaventrite **C** posterio-ventral aspect with ventrites 1–5.

approx. anterior 0.3–0.75; laterobasal impression shallow and indistinct; pronotal disc slightly vaulted; entire pronotum moderately sparsely punctate; punctures very small and shallowly impressed; setae moderately long; interstices glabrous and flat; laterobasal impression and lateral margins rugulose. Hypomeron rugose, moderately densely pubescent.

Prosternum (Fig. 9B) short; lateral portions with very dense, fine pubescence (plastron); median portion including process medially broadly impressed, rugulose except for glabrous median portion; prosternal process sub-quadrate, approx. as wide as long; lateral margins finely striate.

Scutellum sub-triangular, medially slightly impressed, glabrous.

Elytra (Fig. 4) roundly elongate, moderately convex dorsally, 1.29–1.33 mm long (EL), ca. 1.5 times as long as wide (EL/EW), widest at the middle, slightly tapered anteriad; apices separately rounded, with eight longitudinal, slightly impressed rows of punctures; punctures much larger (in row 1: approx. as wide as intervals) and deeper impressed basally, increasingly smaller (in rows 1–4: 0.2 times of intervals) and more

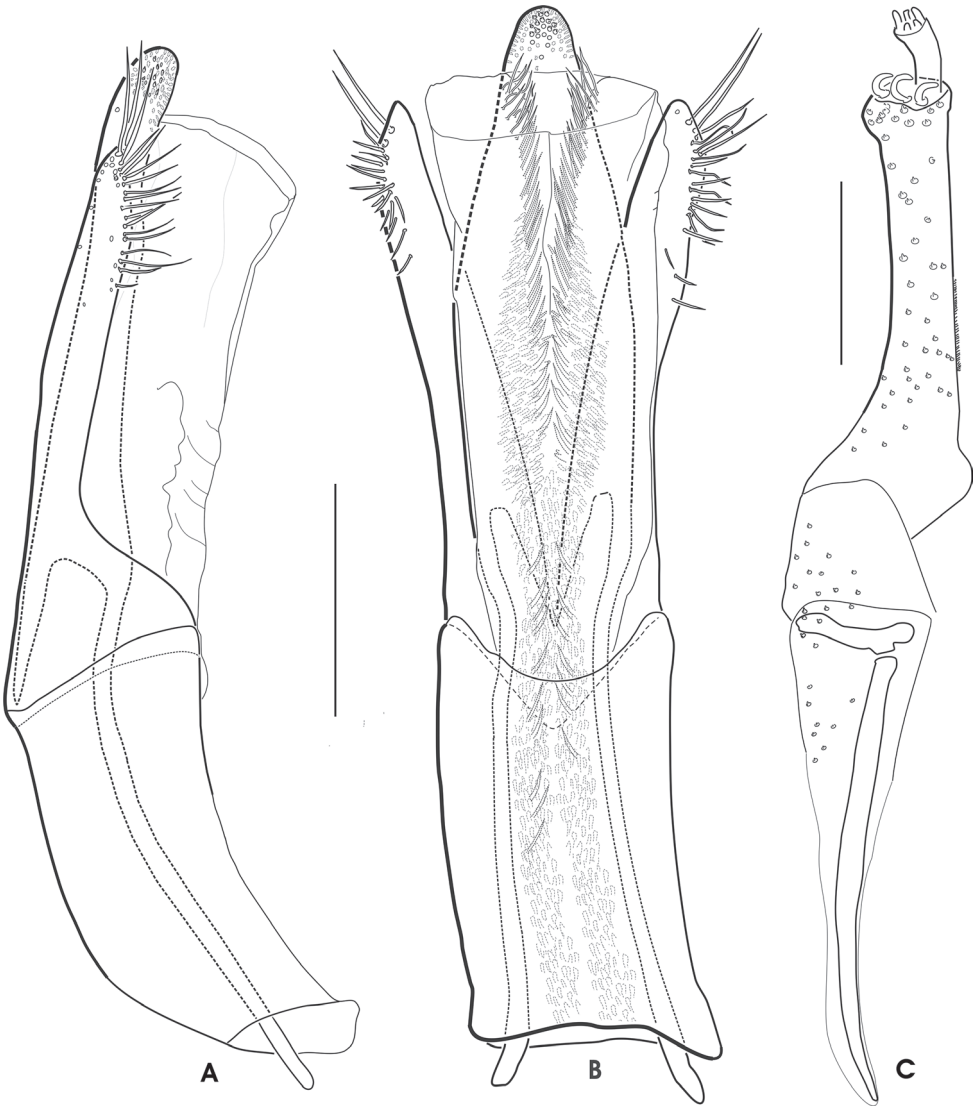

Figure 10. *Grouvellinus andrekuipersi* sp. n. (paratype male & female from 'NepC3g'): **A** aedeagus in lateral view **B** aedeagus in ventral view **C** ovipositor in ventral view (right half). Scale bars: 0.1 mm.

shallowly impressed apically, regularly arranged in median rows only, less regularly arranged in lateral rows; interstices glabrous; only interval 8 with (genus-typical) serrate carina; all carinae with row of yellowish pubescence; lateral elytral margin serrate.

Mesoventrite (Fig. 9C) with two pairs of deep sub-trapezoidal grooves, one behind procoxae, another medially, the latter more distinct in males.

Metaventrite (Fig. 9C) with large glabrous disc; longitudinal impression along median suture limited to posterior half; lateral portions with irregular impressions and irregularly micro-striate interstices; posterior-lateral portions with very dense, fine pubescence (plastron).

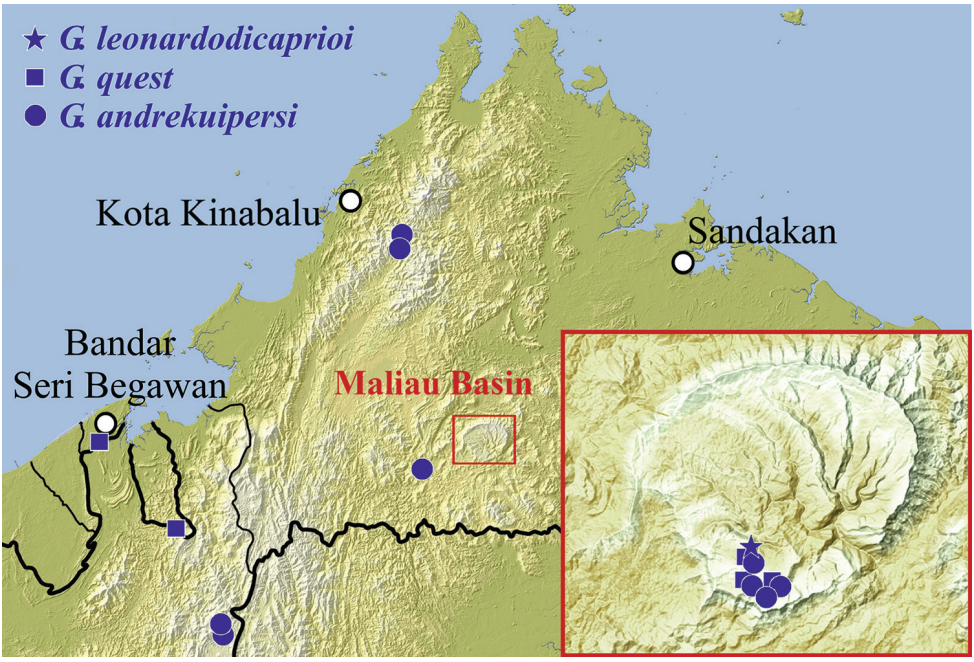

Figure 11. Map of the eastern tip of Borneo with large parts of Sabah, Malaysia and Negara Brunei Darussalam and the collection sites of the new *Grouvellinus* species (additional paratypes from NMW) and enlarged area of the Maliau Basin with collection sites of the first taxon expedition.

Abdominal ventrites (Fig. 9C). Ventrite 1 with pair of longitudinal carinae between glabrous disc and densely finely pubescent lateral portions (plastron); broad lateral portions of ventrites 1–2 and almost entire ventrites 4–5 (Fig. 9B) densely covered with plastron and scattered, moderately long setae; the latter more dense at apex and lateral margins of ventrite 5.

Legs (Fig. 4) approx. as long as body; hind leg longest; tibia longer than tarsus and femur in all legs; outer (dorsal) edge of all femora and tibiae with longitudinal row of robust trichoid setae (in both sexes); coxae and inner (ventral) faces of femora and tibiae densely covered with plastron-like short adpressed setae; inner (ventral) edge of distal tibia and tarsomeres 1–4 with fringe of long trichoid setae and short spine-like setae; apex of tibiae with pair of apical spines and a cluster of long spine-like setae (most conspicuous at hind tibia). Legs not conspicuously varying between sexes.

Aedeagus (Fig. 10A, B) ca. 440 µm long, ca. 100 µm wide. Base reaching basal 0.46 of total aedeagus length. Median lobe ca. four times as long as wide, distinctly overreaching parameres, slightly conical towards round apex in apical third. Ventral sac apically inflated, internally densely stippled and with dense sub-median fringes of moderately long, thin spines. Parameres apically conical (in both, ventral and lateral view), very slender in apical 2/3 in lateral view, usually with more than 20 trichoid setae in apical third, most of them at outer ventral face; most apical 2–4 setae longest and inserted at dorsal face.

Male sternite IX as in previous new species.

Figure 12. Type localities of the new species: **A** Giluk Falls (for *Grouvellinus leonardodicaprioi* sp. n. and *G. andrekuipersi* sp. n. **B** Creek east of 'Nepenthes Camp' (for *G. quest* sp. n.).

Ovipositor (Fig. 10C) similar to that of *Grouvellinus quest* sp. n., but overall slightly shorter (total length ca. 580 µm); stylus slightly shorter (30 µm long), and more bent outwards; coxite relatively longer (260 µm long), apically more broadened, ca. 2.8 times long as proximal portion; valvifer 330 µm long.

Larva. Unknown.

Differential diagnosis. *Grouvellinus andrekuipersi* sp. n. is similar in size, pronotal and elytral surface structure to *G. thienemanni* Jäch, 1984 and *G. sumatrensis* Jäch, 1984, but displays a slenderer pronotum in relation to the elytra and slightly convex lateral elytral margins (vs. slightly concave or straight in basal half in *G. thienemanni* and *G. sumatrensis*). The yellowish elytral patterns commonly seen in *G. andrekuipersi* sp. n. were not observed in any examined specimen (n = 20) of the two congeners. Their entire elytra and pronotum appear overall slightly paler (brown). Additionally, the pronotal basis is entirely rugulose ("shagreened") in *G. thienemanni* and *G. sumatrensis* (vs. glabrous with a pair of median rugose patches in *G. andrekuipersi* sp. n.). In *G. thienemanni*, the pronotal disc is additionally more densely punctate. The aedeagus of the new species is also similar in size and proportions to that of *G. thienemanni*, but in *G. andrekuipersi* sp. n., the paramere tips are distinctly conical (vs. evenly rounded in *G. thienemanni*) and the median lobe is wider and conically tapering towards apex (vs. evenly slender in apical 1/5 in *G. thienemanni*). From the previous new species (*G. quest* sp. n.), *G. andrekuipersi* sp. n. can easily be distinguished by 1) the pale elytral patches; 2) the smoother elytral surface due to the lack of any other elytral carinae than at interval 8; 3) the relatively broader and laterally convex elytra; 4) the sparse punctures of the pronotum; and 5) the smaller aedeagus with distinctly varying base, median lobe, and parameres.

Distribution. This species is known only from Borneo Island, namely the upper Maliau Basin, Tawau Hills Park, and Crocker Range in Sabah and two sites in eastern Sarawak (Fig. 11).

Acknowledgements

We would like to thank Taxon Expeditions participants and instructors Menno Schilthuizen, Carin Bondar, Massimo Delledonne, Mary Erickson, Lilian Seip, Sean Otani, Corlijn de Groot, Paolo Piccoli, and Paul Serail for assistance in the field, Jadda Suhaimi and staff at Maliau Basin Studies Centre for support, Liew Thor Seng, Charles Vairappan, Junn Kitt Foon, and Yeong Kam Cheng of Universiti Malaysia Sabah for assistance in databasing and collection deposition. Thanks are also due to Angelito Felipe L. Puno (Quezon City, Philippines) for the digital improvement of habitus pictures and line drawings. This research was carried out under SaBC access licence No. JKM/MBS.1000-2/2 JLD.5 (51) and under Maliau Basin Management Committee permit YS/MBMC/2016/245. The participation of the second author was partly funded by an Ateneo de Manila University Internationalization Grant.

References

Bian D, Jäch MA (2018) Revision of the Chinese species of the genus *Grouvellinus* Champion, 1923 (Coleoptera: Elmidae). The *G. acutus* species group. Zootaxa 4387: 174–182. http://dx.doi.org/10.11646/zootaxa.4387.1.8

Cardoso P, Erwin T, Borges P, New T (2011) The seven impediments in invertebrate conservation and how to overcome them. Biological Conservation 144: 2647–2655. http://dx.doi.org/10.1016/j.biocon.2011.07.024

Champion GC (1923) On some Indian Coleoptera. Entomologist's Monthly Magazine 59(269): 165–179.

Chandler M, See L, Copas K, Bonde AMZ, López BC, Danielsen F, Legind JK, Masinde S, Miller-Rushing AJ, Newman G, Rosemartin A, Turak E (2017) Contribution of citizen science towards international biodiversity monitoring. Biological Conservation 213: 280–294. https://doi.org/10.1016/j.biocon.2016.09.004

Conrad CC, Hilchey KG (2011) A review of citizen science and community-based environmental monitoring: issues and opportunities. Environmental Monitoring and Assessment 176: 273–291. http://dx.doi.org/10.1007/s10661-010-1582-5

De Kennis van Nu (2017) De nieuwe Darwins. https://www.dekennisvannu.nl/flow/1/denieuwedarwins

EarthWatch Institute (2018) Science in Action. http://earthwatch.org

Florida Lakewatch (2017) Florida LAKEWATCH Volunteer Water Quality Monitoring Program. http://lakewatch.ifas.ufl.edu

Freitag H, Jäch MA, Wewalka G (2016) Diversity of aquatic Coleoptera of the Philippines: checklists, state of knowledge, priorities for future research and conservation. Aquatic Insects 37: 177–213. doi.org/10.1080/01650424.2016.1210814

Grouvelle MA (1896) Potamophilides, Dryopides, Helmides et Heterocerides des Indes orientales. Annali del Museo Civico di Storia Naturale de Genova, Serie 2, 17: 32–56.

Jäch MA (1984) Die Gattung *Grouvellinus* im Himalaya und in Südostasien (Coleoptera, Elmidae). Koleopterologische Rundschau 57: 107–127.

Jäch MA, Kodada J, Brojer M, Shepard W, Ciampor FJr (2016) World catalogue of Insects. Vol. 14. *Coleoptera*: *Elmidae*, *Protelmidae*. Brill, Boston, 318 pp.

Kodada J, Jäch MA, Čiampor FJr (2016) Elmidae Curtis, 1830. In: Beutel, RG, Leschen RAB (Eds) Handbook of Zoology. Vol. IV. Part 38. Coleoptera, Beetles. Vol. 1. Morphology and Systematics (Archostemata, Adephaga, Myxophaga, Polyphaga partim). 2nd Ed. Walter de Gruyter, Berlin, 561–589.

McKinley DC, Miller-Rushing A, Ballard R, Bonney R, Brown S, Cook-Patton SC, Evans DM, French RA, Parrish JK, Phillips TB, Ryan SF, Shanley LA, Shirk JL, Stepenuck KF, Weltzin JF, Wiggins A, Boyle OD, Briggs RD, Chapin SF III, Hewitt DA, Preuss PW, Soukup MA (2017) Citizen science can improve conservation science, natural resource management, and environmental protection. Biological Conservation 208: 15–28. http://dx.doi.org/10.1016/j.biocon.2016.05.015

Opwall (2018) Operation Wallacea. https://www.opwall.com

Pollock RM, Whitelaw GS (2005) Community based monitoring in support of local sustainability. Local Environment 10: 211–228. https://doi.org/10.1080/13549839.2005.9684248

Schilthuizen M, Seip L, Otani S, Njunjić I (2017) Three new minute leaf litter beetles discovered by citizen scientists in Maliau Basin, Malaysian Borneo (Coleoptera: Leiodidae, Chrysomelidae). Biodiversity Data Journal 5: e21947. https://doi.org/10.3897/BDJ.5.e21947

Suprayitno N, Narakusumo R, von Rintelen T, Hendrich L, Balke M (2017) Taxonomy and Biogeography without frontiers – WhatsApp, Facebook and smartphone digital photography let citizen scientists in more remote localities step out of the dark. Biodiversity Data Journal 5: e19938. https://doi.org/10.3897/BDJ.5.e19938

Theobald EJ, Ettinger AK, Burgess HK, DeBey LB, Schmidt NR, Froehlich HE, Wagner C, HilleRisLambers J, Tewksbury J, Harsch MA, Parrish JK (2015) Global change and local solutions: tapping the unrealized potential of citizen science for biodiversity research. Biological Conservation 181: 236–244. http://dx.doi.org/10.1016/j.biocon.2014.10.021

ZooKeys 754: 23–32 (2018)
doi: 10.3897/zookeys.754.23525
http://zookeys.pensoft.net

RESEARCH ARTICLE

A peer-reviewed open-access journal
ZooKeys
Launched to accelerate biodiversity research

Two new species of the genus *Miasa* Distant, 1906 from China, with a key to all species (Hemiptera, Fulgoromorpha, Dictyopharidae)

Yan-Li Zheng[1,2,3], Lin Yang[1], Xiang-Sheng Chen[1], Xu-Qiang Luo[2,3]

1 *Institute of Entomology, Guizhou University; The Provincial Special Key Laboratory for Development and Utilization of Insect Resources of Guizhou, Guizhou University, Guiyang, Guizhou, 550025 P. R. China*
2 *School of Geography and Tourism, Guizhou Education University, Guiyang, Guizhou, 550018 P. R. China*
3 *Institute of Environmental, Resources and Disaster, Guizhou Education University, Guiyang, Guizhou, 550018 P. R.China*

Corresponding author: *Xiang-Sheng Chen* (chenxs3218@163.com)

Academic editor: *M. Wilson* | Received 10 January 2018 | Accepted 3 April 2018 | Published 30 April 2018

http://zoobank.org/5778B262-F79E-4B4B-BB2C-2187F78D4F43

Citation: Zheng Y-L, Yang L, Chen X-S, Luo X-Q (2018) Two new species of the genus *Miasa* Distant, 1906 from China, with a key to all species (Hemiptera, Fulgoromorpha, Dictyopharidae). ZooKeys 754: 23–32. https://doi.org/10.3897/zookeys.754.23525

Abstract

Two new species *Miasa dichotoma* Zheng & Chen, **sp. n.** and *M. trifoliusa* Zheng & Chen, **sp. n.** from China are described and illustrated. A key of identification to all species of the genus is provided.

Keywords

Fulgoroidea, Oriental region, planthopper, taxonomyt. Text.

Introduction

The Oriental genus *Miasa* was established by Distant (1906) for a single species *Elidiptera smaragdilinea* Walker, 1857, from Malacca (Malay Peninsula). Song et al. (2014) reviewed this genus revising the already three known species and adding two

new. In this paper, two new species, *M. dichotoma* sp. n. and *M. trifoliusa* sp. n. are described and illustrated, with photographs of the adult habitus. So far, this genus now includes seven species.

Materials and methods

The morphological terminology and measurements follow Yang and Yeh (1994) and Song et al. (2014). Specimens are deposited in the Institute of Entomology, Guizhou University, Guiyang, China (IEGU). Dry specimens were used for the observation, description, and illustration. Genital segments of the examined specimens were macerated in boiling solution of 10% potassium and drawn from preparations in glycerine jelly under a Leica MZ12.5 stereomicroscope. Color pictures for adult habitus were obtained by a KEYENCE VHX-1000 system. Illustrations were scanned with Canon Cano Scan LiDE 200 and imported into Adobe Photoshop CS6 for labelling and plate composition. The type specimens are deposited in the Institute of Entomology, Guizhou University, China (IEGU).

The following abbreviations are used in the text:

BL body length (from apex of cephalic process to tip of fore wings);
HL head length (from apex of cephalic process to base of eyes);
HW head width (including eyes);
FWL forewing length.

Taxonomy

***Miasa* Distant, 1906**
Figs 1–32

Miasa Distant, 1906: 247; Schmidt 1906: 280; Melichar 1912: 37; Schmidt 1915: 348; Distant 1916: 28; Schmidt 1928: 129; Metcalf 1946: 34; Song et al. 2014: 142. Type species. *Elidiptera smaragdilinea* Walker, 1857, by original designation.
Putalamorpha Bierman, 1910: 9. Type species. *Stenocranus productus* Lethierry, 1888 by original designation. Synonymised by Melichar 1912: 79.

Type species. *Elidiptera smaragdilinea* Walker, 1857.

Diagnosis. For the relationships and diagnosis of *Miasa* see Songet al. (2014).

Distribution. Burma; Indonesia (Borneo, Jawa, Sumatra); Malaysia (Borneo, Sabah, Sarawak, peninsula); China (Yunnan); Thailand; Vietnam; Singapore; Myanmar (ex Burma).

Key to the species of the genus *Miasa* based on males

(Modified from Songet al. 2014 and updated two new species)

1 Frons below eyes including median carina uniformly dull ochreous; pronotum with posterolateral corner pale yellow to ochreous with or without dark spot behind eye; forewings posterior margin broadly dull ochreous; aedeagus with two pairs of ventral lobes and a pair of dorsolateral lobes **2**

– Frons below eyes emerald green, with median carina testaceous or if uniformly dull ochreous medial carina darker; pronotum with lateroventral corner brown, without dark spot behind eye; forewings with inner margin of clavus narrowly dark brown; aedeagus with two pairs of ventral lobes, but without dorsolateral lobes; southern Malay Peninsula, Sumatra and Java..... ..... ***M. smaragdilinea*** **(Walker)**

2 Male segment X broad basally, not hatchet-shaped in lateral view..... **5**

– Male segment X narrow basally, hatchet-shaped in lateral view **3**

3 Aedeagus with membranous phallobase bearing two pair of lobes, a pair of dorsal, a pair of complicated ventral lateral lobes (Fig. 14); southwestern China ..... ***M. dichotoma*** **Zheng & Chen, sp. n.**

– Aedeagus with membranous phallobase bearing three pairs lobes (Fig. 31).. 4

4 Phallobase membranous with a pair of dorsal lobes directed posteriorly, and two pairs of ventral lobes: upper pair large and elongate, directed dorsally; lower pair relatively small and rounded; southwestern China, southeast Asia to North Malay Peninsula..... ***M. wallacei*** **Muir**

– Phallobase membranous with a pair of dorsal lobes directed posteriorly, and two pairs of ventral lobes (Fig. 31): large, almost equal length, apical bifurcate, directed dorsally; southwestern China..... ..... ***M. trifoliusa*** **Zheng & Chen, sp. n.**

5 Preocular field with a blackish brown spot; male segment X with ventral margin weakly incurved in lateral view..... **6**

– Preocular field without blackish brown spot; male segment X with ventral margin distinctly incurved sub-basally in lateral view; Borneo .... ***M. borneensis*** **Song, Webb & Liang**

6 Upper process of gonostyle distinctly broad at apex; basal ventral lobes of aedeagus distinctly short and small; male segment X with apical ventral margin distinctly produced in a long process in lateral view; Borneo..... ..... ***M. nigromaculata*** **Song, Webb & Liang**

– Upper process of gonostyle not broad at apex; basal ventral lobes of aedeagus distinctly long; male segment X with ventral margin not protruded in lateral view; Sumatra and Java ..... ***M. producta*** **(Lethierry)**

***Miasa dichotoma* Zheng & Chen, sp. n.**
http://zoobank.org/792EE97D-AA25-4C91-8A93-B771A0B70699
Figs 1–20

Measurements. ♂, BL: 14.8–15.1 mm; HL: 2.0–2.3 mm; HW: 0.8–0.9 mm; FWL: 11.1–11.3 mm. ♀, BL: 15.6 mm; HL: 2.6 mm; HW: 1.0 mm; FWL: 11.5 mm.

Description. General colour in dried specimens ferruginous-brown, marked with pale green and black. Cephalic process of the base brown, terminal black, brown on side. Frons uniformity brown. Frontoclypeal area dark with brown freckles. Compound eyes dark brown; ocelli light pink. Antennae brown. Pronotum and mesonotum brown, the median area emerald green. Forewings with stigmal area and posterior margin broadly dull ochreous, a large oblique triangular apical streak, and a narrow streak along nodal line fuscous; hind wings with an apical fuscous spot. Legs brown with dark spots.

Cephalic (Figs 1, 2, 5–7) process relatively long, distinctly upturned, ratio length to length of pronotum and mesonotum combined 0.8. Vertex (Figs 1, 2, 5–7) with lateral margins carinate, sub-parallel at base, sharply sinuate in front of eyes, then narrowing to arrowhead at apex, ratio of length to width between eyes 4.5. Frons (Fig. 6) elongate, median carina complete and elevated, length approx. 3.9 times long than width. Pronotum (Figs 1, 2, 5–7) distinctly shorter than mesonotum medially in the middle line, median carina obscure, lateral carina distinct, ratio length to length approx. 0.3:1. Mesonotum (Figs 1, 2, 5–7) median carina obscure, lateral carina distinct. Forewings (Figs 1, 8) elongate, with ratio of length to width approx. 4.0:1; CuA vein first branched before Sc+R and M veins near middle; crossveins very scarce, forming a nodal line along Sc+R, M and CuA veins at apical 1/3; apical cells approx. 10–12; Pcu and A_1 veins fused into a long Pcu+A_1 vein at apical 1/6 in clavus; stigmal area clear, with four cells. Legs long and thin, profemur not flattened and dilated, with one minute, short, blunt spine near apex; metatibia with 6 lateral black-tipped spines and 6 apical black-tipped teeth, hind tibiae I with nine and tarsomeres II with 8 black-tipped apical teeth, respectively.

Male genitalia. Pygofer (Figs 10–12) wider ventrally than dorsally (approx. 5.8:1), hatchet-shaped in lateral view. Gonostyles (Figs 10, 11) relatively large, broadening towards apex in lateral view (Fig. 10), posterior margin straight, upper margin with dorsally directed, black-tipped process near middle, with ventrally directed, hook-like process near sub-middle on outer upper edge. Anal tube (Figs 10, 12) wide and narrow down in dorsal view, ratio length to width approx. 1.1:1. Aedeagus (Figs 13–15) with one pair of special long endosomal processes, processes with apex acute, sclerotised and pigmented. Phallobase sclerotised and pigmented at base, with two pairs of membranous lobes at apex (Figs 13–15): the dorsal lobes relatively small and the ventral lobes large with complicated ventral lateral lobes in lateral view (Fig. 13), one pair of large lobes in dorsal view (Fig. 15), one pair of large and complicated lobes in ventral view (Fig. 14).

Female genitalia. Segment X (Fig. 17) round and large in dorsal view, ratio length to width at middle approx. 1.3. Gonocoxae VIII with two endogonocoxal processes membranous and flattened on endogonocoxal lobe. Gonopophyses VIII (Fig. 18) scle-

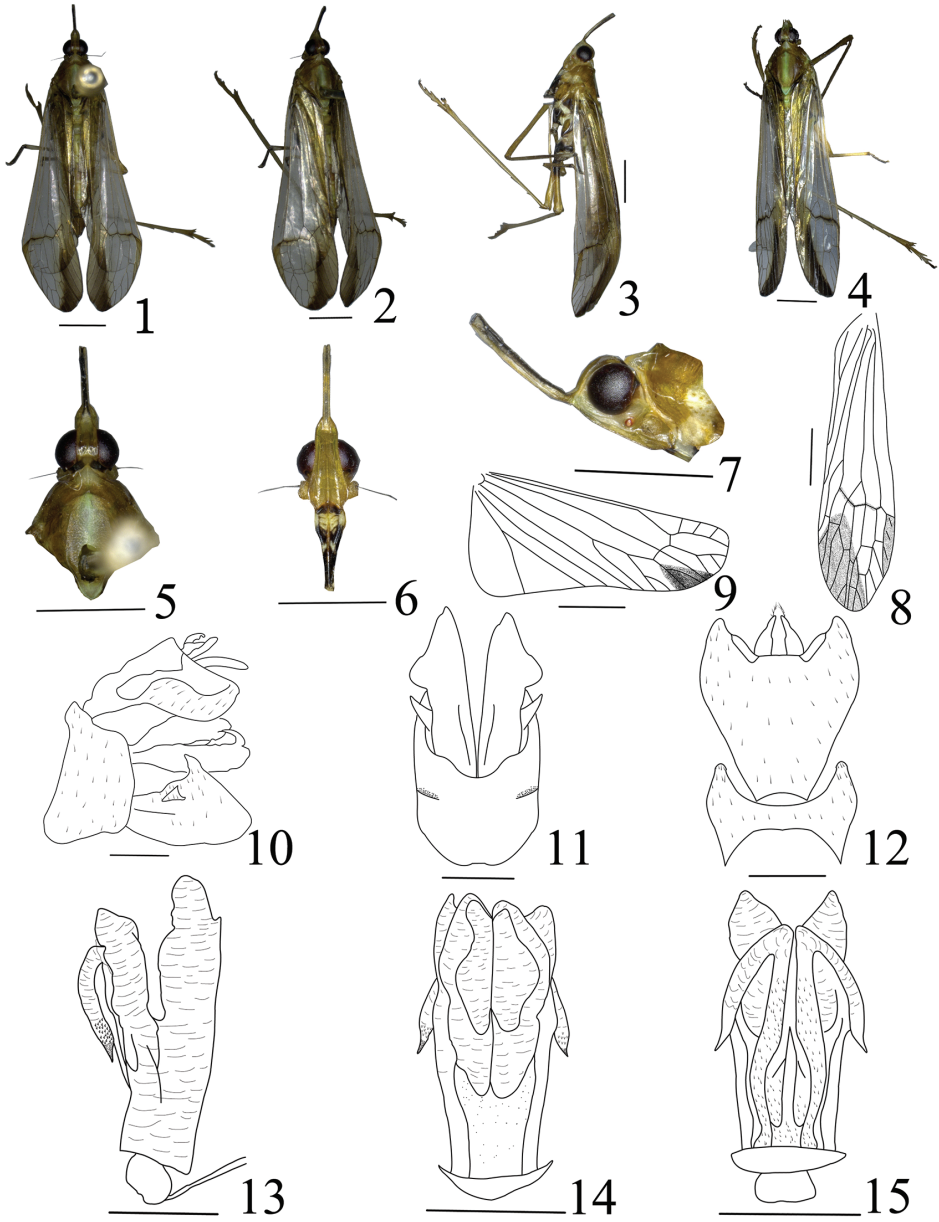

Figures 1–15. *Miasa dichotoma* sp. n.: **1** male, holotype, dorsal view **2** male, oblique side view **3** male, lateral view **4** female, dorsal view, spoiled **5** male, head and thorax, dorsal view **6** male, frons and clypeus, ventral view **7** male, head and pronotum, lateral view **8** male, forewing **9** male, hind wing **10** genitalia, lateral view **11** pygofer and parameres, ventral view **12** pygofer and anal tube, dorsal view **13** aedeagus, lateral view **14** aedeagus, ventral view **15** aedeagus, dorsal view. Scale bars: 2 mm (**1–9**), 0.5 mm (**10–15**).

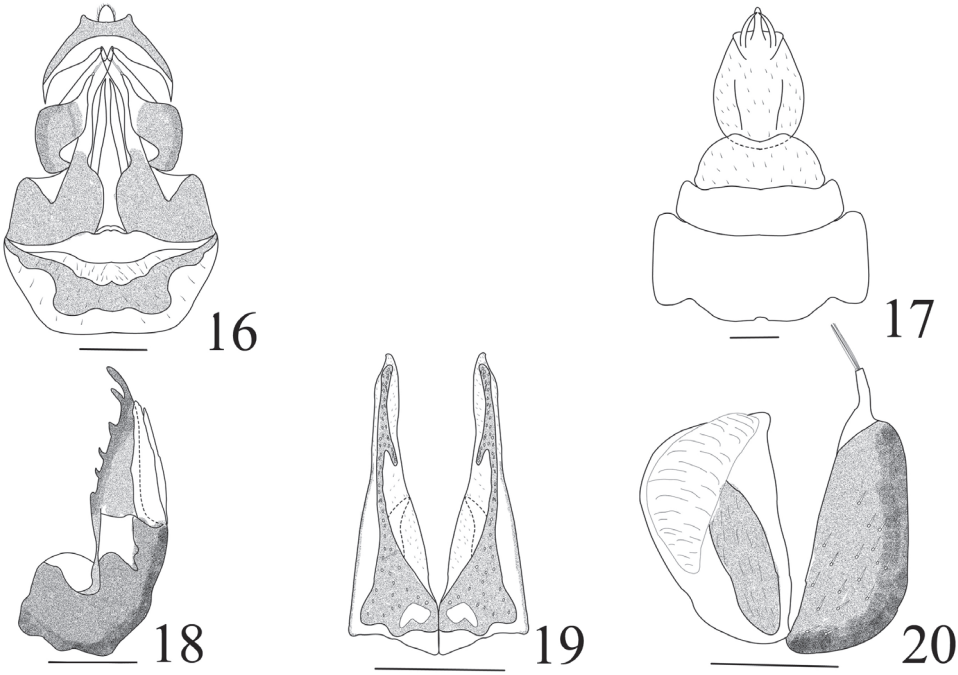

Figures 16–20. *Miasa dichotoma* sp. n.: **16** genitalia ventral view of female **17** genitalia dorsal view of female **18** gonocoxae VIII (lateral view) **19** gonopophyses IX (ventral view) **20** gonoplacs (lateral view). Scale bars: 0.5 mm.

rotised with six differently sized teeth in lateral view. Gonopophyses IX (Fig. 19) triangular, symmetrical in ventral view, connected at base and separated from 2/3 base. Gonoplacs (Fig. 20) with two sclerotised lobes, ventral lobe with a membranous structure at the top, and lateral lobe with 3-4 long spines at apex.

Type material. Holotype ♂, China, Yunnan, Xishuangbanna, Mengla, 23.VIII.2013, Guo Mei-Na. Paratypes, 1♀, same data as Holotype; 1♂, China, Yunnan, Xishuangbanna, Menglun, 30.VII.2012, Zheng Wei-Bin.

Distribution. China (Yunnan).

Differential diagnosis. This species is similar to *M. trifoliusa* sp. n. but can be distinguished from phallobase. The former has two pairs of membranous lobes of the phallobase at apex, the latter with three pairs of membranous lobes at apex.

Etymology. This new species is named for the Greek word "*dichotoma*" referring to aedeagus that is dichotomous at its apex.

***Miasa trifoliusa* Zheng & Chen, sp. n.**
http://zoobank.org/071117C8-A54B-49A5-8FD7-FB582E751618
Figs 21–32

Measurements. ♂, BL: 14.2 mm; HL: 1.8 mm; HW: 0.4 mm; FWL: 10.7 mm.

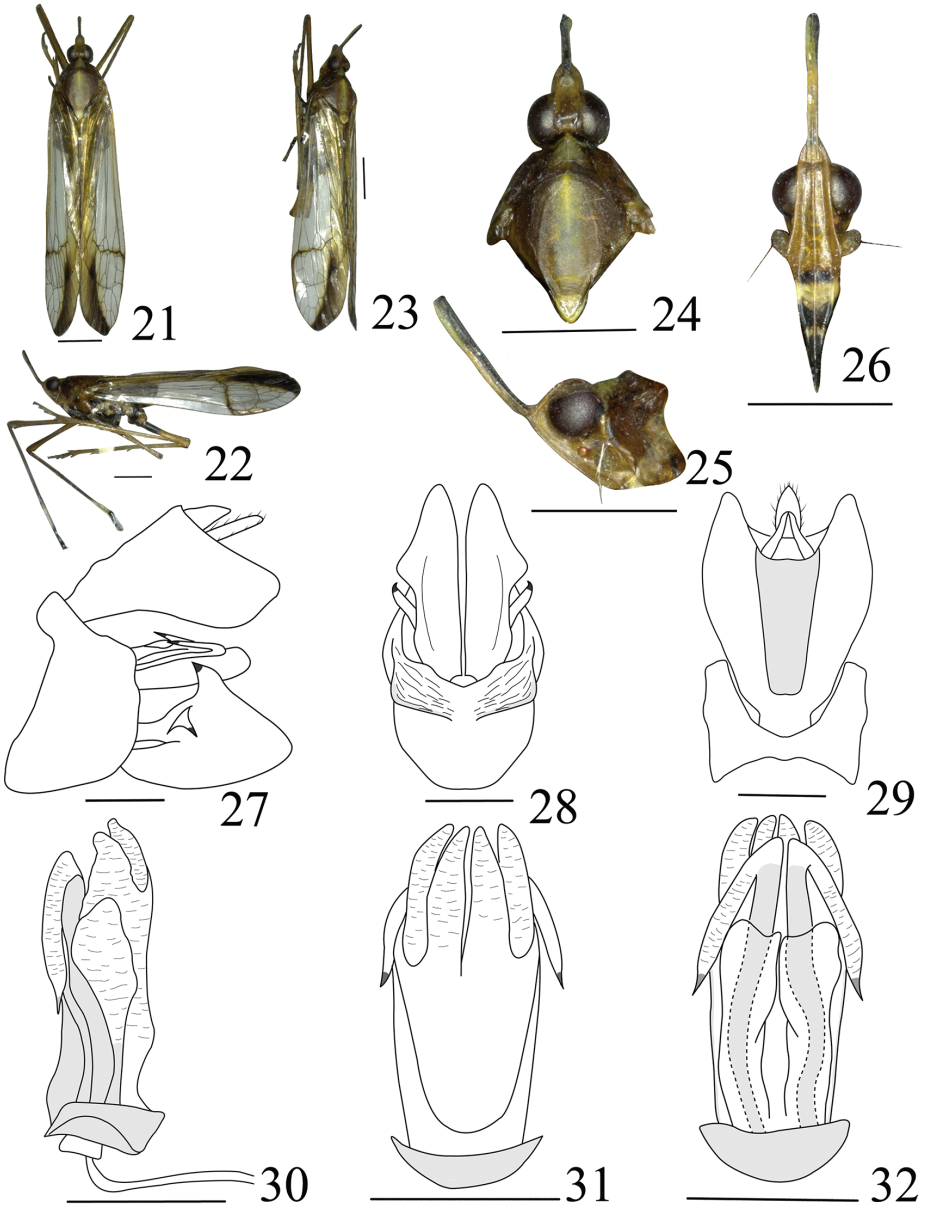

Figures 21–32. *Miasa trifoliusa* Zheng & Chen, sp. n.: **21** male, holotype, dorsal view **22** male, lateral view **23** male, oblique side view **24** male, head and thorax, dorsal view **25** male, head and pronotum, lateral view **26** male, frons and clypeus, ventral view **27** genitalia, lateral view **28** pygofer and parameres, ventral view **29** pygofer and anal tube, dorsal view **30** aedeagus, lateral view **31** aedeagus, ventral view **32** aedeagus, dorsal view. Scale bars: 2 mm (**21–26**), 0.5 mm (**27–32**).

Description. General colour in dried specimens ferruginous-brown, marked with faint yellow and reddish brown. Cephalic process of the base brown, terminal black, brown on side. Frons brown with faint yellow marks. Frontoclypeal dark with paired

brown blotchy markings. Compound eyes dark brown, ocelli light pink. Antennae brown. Pronotum and mesonotum brown, the middle faint yellow. Forewings with stigmal area and posterior margin broadly dull ochreous, a large oblique triangular apical streak, and a narrow streak along nodal line fuscous; hind wings with an apical fuscous spot. Legs brown with dark spot.

Cephalic (Figs 21–25) process relatively long, distinct upturned, ratio length to length of pronotum and mesonotum combined 0.7. Vertex (Figs 21–25) with lateral margins carinate, sub-parallel at base, sharply sinuate in front of eyes, then narrowing to arrowhead at apex, ratio of length to width between eyes 3.5. Frons (Fig. 26) elongate, median carina complete and elevated, length approx. 4.8 times long than width. Pronotum (Figs 21–24) distinctly shorter than mesonotum medially in the middle line, median carina obscure, lateral carina distinct, ratio length to length approx. 0.3:1. Mesonotum (Figs 21–24) median carina obscure, lateral carina distinct. Forewings (Figs 22, 23) elongate, with ratio of length to width approx. 4.0:1; stigma distinct, with four cells, CuA vein first branched before Sc+R and M veins near middle; cross-veins very scarce, forming a nodal line along Sc+R, M and CuA veins at apical 1/3; apical cells approx. 12; Pcu and A_1 veins fused into a long Pcu+A_1 vein at apical 1/6 in clavus. Legs long and thin, fore femur not flattened and dilated, with one minute, short, blunt spine near apex; hind tibia with five lateral black-tipped spines and six apical black-tipped teeth, hind tibiae I with ten and tarsomeres II with eight black-tipped apical teeth, respectively.

Male genitalia. Pygofer (Figs 27–29) wider ventrally than dorsally (aprpox. 4.5:1), hatchet-shaped in lateral view. Gonostyles (Figs 27, 28) relatively large, broadening towards apex in lateral view (Fig. 27), posterior margin straight, upper margin with dorsally directed, black-tipped process near middle, with ventrally directed, hook-like process near sub-middle on outer upper edge. Anal tube (Figs 27, 29) wide and narrow down in dorsal view, ratio length to width approx. 1.4:1. Aedeagus (Figs 30-32) with one pair of special long endosomal processes, processes with apex acute, sclerotised and pigmented. Phallobase sclerotised and pigmented at base, with three pairs of membranous lobes at apex: the dorsal lobes relatively small and the ventral two pairs of membranous lobes large and connected in ventral view (Fig. 31).

Type material. Holotype ♂, China, Yunnan, Xishuangbanna Menglun. 18.VIII.2014, Wang Ying-Jian.

Distribution. China (Yunnan).

Differential diagnosis. This species is similar to *M. wallacei* Muir, but can be distinguished most easily by the phallobase conformation. The former is membranous with a pair of dorsal lobes directed posteriorly, and two pairs of ventral lobes: large, almost equal in length, apically bifurcate, directed dorsally, the latter membranous with a pair of dorsal lobes directed posteriorly, and two pairs of ventral lobes: upper pair large and elongate, directed dorsally; lower pair relatively small and rounded. There have differences in body colour and in the lengths and widths of the forewings, but the differences are not obvious.

Etymology. This new species is named with the Greek word "*trifoliusa*" referring to phallobase with three pairs of membranous lobes at apex.

Discussion

The discovery of these two new species broadens our knowledge of the morphology and biogeography of the genus, although it is not a new record of the genus for China. The two new species occur in Yunnan, China (as does *M. wallacei*). This might be related with the special geographical position and climate of Yunnan.Tto the northwest lies Lancang County; to the southeast, south, and southwest respectively there are borders with Laos, Burma, and Vietnam. These regions and countries are linked by mountains and rivers and are located on the Tropic of Cancer in tropical humid areas.

Acknowledgments

This work was supported by the Program of Science and Technology Innovation Talents Team, Guizhou Province (No. 20144001), the Program of Excellent Innovation Talents, Guizhou Province (No. 20154021), the Special Foundation for Excellent Young Scientist of Guizhou Province (No. [2015]21), the National Natural Science Foundation of China (No. 31472033, 41563007), Scientific research fund project of Guizhou Education University (2015BS012), and the International Science and Technology Cooperation Program of Guizhou (20165802).

References

Bierman CJH (1910) Homopteren aus Niederländisch Ost-Indien. II; herausgegeben von D. Mac Gillavry und K.W. Dammerman. Notes Leyden Museum 33: 1–68.

Distant WL (1906) The Fauna of British India, including Ceylon and Burma. Rhynchota Vol. III (Heteroptera-Homoptera). Taylor & Francis, London, 503 pp.

Distant WL (1916) The Fauna of British India, including Ceylon and Burma. Rhynchota Vol. VI (Heteroptera-Homoptera). Taylor & Francis, London, 248 pp.

Lethierry LF (1888) Liste des Hemiptères recueillis à Sumatra et dans l'ile de Nias par M. E. Modigliani. Annali del Museo Civico di Storia Naturale di Genova, Genova (Ser. 2) 6: 460–470.

Melichar L (1912) Monographie der Dictyophorinen (Homoptera). Abhandlungen der K. K. Zoologisch-Botanischen Gesellschaft, Wien 7(1): 1–221.

Metcalf ZP (1946) General catalogue of the Hemiptera, Fasci. IV. Fulgoroidea, Part 8 Dictyopharidae. Smith College, Northampton, Mass., USA, 245 pp.

Schmidt E (1906) Beitrag zur Kenntnis der Fulgoriden. Die Gattung *Miasa* Distant. Stettiner Entomologische Zeitung 67: 280–286.

Schmidt E (1928) Die Zikaden des Buitenzorger Museums (Hemipt.-Homopt.). I. Treubia 10: 107–144.

Song Z-S, Webb MD, Liang A-P (2014) Systematic revision of the Oriental planthopper genus Miasa Distant (Hemiptera: Fulgoromorpha: Dictyopharidae), with description of a new genus from southern India. Arthropod systematics 72(2): 137–164.

Walker F (1857) Catalogue of the homopterous insects collected at Sarawak, Borneo, by Mr. A. R. Wallace, with descriptions of new species. Journal of the Proceedings of the Linnean Society 1: 82–100. https://doi.org/10.1111/j.1096-3642.1856.tb00958.x

Yang C-T, Yeh W-B (1994) Nymphs of Fulgoroidea (Homoptera: Auchenorrhyncha) with descriptions of two new species and notes on adults of Dictyopharidae. Chinese Journal of Entomology, Special Publication 8: 1–187.

ZooKeys 754: 33–46 (2018)
doi: 10.3897/zookeys.754.24210
http://zookeys.pensoft.net

RESEARCH ARTICLE

A peer-reviewed open-access journal
ZooKeys
Launched to accelerate biodiversity research

Study on the Pauropoda from Tibet, China. Part I. The genera *Decapauropus* and *Hemipauropus* (Myriapoda)

Chang-Yuan Qian[1], Yun Bu[2], Yan Dong[3], Yun-Xia Luan[1]

1 *Key Laboratory of Insect Developmental and Evolutionary Biology, Institute of Plant Physiology and Ecology, Chinese Academy of Sciences, Shanghai 200032, China* **2** *Natural History Research Center, Shanghai Natural History Museum, Shanghai Science & Technology Museum, Shanghai 200041, China* **3** *College of Biology and Food Engineering, Chuzhou University, Chuzhou 239000, China*

Corresponding authors: *Yun Bu* (buy@sstm.org.cn); *Yun-Xia Luan* (yxluan@sibs.ac.cn)

Academic editor: *P. Stoev* | Received 3 February 2018 | Accepted 15 April 2018 | Published 30 April 2018

http://zoobank.org/263A73C9-6E31-492B-A5DD-B3F08EB2EB17

Citation: Qian C-Y, Bu Y, Dong Y, Luan Y-X (2018) Study on the Pauropoda from Tibet, China. Part I. The genera *Decapauropus* and *Hemipauropus* (Myriapoda). ZooKeys 754: 33–46. https://doi.org/10.3897/zookeys.754.24210

Abstract

Three new species of family Pauropodidae: *Decapauropus biconjugarus* Qian & Bu, **sp. n.**, *D. tibeticus* Qian & Bu, **sp. n.** and *Hemipauropus quadrangulus* Qian & Bu, **sp. n.** are described and illustrated from southeastern Tibet, China. The genus *Hemipauropus* is recorded for the first time from China. This is the second report of pauropods from Tibet.

Keywords

diversity, Motuo County, new record, new species, Pauropodidae, taxonomy

Introduction

To date, there is only one species of Pauropoda reported in Tibet (Zhang and Chen 1988). Since only a single specimen was obtained and was tentatively identified as *Sphaeropauropus* sp. of the family Sphaeropauropodidae, Silvestri, 1930. For the last thirty years, this remained the only record of Pauropoda from Tibet. In November 2015,

a short expedition to Motuo and Bomi counties, southeastern Tibet of China was carried out. In total, 50 specimens of Pauropoda were obtained during the expedition. In the present study, we describe and illustrate three new species of the family Pauropodidae Lubbock, 1867, including one species belonging to the genus *Hemipauropus*, which is recorded for the first time from China. The other two species belong to the genus *Decapauropus*. This is the second report of pauropods from the territory of Tibet.

Materials and methods

Sampling was made in three areas of southeastern Tibet in 2015: Dexing town, Motuo County; Beibeng town, Motuo County, and Songzong town, Bomi County. Pauropods were collected by means of Tullgren's funnel. Specimens were sorted under a stereo dissection microscope and preserved in 80% alcohol. Each specimen was mounted with Hoyer's solution and identified under a phase contrast microscope (Nikon ECLIPSE N*i*, objective lens 100X / 1.30 Oil, ∞/ 0.17 WD 0.20 (0.16)). All specimens were deposited in the collection maintained by the Shanghai Natural History Museum (**SNHM**) and the Shanghai Entomological Museum (**SEM**).

Abbreviations used in the descriptions:

Head. $\boldsymbol{a_1}$ – a submedian pair of setae on tergal side of head, $\boldsymbol{a_2}$ – an intermediate pair of setae on tergal side of head, $\boldsymbol{a_3}$ – a sublateral pair of setae on tergal side of head, $\boldsymbol{a_4}$ – a posterolateral pair of setae on head.

Antenna. ***bs*** – base segment of antennal flagellum, $\boldsymbol{F_1}$ – flagellum of tergal antennal branch; $\boldsymbol{F_2}$ – anterior flagellum of sternal antennal branch, $\boldsymbol{F_3}$ – posterior flagellum of sternal antennal branch, ***g*** – globulus of sternal antennal branch, ***p*** – a tergal seta on fourth antennal segment, ***p'*** – an anterior seta on fourth antennal segment, ***p"*** – a sternal seta on fourth antennal segment, ***q*** – a seta on sternal side of sternal antennal branch, ***r*** – a posterior seta on fourth antennal segment, ***s*** – sternal antennal branch, ***t*** – tergal antennal branch.

Trunk. $\boldsymbol{T_{1–5}}$ – first to fifth pair of bothriotricha on tergites.

Pygidial tergum. $\boldsymbol{a_1}$ – (sub) median pair of setae, $\boldsymbol{a_2}$ – intermediate pair of setae, $\boldsymbol{a_3}$ – sublateral pair of setae, ***st*** – styli.

Pygidial sternum. $\boldsymbol{b_1}$ – posterior pair of setae, $\boldsymbol{b_2}$ – lateral pair of setae, $\boldsymbol{b_3}$ – anterior pair of setae.

Measurements are provided as length of body in mm; the range of variation in adult paratypes is given in brackets. Absolute lengths of all other body parts are given in μm. Otherwise, the text refers relative lengths.

Results

Taxonomy
Family Pauropodidae
Genus *Decapauropus* Remy, 1931

***Decapauropus biconjugarus* Qian & Bu, sp. n.**
http://zoobank.org/2E2C1271-92AD-4001-8192-9A652779E81D
Figs 1, 2

Material examined. Holotype, adult with 9 pairs of legs, female (slide no. XZ-PA2015025) (SNHM), China, Tibet, Motuo county, Dexing town, extracted from soil samples in a broad-leaved forest, alt. 1100 m, 29°40'N, 95°26'E, 3-XI-2015, coll. Y. Bu & G. Yang. Paratypes, 2 adults, with 9 pairs of legs, females (slides no. XZ-PA2015019 (SNHM), XZ-PA2015026 (SEM)), 2 subadults, with 8 pairs of legs (slides no. XZ-PA2015027 (SNHM), XZ-PA2015031 (SEM)), same data as holotype.

Etymology. From the Latin *biconjugarus* referring to the anal plate with two pairs of clavate appendages.

Diagnosis. *Decapauropus biconjugarus* sp. n. is distinguished from the other species in the genus by the shape of the anal plate: subquadrate, with obvious U-shape and concave lateral margins; distal part with 4 posteriorly directed clavate appendages, dorsal ones thickest, straight, annulate, those protruding from sternal side shorter and thinner, straight, glabrous. Posterior part of the pygidial sternum evenly rounded.

Description. Holotype length 0.6 mm (Fig. 2A).

Head (Figs 1B, 2E). Dorsal head setae short to moderately long, clavate, lateral ones cylindrical. Relative lengths of setae, 1st row: a_1 = 10, a_2 = 8 (10); 2nd row: a_1 = (9) 10, a_2 = 18 (19) a_3 = 14; 3rd row: a_1 = 8 (10), a_2 = (10) 12; 4th row: a_1 = 8, a_2 = (16) 18, a_3 = (18) 20, a_4 = (30) 32; lateral group setae l_1 =26 (27), l_2 = 22 (25) l_3 = 20 (30); the ratio a_1/a_1–a_1 in 1st row 0.8, 2nd row 0.4, 3rd row 0.4 and 4th row 0.4. Temporal organs oval in dorsal view, their length 1.4 times as long as their shortest distance apart. Head cuticle glabrous.

Antennae (Figs 1A, 2B, 2C). Antennal segment 4 with four cylindrical setae; relative lengths of setae: *p* = 100, *p*' = (39.9) 41.4, *p*" = 62.5 (63.8), *r* = (26) 27.6; tergal seta *p* (1.2) 1.3 times as long as tergal branch *t*. The latter cylindrical, 2.2 (2.3) times as long as its greatest diameter and (1.6) 1.7 times as long as sternal branch *s*, which itself is 2.3 times as long as its greatest diameter. Seta *q* cylindrical, blunt, 1.3 times as long as *s*. F_3 very thin with small base segment. Relative lengths of flagella (base segments included) and base segments: F_1 = 100, bs_1 = 6; F_2 = 44.4, bs_2 = 4; F_3 =83.3, bs_3 = 5. F_1 4.5 times as long as *t,* F_2 and F_3 2.7 and 5.0 times as long as *s* respectively. Distal calyces small; F_1 and F_2 with fusiform flagella axes just below calyx. Distal calyces spherical; distal part of flagella axes fusiform. Globulus *g* 1.75 times as long as wide; about 12 bracts, capsule subspherical; width of *g* 0.67 of the greatest diameter of *t*. Antennae nearly glabrous.

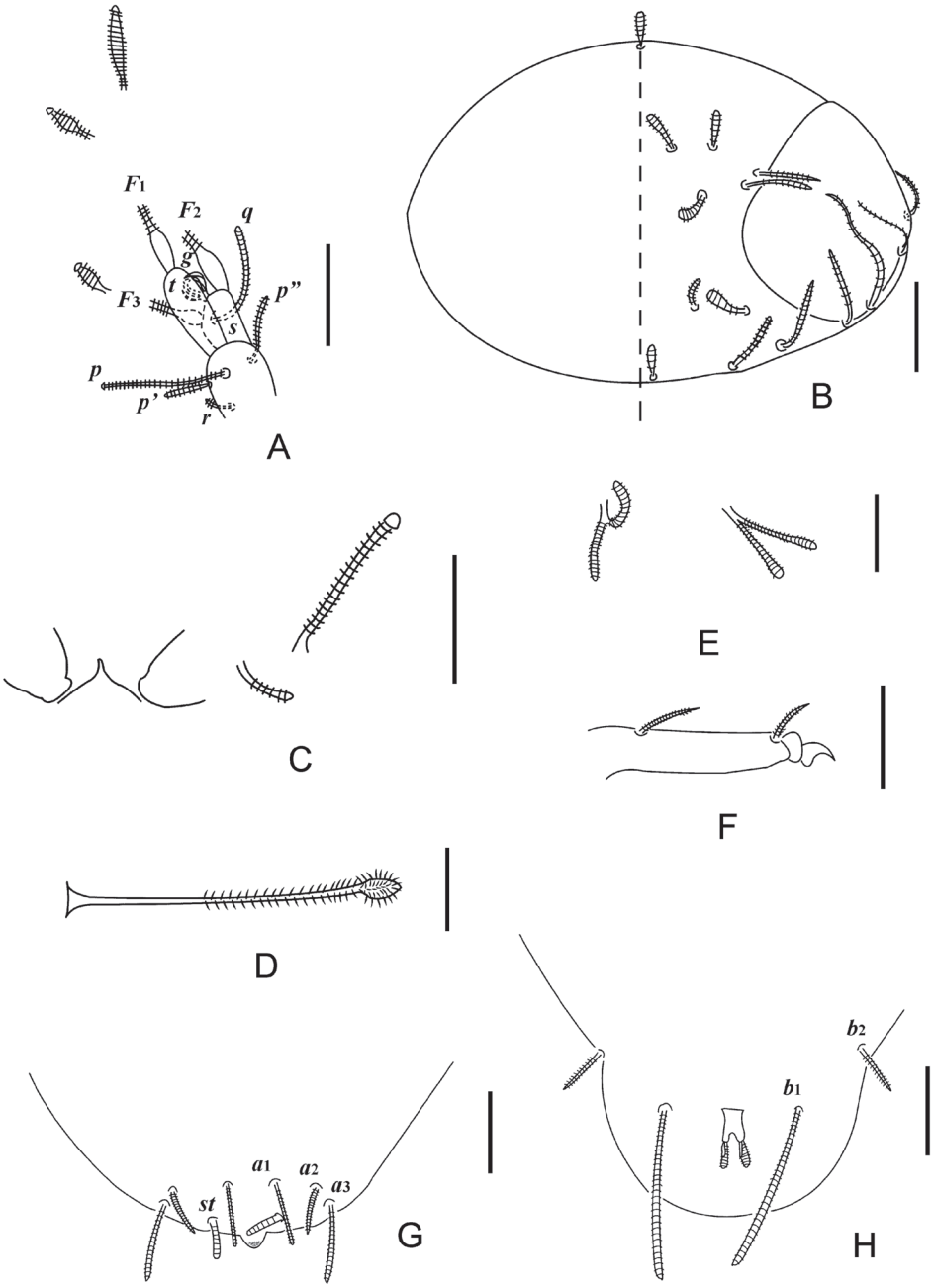

Figure 1. *Decapauropus biconjugarus* sp. n. (holotype) **A** Left antenna, tergal view **B** Head, median and right part, dorsal view **C** Collum segment, median and left part, sternal view **D** T_3 **E** Setae on coxa (left) and trochanter (right) of leg IX **F** Tarsus of leg IX **G** tergum of pygidum **H** sternum of pygidum. Scale bars: 20 μm.

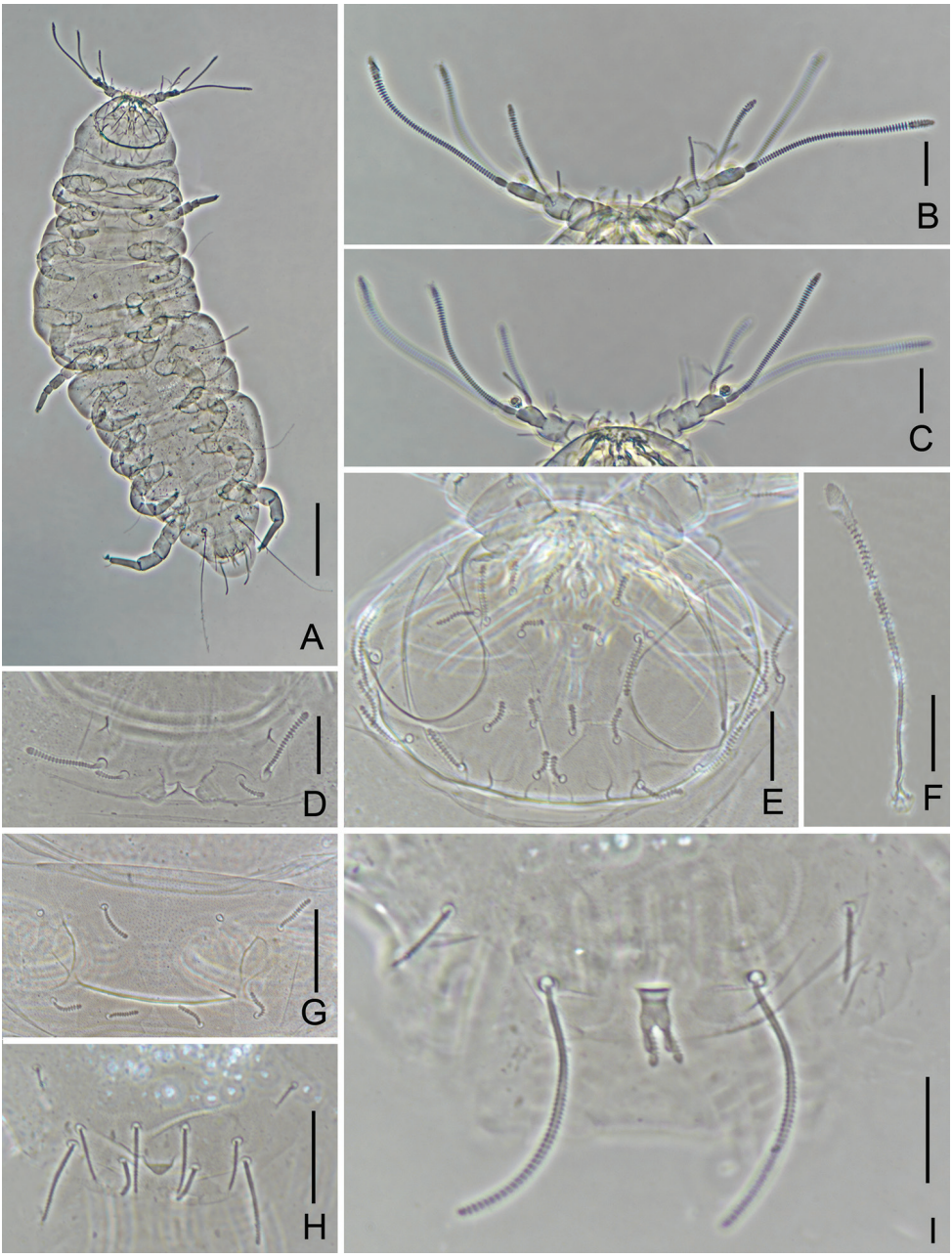

Figure 2. *Decapauropus biconjugarus* sp. n. (holotype) **A** Habitus **B** Antenna, tergal view **C** Antenna, sternal view **D** Collum segment, sternal view **E** Head, dorsal view **F** T_3 **G** Tergite I **H** Tergum of pygidum **I** Sternum of pygidum. Scale bars: 100 μm (**A**), 20 μm (**B–I**).

Trunk. Setae on collum subcylindrical, striate, and appearing simple. Sublateral setae length 27 μm, 2.5 times as long as submedian setae (Figs 1C, 2D); sternite process triangular, pointed; appendages narrowing distally and with flat caps (Figs 1C, 2D). Setae on tergites thin, cylindrical; 4 + 4 setae on tergite I (Fig. 2 G), 6 + 6 on II–IV, 6 + 4 on V, 4 + 2 on VI. Tergites glabrous.

Bothriotricha. Relative lengths: T_1 = 100, T_2 = 126.7, T_3 = 106.7, T_4 =128.0, T_5 = 206.7. Axes simple, straight, in all but T_3 very thin; axes of T_3 thickened in distal half (Figs 1D, 2F). Pubescent hairs simple, short, thin, strongest on distal half of T_3.

Legs. Setae on coxa and trochanter of leg IX length 20 and 23 μm respectively, furcate with subcylindrical, annulate, blunt branches (Fig. 1E). Tarsus of leg IX long, 45 μm, tapering, 4.1 times as long as its greatest diameter (Fig. 1F). Proximal seta long, 14 μm, tapering, striate; distal seta 11 μm, tapering, striate; their lengths 0.35 and 0.30 of the tarsal length, respectively. Cuticle of tarsus glabrous.

Pygidum. Tergum (Figs 1G, 2H). Posterior margin evenly rounded but with small median triangular lobe between a_1 and *st*, the lobe granulated distally. Relative lengths of setae: a_1 = 100, a_2 = 82.4, a_3 = 117.6, *st* = 58.8. All setae subcylindrical, blunt, striate; *st* convergent; Distance a_1–a_1 0.64 of length of a_1; distance a_1–a_2 3.3 times as long as a_2–a_3; distance *st*–*st* 1.5 times as long as *st* and 1.4 times as long as distance a_1–a_1. *Sternum* (Figs 1H, 2I). Posterior margin evenly rounded and smooth between b_1. Relative lengths of setae (a_1 =100): b_1 = 235.3, b_2 = 82.4. All setae subcylindrical, blunt, striate. Distance b_1–b_1 0.7 of length of b_1; distance b_1–b_2 1.1 times as long as b_2.

Anal plate subquadrate, with obvious U shape concave lateral margins; distal part with four posteriorly directed clavate appendages, tergal ones thickest, straight, annulate, those protruding from sternal side shorter and thinner, straight, glabrous. Tergal and sternal appendages 0.9 and 0.5 times as long as plate respectively. Plate and sternum glabrous.

Remarks. This new species seems to be a very close relative of *D. bedosae* Scheller from north-western Thailand (Scheller 1995) and *D. cibodasensis* Scheller from Singapore (Scheller 2007). They can be distinguished by the shape of the posterior part of the pygidial sternum (margin evenly rounded in the new species vs. straight in *D. cibodasensis*; with broad indentation in *D. bedosae*) and by the shape of the anal plate (plate short with medium appendages in *D. biconjugarus*; plate short with long appendages in *D. cibodasensis*; plate longer with sort appendages, especially the sternal ones in *D. bedosae*).

Decapauropus tibeticus Qian & Bu, sp. n.

http://zoobank.org/353D5D52-EE05-4DA6-A063-77441C7E6C61
Figs 3, 4

Material examined. Holotype, adult with nine pairs of legs, female (slide no. XZ-PA2015007) (SNHM), China, Tibet, Linzhi City, Bomi county, Songzong town, extracted from soil samples in a broad-leaved forest, Alt. 3000 m, 29°76'N, 95°96'E, 7-XI-2015, coll. Y. Bu & G. Yang. Paratype, adult with 9 pairs of legs, female (slide no. XZ-PA2015009) (SNHM), same data as holotype.

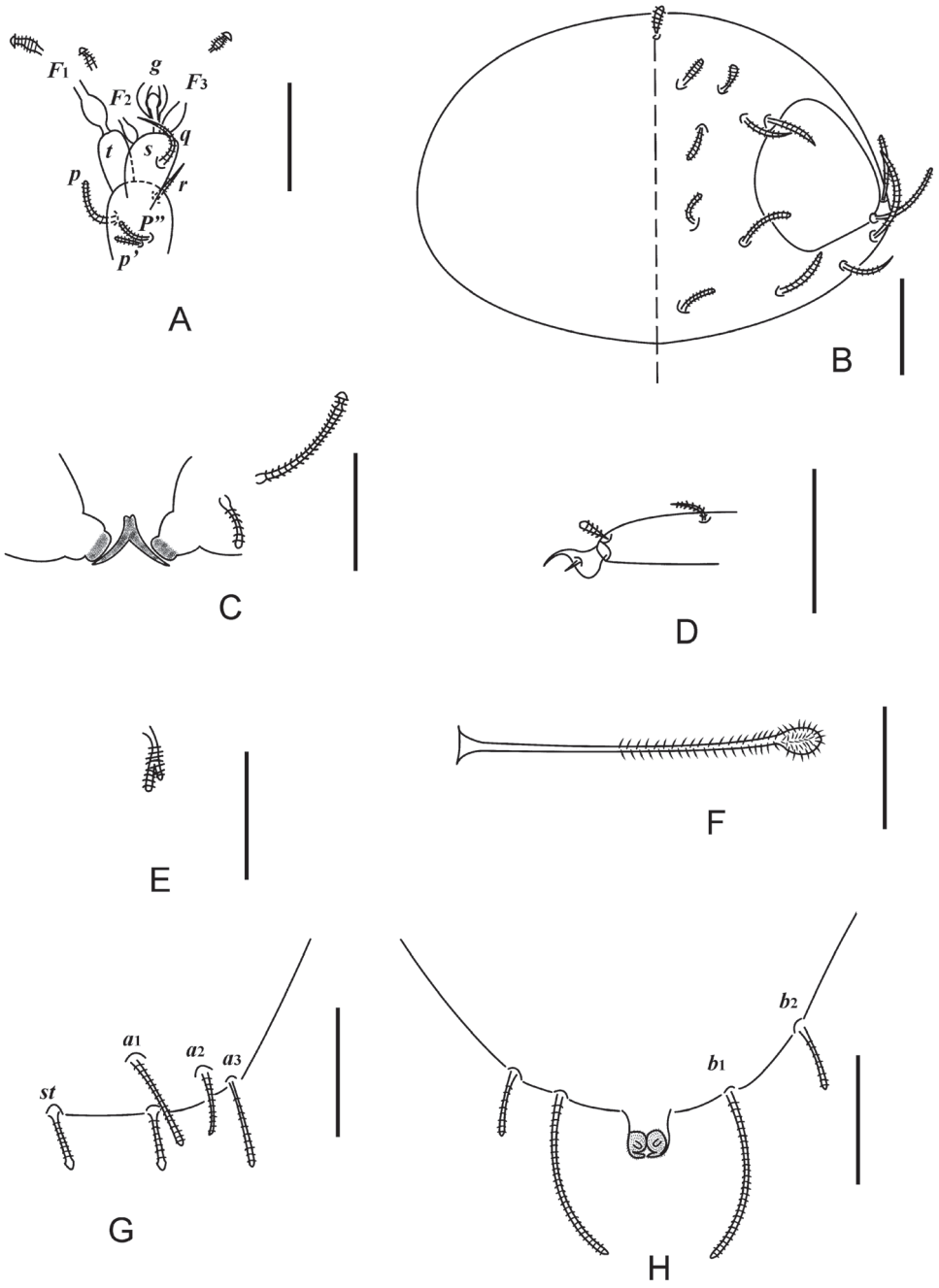

Figure 3. *Decapauropus tibeticus* sp. n. (holotype) **A** Right antenna, sternal view **B** Head, median and right part, dorsal view **C** Collum segment, median and left part, sternal view **D** Tarsus of leg IX **E** Setae on trochanter of leg IX **F** T3 **G** Tergum of pygidum **H** Sternum of pygidum. Scale bars: 20 μm.

Etymology. The species is named after Tibet.

Diagnosis. *Decapauropus tibeticus* sp. n. is distinguished from the other species in the genus by the shape of the anal plate bearing comma shaped appendages with pubescence. This in combination with *st* expanded and annulate distally is a very peculiar character for members of this genus.

Description. Holotype length 0.72 mm (Fig. 4A), paratype length 0.77 mm.

Head (Figs 3B, 4E). Dorsal head setae short, blunt, densely annulate. Relative lengths of setae: 1st row: a_1 = 10, a_2 = 12 (8.6); 2nd row: a_1 = 12 (10), a_2 = 22 (14.3), a_3 = 18 (14.3); 3rd row: a_1 = 16 (10), a_2 = 18 (12.9); 4th row: a_1 = 18 (8.6), a_2 = 24 (17.1), a_3 = 26 (12.9), a_4 = 22.9 (?); lateral group setae l_1 = (20) 22.5, l_2 = (17) 20, l_3 = 14 (?). Ratio $a_1/a_1{-}a_1$ in 1st row 0.6, in 2nd row 0.4, in 3rd row 0.3, in 4th row 0.75. Length of temporal organs 1.2 times as long as shortest interdistance. Head cuticle glabrous.

Antennae (Figs 3A, 4B). Antennal segment 4 with four cylindrical, annulate setae. Relative lengths of setae: p = 100, p' = 46.2 (77.8), p'' = 53.8 (66.7), r = 61.5 (88.9). Tergal seta p 1.3 (0.9 of) times as long as tergal branch t. The latter slender, cylindrical, 1.7 times as long as greatest diameter and 0.8 of sternal branch s which is 2.2 (1.5) times as long as greatest diameter; seta q 0.9 of sternal branch s. Relative lengths of flagella (base segment included) and base segments: F_1 = 100, bs_1 = 7.9 (8), F_2 = 36.5 (33.3), bs_2 = 13 (12), F_3 = 85.7 (73.3), bs_3 = 9.3 (9.1). F_1 6.3 (7.5) times as long as t. F_2 and F_3 1.8 (2.1) and 4.2 (4.6) times as long as s, respectively. Globulus g 1.8 (1.6) times as long as greatest diameter; width of g 0.7 (0.8) of greatest diameter of t.

Trunk. Setae on collum segment subcylindrical, simple, annulate (Figs 3C, 4D). Sublateral setae length 21 μm, 2.1 times as long as submedian setae (10 μm); sternite process thin, pointed anteriorly, with a little incision; appendages with low caps (Fig. 3C). Process and appendages with particles. Seta on tergites annulate, 4+4 on tergite I (Fig. 4F), 6+6 on II–IV (Fig. 4G), 6+4 on V, 4+2 on VI (Fig. 4H).

Bothriotricha. Relative lengths: T_1 = 100, T_2 = 107.7 (107.1), T_3 = 92.3 (92.9), T_4 = 107.7 (107.1), T_5 = 123.1 (121.4). All but T_3 with very thin, simple straight axes and with short oblique pubescence. Axes of T_3 thickened in distal half. Pubescent hairs simple, short, thin, strongest on distal half of T_3 (Figs 3F, 4C)

Legs. Coxa and trochanter of leg IX with furcate setae, lengths 10 and 11 μm respectively, branches subcylindrical, blunt (Fig. 3G). Tarsus of leg IX short, 23 μm (Fig. 3D), somewhat tapering, 2.7 (2.9) times as long as greatest diameter; setae on similar appearance, thin, cylindrical, annulate, length 6–7 μm, approx. 0.2 of length of tarsus.

Pygidum. Tergum (Fig. 3G). Posterior margin of pygidial tergum evenly rounded. Relative lengths of setae: a_1=100, a_2 = 86.7, a_3 = 113.3, st = 66.7. All setae but st blunt, annulate; st subcylindrical, straight, annulate, with a little expanding distally; Distance $a_1{-}a_1$ 0.73 of a_1; distance $a_1{-}a_2$ 2.7 times as long as $a_2{-}a_3$; distance st–st 1.7 times as long as st and st–st 1.3 times as long as distance $a_1{-}a_1$. *Sternum* (Fig. 3H). Posterior margin of sternum evenly rounded. Relative lengths of setae (a_1=100): b_1 = 233.3 (187.5), b_2 = 80 (68.8). All setae cylindrical, annulate. Distance $b_1{-}b_1$ 1.8 times as long as length of b_1; distance $b_1{-}b_2$ 0.16 of length of b_2.

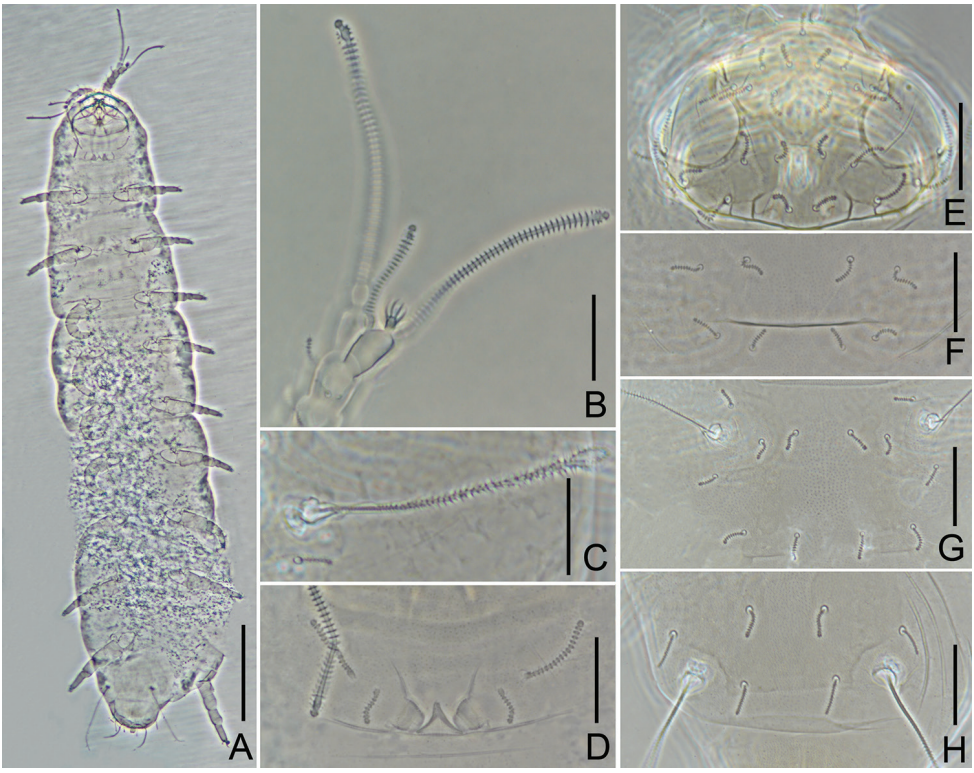

Figure 4. *Decapauropus tibeticus* sp. n. (holotype) **A** Habitus **B** Right antenna, sternal view **C** T_3 **D** Collum segment, sternal view **E** Head, dorsal view **F** Tergite I **G** Tergite II **H** Tergite VI. Scale bars: 100 μm (**A**), 20 μm (**B–H**).

Anal plate subsquare, glabrous, width 0.9 of length, posterior margin with two short, comma shaped, pubescent appendages, appendages with a pair of little stubs that are almost half length of plate.

Remarks. The species differs significantly from the other congeners. The comma shaped appendages of the anal plate with a pair of little stubs are characters unknown in other members of the genus.

Genus *Hemipauropus* Silvestri, 1902, new record to China

Type species. *Hemipauropus leptoproctus* Silvestri, 1902

Diagnosis. Preanal segment much narrower than other body segments, cuticles of tergites with reticulations, particularly on most anterior and posterior parts; pygidial sternum with one pair of seta, b_1.

Distribution. Palaearctic region; Neotropical region; Ethiopian region; Oriental region; Australian region.

Hemipauropus quadrangulus **Qian & Bu, sp. n.**
http://zoobank.org/15D1D101-8426-49BC-A74B-AC15355BA09E
Figs 5, 6

Material examined. Holotype, adult with nine pairs of legs, male (slide no. XZ-PA2015037) (SNHM), China, Tibet, Motuo county, Beibeng town, extracted from the soil samples in a broad-leaved forest, alt. 1500 m, 29°30'N, 95°38'E, 5-XI-2015, coll. Y. Bu & G. Yang.

Etymology. From Latin *quadrangulus* meaning four angles and referring to the shape of the base of the anal plate.

Diagnosis. *Hemipauropus quadrangulus* sp. n. is distinguished from the other species in the genus by the shape of the anal plate, which has a peculiar small Shuriken base and 6+6 setae on tergite IV.

Description. Length. 0.85 mm (Fig. 6A).

Head (Fig. 5B). Tergal setae rather long, leaf-shaped, with short pubescence, lateral setae including *a*3 of 2nd row and *a*4 of 4th row, cylindrical, tapering in distal half, pointed. Relative lengths of setae, 1st row: a_1 = ?, a_2 =10; 2nd row: a_1 = ?, a_2 = ?; a_3 = 15; 3rd row: a_1 = ?, a_2 = 10.7; 4th row: a_1 = 11.4, a_2 = 12.9, a_3 = ?, a_4 = 10; lateral group setae: l_1 = 24.3, l_2 = 25.7, l_3 = 20. Ratio a_1/a_1–a_1 in 1st to 3rd row unknown, in 4th row 0.9. Temporal organs oval in tergal view, length 1.4 of shortest interdistance; pistil absent. Head cuticle with very fine granules, temporal organs glabrous.

Antennae (Figs 5A, 6H). Setae on segments 1–3 folioform. Segment 4 with four setae, *p* and *p'* subcylidrical, *p"* leaf-shaped, *r* very thin, *p'* and *p"* striate; relative lengths of setae: *p* = 10, *p'* = 9.3, *p"* = 3.3, *r* = 4. Tergal branch *t* somewhat fusiform, 3.8 times as long as greatest diameter and 0.95 of the length of sternal branch *s*; that branch 2.9 times as long as greatest diameter; anterodistal corner truncated. Seta *q* 1.3 times as long as seta *p'* of segment 4, 0.95 of the length of *s.* Relative lengths of flagella (base segments included) and base segments: F_1 = 100, bs_1 = 17.3; F_2 = 46.7, bs_2 = 14.7; F_3 = 101.3, bs_3 = 14.7. F_1 3.3 times as long as *t,* F_2 and F_3 1.2 and 2.5 times as long as *s* respectively. Distal organ of F_1 and F_2 consisting of densely arranged pubescent bracts around sessile capsule, F_3 with flat calyx; flagella axes below distal organs not widened in F_1 and F_2, slightly in F_3. Globulus *g* pyriform, 0.2 of the length of *s*, diameter 0.8 of greatest diameter of *t*; 8–10 bracts; capsule subspherical. Antennae almost glabrous.

Trunk. Setae of collum segment broad, phylliform, pubescent, secondary branch rudimentary and inserted just below the middle; sublateral setae length 20 μm, 1.3 times as long as submedian setae; sternite process broad, pointed anteriorly; appendages two-parted with low caps. Process with pubescence and appendages glabrous (Figs 5C, 6B). Tergites indistinctly divided transversally, II–IV with reticular pattern on both sides of the dividing line, only posterior of that line on VI (Fig. 6C–G). Setae cylindrical, 4+4 setae on tergite I (Fig. 6C), 6+6 on II–V (Figs 6 D–G), 4 only on VI (Fig. 6G). Submedian posterior setae on VI 0.2 of inter-distance and 0.4 (–0.5) of the length of pygidial setae a_1. Tergites glabrous.

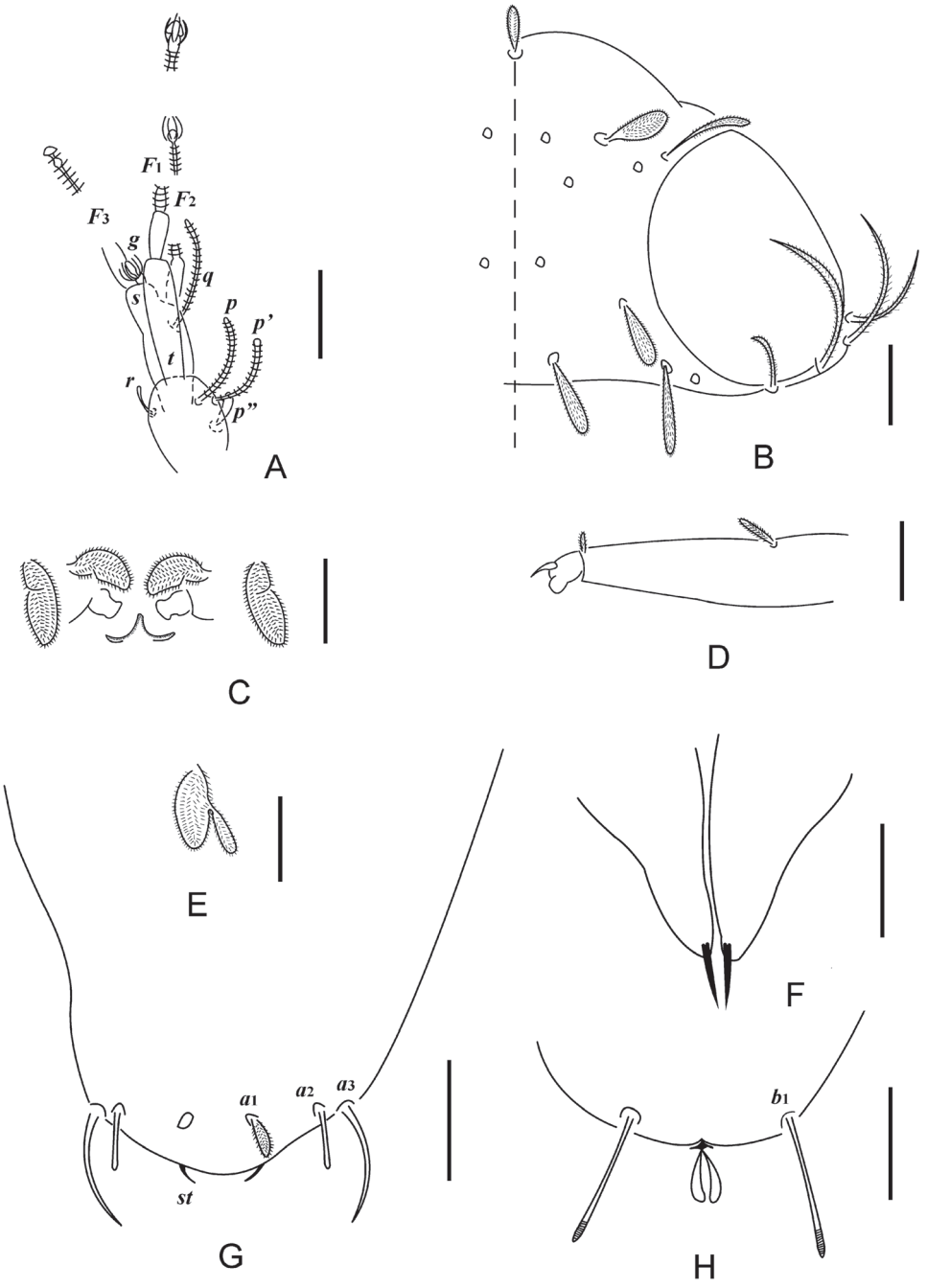

Figure 5. *Hemipauropus quadrangulus* sp. n. (Holotype) **A** Left antenna, tergal view **B** Head, median and right part, dorsal view **C** Collum segment, sternal view **D** Tarsus of leg IX **E** Setae on trochanter of leg IX **F** Genital papillae **G** Tergum of pygidum **H** Sternum of pygidum. Scale bars: 20 μm.

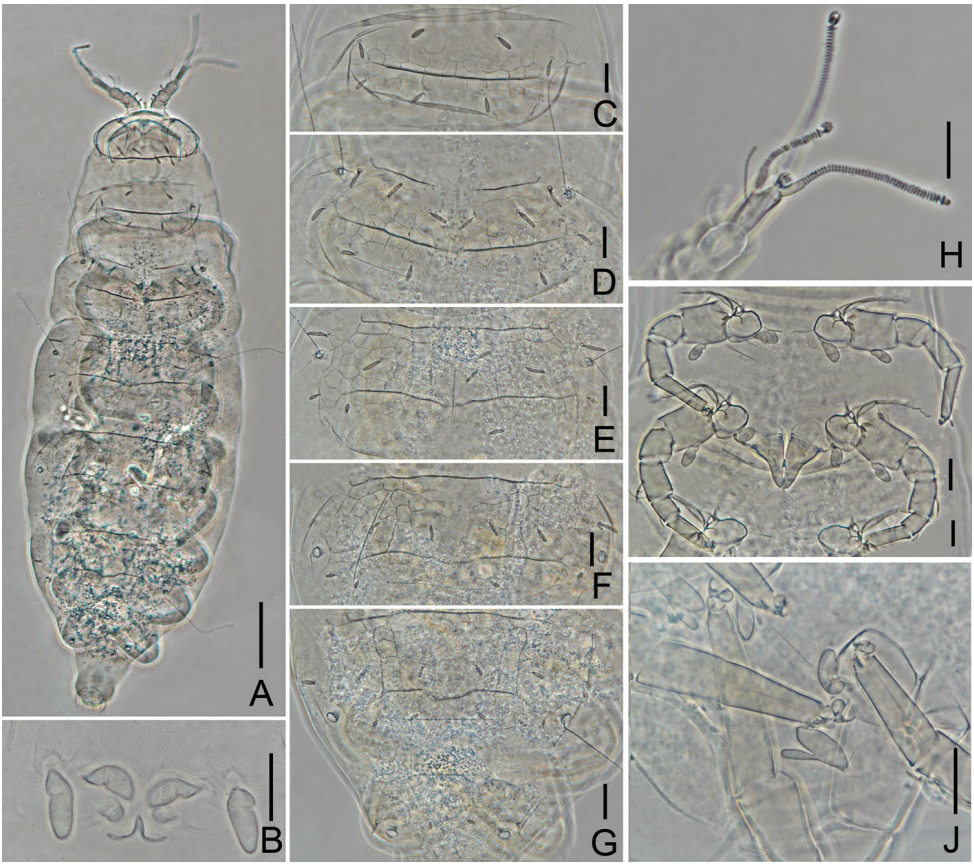

Figure 6. *Hemipauropus quadrangulus* sp. n. (Holotype) **A** Habitus **B** Collum segment, sternal view **C** Tergite I **D** Tergite II **E** Tergite III **F** Tergite IV **G** Tergite V–VI **H** Right antenna, sternal view **I** Legs I–II and genital papillae **J** Leg IX. Scale bars: 100 μm (**A**), 20 μm (**N–J**).

Bothriotricha. Relative lengths: T_1 = 100, T_2 = 104.8, T_3 = ?, T_4=104.8, T_5 = ?. Axes thin, simple, straight, pubescence hairs exceedingly short.

Genital papillae (Figs 5F, 6I). Longish, conical with narrowing and extended distal half, 1.6 times as long as wide, seta short, 0.3 of the length of papilla. Coxal seta of leg II as on leg I, length 10 μm (Fig. 6I).

Legs. Fairly long. Setae on coxa and trochanter of leg IX furcate, main branch leaf-shaped, secondary branch subcylindrical, blunt, 0.5 of the length of seta (Figs 5E, 6J). Tarsus of leg IX long, broad, 60 μm in length, 4.3 times as long as greatest diameter; proximal seta short, blunt, length 10 μm, with pubescence, distal seta shorter and blunt, length 9 μm, with pubescence. Proximal seta 0.2 of the length of tarsus, 2.5 times as long as distal seta. Cuticle of tarsus almost glabrous (Fig. 5D).

Pygidium. Tergum (Fig. 5G). Cuticle glabrous. Posterior margin smooth and round between *st*. Setae of very different lengths, a_1 leaf shaped, pubescent, a_2 subcylindrical, almost straight, a_3 thin, tapering, pointed, a_2 and a_3 glabrous. *st* very short, pointed,

converging; relative lengths of setae: a_1 = 10, a_2 = 13.8, a_3 = 31.3, *st* = 6.3. Distance a_1–a_1 1.6 times as long as a_1; distance *st*–*st* 3.0 times as long as *st* and 1.2 times as long as distance a_1–a_1. *Sternum* (Fig. 5H). Posterior margin with a little indention; b_1 blunt, striate distally. Relative lengths (pygidial a_1 = 10), b_1 = 27.8, 0.8 of their inter-distance.

Anal plate simple and glabrous, with a little base, the base like a Shuriken; posterior median forked part 5.8 times as long as broadest basal part.

Remarks. This species resembles *H. macropus* Scheller, 2009 from the Philippines and *H. clava* Scheller, 2013 from Australia. They can be readily distinguished by the shape of the anal plate (with little Shuriken base in *H. quadrangulus* sp. n. vs. broad base and two lateral spines in both *H. macropus* and *H. clava*) and by the numbers of the setae on tergite IV (6+6 setae in *H. quadrangulus* sp. n. and *H. clava* vs. 6+4 setae in *H. macropus*).

Discussion

Pauropoda is a group of tiny soil myriapods, usually less than 2 mm, with unique branched antennae, having 11 (or 12) body segments and 9 (or 10 or 11) pairs of legs (Scheller 2011b). All species lack eyes and most of them also lack a tracheal system. More than 900 species grouped in 12 families have been found in the world (Qian et al. 2015). However, pauropods are still poorly known in China. Up to now, only 42 species belonging to 12 genera and 4 families have been recorded in China, as most of them were found in southeast and east China (Qian et al. 2015). This study increased our knowledge of pauropod diversity in Tibet.

As one of the most ecologically diverse landscapes on earth, the Tibetan Plateau is home to numerous rare and endangered species, and has attracted so many taxonomists to explore the biodiversity, although it is a remote area at a high altitude. However, there is only one report on the pauropods in Tibet (Zhang and Chen 1988) before our study, probably due to their small size, cryptic behavior, and the difficulties in identification.

Two of three new species reported in this study were collected from Motuo County (northern latitude 27°33' to 29°55', east longitude 93°45' to 96°05'), in the Linzhi area of southeastern Tibet. Standing 1,000 meters above the sea level on average, Motuo is surrounded by snow-capped mountains. Meanwhile, located in the lower reaches of the Yarlung Zangbo River, Motuo has a typical sub-tropical climate, warm and rainy all year round. The diversity of plants and animals in Motuo is rich in tropical species, with many endemic species (Wu et al. 2005, Zhang 2011). In this study, a similar situation in soil-dwelling pauropods was found, especially for the genus *Hemipauropus*, which is recorded for the first time in China. This genus has been found in all main zoogeographical regions, but rarely in temperate areas (Scheller 2011b). The morphology of the *Hemipauropus* species are very close to some genera of the Pauropoda distributed in the tropics.

Since our collecting sites in Tibet are still very sparse, we have not found the species of *Sphaeropauropus* sp. reported by Zhang and Chen (1988) and further investigations should be made in the future so as to reveal the diversity of Pauropoda in this area.

Acknowledgements

We give our cordial gratitude to Dr. Gang Yang for his generous help during the field work and two reviewers for their valuable comments during the review of this manuscript. This research was supported by the National Natural Science Foundation of China (nos: 31471958, 31772510, 31772509, 31401971) and the Natural Science Foundation of Shanghai (no: 17ZR1418700).

References

Qian CY, Dong Y, Bernard EC, Sun HY (2015) Records of Pauropoda (Pauropodidae, Brachypauropodidae, Eurypauropodidae, Sphaeropauropodidae) from China, with a key to the species and descriptions of three new species of *Decapauropus*. Zootaxa 4006(3): 521–539. http://dx.doi.org/10.11646/zootaxa.4006.3.6

Scheller U (1995) Pauropoda (Pauropodidae, Eurypauropodidae) from north-western Thailand. Tropical Zoology 8: 7–41. https://doi.org/10.1080/03946975.1995.10539270

Scheller U (2007) Records of Pauropoda (Pauropodidae; Brachypauropodidae; Eurypauropodidae) from Singapore, Indonesia and Malasia with the description of 18 new species (Pauropoda and Symphyla of the Geneva Museum XV). Revue Suisse de Zoologie 114(3): 521–572. https://doi.org/10.5962/bhl.part.80403

Scheller U (2009) Records of Pauropoda (Pauropodidae, Brachypauropodidae, Eurypauropodidae) from Indonesia and the Philippines with descriptions of a new genus and 26 new species. International Journal of Myriapodology 2: 69–148. https://doi.org/10.1163/187525409X12577705044548

Scheller U (2011a) New records of Pauropoda (Myriapoda) from north-western Thailand. International Journal of Myriapodology 4: 51–77. https://doi.org/10.3897/ijm.4.1103

Scheller U (2011b) Pauropoda. In: Minelli A (Ed.) Treatise on Zoology-Anatomy, Taxonomy, Biology: The Myriapoda, Vol. 1. Brill, Leiden, 467–508. https://doi.org/10.1163/9789004188266_022

Scheller U (2013) Pauropoda (Myriapoda) in Australia, with descriptions of new species from Western Australia. Records of the western Australian Museum 82(supplement): 1–133. https://doi.org/10.18195/issn.0313-122x.82.2013.001-133

Wu ZY, Sun H, Zhou ZK, Peng H, Li DZ (2005) Origin and differentiation of endemism in the flora of China. Acta Botanica Yunnanica 27(6): 577–604. [In Chinese with English summary]

Zhang CZ, Chen ZP (1988) a preliminary study on a new record of the class Pauropoda (Myriapoda) from China. Sinozoologia 6: 39–54. [In Chinese with English summary]

Zhang RZ (2011) Zoogeography of China. Science Press, Beijing, 330 pp. [In Chinese]

ZooKeys 754: 47–62 (2018)
doi: 10.3897/zookeys.754.22884
http://zookeys.pensoft.net

RESEARCH ARTICLE

A peer-reviewed open-access journal
ZooKeys
Launched to accelerate biodiversity research

A taxonomic revision helps to clarify differences between the Atlantic invasive *Ptilohyale littoralis* and the Mediterranean endemic *Parhyale plumicornis* (Crustacea, Amphipoda)

Sabrina Lo Brutto[1], Davide Iaciofano[1]

1 *Department STeBiCeF, Section of Animal Biology, via Archirafi 18, University of Palermo, Palermo, Italy*

Corresponding author: *Sabrina Lo Brutto* (sabrina.lobrutto@unipa.it)

Academic editor: *C.O. Coleman* | Received 9 December 2017 | Accepted 7 March 2018 | Published 30 April 2018

http://zoobank.org/A687380F-D4DB-407A-B9DE-8F205EF78DB6

Citation: Lo Brutto S, Iaciofano D (2018) A taxonomic revision helps to clarify differences between the Atlantic invasive *Ptilohyale littoralis* and the Mediterranean endemic *Parhyale plumicornis* (Crustacea, Amphipoda). ZooKeys 754: 47–62. https://doi.org/10.3897/zookeys.754.22884

Abstract

Ptilohyale explorator (formerly *Parhyale explorator*), described by Arresti (1989), can be considered to be a synonym of west-Atlantic *Ptilohyale littoralis* (Stimpson, 1853), based on morphological observations of paratypes and specimens recently collected in the type locality of *Ptilohyale explorator*. The first collections of *Ptilohyale littoralis*, from the eastern Atlantic were from the port of Rotterdam (The Netherlands) in 2009 and later in Wimereux, Opal Coast (France) in 2014; however, the synonymy of *Ptilohyale explorator* with *Ptilohyale littoralis* backdates to the first European record of *Ptilohyale littoralis* in 1985 at La Vigne, Bay of Arcachon (France). This indicates that *Ptilohyale littoralis* has been established along European Atlantic coast for many years.

An assessment of the nominal valid species belonging to the genus *Ptilohyale* was carried out and a comparison between the Atlantic *Ptilohyale littoralis* and the very similar Mediterranean hyalid species, *Parhyale plumicornis*, is presented based on morphological features and distribution. Due to the invasive ability of *Ptilohyale littoralis*, a comparison between the two species is necessary.

Keywords

Atlantic, Hyalidae, *Invasive species*, Mediterranean Sea, *Parhyale plumicornis*, *Ptilohyale littoralis*

Introduction

Ptilohyale explorator (formerly *Parhyale explorator*) was described by Arresti (1989) from La Vigne, Bay of Arcachon, France. He collected eleven male and three female specimens in the intertidal zone, on the sand of a semi-enclosed beach under stones, in July 22, 1985; following Barnard's (Barnard 1979: 120) "Key to the Species of Parhyale and Parallorchestes", he established that the specimens sampled showed a feature that was not included in the key, i.e., the presence of long tufts of plumose setae in antenna II starting at the 5th peduncular segment. However, as Barnard's taxonomic key (Barnard 1979) had omitted some hyalid species already described at that time, Arresti did not take into consideration some preceding descriptions (listed in Table 1) that could fit with his collected specimens.

As a consequence, Arresti described a new hyalid species under the name *Parhyale explorator*, and deposited eight males and two females in the laboratory of the University of the Basque Country (Spain; holotype; allotype; six males and one female paratypes), one male paratype in the Carcinology Laboratory of Natural History Museum of Paris (France), and one male and one female paratypes in the Laboratory of Dr. S. Ruffo in the Museum of Natural History of Verona (Italy).

In 2008, *Ptilohyale explorator* (Arresti 1989) was reported as a new alien species within the Mediterranean Sea (Bakir et al. 2008), but later acknowledged to be a misidentification (Bakir et al. 2013), who re-identified the samples as *Parhyale plumicornis* (Heller, 1886), an endemic Mediterranean species (Iaciofano and Lo Brutto 2017). Regrettably, the case of this erroneous identification caused a cascade-effect on successive papers and documents that reported a further non-indigenous species (NIS) within Mediterranean (Bakir et al. 2010, Christodoulou et al. 2013, Faasse 2014, Zenetos 2010, Zenetos et al. 2010), although this was not the case.

Ptilohyale explorator is currently considered a valid species even if some authors have already highlighted the need of further investigations, in light of its high similarity with *Ptilohyale littoralis* (Faasse 2014, Spilmont et al. 2016, Marchini and Cardeccia 2017).

To clarify the position of *Ptilohyale explorator*, here considered *species inquirenda*, the paratypes deposited at the Natural History Museum of Verona and at the Natural History Museum of Paris were examined, together with some topotypic specimens collected in the type locality of the species, Bay of Arcachon, France. Descriptions and illustrations of current species belonging to the genus *Ptilohyale* were also consulted, and it was observed that some of them were not ascribable to this genus.

Materials and methods

The paratypes of *Parhyale explorator* (voucher number 330/P) deposited in Sandro Ruffo's collection of the Museum of Natural History of Verona, Verona (Italy) and the *Ptilohyale explorator* paratype (voucher number MNHN-Am3957) deposited at

Table 1. List of *Parhyale* and *Ptilohyale* species excluded by Barnard's taxonomy key (Barnard 1979: 120) and by Arresti (1989), here named according to Lowry (2010) and Lowry et al. (2010).

Ptilohyale littoralis (Stimpson, 1853) – formerly *Allorchestes littoralis*
Ptilohyale plumulosus (Stimpson, 1857) – formerly *Allorchestes plumulosus*
Ptilohyale crassicornis (Haswell, 1879) – formerly *Allorchestes crassicornis*
Parhyale inyacka KH Barnard, 1916
Ptilohyale barnardi (Chevreux, 1926) nomen dubium – formerly *Hyale barnardi*
Ptilohyale ptilocerus (Derzhavin, 1937) – formerly *Allorchestes ptilocerus*
Ptilohyale tristanensis (Macnae, 1953) nomen dubium – formerly *Allorchestes tristanensis*
Ptilohyale iole (JL Barnard, 1970) – formerly *Hyale iole*
Ptilohyale barbicornis (Hiwatari & Kajihara, 1981) – formerly *Hyale barbicornis*

the crustaceans collection of the Natural History Museum of Paris (MNHN), Paris (France) were examined under a stereo-microscope, and photos were produced.

Additionally, a total of 126 specimens of *Ptilohyale* sp. (84 females and 42 males) was collected in the intertidal zone associated with mussel beds (*Mytilus edulis*), from Bay of Arcachon, France (the type locality of *Ptilohyale explorator*), 43°34'N, 1°14'W (DDM), in October 2015, and fixed in 95% ethanol. Their body lengths, from tip of rostrum to apex of telson, were measured using ImageJ software after placement on graph-paper and photography (FINEPIX S1800, FUJIFILM); pencil drawings were scanned and 'inked' using the software Adobe Illustrator CS5. The specimens were identified as *Ptilohyale littoralis* and deposited at the Museum of Zoology of the University of Palermo (MZPA), Palermo (Italy), Voucher Number MZPA-AMPH-0024.

Descriptions of the 12 world species of the genus *Ptilohyale*, according to the World Amphipoda Database (Horton et al. 2017), were consulted and the diagnostic characters delimiting *Ptilohyale* Bousfield & Hendrycks, 2002 were verified: (1) heavily plumose (finely brush-setose) antenna II starting at the 5th peduncular article (both sexes); (2) lack of a guiding robust seta on the medial face of the propodus of gnathopod I (male); (3) variously developed carpal lobe of gnathopod II (male); (4) distomedial robust seta on the peduncle of uropod I; (5) inner ramus of uropod III more or less fused to the peduncle. The subsequent generic status for each of these species was then revised.

Results

The paratypes of *Ptilohyale explorator* preserved in the Museum of Natural History of Verona were entire and in good condition for observations (Fig. 1), while the paratype stored in the Carcinology Laboratory of Natural History Museum of Paris had deteriorated and some body parts were lost (i.e., heads).

Comparison with the description of *Ptilohyale explorator* (Arresti 1989: 103–111) and the paratypes stored at the museums of Verona and Paris showed some incongru-

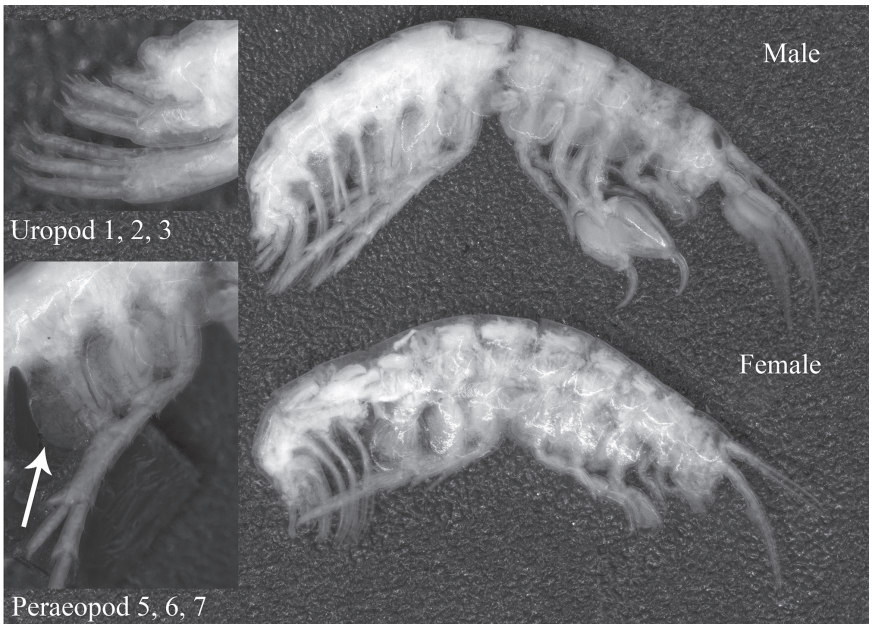

Figure 1. Male and female paratypes of *Parhyale explorator* (subsequently synonymised *Ptilohyale explorator*) from Ruffo's collection (Museum of Natural History of Verona, Italy), entire samples; male peraeopods and uropods, with focus (arrow) on basipodite of peraeopod VII.

Table 2. Diagnostic character states observed in the *Ptilohyale explorator* (*species inquirenda*) paratypes stored at the Museum of Natural History of Verona (Italy) and the Natural History Museum of Paris (France), and in the *Ptilohyale littoralis* sampled in the Bay of Arcachon (France); compared with Arresti's description of *Ptilohyale explorator* and Bousfield and Hendricks's *Ptilohyale littoralis* description. The table shows the incongruences (*) between the description of *Ptilohyale explorator* by Arresti and the deposited paratypes.

Characters	Samples of *Ptilohyale littoralis* (this paper)	Bousfield and Hendricks's description of *Ptilohyale littoralis*	Paratypes of *Ptilohyale explorator* (deposited by Arresti at Museum of Verona)	Paratype of *Ptilohyale explorator* (deposited by Arresti at Museum of Paris)	Arresti's description of *Ptilohyale explorator*
Antenna II, flagellar articles ventrally setose *	4–9	NA	8	NA	10–11
Coxal plate I	subquadrate	subquadrate	subquadrate	NA	subquadrate
Gnathopod I, basis distinct anterodistal lobe	absent	absent	absent	NA	absent
Peraeopod VII basis*	without strong depression on posterior margin	without strong depression on posterior margin	without strong depression on posterior margin	without strong depression on posterior margin	with strong depression on posterior margin
Uropod I rami spines*	3–4 outer; 1–2 inner	2–3 outer	3 outer; 2 inner	NA	6 outer; 2 inner
Uropod II rami	subequal	subequal	subequal	subequal	subequal
Uropod III apical spines*	5–9	5–6	5–6	NA	8–10

NA, not available

ences (Table 2). The most significant difference was the absence of a strong depression on the basipodite of peraeopod VII in all paratypes, conversely to what was indicated in the description. Other diagnostic characters described by Arresti (1989) were also unlike the paratypes, including the number of plumose articles on antenna II, and the arrangement of setae on uropods I and III (see Table 2 for details).

Following the detailed description updated by Faasse (2014) and the recent Hyalidae taxonomic key presented by Bousfield and Hendrycks (2002), the paratypes of Ruffo's collection and all 126 specimens sampled at the Bay of Arcachon (France), were identified as specimens of *Ptilohyale littoralis*. *Ptilohyale explorator* (formerly *Parhyale*) (Arresti, 1989) can be considered synonym of *Ptilohyale littoralis* (Stimpson, 1853).

Systematics

Suborder SENTICAUDATA Lowry & Myers, 2013
Infraorder TALITRIDA Rafinesque, 1815
Superfamily TALITROIDEA Rafinesque, 1815
Family HYALIDAE Bulycheva, 1957
Subfamily HYALINAE Bulycheva, 1957
Genus *Ptilohyale* Bousfield & Hendrycks, 2002

***Ptilohyale littoralis* (Stimpson, 1853)**
Figures 2–3

Allorchestes littoralis Stimpson, 1853: 49, t 3, fig. 36; Smith 1873: 556; Stebbing 1906: 595; Miner 1950: 462, pl. 148.
Hyale littoralis (Stimpson, 1853) Holmes 1905: 472, pl. 3, fig. 2; Barnard and Karaman 1991: 369.
Hyale prevosti (part) Della Valle, 1893: 519.
Hyale plumulosa (Stimpson, 1853) Bousfield 1973: 155, pl. XLIV.2; Pollock 1998: 241, fig. 15.120.
Plumulohyale plumulosa (Stimpson, 1853) Bousfield 2001: 104.
Ptilohyale littoralis (Stimpson, 1853) Bousfield and Hendrycks 2002: 103; Faasse 2014: 1.
Parhyale explorator Arresti, 1989: 101–115.
Ptilohyale explorator (Arresti, 1989) Bousfield and Hendrycks 2002: 98–99.

Type. Neotype deposited in Canadian Museum of Nature Collection; voucher number CMNC 2002-0071 (Bousfield and Hendrycks 2002).

Type locality. Grand Manan Island (Canada), northern eastern Atlantic coast.

Material examined. One hundred and twenty-six specimens were collected at the Bay of Arcachon France (43°34'N, 1°14'W), 13October 2015; intertidally, 0 m, on the heavy substrate of the semi-closed beach (MZPA-AMPH-0024).

Figure 2. Male of *Ptilohyale littoralis*, sampled in October 2015, from Bay of Arcachon, France. Scale bar 1 mm.

Description. ***Male.*** 11.4 mm length specimen. Antenna II ventral margins of the 5th peduncular article and first 4–9 flagellar articles (other one or two articles with sparse plumose setae) densely covered with plumose setae (brush setae). Palp of maxilla I with median constriction. Coxal plate I sub-quadrate with distinctive cups; Gnathopod I, basis lacking distinct anterodistal lobe (hydrodynamic lobe). Gnathopod II, carpus lobe present in juvenile male and absent on adult male. Coxal plate V posterior lobe smaller than anterior lobe; Peraeopod V, basis rounded. Peraeopod VII slender, basis rounded. Uropod I, peduncle with one distomedial robust seta; rami subequal with 3–4 robust setae on outer ramous and 1–2 robust setae on inner ramus. Uropod II, rami sub-equal in length. Uropod III, outer ramus with 5–9 apical robust setae. Telson acute. ***Female.*** Description based on a 10.6 mm length specimen. Gnathopod I, basis with anterodistal lobe.

Distribution. Northern, western, and eastern Atlantic coasts; north eastern Pacific coast.

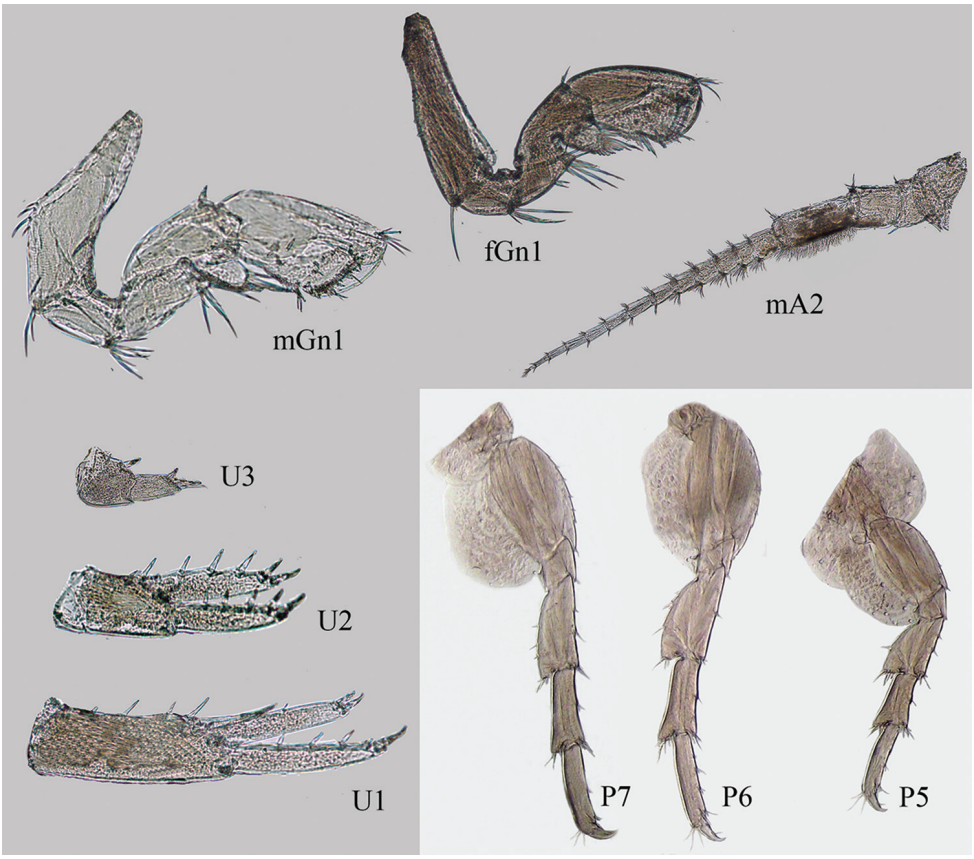

Figure 3. *Ptilohyale littoralis*, antenna II male (mA2), gnathopod I male (mGn1), gnathopod I female (fGn1), peraeopods V (P5), VI (P6) and VII (P7), uropods I (U1), II (U2) and III (U3).

Remarks. The genus *Ptilohyale* includes 12 species: *P. barbicornis* (Hiwatari & Kajihara, 1981); *P. barnardi* (Chevreux, 1925); *P. bisaeta* (Kim & Kim, 1991); *P. brevicrus* Eun et al., 2014; *P. crassicornis* (Haswell, 1879); *P. eburnea* (Krapp-Schickel, 1974); *P. explorator* (Arresti, 1989); *P. iole* (Barnard, 1970); *P. littoralis* (Stimpson, 1853); *P. plumulosus* (Stimpson, 1857); *P. ptilocerus* (Derzhavin, 1937); *P. tristanensis* (Macnae, 1953) (Bousfield and Hendrycks 2002, Eun et al. 2014, Lowry 2010). Of these, the descriptions of three of the species showed characters not ascribable to *Ptilohyale sensu* Bousfield & Hendrycks (2002). *Ptilohyale barnardi* (formerly *Hyale barnardi*) has brush-setae in antenna II that start at the 4th peduncular article (see Chevreux 1925, Fig. 4A); *P. tristanensis* (formerly *Allorchestes tristanensis*) (see Macnae 1953, Fig. 4B) and *P. eburnea* (see Krapp-Schickel 1974, Fig. 4C), do not have brush-setae in antenna II. The absence of some diagnostic character states makes us consider *Ptilohyale barnardi*, *P. tristanensis*, and *P. eburnea* as *nomina dubia*, and we encourage further investigations.

Discussion

Ptilohyale (formerly *Parhyale*) *explorator* was described by Arresti (1989) using the dichotomous key to "*Parhyale* and *Parallorchestes*" of Barnard (1979: 120); he observed that the specimens collected were not ascribable to any of the species listed therein, due to the presence of *dense elongate tufts of plumose setae ventrally on the peduncular article 5 of the antenna II* and *peduncle of uropod I with distomedial robust seta*. These characters (and others listed in Table 3) prompted Arresti to describe a new species, and to revise Barnard's key; however, both authors had excluded some hyalid species that could be identified with Arresti's specimens (Table 1).

The following character states are considered diagnostic of *Ptilohyale explorator*: the arrangement of setae on the uropods and the presence of a strong depression on the posterior margin of the basis of peraeopod VII (Table 2). Here, it has been verified that these characters described in Arresti (1989) did not match with the paratypes (Fig. 5). The setae arrangement on uropod III and the posterior margin of basis of peraeopod VII of the paratypes, on the contrary, matched with specimens recently sampled from the *explorator* type locality and were identified as *Ptilohyale littoralis*. In fact, following the dichotomous key to Hyalidae of Bousfield and Hendrycks (2002), the detailed description of Faasse (2014), the paratypes in Ruffo's collection, and the present specimens collected in Bay of Arcachon can all be identified as *Ptilohyale littoralis* (Stimpson, 1853). For these reasons, *Ptilohyale explorator* (Arresti, 1989) is proposed as a synonym of *Ptilohyale littoralis* (Stimpson, 1853), which, on base of the Principle of Priority, article 23 of the ICZN Code (Ride Chairman et al. 1999), becomes the valid name of this taxon.

Bousfield (1973) synonymised *Ptilohyale littoralis* with *Ptilohyale plumulosus*, a species distributed along the Pacific coast of North America. This synonymy was subsequently rejected (Bousfield and Hendrycks 2002), thus limiting the distribution of *Ptilohyale littoralis* to the western Atlantic coast of North America (Bousfield and Hendrycks 2002).

Recently, *Ptilohyale littoralis* was declared as a recent alien species spreading along the eastern Atlantic coast since 2009 (Faasse 2014, Spilmont et al. 2016, Marchini and Cardeccia 2017), but this study has shown that the species inhabited the Atlanto-European coast at least since 1985.

Moreover, *Ptilohyale littoralis* was recently recorded along the eastern Pacific coast of North America (Campbell River, Vancouver, Choi et al. 2016; and Puget Sound, Washington State, Heerhartz et al. 2016), suggesting an extension of the species' range.

The genus *Ptilohyale* has been diagnosed with plumose setae on ventral margins of antenna II that start at the 5th peduncular segment and distomedial robust seta on peduncle of uropod I. Behaviourally, it is described as saltatory and occurring in brackish and estuarine waters (Bousfield and Hendrycks 2002).

Ptilohyale is distributed along both the Atlantic and Pacific coasts (Bousfield and Hendrycks 2002, Eun et al. 2014, Faasse 2014, Haswell 1879, Heerhartz et al. 2016, Hiwatari and Kajihara 1981, Hutchings et al. 2013, Kim and Kim 1987,

Table 3. Characters used by Arresti (1989) for diagnosing *Parhyale explorator* (subsequently synonymised *Ptilohyale explorator*) from the other species of the genus *Parhyale*.

Parhyale explorator	*Parhyale eburnea* Krapp-Schickel, 1974
Uropod I with robust seta on peduncle; Rami of uropods I and II with strong dorsal setae.	Uropod I without robust seta on peduncle; Rami of uropods I and II without strong dorsal setae.
Parhyale explorator	*Parhyale plumicornis* (Heller, 1866)
Uropod III with only apical setae; Inner ramous of uropod III poorly defined and fused to the peduncle; Carpus of gnathopod II male with stout process.	Uropod III with apical and dorsal setae; Inner ramous of uropod III well defined and not fused to the peduncle; Carpus of gnathopod II male with evident process.
Parhyale explorator	*Parhyale aquilina* (Costa, 1857)
Uropod I with robust seta on peduncle.	Uropod I without robust seta on peduncle;
Parhyale explorator	*Parhyale* ? *zibellina* (Derzhavin, 1937)
Uropod III with only apical setae; Inner ramous of uropod III poorly defined and fused to the peduncle; Uropod I with robust seta on peduncle.	Uropod III with apical and dorsal setae; Inner ramous of uropod III well defined and not fused to the peduncle; Uropod I without robust seta on peduncle.
Parhyale explorator	*Parhyale* ? *iwasai* (Shoemaker, 1956)
Uropod III with only apical setae; Propodus of peraeopod VII without setae on posterior margin.	Uropod III with apical and dorsal setae; Propodus of peraeopod VII with setae on posterior margin.
Parhyale explorator	*Parhyale hawaiiensis* (Dana, 1853)
Inner ramous of uropod III poorly defined and fused to the peduncle; Propodus of peraeopod VII without setae on posterior margin.	Inner ramous of uropod III well defined and not fused to the peduncle; Propodus of peraeopod VII with setae on posterior margin.
Parhyale explorator	*Parhyale penicillata* Shoemaker, 1956
Inner ramous of uropod III poorly defined and fused to the peduncle; Rami of uropods I and II with strong dorsal setae.	Inner ramous of uropod III well defined and not fused to the peduncle; Rami of uropods I and II without strong dorsal setae.
Parhyale explorator	*Parhyale fascigera* Stebbing, 1897
Inner ramous of uropod III poorly defined and fused to the peduncle; Rami of uropods I and II with strong dorsal setae.	Inner ramous of uropod III well defined and not fused to the peduncle; Rami of uropods I and II without strong dorsal setae.
Parhyale explorator	*Parhyale* of Bulycheva
Inner ramous of uropod III poorly defined and fused to the peduncle; Basipodite of peraeopod VII with rounded posteroventral lobe.	Inner ramous of uropod III well defined and not fused to the peduncle; Basipodite of peraeopod VII without rounded posteroventral lobe.
Parhyale explorator	*Parhyale basrensis* Salman, 1986
Inner ramous of uropod III poorly defined and fused to the peduncle; Uropod I with robust seta on peduncle; Propodus of peraeopod VII without setae on posterior margin.	Inner ramous of uropod III well defined and not fused to the peduncle; Uropod I without robust seta on peduncle; Propodus of peraeopod VII with setae on posterior margin.
Parhyale explorator	*Parhyale multispinosa* Stock, 1987
Inner ramous of uropod III poorly defined and fused to the peduncle; Propodus of peraeopod VII without setae on posterior margin.	Inner ramous of uropod III well defined and not fused to the peduncle; Propodus of peraeopod VII with setae on posterior margin.

1991, Macnae 1953, McDermott 1998, Peart 2004, Spilmont et al. 2016, Tsoi and Chu 2005, Tunnell and Withers 2009, Turbeville and Caplins 2010). The genus still includes 12 species in some documents (e.g., Bousfield and Hendrycks 2002, Eun et al. 2014, Horton et al. 2017, Lowry 2010) instead of the eight nominal valid species (Table 4).

Table 4. List of *Ptilohyale* species exhibiting diagnostic generic characters, and their distribution.

Ptilohyale species	Distribution	Reference
Ptilohyale barbicornis (Hiwatari and Kajihara, 1981)	Japan Sea, Korea and Japan	Hiwatari and Kajihara 1981, Eun et al. 2014
Ptilohyale bisaeta (Kim and Kim, 1991)	Japan Sea, Korea	Kim and Kim 1991
Ptilohyale brevicrus Eun et al., 2014	Japan Sea, Korea	Eun et al. 2014
Ptilohyale crassicornis (Haswell, 1879)*	Tasman Sea, Australia; Yellows and Japan Seas, China and Korea	Haswell 1879, Hiwatari and Kajihara 1981, Kim and Kim 1987, Peart 2004, Tsoi and Chu 2005, Hutchings et al. 2013
Ptilohyale iole (JL Barnard, 1970)	Pacific Ocean, Hawaii	Hiwatari and Kajihara 1981
Ptilohyale littoralis (Stimpson, 1853)	Atlantic Ocean, France, Netherlands, United States and Canada; Pacific Ocean, Canada	Bousfield and Hendrycks (2002), Choi et al. 2016, Faasse 2014, Spilmont et al. 2016, Heerhartz et al. 2016; this paper;
Ptilohyale plumulosus (Stimpson 1857)**	Pacific Ocean, Alaska, Canada and United States	McDermott 1998, Bousfield and Hendrycks 2002, Tunnell and Withers 2009, Turbeville and Caplins 2010, Heerhartz et al. 2016
Ptilohyale ptilocerus (Derzhavin, 1937)	Japan Sea, Russia	Hiwatari and Kajihara 1981

* erroneously named *crassicorne* in Bousfield and Hendrycks (2002) instead of *crassicornis*

** erroneously named *plumulosa* in Bousfield and Hendrycks (2002) instead of *plumulosus*

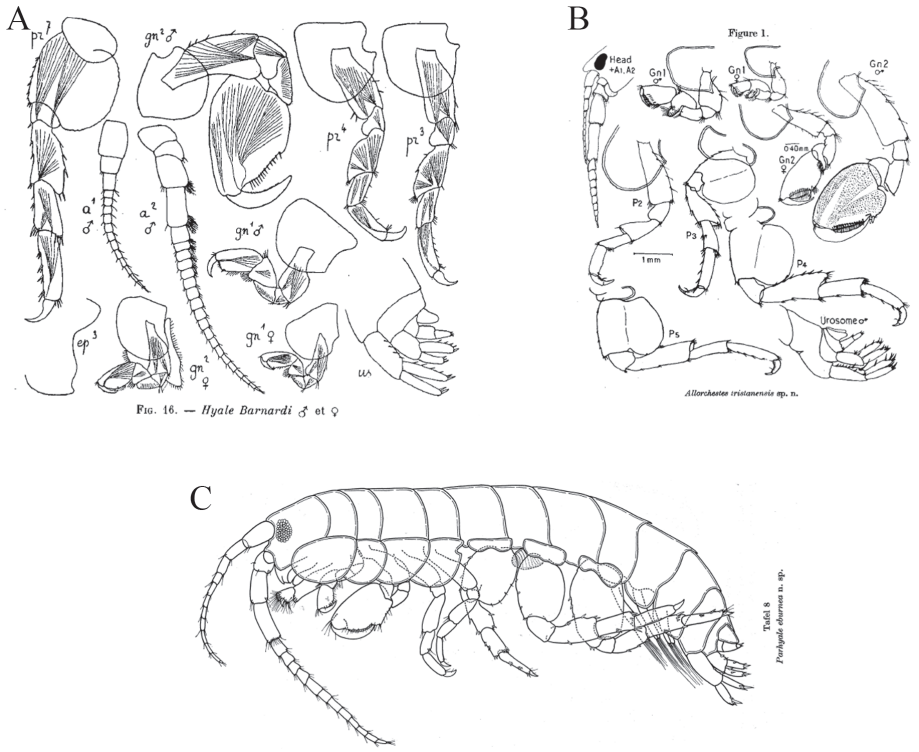

Fig. 16. — *Hyale Barnardi* ♂ et ♀

Figure 4. Illustrations from the literature of: **A** *Ptilohyale barnardi* (Chevreux, 1925) **B** *Ptilohyale tristanensis* (Macnae, 1953) **C** *Ptilohyale eburnea* (Krapp-Schickel, 1974).

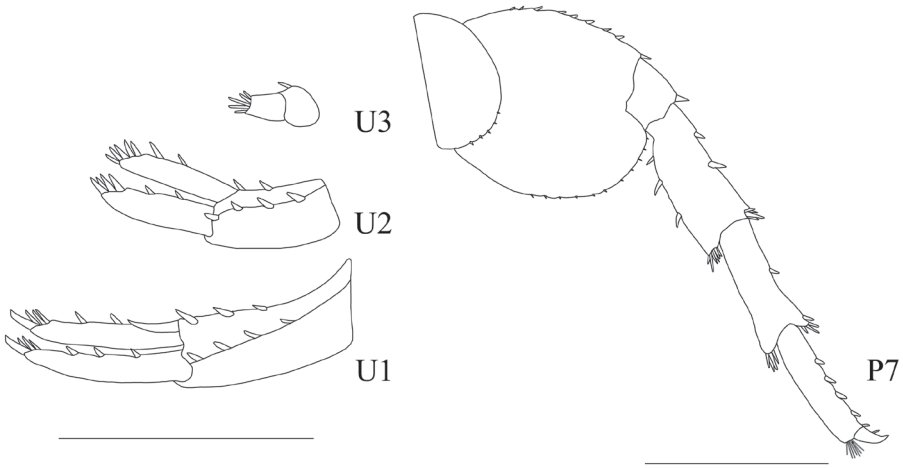

Figure 5. Illustration of male paratype of *Parhyale explorator*, from Ruffo's collection, uropods I (U1), II (U2), III (U3) and peraeopod VII (P7). Scale bars 1 mm.

The Atlantic *Ptilohyale littoralis* vs. the Mediterranean *Parhyale plumicornis*

Due the high connectivity between eastern Atlantic and Mediterranean area, which has already caused a high similarity in the Portuguese and Mediterranean amphipod fauna (Plicanti et al. 2016) it can be supposed that the Atlantic *Ptilohyale littoralis* may have spread into the Mediterranean, or vice versa, *Parhyale plumicornis* into the Atlantic Ocean.

Parhyale plumicornis belongs to the Mediterranean fauna and it is the most similar hyalid species to *Ptilohyale littoralis* due to the overlapping morphological and ecological characters such as the brush setae along ventral margin of antennae II (Bakir et al. 2013, Iaciofano and Lo Brutto 2017); and both their presences in the intertidal habitat in slow-drying sediments (Arresti 1989, Bousfield and Hendrycks 2002, Iaciofano and Lo Brutto 2017).

Some morphological character states are presented in Fig. 6 as a guide to the correct identifications: *Ptilohyale littoralis* (Fig. 6A) has brush setae on the ventral margin of antenna II that start at the 5th peduncular article (Fig. 6B) and distomedial robust setae on the peduncle of uropod I (Fig. 6C). In contrast, *Parhyale plumicornis* (Fig. 6E) has brush setae on the ventral margin of antenna II that start at the 4th peduncular article (Fig. 6F) and has a distolateral robust seta on the peduncle of uropod II (Fig. 6G).

These two species show a different and non-overlapping distributions: *Ptilohyale littoralis* was recorded along European Atlantic coast (Fig. 6D; Table 4), whereas *Parhyale plumicornis* was recorded along Mediterranean and Red Sea coasts (Fig. 6H; Iaciofano and Lo Brutto 2017 and reference therein). In light of the range extension of *Ptilohyale littoralis* already recorded over long distances, a clear representation of diagnostic character states is needed. *Ptilohyale littoralis* may be invading the Mediterranean Sea where it could probably be a competitor of the Mediterranean endemic *Parhyale plumicornis* as it occupies the same habitat.

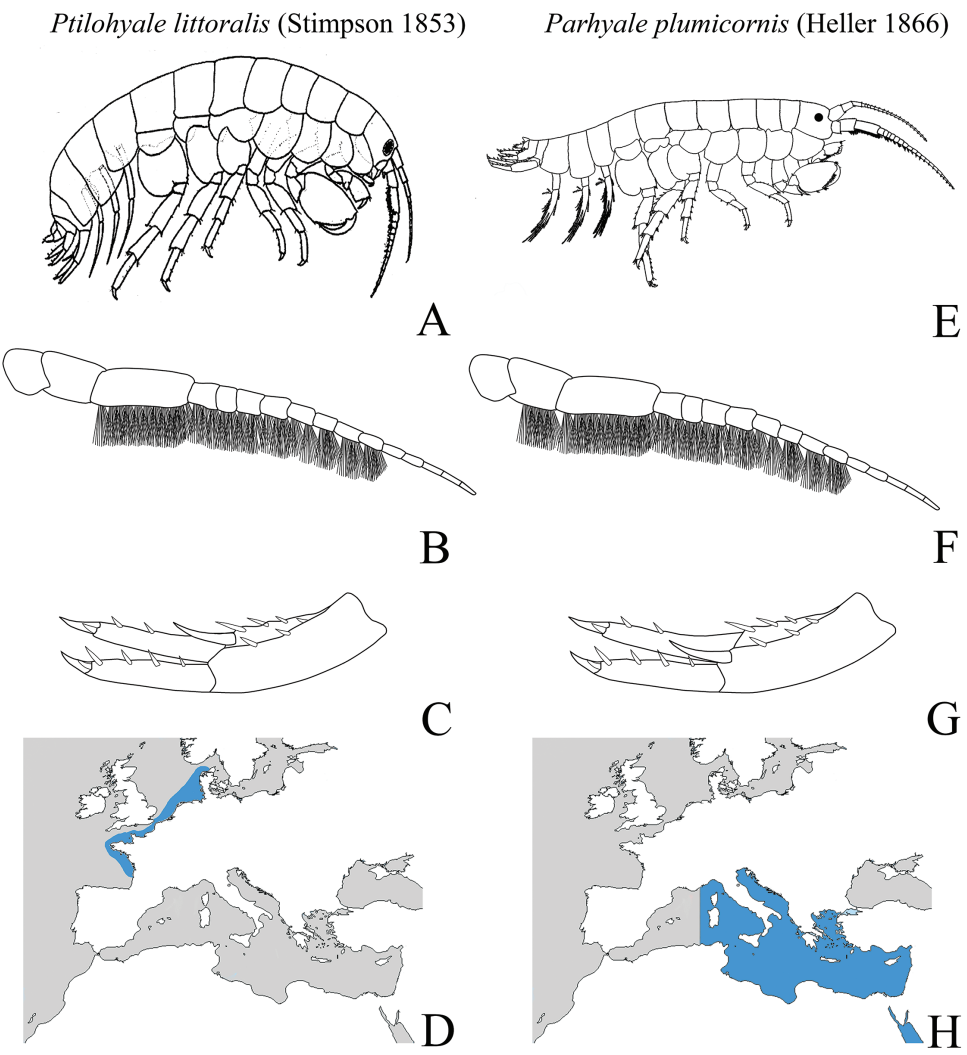

Figure 6. Comparison between *Ptilohyale littoralis* and *Parhyale plumicornis* diagnostic characters and distributions. *Ptilohyale littoralis*: **A** illustration of male (Bousfield and Hendrycks 2002) **B** antenna II male with brush-setae starting at the 5th peduncular segment **C** right uropod I with peduncular distomedial robust seta **D** species distribution along the Atlantic coast. *Parhyale plumicornis*: **E** illustration of male (Iaciofano and Lo Brutto 2017) **F** antenna II male with brush setae starting at the 4th peduncular segment **G** right uropod I with peduncular distolateral robust seta **H** species distribution along the Mediterranean and Red Sea coasts.

Acknowledgements

The authors are grateful to Dr. Leonardo Latella and Dr. Roberta Salmaso who provided laboratory facilities and access to the Sandro Ruffo's collection at the Museum of Natural History of Verona; to Dr. Laure Corbari who provided laboratory facilities

and access to the collection of the Muséum national d'Histoire naturelle, Departement Systematique et Evolution (Paris, France); to Dr. Benoit Gouillieux of French National Centre for Scientific Research (Paris, France) for providing the authors of this paper with specimens of *Ptilohyale littoralis* from Arcachon bay. The authors are grateful to reviewers who provided valuable suggestions and comments during revision of the manuscript.

This work was supported by the University of Palermo (Grant FFR 2012/2013).

References

Arresti A (1989) *Parhyale explorator*, a new species of talitroid amphipod from the bay of Arcachon, France. Bulletin du Muséum national d'Histoire naturelle. Section A, Zoologie, biologie et écologie animales 11: 101–115.

Bakir K, Katağan T, Sezgin M (2008) *Parhyale explorator* Arresti, 1989 (Amphipoda, Talitroidea): First Mediterranean record of this Atlantic amphipod. Crustaceana 81: 557–562. https://doi.org/10.1163/156854008784092247

Bakir K, Katağan T, Sezgin M (2013) Correction about the existence of *Parhyale explorator* Arresti, 1989 (Amphipoda, Talitroidea) in the Mediterranean Sea. Crustaceana 86: 1297–1298. https://doi.org/10.1163/15685403-00003225

Bakir K, Sezgin M, Katağan T (2010) Alien amphipods on the Turkish Coasts. Zoologica baetica 21: 191–196.

Barnard JL (1970) Sublittoral Gammaridea (Amphipoda) of the Hawaiian Islands. Smithsonian Contributions to Zoology 34: 1–286. https://doi.org/10.5479/si.00810282.34

Barnard JL (1979) Littoral gammaridean Amphipoda from the Gulf of California and the Galapagos Islands. Smithsonian Contributions to Zoology 271: 1–149. https://doi.org/10.5479/si.00810282.271

Barnard JL, Karaman GS (1991) The families and genera of marine gammaridean Amphipoda (except marine gammaroids). Part 2. Records of the Australian Museum 13: 1–866. https://doi.org/10.3853/j.0812-7387.13.1991.91

Barnard KH (1916) Contributions to the crustacean fauna of South Africa. 5. The Amphipoda. Annals of the South Africa Museum 15: 105–302. https://doi.org/10.5962/bhl.part.22196

Bousfield EL (1973) Shallow-water Gammaridean Amphipods of New England. Comstock publishing associates, Cornell University Press, Ithaca and London, 312 pp.

Bousfield EL (2001) Phyletic classification as applied to amphipod crustaceans of North America. Amphipacifica 3: 49–119.

Bousfield EL, Hendrycks EA (2002) The Talitroidean amphipod family Hyalidae revised, with emphasis on the North Pacific fauna: Systematics and distributional ecology. Amphipacifica 3: 17–134.

Bulycheva AI (1957) Beach-fleas of the seas of the USSR and adjacent waters (Amphipoda- Talitroidea). Akademiya Nauk SSSR, Opredeliteli po Faune SSSR 65: 1–185.

Chevreux E (1925) Amphipodes I. Gammariens (suite). Voyage de la goéllette *Melita* aux Canaries et au Senegal 1889–1890. Bulletin de la Société zoologique de France 50: 365–398.

Choi FM, Murray CC, Therriault TW, Pakhomov EA (2016) Intertidal invasion patterns in Canadian ports. Marine Biology 163: 183. https://doi.org/10.1007/s00227-016-2957-0

Christodoulou M, Paraskevopoulou S, Syranidou E, Koukouras A (2013) The amphipod (Crustacea: Peracarida) fauna of the Aegean Sea, and comparison with those of the neighbouring seas. Journal of the Marine Biological Association of the United Kingdom 93: 1303–1327. https://doi.org/10.1017/S002531541200183X

Costa A (1857) Ricerche sui crostacei amfipodi del regno di Napoli. Memorie della Reale Accademia delle Scienze di Napoli, 1: 181–183. https://doi.org/10.5962/bhl.title.2070

Dana JD (1853) Crustacea, Part II United States Exploring Expedition during the years 1838, 1839, 1840, 1841, 1842, under the command of Charles Wilkes. U.S. Navy 14: 686–1618. https://doi.org/10.5962/bhl.title.63979

Della Valle A (1893) Gammarini del golfo di Napoli. Fauna und Flora des Golfes von Neapel und der angrenzenden Meeres-Abschnitte. Herausgegeben von der Zoologischen Station zu Neapel 20: XI–948.

Derzhavin AN (1937) Talitridae of the Soviet coast ofthe Japan Sea. Issledovaniya Morei SSSR 3: 87–112.

Eun Y, Kim YH, Hendrycks EA, Lee KS (2014) The family Hyalidae (Crustacea: Amphipoda: Talitroidea) from Korean waters. 1. Genus *Ptilohyale* Bousfield & Hendrycks, 2002. Zootaxa 3802: 583–595. https://doi.org/10.11646/zootaxa.3802.4.8

Faasse MA (2014) Introduction of *Ptilohyale littoralis* to The Netherlands. Marine Biodiversity Records 7: e28. https://doi.org/10.1017/S1755267214000293

Haswell WA (1879) On Australian Amphipoda. Proceedings of the Linnean Society of New South Wales 4: 245–279. https://doi.org/10.5962/bhl.part.22848

Heller C (1866) Beiträge zur näheren Kenntniss der Amphipoden des Adriatischen Meeres. Denkschriften der Kaiserlichen Akademie der Wissenschaften, Mathematisch Naturwissenschaftliche Klasse 26: 1–62. https://doi.org/10.5962/bhl.title.6483

Heerhartz SM, Toft JD, Cordell JR, Dethier MN, Ogston AS (2016) Shoreline armoring in an estuary constrains wrack-associated invertebrate communities. Estuaries and Coasts 39: 171–188. https://doi.org/10.5962/bhl.part.22848

Hiwatari T, Kajihara T (1981) A new species of the genus *Hyale*. Ibid 20: 35–40.

Holmes SJ (1905) The amphipods of southern New England. Bulletin of the United State. Fish Commission 24: 459–529.

Horton T, Lowry J, De Broyer C, Bellan-Santini D, Zeidler W (2017) World Amphipoda Database. http://www.marinespecies.org/amphipoda [accesed on 2017-08-01]

Hutchings P, Ahyong S, Ashcroft M, McGrouther M, Reid A (2013) Sydney Harbour: its diverse biodiversity. Australian Zoologist 36: 255–320. https://doi.org/10.7882/AZ.2012.031

Iaciofano D, Lo Brutto S (2017) *Parhyale plumicornis* (Heller, 1866) (Crustacea: Amphipoda: Hyalidae): is this an anti-lessepsian Mediterranean species? Morphological remarks, molecular markers and ecological notes as tools for future records. Systematics and Biodiversity 15: 238–252. https://doi.org/10.1080/14772000.2016.1248519

Kim HS, Kim CB (1987) Marine gammaridean Amphipoda (Crustacea) of Cheju Island and its adjacent waters, Korea. The Korean Journal of Systematic Zoology 3: 1–23.

Kim W, Kim CB (1991) The marine amphipod crustaceans of Ulreung Island, Korea: Part II. The Korean Journal of Systematic Zoology 7: 13–38.

Krapp-Schickel G (1974) Camill HELLERS Sammlung adriatischer Amphipoden – 1866 und heute. Annalen des Naturhistorischen Museums in Wien 78: 319–379.

Lowry J (2010) *Ptilohyale* Bousfield & Hendrycks, 2002. In: Horton T, Lowry J, De Broyer C, Bellan-Santini D, Coleman CO, Zeidler W (Eds) World Amphipoda Database. http://www.marinespecies.org/amphipoda/ [accessed on 12 Jan 2017]

Lowry J, Costello M, Bellan-Santini D (2010) *Parhyale* Stebbing, 1897. In: Horton T, Lowry J, De Broyer C, Bellan-Santini D, Coleman CO, Zeidler W (2016) World Amphipoda Database. http://www.marinespecies.org/amphipoda/ [accessed on 12 Jan 2017]

Lowry JK, Myers AA (2013) Phylogeny and Classification of the Senticaudata subord. nov. (Crustacea: Amphipoda). Zootaxa 3610: 1–80. https://doi.org/10.11646/zootaxa.3610.1.1

Marchini A, Cardeccia A (2017) Alien amphipods in a sea of troubles: cryptogenic species, unresolved taxonomy and overlooked introductions. Marine Biology 164(4): 69. https://doi.org/10.1007/s00227-017-3093-1

McDermott JJ (1998) The western Pacific brachyuran (*Hemigrapsus sanguineus*: Grapsidae), in its new habitat along the Atlantic coast of the United States: geographic distribution and ecology. ICES Journal of Marine Science: Journal du Conseil 55: 289–298. https://doi.org/10.1006/jmsc.1997.0273

Macnae W (1953) On a small collection of amphipods from Tristan da Cunha. Proceedings of the Zoological Society of London 122: 1025–1033. https://doi.org/10.1111/j.1096-3642.1953.tb00361.x

Miner RW (1950) Field book of seashore life. Putnam & Sons, New York, 890 pp. [251 pls]

Peart RA (2004) Amphipoda (Crustacea) collected from the Dampier Archipelago, Western Australia. Records of the Western Australian Museum Supplement 66: 159–167. https://doi.org/10.18195/issn.0313-122x.66.2004.159-167

Plicanti A, Iaciofano D, Bertocci I, Lo Brutto S (2016) The amphipod assemblages of *Sabellaria alveolata* reefs from the NW coast of Portugal: An account of the present knowledge, new records, and some biogeographic considerations. Marine Biodiversity 47(2): 521–534. https://doi.org/10.1007/s12526-016-0474-5

Pollock LW (1998) A practical guide to the marine animals of northeastern North America. Rutgers University Press, New Brunswick, New Jersey, 371 pp.

Rafinesque CS (1815) Analyse de la nature ou tableau de l'université des corps organisés par C.S. Rafinesque. Palerme. https://doi.org/10.5962/bhl.title.106607

Ride Chairman WDL, Cogger HG, Dupuis C, Kraus O, Minelli A, Thompson FC, Tubbs PK (Eds) (1999) International Code of Zoological Nomenclature. International Trust for Zoological Nomenclature. The Natural History Museum, London, 1–106.

Salman SO (1986) *Parhyale basrensis*, a new species of talitrid amphipod from the Shutt AI-Arab region, Iraq. Crustaceana 50: 287–294. https://doi.org/10.1163/156854086X00313

Shoemaker CR (1956) Observations of the amphipod genus. Proceedings of the United States National Museum 106: 345–358. https://doi.org/10.5479/si.00963801.106-3372.345

Smith SI (1873) Crustacea ex Isopoda. In: Verrill AE (Ed.) Report upon the invertebrate animals of Vineyard Sound. Report of the United States Commissioner of Fisheries 1: 295–778.

Spilmont N, Hachet A, Faasse MA, Jourde J, Luczak C, Seuront L, Rolet C (2016) First records of *Ptilohyale littoralis* (Amphipoda: Hyalidae) and *Boccardia proboscidea* (Polychaeta: Spionidae) from the coast of the English Channel: habitat use and coexistence with other species. Marine Biodiversity, 1–11. https://doi.org/10.1007/s12526-016-0557-3

Stebbing TR (1897) II. Amphipoda from the Copenhagen Museum and other Sources. Transactions of the Linnean Society of London, 2nd Series: Zoology 7: 25–45. https://doi.org/10.1111/j.1096-3642.1897.tb00400.x

Stebbing TRR (1906) Amphipoda. I. Gammaridea. Das Tierreich 21: XXXIX–806.

Stimpson W (1853) Synopsis of the marine invertebrate of Grand Manan: or the region about the mouth of the Bay of Fundy. Smithsonian Contributions to Zoology 6: 5–66.

Stimpson W (1857) The Crustacea and Echinodermata of the Pacific shores of North America. Boston Society of Natural History 6: 1–92.

Stock JH (1987) Stygofauna of the Canary Islands. 5. A hypogean population of *Parhyale* (Amphipoda) in the Jameos del agua Lava Tunnel (Lanzarote) a supposed case of recent evolution. Stygologia 3: 167–184.

Tsoi KH, Chu KH (2005) Sexual dimorphism and reproduction of the amphipod *Hyale crassicornis* Haswell (Gammaridea: Hyalidae). Zoological studies 44: 382–392.

Tunnell KD, Withers K (2009) Macrofauna Associate with Ungrounded Prop Roots of *Rhizophora mangle* in Veracruz and Quintana Roo, Mexico. Gulf and Caribbean Research 21: 67–72. https://doi.org/10.18785/gcr.2101.08

Turbeville JM, Caplins SA (2010) First record for *Prosorhochmus americanus* (Nemertea Hoplonemertea) in Virginia with notes on its natural history and morphology. Banisteria 35: 61–65.

Zenetos A (2010) Trend in aliens species in the Mediterranean. An answer to Galil, 2009 «Taking stock: inventory of alien species in the Mediterranean Sea». Biological invasions 12: 3379–3381. https://doi.org/10.1007/s10530-009-9679-x

Zenetos A, Gofas S, Verlaque M, Cinar ME, Garcia Raso JE, Bianchi CN, Morri C, Azzurro E, Bilecenoglu M, Froglia C, Siokou I, Violanti D, Sfriso A, San Martin G, Giangrande A, Katagan T, Ballesteros E, Ramos-Espla AA, Mastrototaro F, Ocana O, Zingone A, Gambi MC, Streftaris N (2010) Alien species in the Mediterranean Sea by 2010. A contribution to the application of European Union's Marine Strategy Framework Directive (MSFD). Part I. Spatial distribution. Mediterranean Marine Science 11: 381–493. https://doi.org/10.12681/mms.87

ZooKeys 754: 63–101 (2018)
doi: 10.3897/zookeys.754.23368
http://zookeys.pensoft.net

RESEARCH ARTICLE

A peer-reviewed open-access journal
ZooKeys
Launched to accelerate biodiversity research

Evaluating the genus *Cespitularia* MilneEdwards & Haime, 1850 with descriptions of new genera of the family Xeniidae (Octocorallia, Alcyonacea)

Yehuda Benayahu[1], Leen P. van Ofwegen[2], Catherine S. McFadden[3]

1 *School of Zoology, George S. Wise Faculty of Life Sciences, Tel Aviv University, Ramat Aviv, 69978, Israel* **2** *Naturalis Biodiversity Center, P.O. Box 9517, 2300 RA Leiden, The Netherlands* **3** *Department of Biology, Harvey Mudd College, Claremont, CA 91711, USA*

Corresponding author: *Yehuda Benayahu* (yehudab@tauex.tau.ac.il)

Academic editor: *B.W. Hoeksema* | Received 2 January 2018 | Accepted 22 February 2018 | Published 26 April 2018

http://zoobank.org/71608A76-1D72-4692-AA7F-BFB0E352DC60

Citation: Benayahu Y, van Ofwegen LP, McFadden CS (2018) Evaluating the genus *Cespitularia* Milne Edwards & Haime, 1850 with descriptions of new genera of the family Xeniidae (Octocorallia, Alcyonacea). ZooKeys 754: 63–101. https://doi.org/10.3897/zookeys.754.23368

Abstract

Several species of the family Xeniidae, previously assigned to the genus *Cespitularia* Milne Edwards & Haime, 1850 are revised. Based on the problematical identity and status of the type of this genus, it became apparent that the literature has introduced misperceptions concerning its diagnosis. A consequent examination of the type colonies of *Cespitularia coerulea* May, 1898 has led to the establishment of the new genus *Conglomeratusclera* **gen. n.** and similarly to the assignment of *Cespitularia simplex* Thomson & Dean, 1931 to the new genus, *Caementabunda* **gen. n.** Both new genera are described and depicted and both feature unique sclerite morphology, further highlighting the importance of sclerite microstructure for generic position among Xeniidae. Freshly collected material was subjected to molecular phylogenetic analysis, whose results substantiated the taxonomic assignment of the new genera, as well as the synonymies of several others.

Keywords

Indo-Pacific Ocean, new genera, phylogeny, sclerite microstructure, taxonomy

Introduction

Members of the octocoral family Xeniidae form a major faunistic component on shallow Indo-Pacific coral reefs (e.g., Alderslade 2001, Janes 2013, McFadden et al. 2014, Halàsz et al. 2014, 2015). They play a significant ecological role in coral reef ecosystems, exhibiting a rapid colonization rate (e.g., Tilot et al. 2008, Wild and Naumann 2013) as well as invasive capabilities (Ruiz-Allais et al. 2014). Uniquely among Octocorallia, in xeniids the pinnules along the margins of the polyp tentacles are commonly arranged in more than one longitudinal row. The number of pinnule rows and the number of pinnules in the outermost row have been considered taxonomically diagnostic (e.g., Hickson 1931a, Reinicke 1997, Halàsz et al. 2014). However, Halàsz et al. (2015) and subsequently McFadden et al. (2017) demonstrated that this character is not informative for species delineation among members of the xeniid genus *Ovabunda* Alderslade, 2001. The taxonomic literature on Xeniidae also considers several other morphological characters to be informative, such as colony shape, dimensions and coloration, as well as polyp retractability and pulsation in the live state (e.g., Reinicke 1997, Halàsz et al. 2014, 2015).

The majority of the described Xeniidae taxa have a high density of minute sclerites in their tissues, although some have only a few or none (e.g., Halàsz et al. 2014). This family has been considered to exhibit less diversity of sclerites than most other octocoral families, with the commonly held notion that most of the species feature relatively simple sclerites in the form of round platelets (Fabricius and Alderslade 2001). Consequently, most of the old taxonomic literature does not depict xeniid sclerites, although their size-range has occasionally been recorded (Halàsz et al. 2014 and references therein). Among the few studies that have included drawings of xeniid sclerites are those of *Cespitularia mantoni* Hickson, 1931, *C. multipinnata* Quoy & Gaimard, 1833 (in Hickson 1931: 168, fig. 5), and *C. stolonifera* Gohar, 1938 (in Utinomi 1950: 80, fig. 3f) (see also Halàsz et al. 2014). With the use of scanning electron microscopy (SEM), the diverse microstructural features of xeniid sclerites have now become evident (e.g., Benayahu 1990, 2010, Reinicke 1997, Alderslade 2001, Janes 2008, Aharonovich and Benayahu 2011, Halàsz et al. 2014). Subsequently, several new genera have been described, such as *Bayerxenia* Alderslade, 2001, *Ingotia* Alderslade, 2001, *Ixion* Alderslade, 2001, *Orangaslia* Alderslade, 2001, and *Yamazatum* Benayahu, 2010. Alderslade (2001) established the genus *Ovabunda* Alderslade, 2001 for previously described species of *Xenia* Lamarck, 1816 with the corpuscular sclerite-type, while retaining those with a dendritic surface in the original genus. To date, the phylogenetic studies on Xeniidae support the hypothesis that their distinct sclerite microstructure justifies establishing generic boundaries within this family (Haverkort-Yeh et al. 2013, McFadden et al. 2014).

There is considerable confusion in the literature concerning the diagnosis of the xeniid genus *Cespitularia*. This genus was erected by Valenciennes in an unpublished manuscript and later published by Milne Edwards and Haime (1850). The type of

Cornularia multipinnata Quoy & Gaimard, 1833 collected in Tonga (West-Pacific) was designated to be the type species of the genus; Quoy and Gaimard (1833) also described *Cornularia subviridis* from the same locality. According to Milne Edwards and Haime (1850), the genus *Cespitularia* features non-retractile polyps arranged in fasciculi (=longitudinal groups) and united along the greatest part of their length by dense tough tissue; their description does not note the presence of sclerites. Our attempts to trace the types of both these *Cornularia* species have failed and therefore they are considered lost. Later, May (1899: 89) synonymized the genera *Cornularia* Quoy & Gaimard, 1833 and *Suensonia* Brundin, 1896 (see ahead) under *Cespitularia* Valenciennes; his description too does not note the presence of sclerites.

Drawings of the type of *Cornularia multipinnata* Quoy & Gaimard (1833) (plate 22, figs 1–4), depict a colony with a distinct dome–shaped capitulum bearing polyps as well as a bare stalk with no polyps (fig. 4), thus resembling *Xenia* (see e.g., Fabricius and Alderslade 2001). *Cornularia subviridis* (plate 22, figs 5–7) was described as a colony with three elongated stems arising from a common base, each bearing polyps along half of its length (fig. 5). The depicted sclerites of this species are spindles (fig. 5'), but no information is given on those of *C. multipinnata*. Hickson's (1931) revision of the Xeniidae (p. 162) referred to this original description, but erroneously stated that *C. multipinnata* featured spindle-shaped sclerites and *C. subviridis* had *Xenia*-like sclerites. Consequently, his conclusion that *C. subviridis* is probably *X. umbellata* would appear to be an error. Hickson's revision also indicated that Quoy & Gaimard (1833) had provided errata, arguing that their original drawing of the two *Cornularia* species had been switched, and thus figs 1–4 should refer to *C. subviridis* and figs 5–7 to *C. multipinnata*. It should be noted that although the colony shape depicted in plate 22, fig. 5 might be considered to be *Cespitularia* (see Fabricius and Alderslade 2001), doubts nonetheless exist because of the spindle-shaped sclerites (fig. 5'). Such sclerites have never been recorded among Xeniidae and, therefore, doubt exists as to whether *Cornularia multipinnata* Quoy & Gaimard, 1833 should be assigned to the family Xeniidae. Until new xeniid material can be obtained from the original type locality (Tonga), the taxonomic status of *Cespitularia sensu stricto* Quoy & Gaimard (1833) cannot be unequivocally determined.

The genus *Cespitularia* Milne Edwards & Haime, 1850 was first revised by Kükenthal (1902), who diagnosed it as forming tree-like colonies, with polyps not positioned on a defined polypary. That revision listed the following species under the genus: *C. subviridis* (Quoy & Gaimard, 1833); *C. multipinnata* (Quoy & Gaimard, 1833) as well as the subsequently described species *C. mollis* (Brundin, 1896); *C. coerulea* May, 1898; and *C. taeniata* May, 1899. The revision by Hickson (1931) similarly diagnosed the genus as having dendritic branches with the margins of the capitulum not sharply defined, i.e., its polyps do not arise only from the summit of the branches but also from lower down, albeit gradually diminishing in number. Based on the problematical identity and status of the type of the genus *Cespitularia*, as detailed above, it is apparent that both of these revisions introduced further misperceptions concerning its diagnosis.

The ambiguity concerning the diagnosis of *Cespitularia* is further demonstrated in *C. mollis* (Brundin, 1896), originally described as *Suensonia mollis*, whose type locality is the Korean Straits (120 m depth). May (1899) assigned this species to *Cespitularia*, but Hickson (1931) stated that it "must be regarded as a distinct species" because of its geographical origin and depth of collection. Hickson (1931) also indicated that the sclerites of *S. mollis* are "twins, quadruplets and hour-glass shaped", but no drawings were presented. Although Utinomi (1950:81) stated that this species is "a member of *Cespitularia*", the type locality of *S. mollis* certainly departs from that of the tropical coral-reef systems. It can therefore be concluded that *C. mollis* is not a xeniid.

At present, the literature refers to 18 species of the genus *Cespitularia* (Cordeiro et al. 2018). Considering the fact that the type species of the genus *Cespitularia* is missing and presumed lost, we searched for the types of species that were originally assigned to the genus subsequent to the species noted above, i.e., from May (1898) onwards. Accordingly, the current study examined the following types: *C. coerulea* May, 1898, *C. taeniata* May, 1898, *C. simplex* Thomson & Dean, 1931, *C. robusta* Tixier-Durivault, 1966, and *C. turgida* Verseveldt, 1971. Freshly collected material was subjected to molecular phylogenetic analyses whose results also substantiated the taxonomic findings that have led us to assign new xeniid genera as well as to synonymize several others. Examination of diverse, related museum material provided data on intraspecific variation and the zoogeographical distribution of the taxa.

Materials and methods

The study examined preserved type specimens obtained on loan from the British Museum of Natural History (**BMNH**); Muséum National d'Histoire Naturelle, Paris (**MNHN**); Naturalis Biodiversity Center, formerly Rijksmuseum van Natuurlijke Historie, Leiden (**RMNH**); Zoologisches Museum, Hamburg (**ZMH**); Zoologisches Museum Berlin (**ZMB**); Smithsonian National Museum of Natural History, Washington DC (**USNM**), and the Steinhardt Museum of Natural History at Tel Aviv University (**ZMTAU**).

Morphological features of the preserved colonies were recorded, comprising dimensions, branching and stalk length, and width of the stalk at the colony base. The number of rows of pinnules and number of pinnules on the aboral side of the tentacles were counted under a dissecting microscope, whenever possible from multiple polyps. The length of the anthocodiae, consisting of the polyp body and extended tentacles, and the dimensions and shape of the pinnules were also recorded (see also Halàsz et al. 2014). To examine the sclerites, the tissue samples were treated with 10 % sodium hypochlorite followed by repeated rinses in distilled water. Wet preparations of the clean sclerites from polyps and the colony base were examined under a Nikon Optiphot light microscope at 400× magnification. Observed differences led to preparation of SEM mounts from both regions; otherwise only those from the polyp were used (see Aharonovich and Benayahu 2011); each stub usually contained numerous sclerites and

samples were coated with Pd/Au and viewed under a Quanta 200 FEG (Field Emission Gun) ESEM at 5–20 kV. SEM was used to examine sclerites of almost all the studied material; in certain cases, wet preparations were prepared and examined under the light microscope (×200–400). Both SEM and wet preparations were prepared from the same colonies in order to correctly visualize the unique structure of the corresponding sclerites. The zoogeographical species distributions were determined by the examination of types and other material.

Freshly collected material used for molecular and morphological studies was collected by YB in Yonaguni Is., Ryukyu Archipelago, Japan (in 2010); Green Is., Taiwan (2012) and Nosy Be, Madagascar (2015). Xeniidae colonies tend to release large quantities of mucus, especially when being detached from the reef and brought onboard, which is particularly relevant to the taxa studied here. This usually causes rapid colony disintegration and poor condition of museum material. Therefore, upon collection samples were immediately preserved in 95 % ethanol and subsamples were removed and preserved in absolute ethanol for molecular studies and then placed on ice in cool boxes until brought to the laboratory. In order to ensure appropriate preservation, the fixatives were replaced twice within 24 hours after collection, and throughout all preservation steps, the bottles were shaken to enhance infiltration of the fixative into the tissues.

DNA was extracted from ethanol-preserved tissue samples using the Qiagen DNEasy Blood & Tissue kit, and three gene regions were subsequently amplified by polymerase chain reaction (PCR) using previously published primers and PCR protocols (McFadden et al. 2011). For most specimens, we amplified the octocoral-specific mitochondrial *mutS* homolog (*mtMutS*) using primers ND42625F (McFadden et al. 2006) and mut3458R (Sánchez et al. 2003); cytochrome oxidase I (*COI*) and the adjacent intergenic region, *igr1*, using primers COII8068F (McFadden et al. 2004) and HC02198 (Folmer et al. 1994); and a fragment of 28S rDNA using primers 28S-Far and 28S-Rar (McFadden and Ofwegen 2013). The L-INS-i method in MAFFT (Katoh et al. 2005) was used to align sequences to a reference dataset consisting of previously published sequences for other genera of xeniids and three outgroup taxa, *Coelogorgia*, *Paralemnalia*, and *Rhytisma* (McFadden et al. 2014). Pairwise measures of genetic distance (Kimura 2-parameter) among sequences were computed using MEGA v.5 (Tamura et al. 2011). jModelTest2 (Darriba et al. 2012) was used to select appropriate models of evolution for maximum likelihood analyses that were run using GARLI 2.0 (Zwickl 2006). Analyses were run for each gene region alone, and for a combined dataset with all three genes concatenated. Each gene was treated as a separate data partition with different models of evolution applied to each (*mtMutS*: HKY+G; *COI*: TIM2+I+G; *28S*: GTR+I+G). Bayesian analyses of the concatenated alignment used MrBayes v. 3.2.1 (Ronquist et al. 2012) with the same data partitions and evolutionary models applied, except that GTR+I+G was substituted for TIM2+I+G. MrBayes was run for 5,000,000 generations (until standard deviation of split partitions < 0.01) with a burn-in of 25 % and default Metropolis coupling parameters.

Systematics

Class Anthozoa Ehrenberg, 1831
Subclass Octocorallia Haeckel, 1866
Order Alcyonacea Lamouroux, 1812
Family Xeniidae Ehrenberg, 1828

***Conglomeratusclera* gen. n.**
http://zoobank.org/F3E23C0E-B3D8-4C72-9638-33404B685A1B

Type species. *Cespitularia coerulea* May, 1898: 21

Diagnosis. Colonies soft with a short but distinct stalk, ramified into primary branches and occasionally into secondary ones. Polyps monomorphic, found along the branches, sometimes down on the stalk; most are non-retractile. Sclerites of a wide diversity of forms and dimensions, many lacking a distinct repetitive morphology. They include spheres, spherules, and small dumbbell-like sclerites. They are commonly cemented together, forming heterogeneous morphologies of various shapes and sizes. Occasionally, the aggregates form plate-like structures, embedded with spheres and/or spherules. The abundance of sclerites can vary greatly; in some specimens they are rare and then mostly found only at the colony base, and occasionally they may be found in all parts of the colonies, or may even be entirely absent. Zooxanthellate.

Etymology. The generic name is derived from Latin *conglomerātus*, which refers to anything composed of heterogeneous materials or elements and *sclera* from Greek meaning sclerite. Here it denotes the sclerites that resemble the geological structures termed conglomerates, a feature comprising rounded to sub-angular clast of granules, pebbles or cobbles cemented together. Gender female.

***Conglomeratusclera coerulea* (May, 1898)**
Figures 1A–B, 2–4, 5A–B, 7–25

Cespitularia coerulea May, 1898: 21; May 1899: 90, plate I, fig. 10; Kükenthal 1902: 659; Thomson and Henderson 1906: 414–415; Thomson and Mackinnon 1910: 173, plate 12, fig. 5; Hickson 1931: 162 (listed only); Thomson and Dean 1931: 32–33; Roxas 1933: 106, plate 4, fig. 6; Malyutin 1992: 2 (listed only); Benayahu et al. 2004: 551 (listed only).

Cespitularia taeniata May, 1899: 89–90; Kükenthal 1902: 659, Hickson 1931: 162; Utinomi 1950: 14–15, fig 3b, c; 1954: 102 (listed only); Thomson and Mackinnon 1910: 172, Thomson and Dean 1931: 33.

Material. Syntypes: ZANZIBAR: ZMH C 2518, Kokotoni, two colonies and two fragments, Tumbatu (southern reef), 24 July 1885, coll. Stuhlmann; ZMB Cni 3671, two colonies, 1885, coll. Sander; **types** of *Cespitularia taeniata*; **MOZAMBIQUE**: ZMH C 2519, three colonies and three fragments, coll. Philippi, 1884.

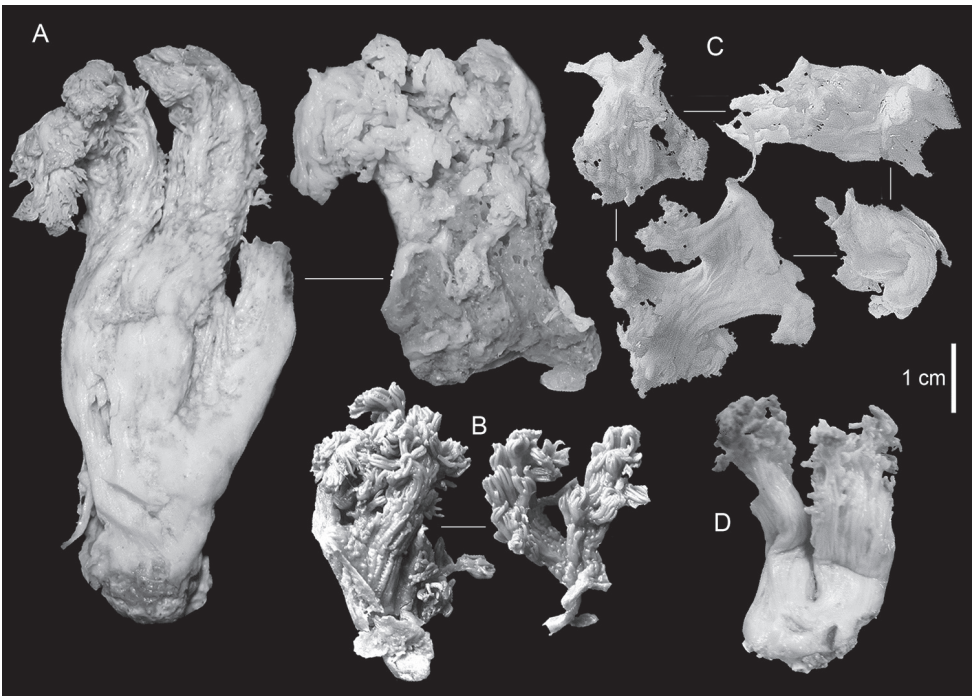

Figure 1. A *Conglomeratusclera coerulea* (May, 1898), syntypes ZMH C 2518 **B** *Conglomeratusclera coerulea* (May, 1898), type ZMB Cni 3671 **C** *Cespitularia taeniata* May, 1898, syntypes ZMH C 2519 **D** *Ammothea bauiana* May, 1898, type ZMH C 2375.

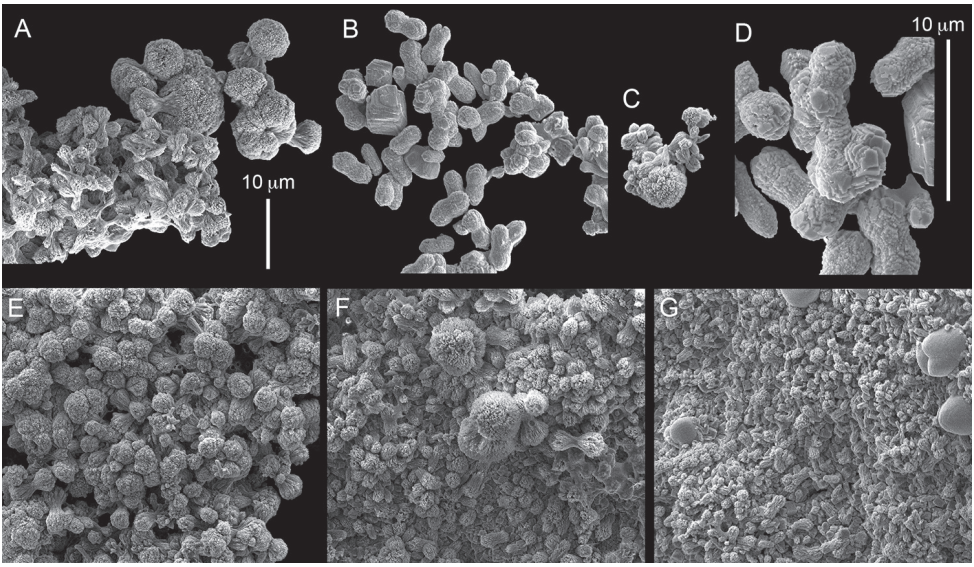

Figure 2. *Conglomeratusclera coerulea* (May, 1898), syntypes ZMH C 2518. **A** aggregate of spherules **B** conglomerate of dumbbells **C** conglomerate of spherules of various diameters **D** conglomerate of dumbbells **E–G** dense conglomerate of spherules with some dumbbells. Scale bar at **A** also applies to **B**, **C** and **E–G**.

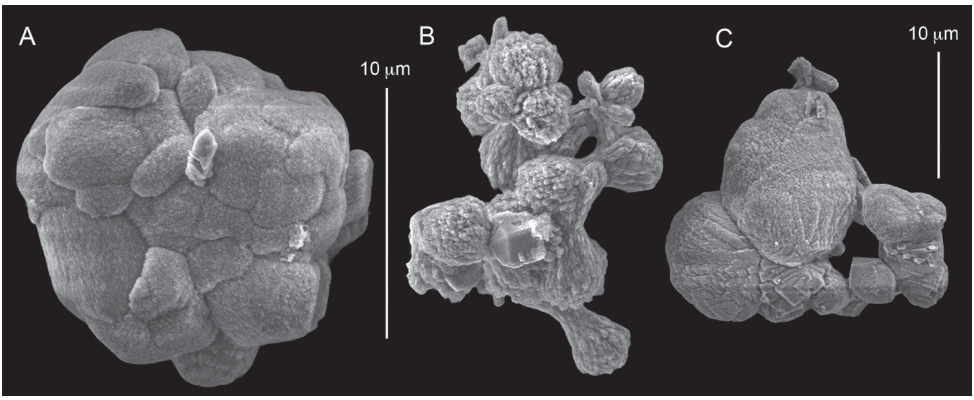

Figure 3. *Conglomeratusclera coerulea* (May, 1898), type ZMB Cni 3671. **A** conglomerate sclerites composed of spheres and spherules **B** conglomerate sclerite composed of spheres and dumbbells **C** conglomerate sclerite composed of spheres and spherules. Scale at **A** also applies to **B**.

Other material. JAPAN: ZMTAU Co 29285, Yonaguni Is., Ryukyu Archipelago, coll. Y. Benayahu, 13 November 1992, ten specimens; ZMTAU Co 29290, Nurugan, Yonaguni Is., Ryukyu Archipelago, 04°05'N, 122°57'E, 23 m depth, coll. Y. Benayahu, 11 November 1992, ZMTAU Co 31699, details as before, six specimens; ZMTAU CO 35129, West Point, Yonaguni Is., Ryukyu Archipelago, 11–22 m depth, coll. Y. Benayahu, 4 July 2010, two specimens; ZMTAU CO 35130, details as before; ZMTAU Co 35131, details as before, four specimens ZMTAU Co 35132, Co 35134, Co 35138, Co 35139, details as before; ZMTAU Co 35142, West Point, Yonaguni Is., Ryukyu Archipelago, 16–22 m depth, coll. Y. Benayahu, 5 July 2010, two specimens; ZMTAU Co 35153, details as before; **KENYA**: ZMTAU Co 31326, Nyali, off Mombasa, 10–16 m depth, coll. Y. Benayahu & S. Perkol, 1 February 2001; ZMTAU Co 31635, Turning Bouya, Shelly Reef, off Likoni, 04°05'S, 39°41.1'E, 15–28 m depth, coll. Y. Benayahu, 27 February 2002, two specimens; **MADAGASCAR**: ZMTAU Co 35982, Riva Be, 12°59.126'S, 48°34.453'E, 8–10 m depth, coll. Y. Benayahu, 27 November 2012, three specimens; ZMTAU Co 35990, Riva Be, 12°59.094'S, 48°34.622'E, 10–11 m depth, coll. Y. Benayahu, 27 November 2012, two specimens; ZMTAU Co 35991, details as before, four specimens; ZMTAU Co 36013, Ankaréa, 12°50.054'S, 48°34.563'E, 6–9 m depth, coll. Y. Benayahu, 29 November 2012; ZMTAU Co 36055, Co 36063, 4 Fréres, 12°59.655'S, 48°29.248'E, 4–15 m depth, coll. Y. Benayahu, 1 December 2012; ZMTAU Co 36101, Ronald Point, Nosy Be, 13°23.530'S, 48°00.143'E, 19–27 m depth, coll. Y. Benayahu, 3 December 2012, two specimens; ZMTAU Co 36129, Ronald Point, Nosy Be, 13°29.032'S, 47°58.721'E, 2–14 m depth, coll. Y. Benayahu, 3 December 2012, two specimens; USNM 54000 Nosy Be; USNM 54003 Nosy Be; **MOZAMBIQUE**: ZMTAU Co 31296, Ilha Sete Paus, 14°58.572'S, 40°47.389'E, 6 m depth, coll. M. Schleyer, 16 November 2000, two specimens; ZMTAU Co 31337, Ilha Caldeira, 16°38'22"S, 39°43'10"E, 4–16 m depth, coll. M. Schleyer, 2 June 2000, four specimens; **TAIWAN**: ZMTAU, Co 32988, Lomen-

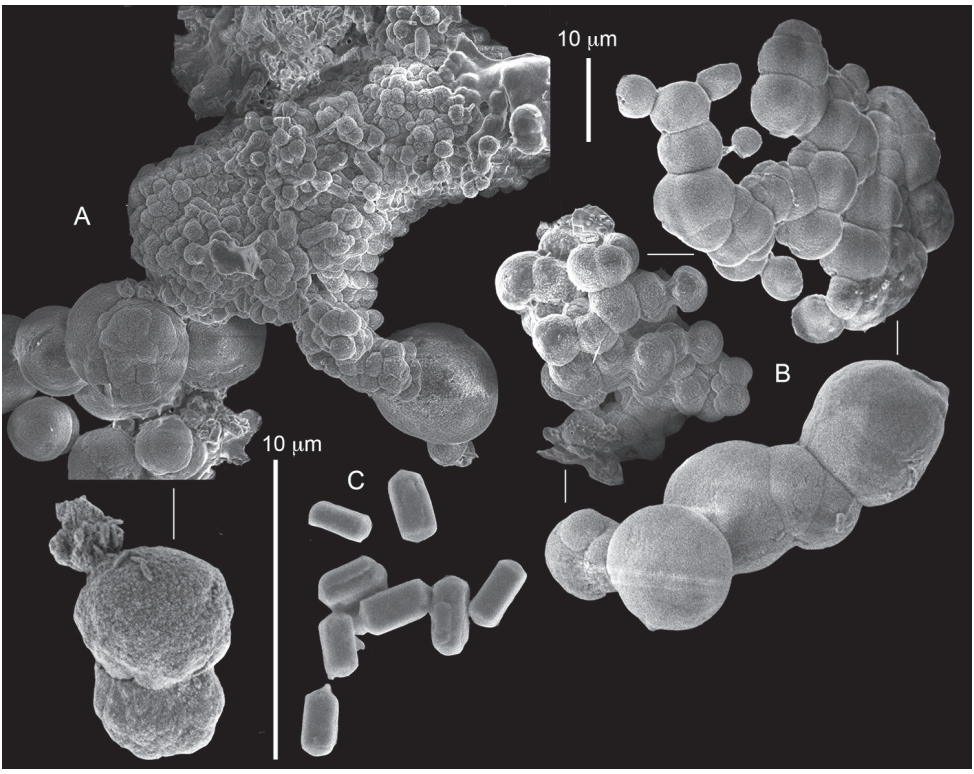

Figure 4. *Cespitularia taeniata* (May, 1898), type ZMH C 2519, synonym of *Conglomeratusclera coerulea* (May, 1898). **A** conglomerate sclerites composed of spherules and spheres **B** conglomerate sclerites composed of mainly spheres **C** cylinder-like small sclerites. Scale at **A** also applies to **B**.

yan, Green Is., 22°40'56"N, 121°30'06"E, 3–25 m depth, coll. Y. Benayahu, 12 July 2005; ZMTAU Co 33006, details as before, seven specimens, Co 33008, details as before; ZMTAU Co 33030, Dabaisha, Green Is., 22°38'25"N, 121°29'04"E, 10–25 m depth, coll. Y. Benayahu, 14 July 2005; ZMTAU Co 33036, Co 33043, 33045, Nanliao, Green Is., 22°39'40"N, 121°27'59"E, 10–25 m depth, coll. Y. Benayahu, 14 July 2005; ZMTAU Co 35693, Co 35699, Co 35708, Co 35709, Co 35712, Co 35714, Co 35716 , Co 35717, (only molecular sample), Shihlang, Green Is., 22°39.425'N, 121°28.399'E, 8–12 m depth, coll. Y. Benayahu, 3 September 2012, ZMTAU Co 35692, details as before, three specimens; ZMTAU Co 35706, Co 35707, details as before, two specimens; ZMTAU Co 35725, Dabaisha, Green Is., 22°38.284'N, 121°29.457'E, 14–25 m depth, coll. Y. Benayahu, 4 September 2012; ZMTAU Co 35729, details as before, two specimens; ZMTAU Co 35731, details as before, three specimens; ZMTAU Co 35736, Co 35737, Dabaisha, Green Is., 22°38.284'N, 121°29.457'E, 11–15 m depth, coll. Y. Benayahu, 4 September 2012; ZMTAU Co 35742, details as before, two specimens; ZMTAU Co 35747, Co 35748, Co 35750, Co 35753, Iron Artificial Reef, Green Is., 22°38'33"N, 121°28'31"E, 20–26 m depth, coll. Y. Benayahu, 5 September 2012; ZMTAU

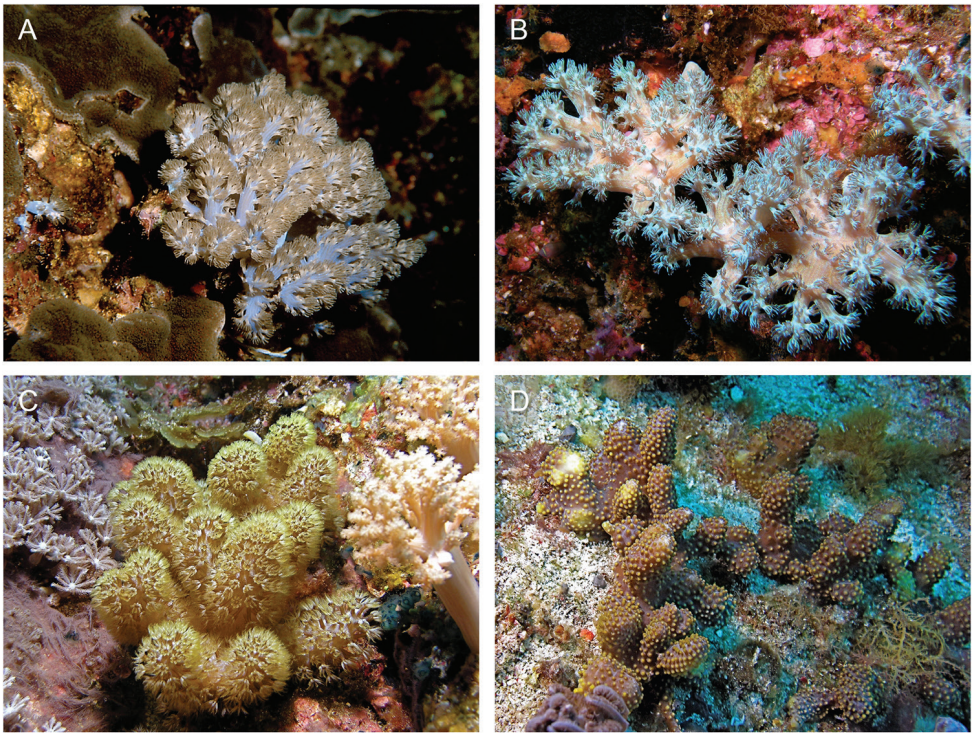

Figure 5. Live colonies on the reefs of Green Is. Taiwan. **A–B** *Conglomeratusclera coerulea* (May, 1898). **C** *Caementabunda simplex* (Thomson & Dean, 1931) with expanded polyps **D** *C. simplex* (Thomson & Dean, 1931) with partially retracted polyps. Photo credit Chang-Feng Dai, National Taiwan University, Taiwan.

Co 35752, details as before, three specimens, ZMTAU Co 35756, Co 35758, Co 35760, Co 35763, Co 35765, Co 35774, Shihlang, Green Is., 22°39.425'N, 121°28.399'E, 7–10 m depth, coll. Y. Benayahu, 5 September 2012; ZMTAU Co 35759, details as before, two specimens; ZMTAU Co 36232, Co 36235, Shihlang, Green Is., 22°39'17.91"N, 121°28'26.41"E, 6–11 m depth, coll. Y. Benayahu, 26 August 2013; ZMTAU Co 36247, details as before, four specimens; ZMTAU Co 36255, Gueiwan, Green Is., 22°38'41"N, 121°28'26"E, 10–18 m depth, coll. Y. Benayahu, 27 August 2013, two specimens; **MAYOTTE**: ZMTAU Co 37403, Glorioso Is., 11°34.880'S, 47°16.862'E, 10–11.5 m depth, coll. M. Schleyer, 20 November 2016, two specimens; ZMTAU Co 37430, Saziley, 12°59.138'S, 45°10.947'E, 3–4 m depth, coll. M. Schleyer, 26 June 2011; ZMTAU Co 37431, Station East Bouzi, 12°48.739'S, 45°14.543'E, 5–10 m depth, coll. M. Schleyer, 24 June 2011; **MAURITIUS**: BMNH 1912.2.24.65; BMNH 1912.2.24.66; Cargados Carajos, 20–25 m depth; BMNH 1933.3.13.175, Cargados Carajos, 20–25 m depth, coll. J.A. Thomson; BMNH 1933.3.13.176, Cargados Carajos, 20–30 m depth, Percy Sladen Trust Expedition, coll. J.A. Thomson; BMNH 1933.5.3.301, Port East Africa, Sir J.A. Thomson Expedition, 11 November 1907; **MALAYSIA**:

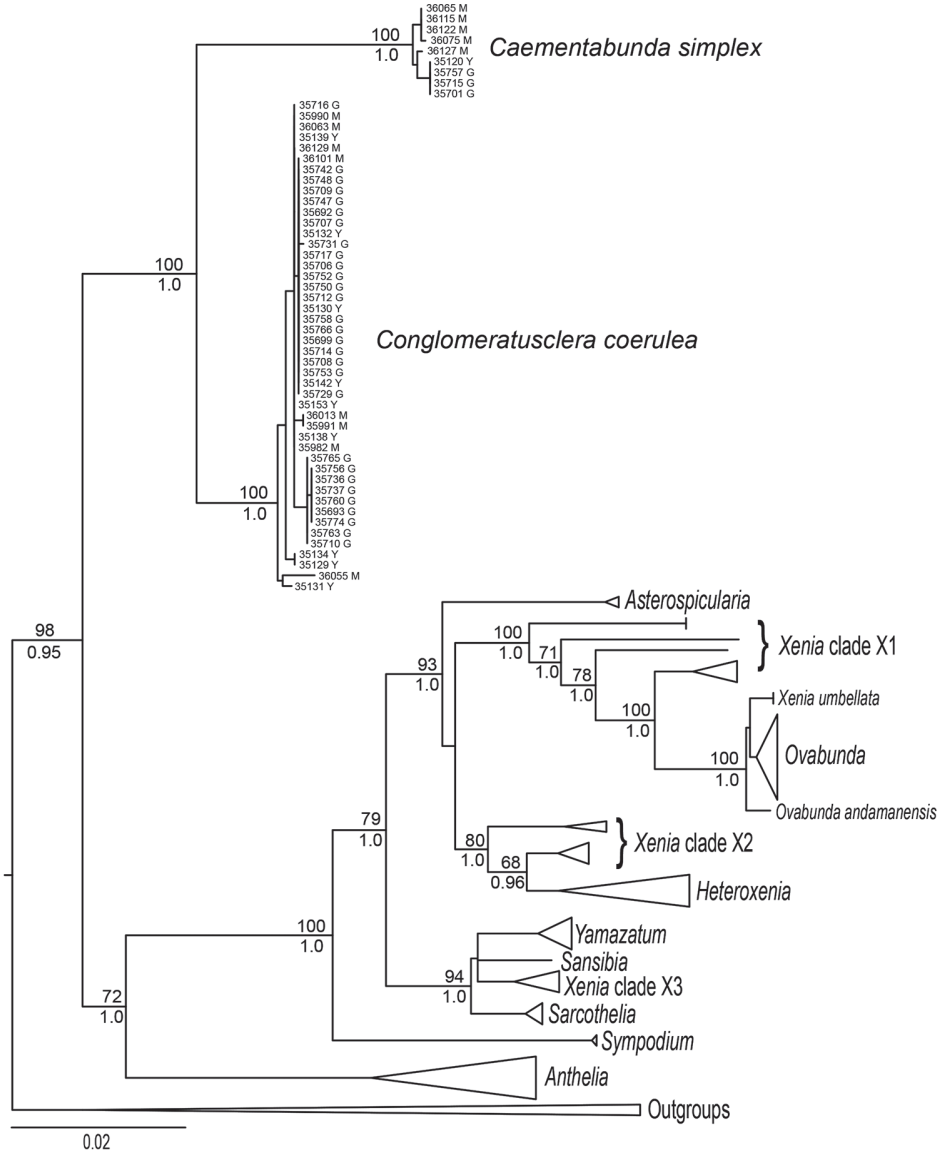

Figure 6. Maximum likelihood tree of family Xeniidae based on a partitioned analysis of concatenated *mtMutS*, *COI* and *28S* rDNA gene regions. Numbers above nodes: ML bootstrap percentages; numbers below nodes: Bayesian posterior probabilities. All genera and major clades of Xeniidae other than *Caementabunda* and *Conglomeratusclera* have been collapsed to facilitate readability. Specimens of *Caementabunda* and *Conglomeratusclera* are identified by ZMTAU catalog number and location of collection (G = Green Is., Taiwan; M = Madagascar; Y = Yonaguni Is., Japan).

BMNH 1985.4.17.20, NE Borneo, Sabah, Semporna, Pulau-Pulau Mantanani. **AUSTRALIA**: USNM 60795, Great Barrier Reef, Myrmidon Reef, Northern Reef, 17°00'S, 146°00'E Queensland, 1982; **INDONESIA**: RMNH Coel 42158, SW

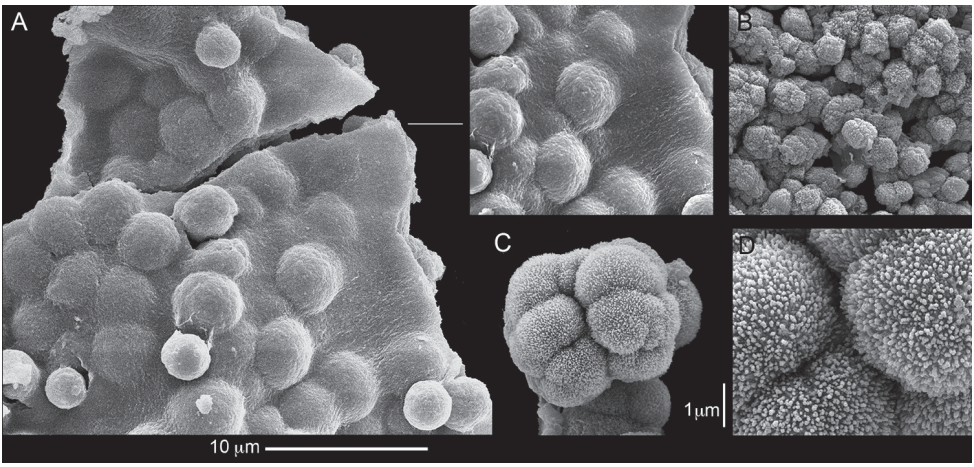

Figure 7. *Conglomeratusclera coerulea* (May, 1898), ZMTAU Co 35692. **A** spheres embedded in a calcareous lamella-like structure **B** conglomerate sclerite composed of spherules **C–D** spherules with bristly surface. Scale at **A** also applies to **B**, scale at **C** also applies to **D**.

Sulawesi, Spermonde Archipelago, west of Lumu-Lumu Is.; RMNH Coel 42159, N Sulawesi, Bunaken park, ESE Siladen Is.; RMNH Coel 42161, Snellius II Exp. Station 4.139, NE Taka Bone Rate (Tiger Is.), S. of Tarupa Kecil, edge of reef flat, 06°30'S, 121°08'E, SCUBA, snorkeling on sea grass bed, 30 m depth, 25–26 September, 13 and 17 October 1984; RMNH Coel 42162, N. Sulawesi, Selat Lembeh, Pulau Lembeh, N of Pulau Burung, 01°29'N, 125°15'E; sandy bay merging to the north in stony boulders beach, stony and soft corals, SCUBA, 22 October 1994, 2–25 m depth, coll. L.P. van Ofwegen; RMNH Coel 42163 N. Sulawesi, Selat Lembeh, Pulau Lembeh, Air Bajo, near Kereko, Nusu Dua; SUL 13, 01°29'N, 125°15'E; sandy bay between rocks, N-exposed, gently sloping bottom with large boulders, snorkeling 5 m depth, 21 October 1994, coll. J.C. Den Hartog; RMNH Coel 42165, Buginesia Prog. UNHAS-NNM, SW Sulawesi. Spermonde Archipelago N of Kudingareg Keke (=14 km WNW of Makassar), 5°06'S, 119°17'E, SCUBA, 5–25 m depth, 1994 Sul. KK SW, 14 October 1994, coll. B.W. Hoeksema; RMNH Coel 42166, Buginesia Prog. UNHAS-NNM, SW Sulawesi, Spermonde Archipelago N of Langkai Is. (=37 km WNW of Makassar), 5°02'S, 119°05'E, coral reef, SCUBA, 24 June 1994, coll. B.W. Hoeksema; RMNH Coel 42167, Buginesia Prog. UNHAS-NNM, SW Sulawesi, Spermonde Archipelago N of Langkai Is. (=37 km WNW of Makassar), 5°02'S, 119°05'E, coral reef, SCUBA, 24 June 1994, coll. B.W. Hoeksema; RMNH Coel 42170, Buginesia Prog. UNHAS-NNM, SW Sulawesi, Spermonde Archipelago, N of Kudingareng Keke (=14 km WNW of Makassar), 5°0'S, 119°17'E, SCUBA, 1994 Sul. KK SW, 5 September 1994, coll. B.W. Hoeksema; **PHILIPPINES**: RMNH Coel 42160, Cebu strait Expedition, Station CEB. 13.

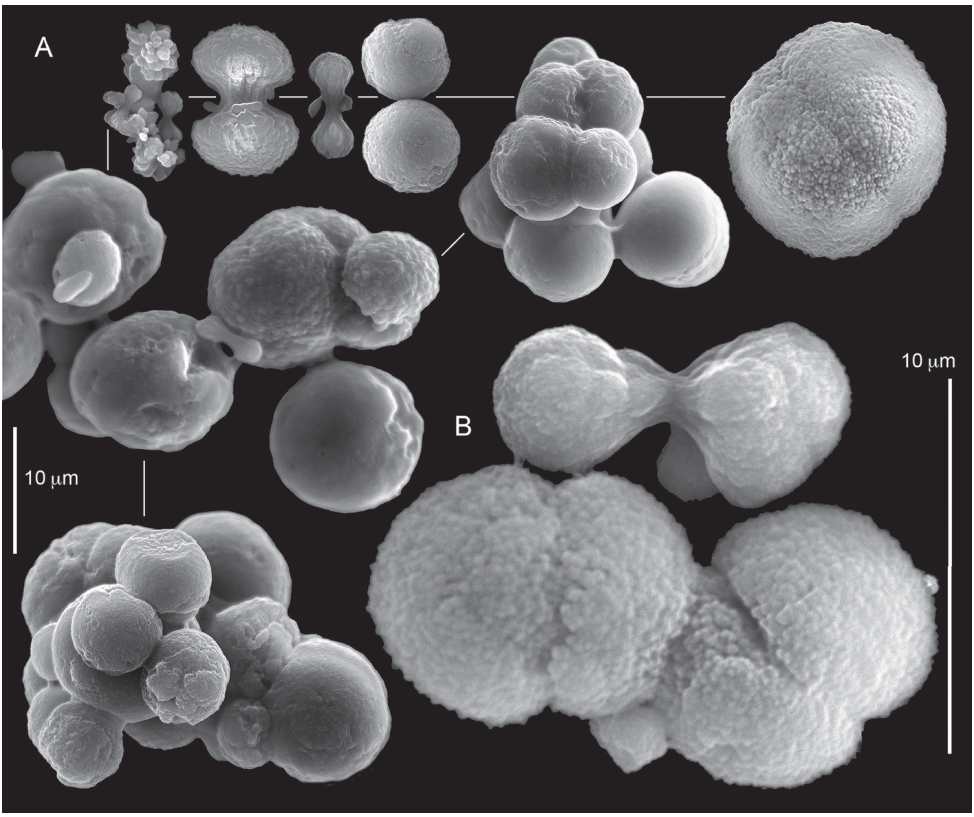

Figure 8. *Conglomeratusclera coerulea* (May, 1898), ZMTAU Co 35737. **A** conglomerate sclerite composed of spherules and of spheres, dumbbells **B** bristly surface of dumbbells and double spheres.

Notes to previous description. The original description of *C. coerulea* by May (1898) referred to a colony from Kokotoni, Zanzibar. Later, May (1899) repeated the description, referring to colonies collected from that location in 1889 by Stuhlmann and from Zanzibar in 1885 by Sander, deposited in Hamburg and Berlin museums, respectively. During a visit by the senior author to ZMH two colonies were found labeled as the type of *C. coerulea*, both collected in Kokotoni, Zanzibar, 24 July 1895 (leg. Stuhlman). Similarly, in a subsequent visit to ZMB two colonies were found, labeled as syntypes of *C. coerulea*, collected in Zanzibar, 1895 (leg. Sander). Both ZMH and ZMB colonies are considered to be the original syntypes of that species and are re-described below.

Description. ZMH C 2518 consists of two colonies; the first is 8.5 cm high by 4.2 cm wide and the second 5 cm high by 4 cm wide (Figure 1A). The polypary of these colonies is branched and their tips are bent. They bear non-retractile polyps, with some occurring towards the upper part of the colony's base. The polyp body is up to 8 mm long and the tentacles are up to 3 mm long; the latter bear one row of pinnules and 16–18 pinnules along each edge. The pinnules are short, pointed and evenly placed along

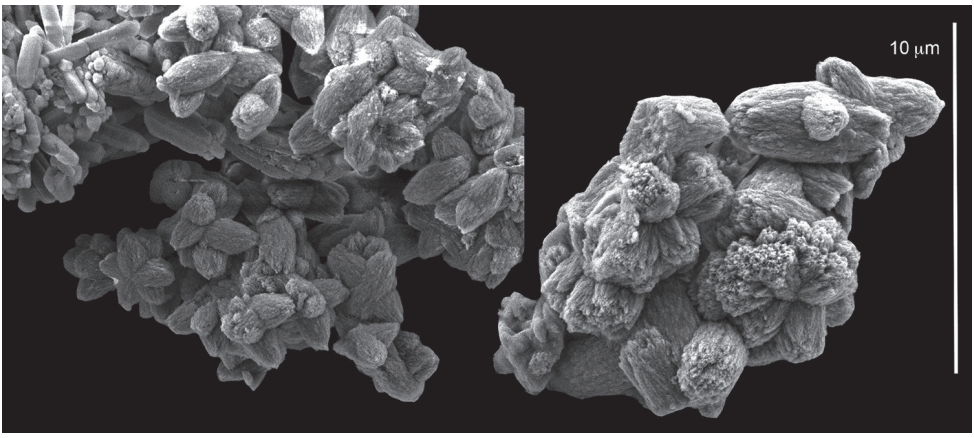

Figure 9. *Conglomeratusclera coerulea* (May, 1898), ZMTAU Co 35765. Conglomerate sclerite composed of striated ovals and cylinder-like small sclerites (left top corner).

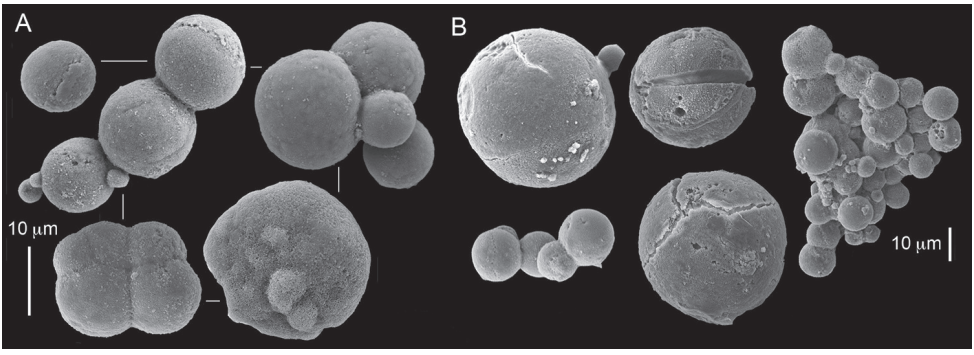

Figure 10. *Conglomeratusclera coerulea* (May, 1898), ZMTAU Co 35709. **A** individual sphere, conglomerate sclerites composed of spheres and spherules **B** individual spheres, conglomerate sclerites composed of spheres and spherules.

the tentacle, with a narrow space of less than a pinnule width between adjacent ones. The preserved colonies are pale gray- almost white. Sclerites could not be found in the upper part of the branches or in the polyps. However, the lower part of the branches, including the base of the colonies, feature conglomerates, comprised of spherules and small dumbbell-like sclerites, mostly cemented (Figure 2). The spherules are about 0.002–0.006 mm in diameter (Figures 2A, E–G), with a rather rough surface-texture. The abundance of the dumbbells (Figures 2B–D, F) may exceed that of the spheroids. The former vary in size, with a length of 0.003–0.006 mm. The conglomerate nature of the sclerites exhibits a large morphological variation as demonstrated in Figure 2. The syntype ZMB Cni 3671 (Figure 1B) resembles syntype ZMH 2518, except for the size of the colonies. Most of the polyps of the former are expanded, well-preserved, and thus recognizable on the branches of the colony. The sclerites are similar, conglomerated spheres and spherules along with some double-heads (Figure 3), but are less

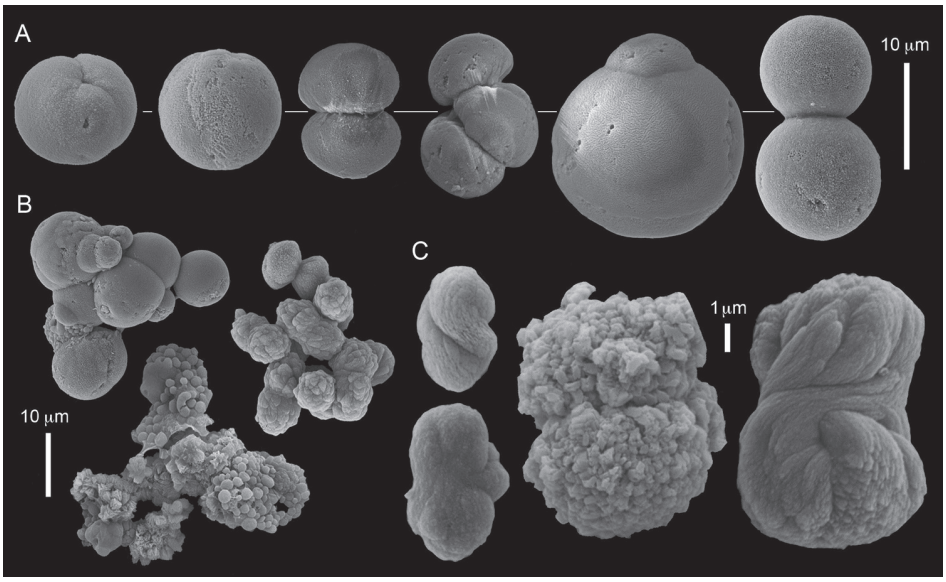

Figure 11. *Conglomeratusclera coerulea* (May, 1898), ZMTAU Co 35707. **A** Spheres and double spheres. **B** conglomerate of spheres and spherules **C** twisted dumbbells.

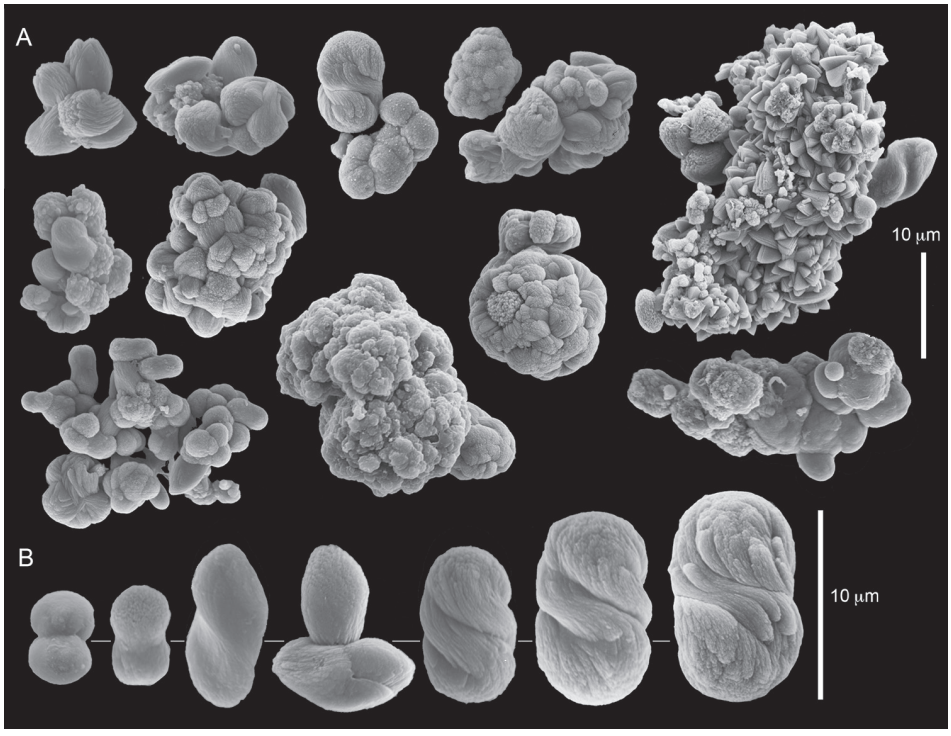

Figure 12. *Conglomeratusclera coerulea* (May, 1898), ZMTAU Co 35710. **A** conglomerate sclerites composed of spherules and twisted dumbbells **B** double heads and twisted dumbbells.

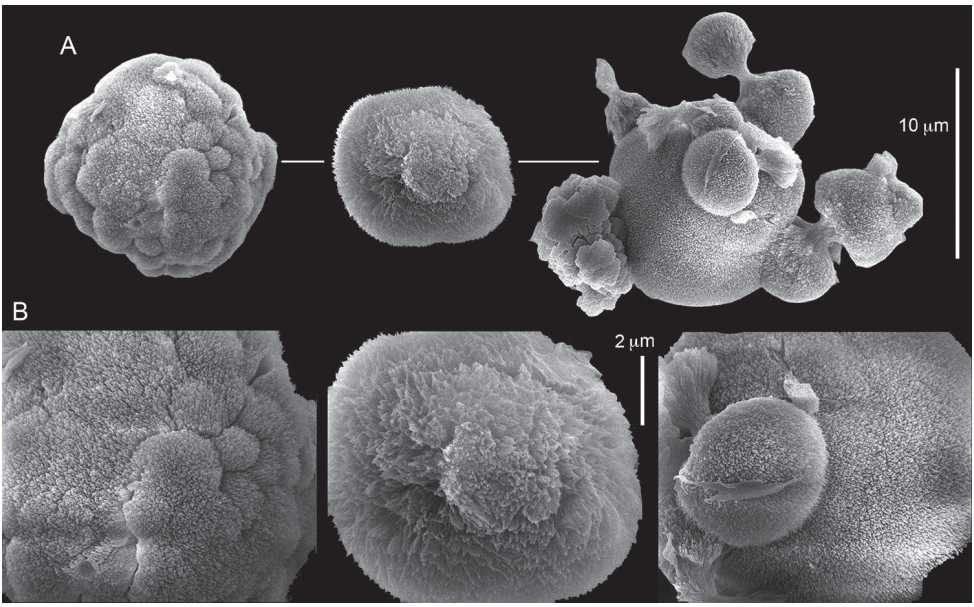

Figure 13. *Conglomeratusclera coerulea* (May, 1898), ZMTAU Co 35712. **A–B** bristly surface of spherules and spheres.

common in the tissues compared to ZMH C 2518. Under the light microscope wet preparations of the tentacles removed from ZMB Cni 3671 revealed some conglomerates along with spheres of various sizes.

The type material of *Cespitularia taeniata* (ZMH C 2519) comprises two flaccid colonies and two additional fragments (Figure 1C). The colonies are 3–4.5 cm high by 2–2.5 cm wide. Their polyparies consist of short branches bearing non-retractile polyps; some polyps were also found on the upper part of the stalk. The tentacles feature one row of 16–18 pointed pinnules, evenly placed along the edges with a free space between adjacent ones. Sclerites were found in the base of the colonies and the branches (Figure 4) but none in the polyps. They are conglomerates comprised mainly of spherules (Figure 4A) and some predominantly of spheres (Figure 4B), the latter measuring up to 0.018 mm in diameter. In addition, some cylinder-like small sclerites featuring round tips are also found, measuring 0.002–0.003 mm (Figure 4C). It should be noted that the aggregates tend to disintegrate during the sclerite preparation and therefore their actual dimensions cannot be determined.

A colony labeled as ZMH C 2375 (Figure 1D) features tentacles with 12–14 pinnules and sclerites similar to ZMH C 2519. ZMH C 2375 is listed in the museum's catalog as the "Typus von *Ammothea bauiana* May, 1898" along with a note that Gohar had corrected the identification in 1938 to *C. taeniata*. Both colonies, ZMH C 2519 and ZMH C 2375, are light gray-beige. *Conglomeratusclera taeniata* was described by Thomson and Dean (1931: 33) as being "near to but distinct from *Cespitularia coerulea*". The current findings indicate that there are only some small morphological differ-

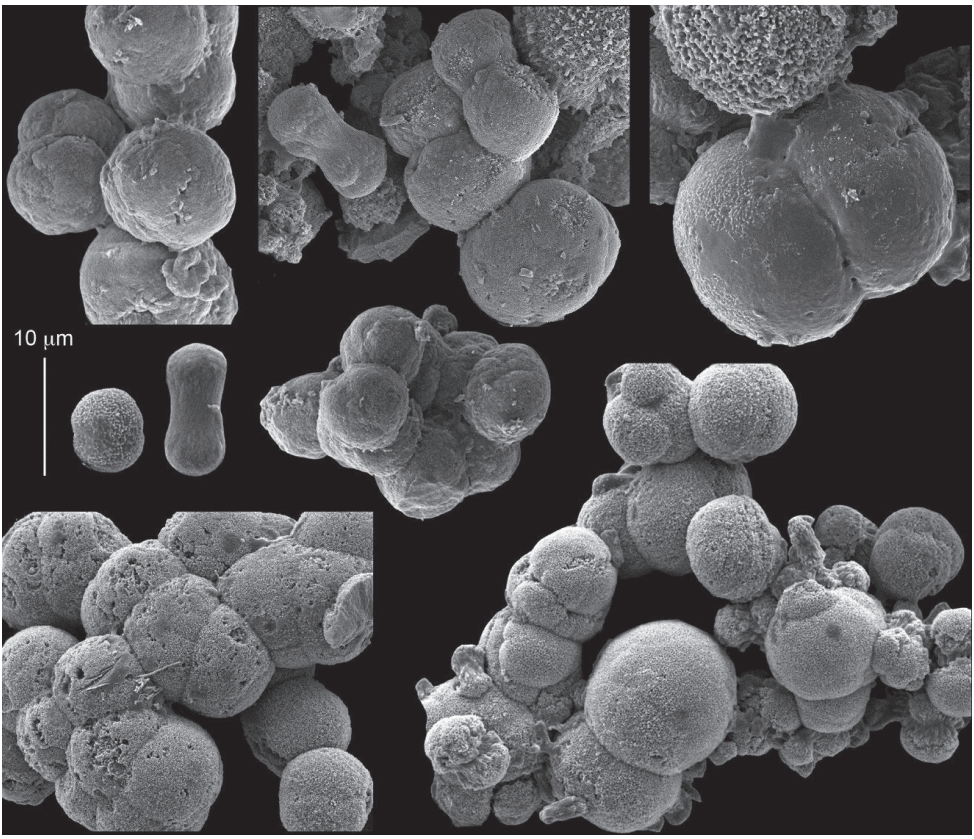

Figure 14. *Conglomeratusclera coerulea* (May, 1898), ZMTAU Co 35131. Conglomerate sclerites composed of spheres and spherules, individual elongate double head.

ences in the colony and polyp dimensions between the two species, and therefore, the above statement appears reasonable. Utinomi (1950) described the *C. taeniata* specimen identified by him as having 10–12 pinnules, slightly lower in range compared to the 12–14 pinnules of C 2375. The current examination of the types of both *C. coerulea* and *C. taeniata* revealed that despite the erroneous statement that they have no sclerites, they feature quite similar sclerites. It is therefore suggested that the similarity between the two species indicates that the above-reported morphological differences in the number of pinnules of the two types represent intra-specific variation. The sequencing results obtained in the current study along with the morphological findings further substantiate this conclusion, as colonies with a single row of 8–22 pinnules share similar DNA sequences (see ahead). Therefore, it is concluded that *C. coerulea* and *C. taeniata sensu stricto* should be synonymized, and both are now designated under *Conglomeratusclera coerulea*.

Remarks. The original descriptions of *Cespitularia coerulea* by May (1898, 1899) indicated an absence of sclerites in the colony. In contrast, the current findings dem-

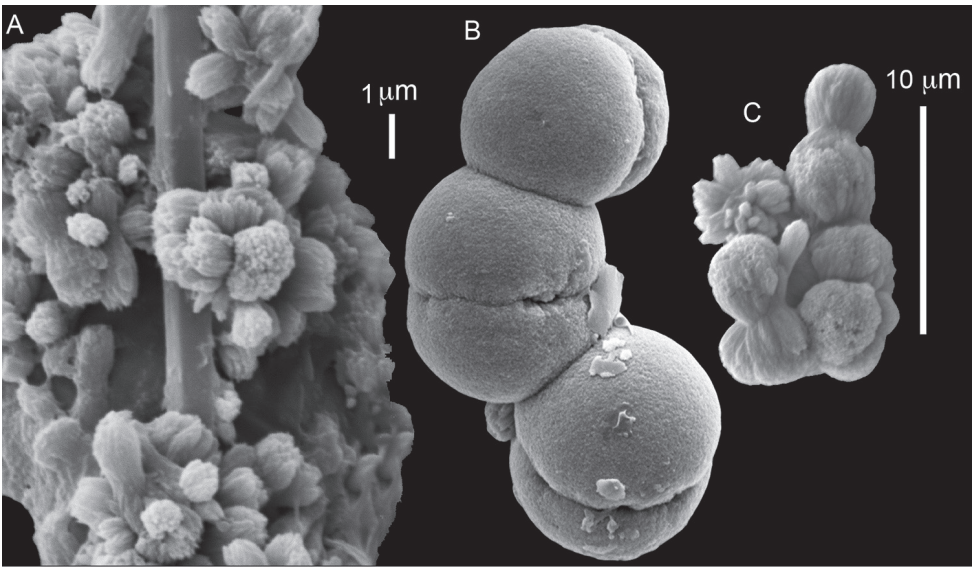

Figure 15. *Conglomeratusclera coerulea* (May, 1898), ZMTAU Co 36129. **A** conglomerate of bristly dumbbells **B** conglomerate of spheres **C** conglomerate of dumbbells. Scale at **A** also applies to **B**.

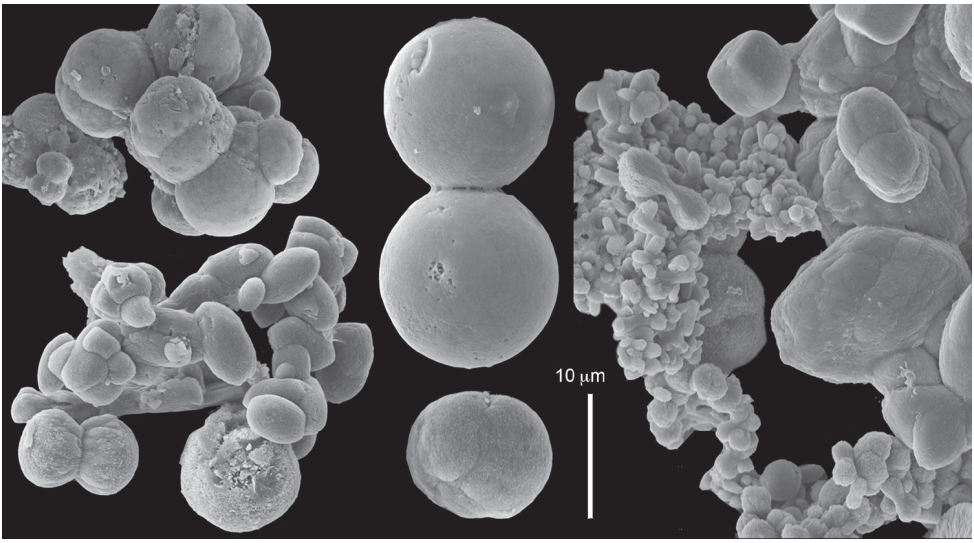

Figure 16. *Conglomeratusclera coerulea* (May, 1898), ZMTAU Co 36013. Conglomerate sclerites composed of spheres, spherules and dumbbells, individual sphere.

onstrate the presence in the syntypes of a novel type of sclerite, depicted here for the first time. These sclerites are composed of agglomerated calcite-constructed minute substructures of various morphologies, mostly spherules, spheres, and double heads appearing in different arrangements. They were probably overlooked in previous stud-

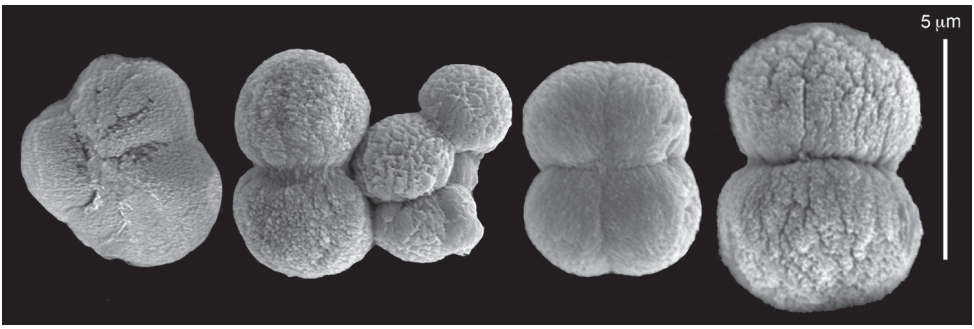

Figure 17. *Conglomeratusclera coerulea* (May, 1898), BMNH 1933.3.13.175. Spheres and double heads with bristly surfaces. Some double heads joined to form a more cross-like sclerite.

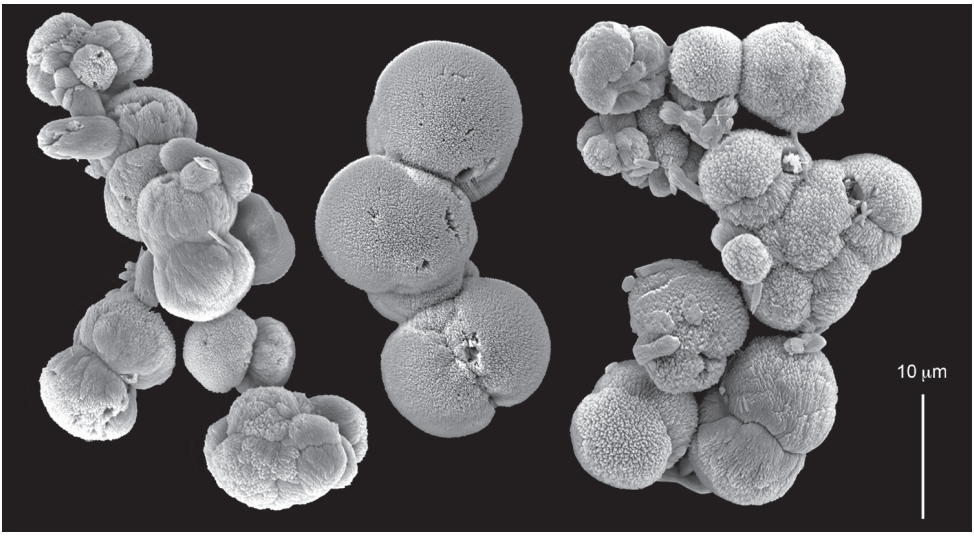

Figure 18. *Conglomeratusclera coerulea* (May, 1898), BMNH 1912.2.24.65. Conglomerate sclerites composed of spheres and spherules. Bristly surface is noted.

ies due to their minute size and also occasional low abundance. Moreover, the unusual irregular sclerite morphology with almost no definite structure (Figures 2–4), may have caused the misinterpretation concerning their potential as octocoral sclerites to be used as diagnostic characters for taxonomic purposes.

Since the original description of *C. coerulea* a number of studies have assigned specimens to that species. Thomson and Henderson (1906) identified a multi-branched colony from Zanzibar, with one row of pinnules and no sclerites. Later, Thomson and Mackinnon (1910) described a similar colony from Cargados Carajos (Mauritius), noting that when alive the colony was "vivid grass green, but after preservation it faded to cream", a feature that has been widely observed in the current study (see below). Thomson and Dean (1931) identified *C. coerulea* from Kawas-

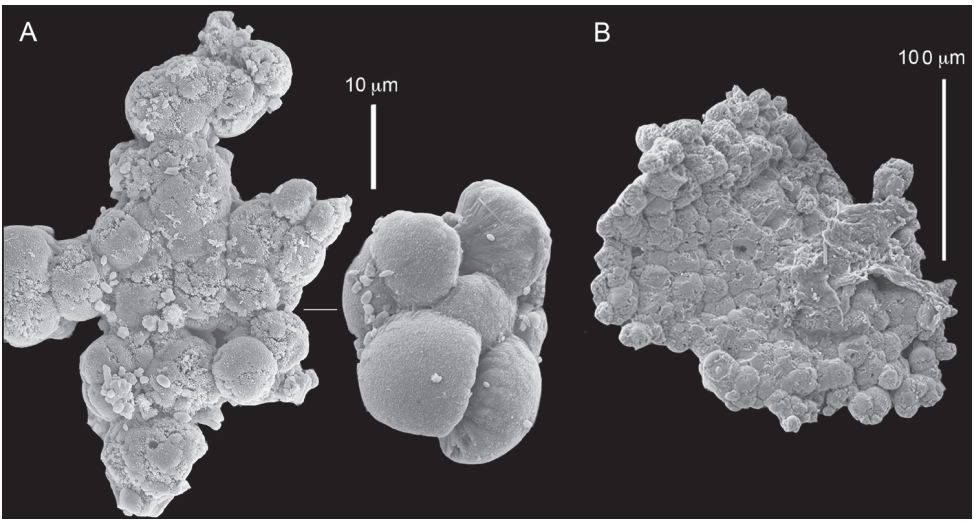

Figure 19. *Conglomeratusclera coerulea* (May, 1898), BMNH 1912.2.24.66. **A** conglomerate sclerites composed of spheres and spherules **B** plate-like conglomerate of spherules.

sang, Indonesia, obtained in the course of the Siboga Expedition, featuring a single row of pinnules and no sclerites, with no mention of the number of pinnules in the polyps. Next, Roxas (1933) identified the same species from Sabang, near Puerto Galera, Mindoro, Philippines, with one row of 14–18 pinnules and no sclerites. Interestingly, that study of Roxas's study was the first to indicate number of the pinnules in that species. In general, the above octocoral samples are in agreement with the original description by May (1898), but all the above authors nonetheless failed to detect any sclerites.

Color. When alive, the color of colonies ranges from vibrantly bluish-purple, light green, light yellow-beige, light cream to almost white (see Figure 5A, B). The alcohol-preserved colonies lose their vibrant colors and mostly become pale cream, gray, or beige.

Morphological variation. In the current study, examination of the colonies from Green Is., Yonaguni Is. and Madagascar was based on both morphological characters (colony shape, pinnule count, and sclerite features), along with DNA sequencing; the latter enabled us to construct a phylogenetic tree (Figure 6). In general, the colony shape of all the colonies listed in Material Examined was in agreement with the syntypes shown above, except for colony size. All colonies exhibited one row of pinnules along the margins of the polyp tentacles, with a variable number of pinnules, ranging from 8 to 22 per row. In some colonies the tentacles were partially or completely withdrawn or the pinnules fully contracted, probably due to the preservation process. In several cases the polyps were fully expanded and in others partially or fully contracted.

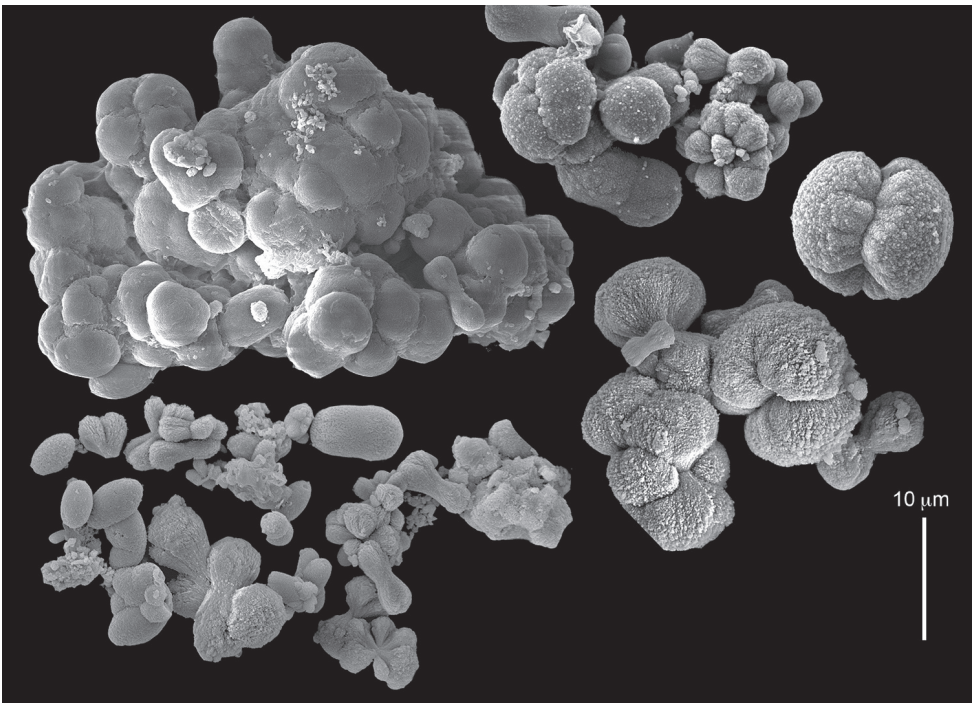

Figure 20. *Conglomeratusclera coerulea* (May, 1898), BMNH 1912.2.24.67. Conglomerate sclerites composed of spheres, spherules and dumbbells. Bristly surfaces of some sclerites is noted.

The following findings denote the number of pinnules found in some of the sequenced colonies (Figure 6), demonstrating the variability in pinnule count. The respective colonies from Green Island are ZMTAU Co 35717: 8, Co 35747: 8, Co 35774: 8, Co 35742: 8–9, Co 35750: 8–9, Co 35753: 8–9, Co 35714: 10–11, Co 35712: 11–12, Co 33045: 11–16, Co 35692: 11–16, Co 35707: 11–16, Co 35699: 12–15, Co 35709: 15, Co 35758: 15, Co 35693: 15–16, Co 35729: 15–18, Co 35693: 16, Co 35725: 16–17, Co 35748: 16–18, Co 35763: 18–20, Co 35756: 20, Co 35760: 20, Co 35736: 21–22 and Co 35737: 21–22; colonies with fully contracted pinnules Co 35706, Co 35708, Co 35710, Co 35731, Co 35752, Co 35765, and Co 35766. Colonies from Yonaguni Is are ZMTAU Co 35131: 9–12 pinnules, Co 35132: 12–14 and Co 35134: 11–13. Colonies from Madagascar: ZMTAU Co 36013: 10–13 pinnules and Co 36129: 12–13.

The sclerites of the colonies noted above featured the full array of morphologies, mostly corresponding to that of the syntypes (Figures 2–3). To demonstrate the vast variation in shape and size of the sclerites, SEM images of sclerites of several sequenced colonies are presented for the Taiwan material: ZMTAU Co 35692 (Figure 7), Co 35737 (Figure 8), Co 35765 (Figure 9), Co 35709 (Figure 10), Co 35707 (Figure 11), Co 35710 (Figure 12), and Co 35712 (Figure 13), Yonaguni: ZMTAU Co 35131 (Figure 14)

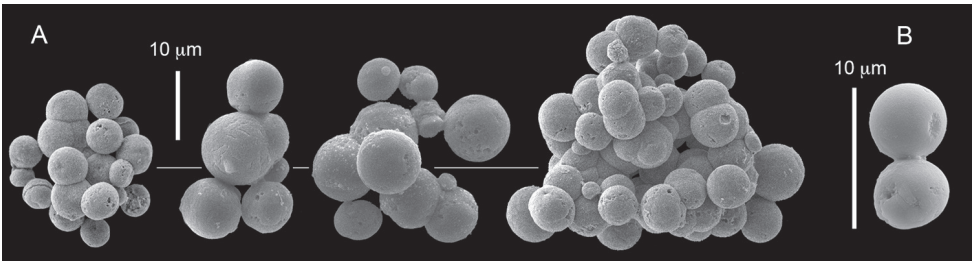

Figure 21. *Conglomeratusclera coerulea* (May, 1898), BMNH USNM 60795. Conglomerate sclerites of spheres and spherules.

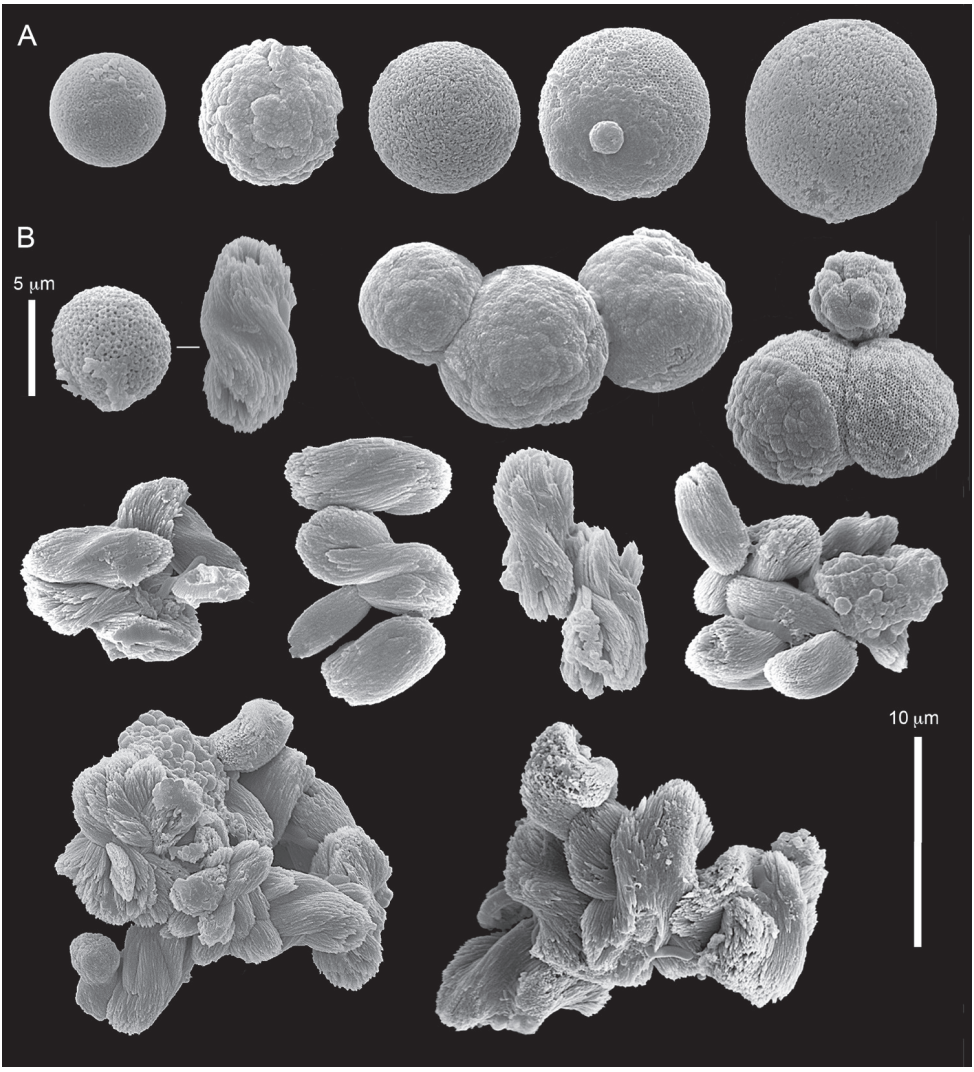

Figure 22. *Conglomeratusclera coerulea* (May, 1898), RMNH Coel 42160. **A** spheres **B** sphere, twisted dumbbell and conglomerate sclerites composed of spheres and twisted dumbbells.

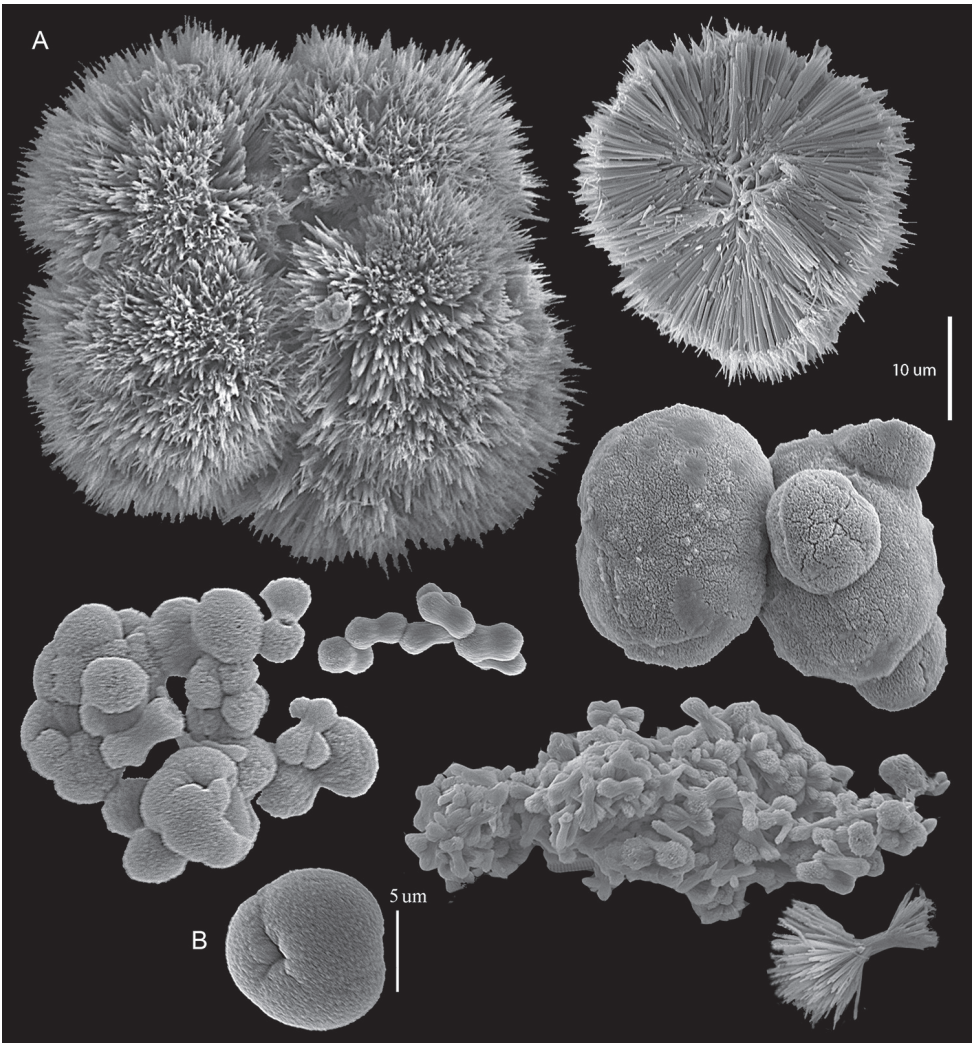

Figure 23. *Conglomeratusclera coerulea* (May, 1898), RMNH Coel 42161. Conglomerate sclerites composed of spheres and spherules. Bristly surface of spheres is noted.

and Madagascar Co 36129 (Figure 15), and Co 36013 (Figure 16). Figures 7–16 demonstrate the morphological variability of the sclerites, with all being conglomerates comprised mainly of spheres and spherules and occasionally dumbbells. The SEM images revealed that their outer surface is sometimes bristly (Figures 7B–D, 8B, 13A–B, 14, 15A, 17) but commonly rather smooth (Figures 8A, 10A–B, 11A–B, 15B, 16). It is interesting to note that the spheres are sometimes embedded in a calcareous lamella-like structure (Figure 7A). Dumbbells were revealed in some colonies (Figures 8B, 12B, 14, 15C, 17) as well as twisted dumbbells (Figures 9, 11C, 12B). Similarly, as noted above for the syntypes, the above SEM images indicate that the aggregates tend to disintegrate during sclerite preparation and therefore their actual dimensions cannot be determined.

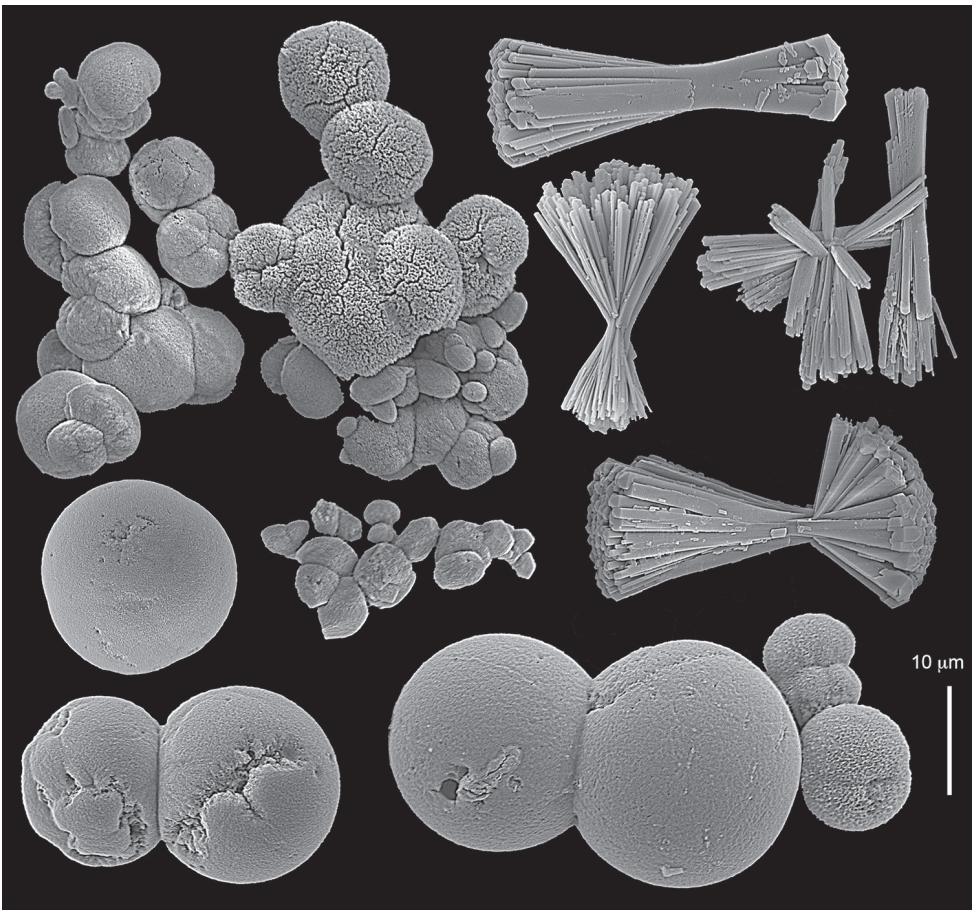

Figure 24. *Conglomeratusclera coerulea* (May, 1898), RMNH Coel 42161. Conglomerate sclerites composed of spheres and spherules. Some crystalline bundles are presented.

The molecular results indicate that despite the differences in pinnule count and sclerite morphology, all the colonies should be assigned to the same species (Figure 6). Consequently, the pinnule count is of no diagnostic value for species delineation within *Conglomeratusclera*. *C. coerulea* thus accommodates colonies with one row of pinnules on the margins of the polyp tentacles, but featuring a remarkable range of pinnule numbers (see above). In addition, the variable sclerite morphologies found in the different colonies (Figures 7–16) both encompass and exceed the range observed among the syntypes of *C. coerulea* (Figures 2A–B). The current results provide further support for the recent findings of McFadden et al. (2017) who argue that the pinnule count used in the taxonomy of Xeniidae, explicitly in the genus *Ovabunda* (see references in Halàsz et al. 2014), is not indicative of species boundaries. It should be noted that in contrast to the relatively uniform morphology of *Ovabunda* sclerites recorded across the four genetic clades presented by McFadden et al. (2017), colonies of *C. coerulea* exhibit an unprecedented and bewildering array of sclerite morphologies (Figures 2A, B, 7–16).

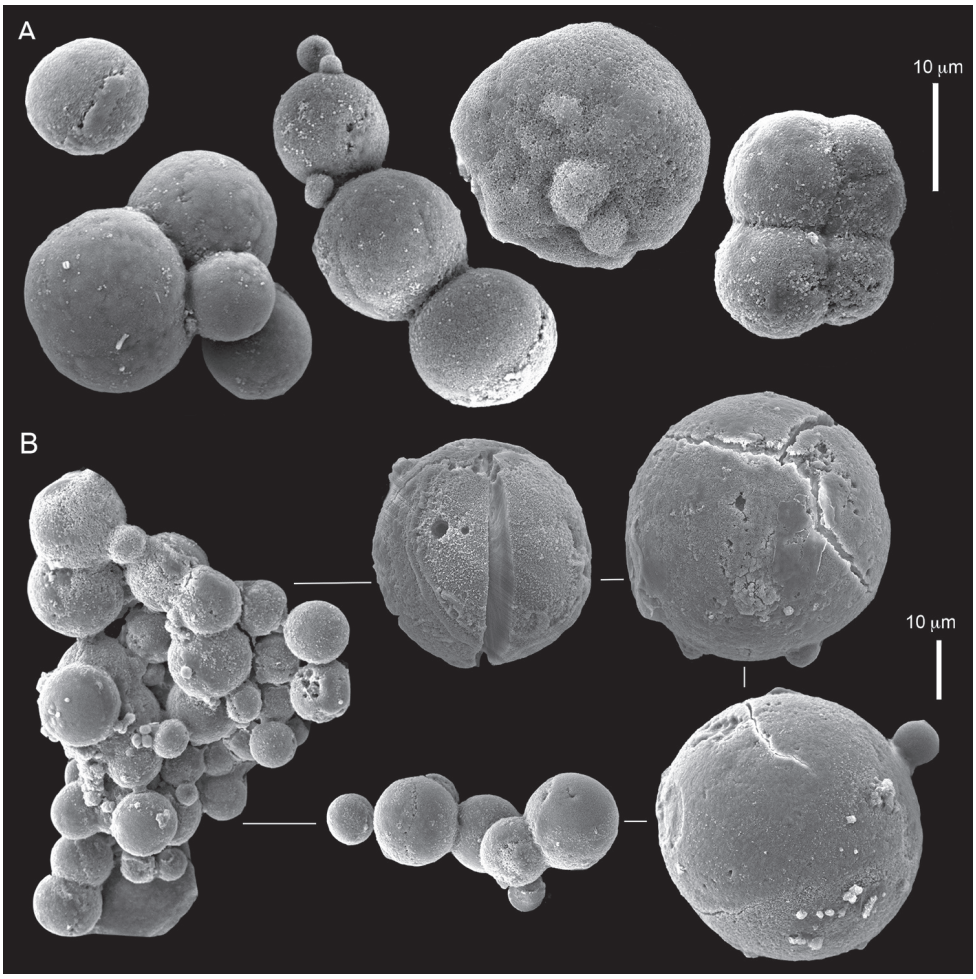

Figure 25. *Conglomeratusclera coerulea* (May, 1898), RMNH Coel 42162. **A–B** Conglomerate sclerites composed of spheres and spherules, some double heads joined to form a more cross-like sclerite.

Material that was examined, but not sequenced, comprised both freshly collected colonies and museum specimens. Their colony and polyp morphologies, including the pinnule counts, are in agreement with the findings presented above. Noteworthy are some colonies for which SEM or light microscopy could not detect any sclerites. There are several suggested reasons for this: (1) actual lack of sclerites; (2) their low incidence which led to a failure to detect them by SEM; or (3) preservation procedures, such as acidic conditions that may have caused sclerite dissolution.

The museum material examined included colonies from the BMNH, all collected from the western Indian Ocean (see above). Some of the colonies were originally identified by L.M.I. Macfadyen as *Cespitularia coerulea* (BMNH 1912.2.24.66 and 1933.3.13.175; Figure 17), *C. mollis* (BMNH 1933.313.177), *C. taeniata* (BMNH 1912.2.24.65, 1933.5.3.301 and 1933.3.13.176) and *Cespitularia wisharti* Hickson,

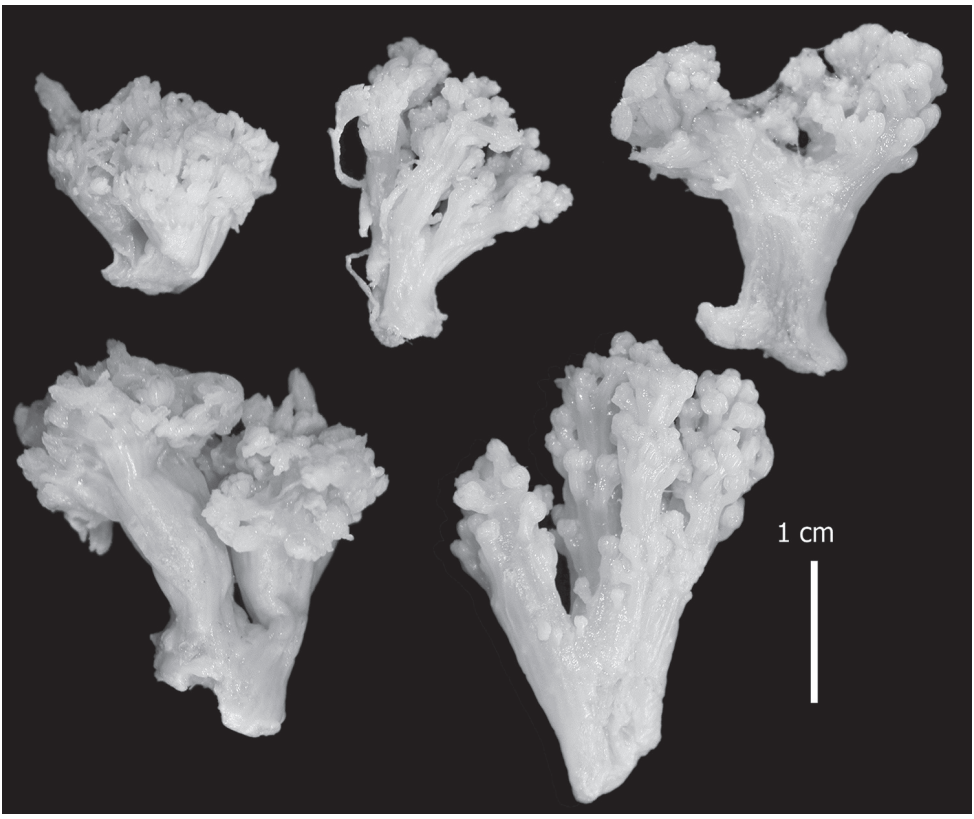

Figure 26. *Conglomeratusclera robusta* (Tixier-Durivault, 1966), syntypes MNH00000167.

1931 (BMNH 1934.3.28.10). These BMNH colonies feature one row of 8–13 pinnules along each side of their tentacles and the morphology of their sclerites corresponds to that of *Conglomeratuscslera coerulea* [e.g., BMNH 1912.2.24.65 (Figure 18), 1912.2.24.66 (Figure 19), 1912.2.24.67 (Figure 20)]. The morphological examination therefore indicates that the BMNH material should be assigned to the above species. The sclerites of the colony from the Great Barrier Reef, Australia, USNM 60795 (Figure 21), as well as those of USNM 54000 and 54003 (sclerites not shown), collected in Madagascar, similarly confirmed them to be *C. coerulea*. The RMNH material too revealed colonies that have now been assigned by us to *C. coerulea*, featuring one row of 8–16 pinnules along each side of their tentacles as well as sclerites: RMNH Coel 42160 (Figure 22), Coel 42161 (Figures 23–24) and RMNH Coel 42162 (Figure 25). These images reveal spheres, either in a conglomerated form or individuals (Figures 22–25), and in other colonies mostly twisted dumbbells, either aggregated or individual (Figure 22). Interestingly, some crystalline bundles were noted among the spheres (Figure 24).

Distribution. Kenya; Zanzibar; Tanzania; Glorioso Islands; Mauritius; Seychelles; Mayotte; Taiwan; Philippines; Japan (Tanabe, Wakayama, Shikoku); Ryukyu Archipelago; Indonesia.

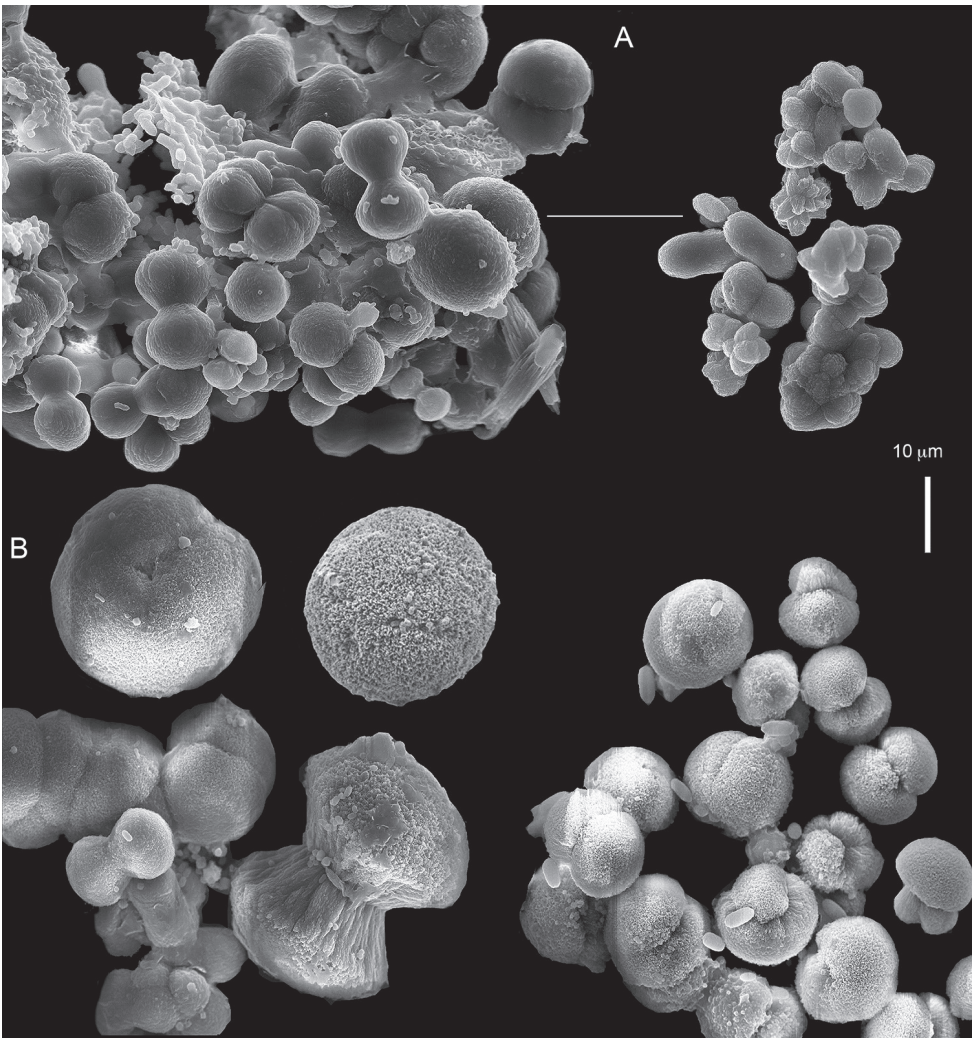

Figure 27. *Conglomeratusclera robusta* (Tixier-Durivault, 1966). **A** Conglomerate sclerites composed of spheres and spherules **B** Spheres, dumbbell, and conglomerate sclerites.

Conglomeratusclera robusta (Tixier-Durivault, 1966)

Figures 26–28

Cespitularia robusta Tixier-Durivault, 1966: 335–356; Janes 2008: 604–605.

Description. Examination of the type material of *Cespitularia robusta* Tixier-Durivault, 1966 (MNH00000167) revealed five colonies (Figure 26), all in agreement with their original description. The tentacles bear two rows of pinnules along each side with an indication of a third row; the outermost row features 12–15 pinnules. The sclerites depicted in the original description are spheres and spherules, also in the form of aggregates (p. 356: fig. 321 C–N). The SEM images of the sclerites (Figure 27) reveal mor-

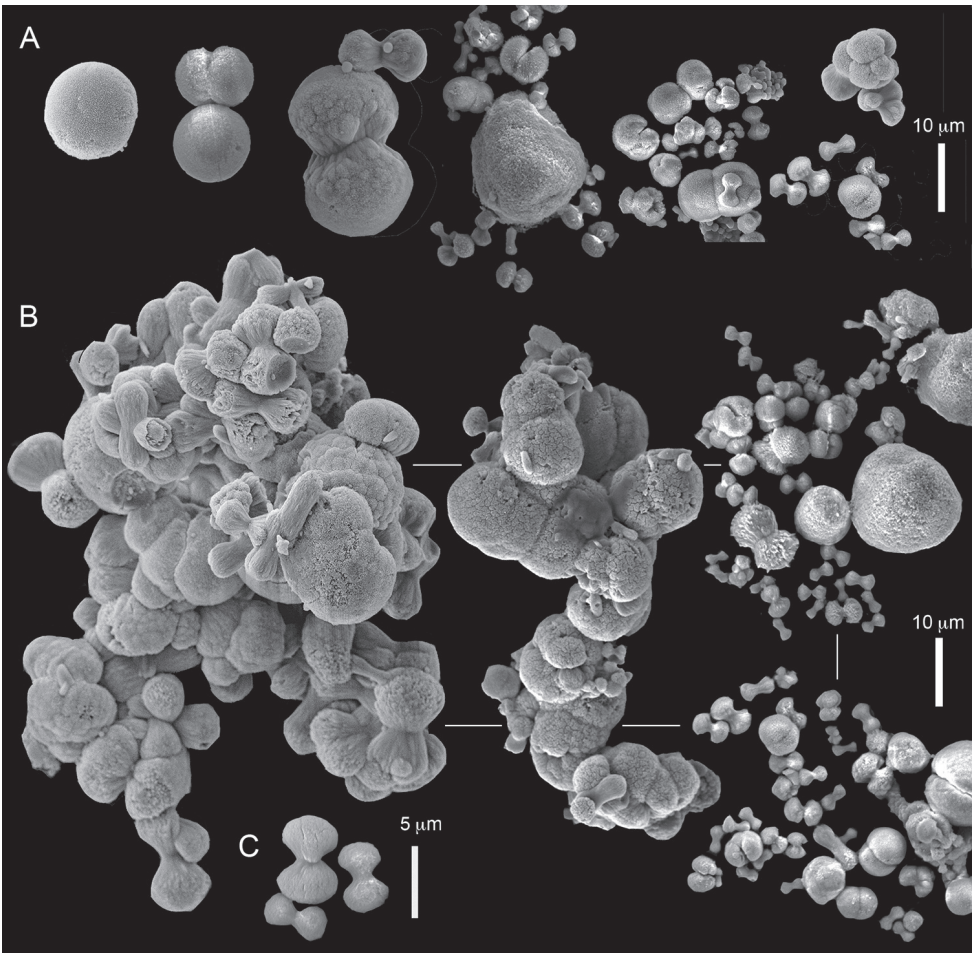

Figure 28. *Conglomeratusclera robusta* (Tixier-Durivault, 1966) RMNH Coel 38672. **A–B** conglomerate sclerites composed of spheres, spherules, and dumbbells. **C** dumbbell sclerites.

phologies similar to those found in *C. coerulea* (see above), and therefore led us to assign the species to *Conglomeratusclera* n. gen instead of *Cespitularia*. Subsequent examination of *C. robusta* (RMNH Coel 38672), identified by Janes (2008), similarly confirmed his findings but based on the sclerite SEM images of that colony (Figure 28), the generic assignment is likewise changed to *Conglomeratusclera*.

The colonies assigned by us to *C. coerulea* feature one row of pinnules along the margins of the tentacles, whereas *C. robusta* has two rows. In order to determine whether a difference in pinnule-row count is indeed diagnostic for species delineation in *Conglomeratusclera*, corresponding fresh colonies with two pinnule-rows should be sequenced. Therefore, for the time being only the generic status of *C. robusta* is changed, making it the second species in the new genus.

Distribution. Mayotte; Aride Island, Seychelles.

***Caementabunda* gen. n.**
http://zoobank.org/899AF711-D0A6-43F7-A3A6-75F481DF29A6

Type species. *Cespitularia simplex* Thomson & Dean, 1931

Diagnosis. Colonies quite flaccid with a distinct but short encrusting base bearing primary lobes, sometimes divided into secondary ones. Non-retractile monomorphic polyps found on the lobes and occasionally down on some parts of the base. The spherical-oval sclerites are composed of a myriad of densely packed chip-like microscleres. Zooxanthellate.

Etymology. The generic name refers to the microstructure of the sclerites, which are composed of multitudes of microscleres, resembling aggregates of cement chips. The name is derived from the Latin *caementum*, cement, and *abunda* meaning copious. Gender feminine.

***Caementabunda simplex* (Thomson & Dean, 1931)**
Figures 5C–D, 29–37

Cespitularia simplex Thomson & Dean, 1931: 33–34; Macfadyen 1936:27; Verseveldt 1971: 62; Janes 2008: 606–608; Janes 2013: 198 (listed only); McFadden et al. 2014: 249 (listed only), *Cespitularia turgida* Verseveldt, 1971: 61–62.

Material. Syntype: INDONESIA: ZMA 2344, Siboga Exped., Sta. 40, 12 m depth, Kawassang**. Other material**: **SEYCHELLES**: RMNH Coel 38673, Southern coast of Aride I. (04°13'S; 55°40'E), <20 m depth, 18 December 1992; **MADAGASCAR**: RMNH Coel 6697, Nosy Be, west of Andilina, 24 August, 1967, 20 m depth; RMNH Coel 42168, Stn. 22, 21 December 1999; RMNH Coel 42169; **PHILIPPINES:** Cebu Strait Exped., Sta. CEB. 1, Cebu Strait, Olango Channel, east side of Olango Is., USNM 60493, Sulu Archipelago, 6°07'N, 121°00'E, R/V Albatross; **AUSTRALIA:** USNM 60794, Flinders Reef, Great Barrier Reef, November 1981; BMNH 1934.3.28.8, Great Barrier Reef Exped., Sta. 10, dredge, 22 February 1929; 1982.11.17, Great Barrier Reef, Flinders Reef, South Coral Sea, southern outer slope, 10–15 m depth, coll. Z. Dinesen; BMNH 1982.11.18, similar details; **JAPAN**: ZMTAU Co 31642, off Danno, Yonaguni Is., Ryukyu Archipelago, 24°27'N, 122°57'E, 15 m depth, coll. Y. Benayahu, 13 November 1992; ZMTAU Co 31638, Mao Cave, Shimoji Is., Ryukyu Archipelago, 10 m depth, coll. Y. Benayahu, 19 November 1992; ZMTAU Co 35120, Umabanazaki Point, Yonaguni Is., Ryukyu Archipelago, 8–12 m depth, coll. Y. Benayahu, 3 June 2010; **MADAGASCAR**: ZMTAU Co 36057, three specimens; ZMTAU Co 36076, 4 Frères, 13°00.142'S, 48°29.099'E, 6–14 m depth, coll. Y. Benayahu, 2 December 2012; ZMTAU Co 36065, 4 Frères, 12°59.655'S, 48°29.248'E, 4–15 m depth, coll. Y. Benayahu, 1 December 2012, four specimens; ZMTAU Co 36115, Ronald Point, Nosy Be, 13°23.530'S, 48°00.143'E, 19–27 m depth, coll. Y. Benayahu, 3 December 2012; ZMTAU Co 36122, Ronald Point, Nosy Be, 13°29.032'S, 47°58.721'E, 2–4 m depth, coll. Y. Benayahu, 03 December

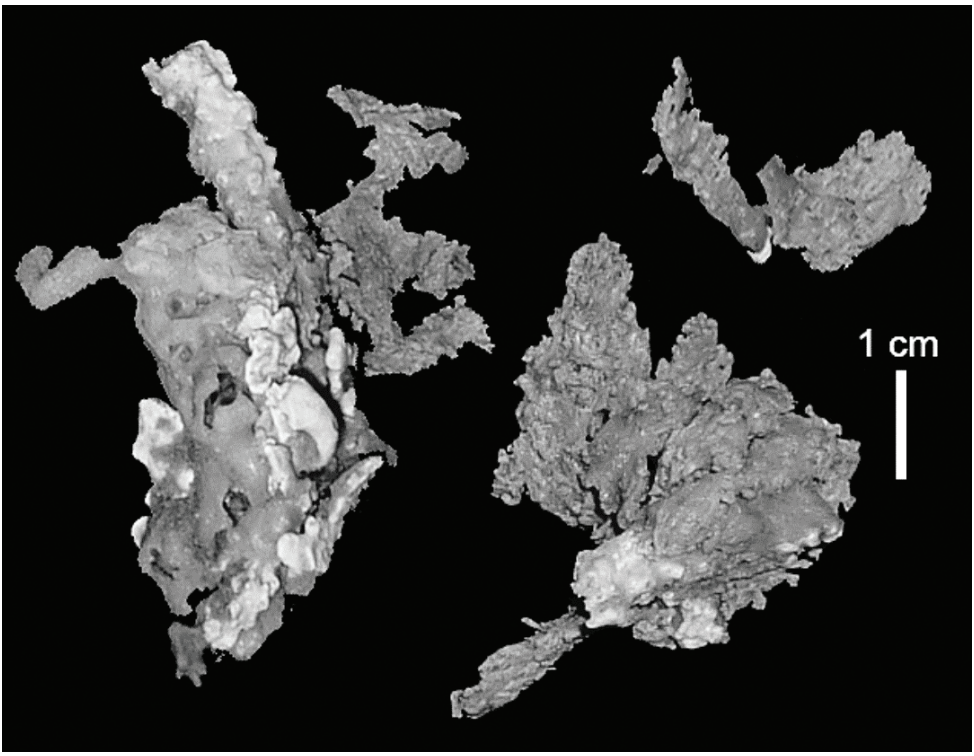

Figure 29. *Caementabunda simplex* (Thomson & Dean, 1931) Syntypes, ZMA 2344.

2012, two specimens; ZMTAU Co 36127, details as before; **TAIWAN**: Co 33021, Chaikou, Green Is., Taiwan, 22°40'40"N, 121°28'20"E, 3–6 m depth, coll. Y. Benayahu, 13 July 2005; ZMTAU Co 35715, Shihlang, Green Is., 22°39.425'N, 121°28.399'E, 8–12 m depth, coll. Y. Benayahu, 3 September 2012; ZMTAU Co 33022, Lomenyen, Green Is., 22°40'56"N, 121°30'06"E, 3–25 m depth, coll. Y. Benayahu, 12 July 2005; ZMTAU Co 35713, details as before, three specimens; ZMTAU Co 35701, details as before, four specimens; ZMTAU Co 35757, Shihlang, Green Is., 22°39.425'N, 121°28.399'E, 7–10 m depth, coll. Y. Benayahu, 5 September 2012, four specimens.

Description. The syntype RMNH Coel 2344 consists of three encrusting lobed colonies attached to calcareous fragments. The largest syntype is 3 cm high by 5 cm wide, the second 1.5 by 2.5 cm, and the third 2 by 3.5 cm (Figure 29). The finger-like lobes feature non-retractile polyps, some of which are found on the colony base. The polyp body is up to 2.8 mm long and the tentacles are up to 1.0 mm long. The tentacles bear one row of 12–14 pinnules along each of their margins. The short pinnules are closely set, with no space between adjacent ones. The preserved colonies are brown-beige. Sclerites are highly abundant and found in all parts of the colony. Under the light microscope they are ovoid or pear-shaped as fully confirmed by SEM (Figure 30A), measuring up to 0.022 mm in length. Occasionally they are arranged in groups (Figure 30B), but during preparation they tend to dissociate and become sin-

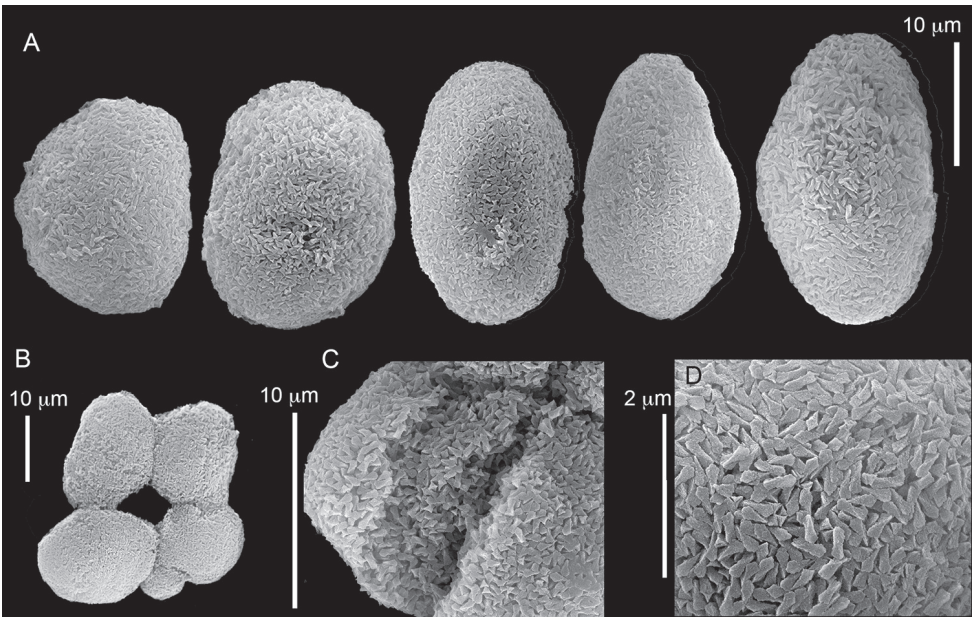

Figure 30. *Caementabunda simplex* (Thomson & Dean, 1931) Syntypes, ZMA 2344**. A** spheroid sclerites **B** cluster of spheroid sclerites **C** fractured spheroid showing densely packed chips-like microscleres **D** densely packed chips-like microscleres of spheroid's surface.

gles. SEM revealed the unique microstructure of the sclerites, which comprise densely packed chip-like microscleres (Figure 30C), giving the sclerite surface the appearance of cement-chip aggregates (Figure 30D).

Color. Live colonies are brown with yellow polyps (Figures 5C–D).

Remarks. The original description of the type by Thomson & Dean (1931: 34) is in agreement with the current findings, and indicates 10–12 pinnules compared to 12–14 noted by us. The sclerite size of 0.01 mm as given in the original description is incorrect and was later corrected by Verseveldt (1971). The latter study provides a better description of the sclerites as oblong, pear-like or angular in shape, 0.015–0.021 mm in diameter. The light microscopy used in the past clearly could not have revealed the unique surface microstructure of that species (Figure 30D).

Examination of the type of *Cespitularia turgida* Verseveldt, 1971 (RMNH Coel 6607) revealed *Caementabunda*-type sclerites (Figure 31). In the original description Verseveldt (1971: 62) presented a comparison between the type of *C. simplex* and his new species and noted the number of pinnules in the single row of both species being 10–12 in the latter *vs.* 5–6 in the former. The current examination of the type of *C. turgida* has confirmed the original morphological findings, while we also present here for the first time images of its sclerites.

Dr. Zena Dinesen (Department of Agriculture, Fisheries and Forestry, Queensland) provided us with an unpublished taxonomic manuscript dealing with some Xeniidae of Flinders Reefs, Great Barrier Reef. Under the collection numbers BMNH

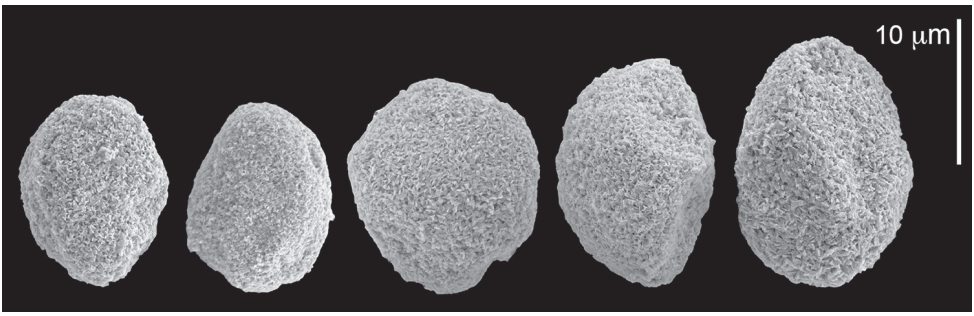

Figure 31. *Cespitularia turgida* Verseveldt, 1971, RMNH Coel 6607.

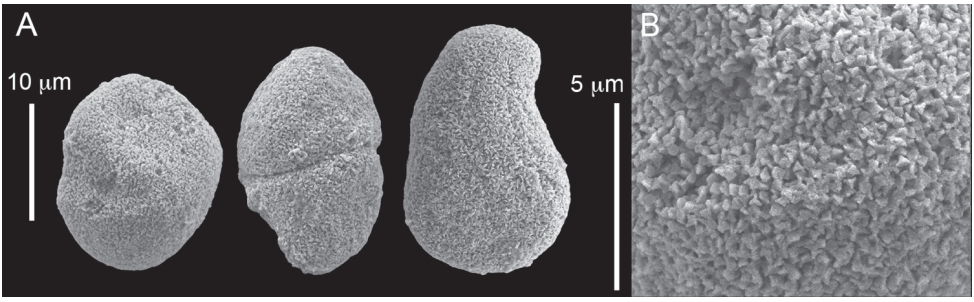

Figure 32. *Caementabunda simplex* (Thomson & Dean, 1931), BMNH 1982.11.17. **A** spheroid sclerites **B** densely packed chips-like microscleres of spheroid's surface.

1982.11.17 and 1982.11.18 there are colonies labeled as paratypes of *Efflatounaria flindensis* Dinesen. Recently Dr. Dinesen confirmed that these two colonies are provisional paratypes of unpublished species presented in her manuscript. Our examination of the colonies revealed *Caementabunda*-type sclerites (BMNH 1982.11.17: figure 32, 1982.11.17: figure 33). In addition, it confirmed the unpublished morphological description of the material which states that the pinnules: "Mostly very contracted, difficult to measure, in one row on each side of the tentacle with 5–12 (6–9) pinnules per row". Hence, the pinnule number corresponds to the original types of both *C. simplex* and of *C. turgida.* Similarly, examination of ZMTAU Co 35757 from Taiwan revealed *Caementabunda*-type sclerites (Figure 34) and 10–12 pinnules in a row, and ZMTAU Co 36127 and Co 36122 from Madagascar both had *Caementabunda*-type sclerites (Co 36122: figure 35) and 7–11 pinnules, thus falling within the range stated above. Based on these findings, it is concluded here that pinnule count is not diagnostic for species delineation in the newly-described genus *Caementabunda*. Similarly, it is concluded that *Cespitularia turgida* is a junior synonym of *Caementabunda simplex* and thus that both should be accommodated within this new genus.

Other material. All other material (see above) features the same sclerites described above for the syntype (Figure 30). Macfadyen (1936: 27) described in a colony from the Great Barrier Reef Expedition numerous minute discs about 0.010 mm in diameter, finely sculptured. The current examination of that colony (BMNH 1934.3.28.8)

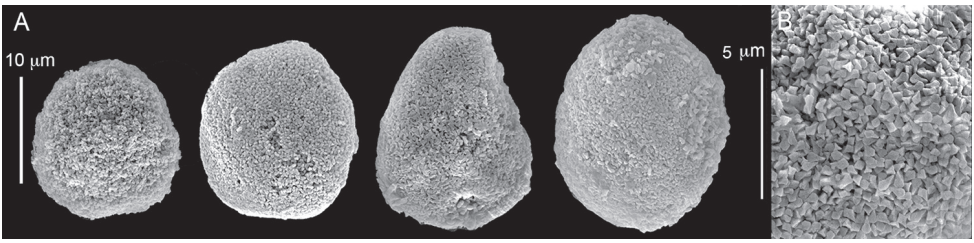

Figure 33. *Caementabunda simplex* (Thomson & Dean, 1931), BMNH 1982.11.18. **A** spheroid sclerites **B** densely packed chips-like microscleres of spheroid's surface.

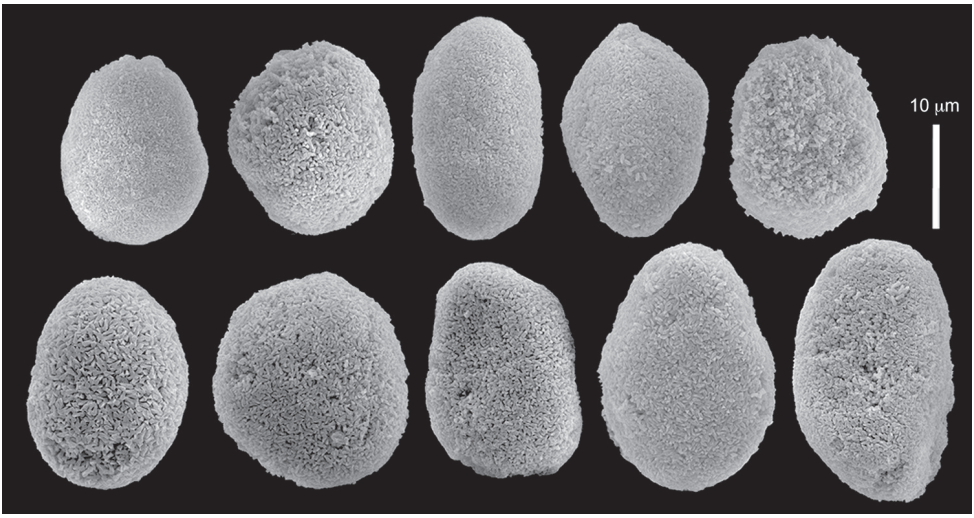

Figure 34. *Caementabunda simplex* (Thomson & Dean, 1931), ZMTAU Co 35757. Spheroid sclerites.

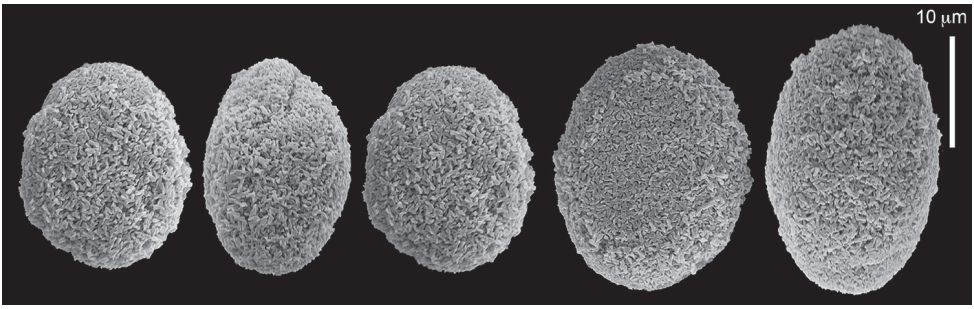

Figure 35. *Caementabunda simplex* (Thomson & Dean, 1931), ZMTAU Co 36122. Spheroid sclerites.

revealed *Caementabunda*-type sclerites. Likewise, RMNH Coel 38673 from Seychelles (see Janes 2008) and ZMTAU Co 31642 (Figure 36) feature this type of sclerite, as do USNM 60793 and 60794 collected in the Philippines (USNM 60793: Figure 37). Based on the current findings all of these colonies were assigned to the new genus.

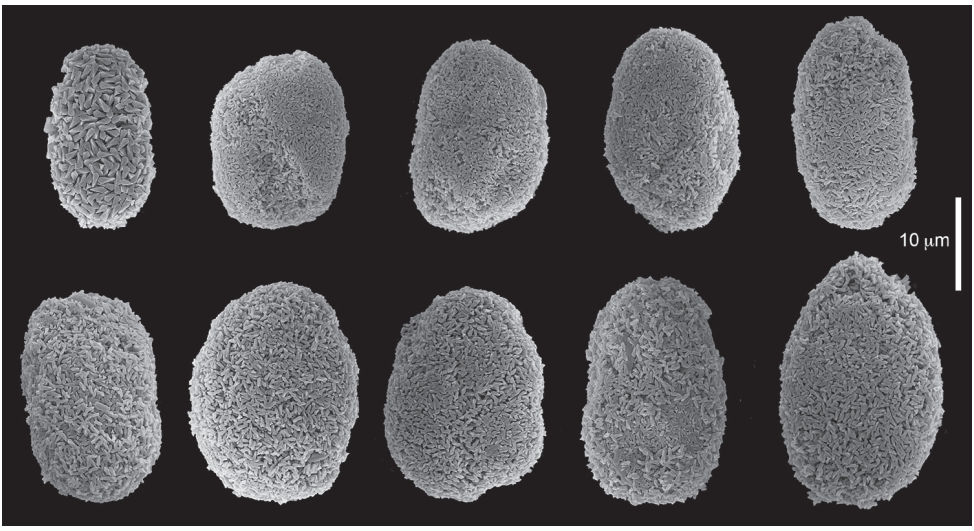

Figure 36. *Caementabunda simplex* (Thomson & Dean, 1931), ZMTAU Co 31642. Spheroid sclerites.

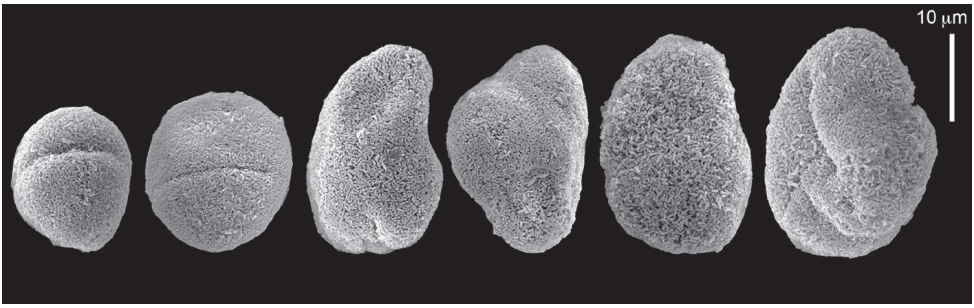

Figure 37. *Caementabunda simplex* (Thomson & Dean, 1931), USNM 60793. Spheroid sclerites.

Distribution. Green Island, Taiwan; Philippines; Great Barrier Reef; Sulawesi; Madagascar; Seychelles.

Molecular phylogenetic results. Sequences of *mtMutS* (582 bp), *igr1+COI* (767 bp) and *28S rDNA* (755 bp) were obtained from 46 individuals of *Conglomeratusclera* and nine individuals of *Caementabunda* from three different geographical locations: Madagascar; Green Is., Taiwan; Yonaguni Is., Japan (GenBank accession nos. MH071812–MH071969). All phylogenetic analyses of individual gene regions as well as the concatenated alignment (2104 bp) recovered trees in which specimens of *Conglomeratusclera* and *Caementabunda* formed two separate, well-supported clades (Figure 6). The average pairwise genetic distance (K2p) among individuals belonging to the two different clades was 3.6%, a value comparable to or higher than that observed among most other genera of xeniids (Figure 6).

All individuals of *Conglomeratusclera* shared identical sequences at *mtMutS* and *COI*, with just two exceptions: a single individual from Taiwan (ZMTAU Co35731) that differed by 0.2% at *mtMutS*; and one from Madagascar (ZMTAU Co36055)

that differed by 0.4% at *COI*. Variation at the *28S rDNA* locus ranged from 0–1.5%. Although a group of nine *Conglomeratusclera* colonies from Taiwan shared a *28S* genotype that differed from all others by three nucleotide substitutions (0.4%), there was no significant bootstrap or *a posteriori* support for them as a separate clade, and no obvious morphological differences to suggest that they might represent a different species.

All *Caementabunda* specimens also shared identical *mtMutS* and *COI* sequences, with the exception of a single individual (ZMTAU Co 36076) that differed by 0.1% at *COI*. At *28S* rDNA pairwise genetic distances (K2p) among individuals ranged from 0–0.8%, and a group of three specimens from Madagascar (ZMTAU Co 36065, Co 36076, Co 36122) differed from all others by three nucleotide substitutions. There was, however, no significant support for this clade, and no apparent morphological differences between these individuals and others of *C. simplex*.

Conclusions

Morphological and molecular phylogenetic analyses support the reassignment of the former species *Cespitularia coerulea* and *C. simplex* into two separate genera; *Conglomeratusclera* n. gen. and *Caementabunda* n. gen., respectively. They are distinguished by differences in sclerite microstructure as well as genetic distances comparable to those among other well-defined genera of the family Xeniidae. In addition, the findings justify synonymy of *C. taeniata* and *C. turgida* with each of these two new genera, respectively. We are at present only able to distinguish a single species in each of the new genera, based on both morphology and genetics. It should be noted that the status of *C. robusta* as a second species of *Conglomeratusclera* remains to be verified genetically. A recent study of the xeniid genus *Ovabunda* found a lack of congruence between the morphological characters traditionally used to diagnose species, in particular the number of rows of pinnules and pinnules per row, and genetic evidence of species boundaries (McFadden et al. 2017). In that case, evidence from multiple segregating nuclear markers was necessary to delineate species that shared identical or very similar mitochondrial haplotypes. Therefore, it is possible that data from additional genetic markers might detect further differences among those individuals with variant 28S rDNA genotypes that we have assigned here to *Conglomeratusclera coerulea* and *Caementabunda simplex*. As currently circumscribed, both of these new genera and in particular the respective species occur over a wide geographic range from the south-western Indian Ocean (Madagascar) to Japan.

Acknowledgements

Part of this research (Applications DE-TAF-662 and GB TAF 3027) received support from the SYNTHESYS Project http://www.synthesys.info/ which is financed by the European Community Research Infrastructure Action under the FP7 “Capacities” Program. It was also in part supported by a Temminck Fellowship, Naturalis Biodiver-

sity Center, and the Israel Cohen Chair in Environmental Zoology to Y.B. We thank the curators at the following museums for enabling examination of material in their possession: A. Cabrinovic, The Natural History Museum London; C. Lüter, Zoologisches Museum Berlin; A. Schmidt-Rhaesa, Zoologisches Museum, Hamburg; J. van Egmond, Naturalis Biodiversity Center, formerly Rijksmuseum van Natuurlijke Historie, Leiden; S.D. Cairns, Smithsonian National Museum of Natural History, Washington DC and A. Andouche, Musee d'Histoire Naturelle, Paris. Support for collection field trips was generously provided in Taiwan by M-S. Jeng, Biodiversity Research Center, Academia Sinica; in Japan by J. Tanaka, Department of Chemistry, Biology and Marine Science, University of the Ryukyus, and in Madagascar by M. Aknin, University of Reunion Island. We acknowledge A. Shlagman for professional curatorial skills, V. Wexler for digital editing, N. Paz for editorial assistance, M. Weis and A. Gonzalez, S. Shi, and P. Hong for technical assistance. We are grateful to the reviewers and the editor for their constructive comments that greatly improved the manuscript.

References

Aharonovich D, Benayahu Y (2011) Microstructure of octocoral sclerites for diagnosis of taxonomic features. Marine Biodiversity 42: 173–177. https://doi.org/10.1007/s12526-011-0102-3

Alderslade P (2001) Six new genera and six new species of soft corals, and some proposed familial and subfamilial changes within the Alcyonacea (Coelenterata: Octocorallia). Bulletin of the Biological Society of Washington 10: 15–65.

Benayahu Y (1990) Xeniidae (Cnidaria: Octocorallia) from the Red Sea with description of a new species. Zoologische Mededelingen Leiden 64: 113–120.

Benayahu Y (2010) A new genus of a soft coral of the family Xeniidae (Cnidaria: Octocorallia) from Japan. Galaxea, Journal of Coral Reef Studies 12: 53–64. https://doi.org/10.3755/galaxea.12.53

Benayahu Y, Jong MS, Perkol-Finkel S, Dai CF (2004) Soft corals (Octocorallia: Alcyonacea) from southern Taiwan: II. Species diversity and distributional patterns. Zoological Studies 43: 548–560.

Brundin JAZ (1896) Alcyonarien aus der Sammlung des zoologischen Museums in Upsala. Bihang till Kongl. Svenska Vetenskaps-Akademiens Handlingar XXII, Afd. IV, N 3: 1–22.

Cordeiro R, Ofwegen L van, Williams G (2018) World List of Octocorallia. *Cespitularia* Milne Edwards & Haime, 1850. Accessed through World Register of Marine Species. http://marinespecies.org/aphia.php?p=taxdetails&id=205452 [2018–02–21]

Darriba D, Taboada GL, Doallo, Posada D (2012) jModelTest 2: more models, new heuristics and parallel computing. Nature Methods 9: 772. https://doi.org/10.1038/nmeth.2109

Fabricius K, Alderslade P (2001) Soft Corals and Sea Fans: A Comprehensive Guide to the Tropical Shallow-Water Genera of the Central-West Pacific, the Indian Ocean and the Red Sea. Townsville, Australian Institute of Marine Science, 264 pp.

Folmer O, Black M, Hoeh W, Lutz R, Vrijenhoek R (1994) DNA primers for amplification of mitochondrial cytochrome c oxidase subunit I from diverse metazoan invertebrates. Molecular Marine Biology & Biotechnology 3: 294–299.

Gohar HAF (1938) On a new species of *Cespitularia* and two invalid species of *Xenia* and *Clavularia*. Journal of Zoology, B108 (3): 483–487. https://doi.org/10.1111/j.1469-7998.1938.tb08526.x

Halàsz A, McFadden CS, Aharonovich D, Toonen R, Benayahu Y (2014) A revision of the octocoral genus *Ovabunda* Alderslade, 2001 (Anthozoa, Octocorallia, Xeniidae). Zookeys 373: 1–41. https://doi.org/10.3897/zookeys.373.6511.

Halàsz A, Reynolds AM, McFadden CS, Toonen RJ, Benayahu Y (2015) Could polyp pulsation be the key to species boundaries in the genus *Ovabunda* (Octocorallia: Alcyonacea: Xeniidae)? Hydrobiologia 759: 95–107. https://doi.org/10.1007/s10750-014-2106-z

Haverkort-Yeh RD, McFadden CS, Benayahu Y, Berumen M, Halàsz A, Toonen RJ (2013) A taxonomic survey of Saudi Arabian Red Sea octocorals (Cnidaria: Alcyonacea). Marine Biodiversity 43: 279–291. https://doi.org/10.1007/s12526-013-0157-4

Hickson SJ (1931) The alcyonarian family Xeniidae, with a revision of the genera and species. Great Barrier Reef Expedition 1928–29, Scientific Reports, British Museum 4(5): 137–179.

Janes MP (2008) A study of the Xeniidae (Octocorallia, Alcyonacea) collected on the "Tyro" expedition to the Seychelles with a description of a new genus and species. Zoologische Mededelingen Leiden 82(49): 599–626.

Janes MP (2013) Distribution and diversity of the soft coral family Xeniidae (Coelenterata: Octocorallia) in Lembeh Strait, Indonesia. Galaxea, Journal of Coral Reef Studies (Special Issue): 195–200. https://doi.org/10.3755/galaxea.15.195

Katoh K, Kuma K, Toh H, Miyata T (2005) MAFFT version 5: improvement in accuracy of multiple sequence alignment. Nucleic Acids Research 33: 551–513. https://doi.org/10.1093/nar/gki198

Kükenthal W (1902) Versuch einer Revision der Alcyonarien: I. Die Familie der Xeniiden. Zoologisches Jahrbüch, Abteilung für systematic, Geographie und Biologie der Tiere 15: 635–662. https://doi.org/10.5962/bhl.part.19040

Lamarck MC (1816) Les Caracteres Generaux et Particuliers de ces Animaux, leur Distribution, leur Classes, leurs Familles, leurs Genres, et la Citation des Principales Especes qui s'y Rapportent. Histoire Naturelle des Animaux sans Vertebres (2): 388–421.

Macfadyen LMI (1936) Alcyonaria (Stolonifera, Alcyonacea, Telestacea and Gorgonacea). Great Barrier Reef Expedition 1928–29, Scientific Reports, British Museum 5(2): 19–71.

Malyutin AN (1992) Octocorallia from the Seychelles Islands with some ecological observations. Atoll Research Bulletin 367: 1–4. https://doi.org/10.5479/si.00775630.367.1

May W (1898) Die von Dr. Stuhlmann im Jahre 1889 gesammelten ostafrikanischen Alcyonaceen des Hamburger Museums. Mitteilungen des naturhistorischen Museums Hamburg 15 (Doctoral dissertation), Supplement 2: 3–38.

May W (1899) Beiträge zur Systematik und Chorologie der Alcyonaceen. Jenaische Zeitschrift Naturwissenschaften 33 (Neue Folge 26): 1–180.

McFadden CS, Tullis ID, Hutchinson MB, Winner K, Sohm JA (2004) Variation in coding (NADH dehydrogenase subunits 2, 3 and 6) and non-coding intergenic spacer regions of the mitochondrial genome in Octocorallia (Cnidaria: Anthozoa). Marine Biotechnology 6: 516–526. https://doi.org/10.1007/s10126-002-0102-1

McFadden CS, France SC, Sánchez JA, Alderslade P (2006) A molecular phylogenetic analysis of the Octocorallia (Coelenterata: Anthozoa) based on mitochondrial protein-coding se-

quences. Molecular Phylogenetics and Evolution 41: 513–527. https://doi.org/10.1016/j.ympev.2006.06.010

McFadden CS, Benayahu Y, Pante E, Thoma JN, Nevarez PA, France SC (2011) Limitations of mitochondrial gene barcoding in Octocorallia. Molecular Ecology Resources 11: 19–31. https://doi.org/10.1111/j.1755-0998.2010.02875.x

McFadden CS, Ofwegen LP van (2013) A second, cryptic species of the soft coral genus *Incrustatus* (Anthozoa: Octocorallia: Clavulariidae) from Tierra del Fuego, Argentina revealed by DNA barcoding. Helgoland Marine Research 67: 137–147. https://doi.org/10.1007/s10152-012-0310-7

McFadden CS, Reynolds AM, Janes MP (2014) DNA barcoding of xeniid soft corals (Octocorallia: Alcyonacea: Xeniidae) from Indonesia: species richness and phylogenetic relationships. Systematics & Biodiversity 12: 247–257. https://doi.org/10.1080/14772000.2014.902866

McFadden CS, Haverkort-Yeh R, Reynolds AM, Halàsz A, Quattrini AM, Forsman Z, Benayahu Y, Toonen RJ (2017) Species boundaries in the absence of morphological, ecological or geographical differentiation in the Red Sea octocoral genus *Ovabunda* (Alcyonacea: Xeniidae). Molecular Phylogenetics & Evolution 112: 174–184. https://doi.org/10.1016/j.ympev.2017.04.025

Milne Edwards H, Haime J (1850) A monograph of the British fossil corals – Part I: Introduction, corals from the Tertiary and Cretaceous formation. Palaeontographical Society, London, 71 pp.

Quoy JRC, Gaimard P (1833) Zoophytes. In: Voyage de découvertes de l'Astrolabe executé par ordre du Roi, pendant les années 1826–1827–1828–1829, sous le commandement de M.J. Dumont d'Urville. Zoologie 4: 1–390.

Reinicke GB (1997) Xeniidae (Coelenterata: Octocorallia) of the Red Sea with descriptions of six new species of *Xenia*. Fauna of Saudi Arabia 16: 5–62.

Ronquist F, Teslenko M, van der Mark P, Ayres D, Darling A, Höhna S, Larget B, Liu L, Suchard MA, Huelsenbeck JP (2012) MrBayes 3.2: Efficient Bayesian phylogenetic inference and model choice across a large model space. Systematic Biology 61: 539–542. https://doi.org/10.1093/sysbio/sys029

Roxas HA (1933) Philippine Alcyonaria. The families Cornulariidae and Xeniidae. The Philippine Journal of Science 50: 49–108.

Ruiz-Allais JP, Amaro ME, McFadden CS, Halàsz A, Benayahu Y (2014) The first incidence of an alien soft coral of the family Xeniidae in the Caribbean, an invasion in eastern Venezuelan coral communities. Coral Reefs 33: 287–287. https://doi.org/10.1007/s00338-013-1122-1

Sánchez JA, McFadden CS, France SC, Lasker HR (2003) Phylogenetic analyses of shallow-water Caribbean octocorals. Marine Biology 142: 975–987. https://doi.org/10.1007/s00227-003-1018-7

Tamura K, Peterson D, Peterson N, Stecher G, Nei M, Kumar S (2011) MEGA5: molecular evolutionary genetics analysis using maximum likelihood, evolutionary distance, and maximum parsimony methods. Molecular Biology and Evolution 28: 2731–2739. https://doi.org/10.1093/molbev/msr121

Thomson JA, Dean LMI (1931) Alcyonacea of the Siboga Expedition. Siboga- Expedition Monograph 13d: 1–227.

Thomson JA, Henderson WD (1906) The Marine Fauna of Zanzibar and British East Africa, from Collections made by Cyril Crossland, MA, B. Sc., FZS, in the Years 1901 and 1902. Alcyonaria. Journal of Zoology 76: 393–443.

Thomson JA, Mackinnon DL (1910) Alcyonarians collected on the Percy Sladen Trust Expedition by Mr. J. Stanley Gardiner. Part II. The Stolonifera, Alcyonacea, Pseudaxonia, and Stelechotokea. Transactions of the Linnean Society of London 13(8): 165–211. [pls. 6–14]

Tilot V, Leujak W, Ormond RFG, Ashworth JA, Mabrouk A (2008) Monitoring of South Sinai coral reefs: influence of natural and anthropogenic factors. Aquatic Conservation: Marine and Freshwater Ecoystems 18: 1109–1126. https://doi.org/10.1002/aqc.942

Tixier-Durivault A (1966) Faune de Madagascar. XXI: Octocoralliaires. ORSTOM, Paris.

Utinomi H (1950) Some Xeniid Alcyonarians from Japan and Adjacent Localities. Publications of the Seto Marine Biological Laboratory 1(3): 7–17. https://doi.org/10.5134/174440

Utinomi H (1954) Some alcyoniid octocorals from Kii coast, middle Japan. Publications of the Seto Marine Biological Laboratory 4(1): 43–55. https://doi.org/10.5134/174502

Verseveldt J (1971) Octocorallia from North-Western Madagascar (Part II). Zoologische Verhandelingen 117: 1–73.

Wild C, Naumann MS (2013) Effect of active water movement on energy and nutrient acquisition in coral reef-associated benthic organisms. Proceedings of the National Academy of Sciences of the United States of America 110: 8767–8768. https://doi.org/10.1073/pnas.1306839110

Zwickl DJ (2006) Genetic algorithm approaches for the phylogenetic analysis of large biological sequence datasets under the maximum likelihood criterion. Ph.D. dissertation, University of Texas: Austin.

ZooKeys 754: 103–111 (2018)
doi: 10.3897/zookeys.754.25704
http://zookeys.pensoft.net

RESEARCH ARTICLE

A peer-reviewed open-access journal
ZooKeys
Launched to accelerate biodiversity research

A new, alpine species of *Lissodesmus* Chamberlin, 1920 from Tasmania, Australia (Diplopoda, Polydesmida, Dalodesmidae)

Robert Mesibov[1]

1 *West Ulverstone, Tasmania 7315, Australia*

Corresponding author: *Robert Mesibov* (robert.mesibov@gmail.com)

Academic editor: *P. Stoev* | Received 11 April 2018 | Accepted 26 April 2018 | Published 3 May 2018

http://zoobank.org/416997CF-8D35-425B-9845-E9DEB46C9CC6

Citation: Mesibov R (2018) A new, alpine species of *Lissodesmus* Chamberlin, 1920 from Tasmania, Australia (Diplopoda, Polydesmida, Dalodesmidae). ZooKeys 754: 103–111. https://doi.org/10.3897/zookeys.754.25704

Abstract

Lissodesmus nivalis **sp. n.** is described from 1450–1550 m elevation on the treeless, alpine Ben Lomond plateau in northeast Tasmania, Australia. The new species is distinguished from all other Tasmanian and Victorian *Lissodesmus* species by a unique combination of gonopod telopodite features: solenomere without a pre-apical process, tibiotarsus Y-shaped, femoral process L-shaped with forked tips, prefemoral process with a long comb of teeth below an irregularly dentate apical margin, and a roughened "shoulder process" near the base of the prefemoral process.

Keywords

Diplopoda, Polydesmida, Dalodesmidae, Tasmania, Australia

Introduction

Several species of the millipede family Dalodesmidae can be found in treeless alpine areas of Tasmania, among them *Dasystigma margaretae* (Jeekel, 1984), which was collected on an alpine "cushion plant" at 1150 m at the type locality on Tasmania's Central Plateau (Mesibov 2003). However, until recently the only Tasmanian dalodesmid known exclusively from above the treeline was *Noteremus summus* Mesibov, 2009 from the summit of Mt Weld (1100–1300 m) in the south of the island (Mesibov 2009). The new species described here is so far known only from ca 1450–1550 m on the Ben Lomond

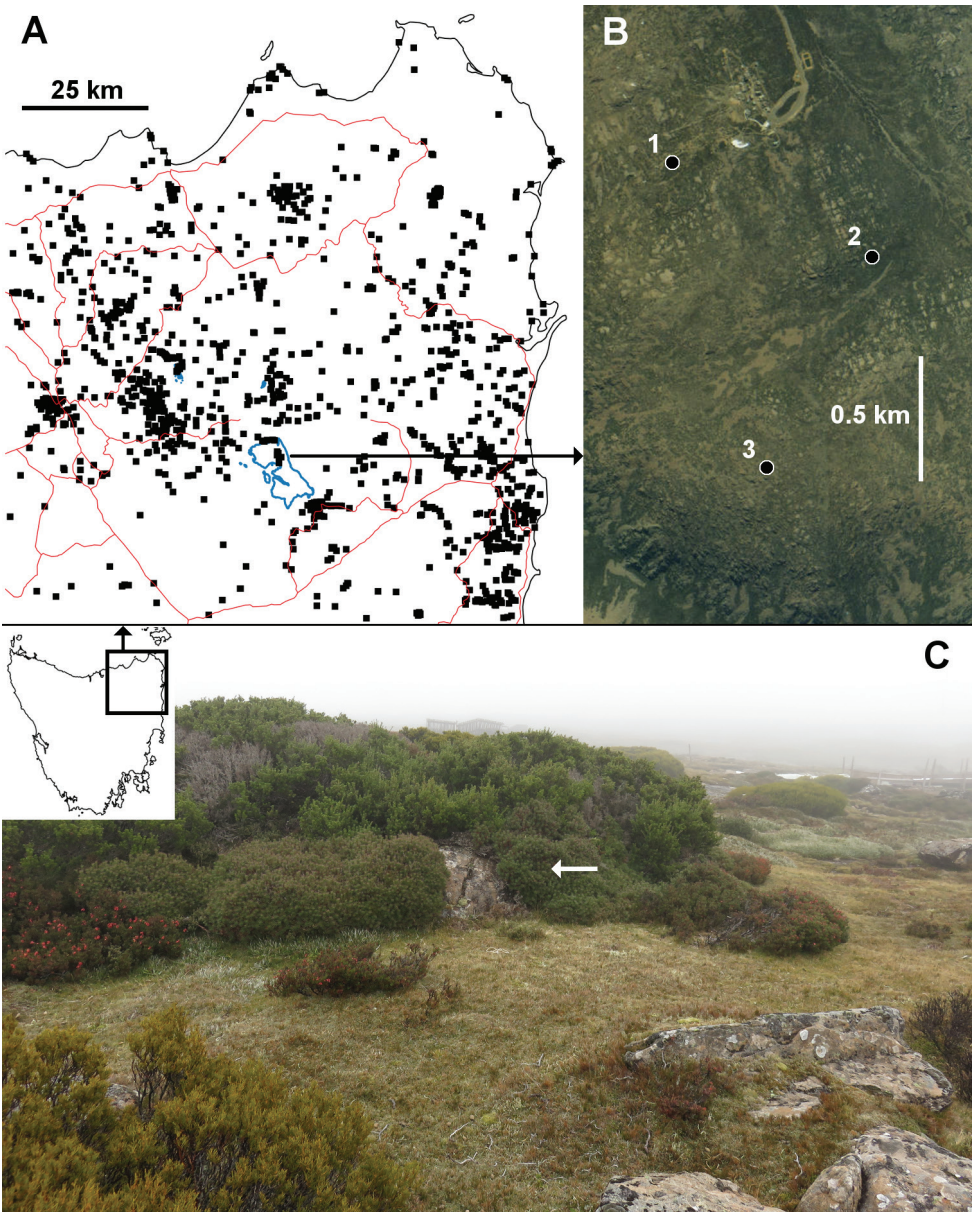

Figure 1.A Northeast Tasmania with millipede sampling sites, 1934–2018 (black squares), major roads (thin red lines) and 1300 m elevation contours (thick blue lines); the large, rectangular block above 1300 m is the Ben Lomond plateau **B** Aerial photograph of part of the Ben Lomond plateau with *Lissodesmus nivalis* sp. n. localities: 1 = Ben Lomond ski village (type locality), 2 = Surprise Vale, 3 = Giblin Fells **C** Ben Lomond ski village collecting site (1 in **B**), 2 April 2018; white arrow indicates the rock-hugging shrub beneath which the holotype and paratypes of *L. nivalis* sp. n. were found. Sampling sites in **A** from Mesibov (2006–2018) for named species, and the author's unpublished records for undescribed species. Image in **B** from https://maps.thelist.tas.gov.au/listmap/app/list/map. Rectangle in inset map in **C** shows extent of map **A** both maps are Mercator projections.

plateau in northeast Tasmania (Fig. 1). Its discovery in 2017 was remarkable for another reason: northeast Tasmania has been intensively sampled for millipedes by the author and other collectors over many years (Fig. 1A). I therefore thought the list of the region's dalodesmid fauna might be complete, apart from very small, inconspicuous and geographically restricted forms yet to be collected. Unexpectedly, the new Ben Lomond species is a large and conspicuous addition to the Tasmanian and Victorian genus *Lissodesmus* Chamberlin, 1920, which now includes 30 species (Mesibov 2006–2018).

Materials and methods

All specimens are stored in 80% ethanol in the Queen Victoria Museum and Art Gallery (QVM). Several legs of the holotype were removed and placed in 95% ethanol before the rest of the specimen was preserved. Freshly collected specimens were examined and measured using a Nikon SMZ800 binocular dissecting microscope, and stacks of colour images were manually generated using a Canon EOS 1000D digital SLR camera mounted on the Nikon SMZ800 fitted with a beam splitter. Images were then focus-stacked with Zerene Stacker 1.04 software. The gonopods and one leg 7 of the male paratype were cleared in 80% lactic acid and temporarily mounted in a 1:1 glycerol:water mixture for examination. The gonopods were imaged using an eyepiece video camera mounted on an Amscope binocular microscope. Preliminary drawings were traced from printed copies of the images, then corrected by reference to the actual gonopod. Figures were composed using GIMP 2.8 and maps with QGIS 2.14.

Locality details are given with latitude and longitude in decimal degrees based on the WGS84 datum. The estimated uncertainty for a locality is the radius of a circle around the given position in metres.

Terminology of gonopod telopodite parts as in Mesibov (2006).

Abbreviation: QVM = Queen Victoria Museum and Art Gallery, Launceston, Tasmania, Australia.

Results

Order Polydesmida Pocock, 1887
Suborder Dalodesmidea Hoffman, 1980
Family Dalodesmidae Cook, 1896

Genus *Lissodesmus* Chamberlin, 1920

Lissodesmus: Chamberlin 1920: 135; Attems 1940: 490; Jeekel 1971: 336; Hoffman 1980: 185; Jeekel 1982: 12; 1983: 146, 150; 1984: 85, 89; 1985: 50, 51; Mesibov 2003: 198; 2004: 21; 2006: 108; 2008: 2, 49.

Australopeltis: Johns 1964: 47 (as subgenus of *Pseudoprionopeltis* Carl, 1902); Hoffman 1980: 184 (raised to genus); Jeekel 1982: 12; 1983: 150 (synonymised with *Lissodesmus*); Shelley et al. 2000: 86; Mesibov 2006: 108; 2008: 49. (Type species *Pseudoprionopeltis martini* Carl, 1902, by original designation.)

Type species. *Lissodesmus modestus* Chamberlin, 1920, by original designation.

Other assigned species. *Lissodesmus adrianae* Jeekel, 1984, *L. alisonae* Jeekel, 1984, *L. anas* Mesibov, 2006, *L. bashfordi* Mesibov, 2006, *L. blackwoodensis* Mesibov, 2006, *L. catrionae* Mesibov, 2006, *L. clivulus* Mesibov, 2006, *L. cognatus* Mesibov, 2006, *L. cornutus* Mesibov, 2006, *L. devexus* Mesibov, 2006, *L. dignomontis* Mesibov, 2006, *L. gippslandicus* Mesibov, 2006, *L. grampianensis* Mesibov, 2008, *L. hamatus* Mesibov, 2006, *L. horridomontis* Mesibov, 2006, *L. inopinatus* Mesibov, 2006, *L. johnsi* Mesibov, 2006, *L. latus* Mesibov, 2006, *L. macedonensis* Mesibov, 2006, *L. martini* (Carl, 1902), *L. milledgei* Mesibov, 2006, *L. montanus* Mesibov, 2006, *L. nivalis* sp. n., *L. orarius* Mesibov, 2006, *L. otwayensis* Mesibov, 2006, *L. peninsulensis* Mesibov, 2006, *L. perporosus* Jeekel, 1984, *L. plomleyi* Mesibov, 2006, *L. tarrabulga* Mesibov, 2006.

Lissodesmus nivalis sp. n.

http://zoobank.org/688C85B2-1C5F-4ACE-AA6C-6C663BF25788
Figs 2, 3

Holotype. Male, Ben Lomond ski village, Tasmania, -41.5357, 147.6618, ±25 m, 1490 m a.s.l., 2 April 2018, K. Bonham and R. Mesibov, QVM 2018:23:0038.

Paratypes. 1 male, 1 female, details as for holotype, QVM 2018:23:0039.

Other material. Tasmania, QVM: 1 male, Giblin Fells, Ben Lomond, -41.5471, 147.6666, ±100 m, 1540 m a.s.l., 15 April 2017, K. Bonham, 2017:23:0185, gonopod telopodite with femoral processes broken off; 1 stadium VI male, Surprise Vale, Ben Lomond, -41.5392, 147.6719, ±50 m, 1450 m a.s.l., 20 November 2017, R. Mesibov, 2017:23:0244.

Diagnosis. Distinguished from all other *Lissodesmus* species by a unique combination of character states of gonopod telopodite processes: solenomere without pre-apical process, tibiotarsus Y-shaped, femoral process L-shaped with forked tips, prefemoral process with long comb of teeth below irregularly dentate apical margin, roughened "shoulder process" near base of prefemoral process.

Description. Male/female approximate measurements: length 25/25 mm, midbody vertical diameter 2.1/2.5 mm, midbody width across paranota 3.2/3.5 mm. Live specimens yellowish-brown to chestnut brown with pinkish red antennae (darker distally) and pinkish red legs (darker basally); rings darkest at posterior metatergal margin and along paranotal margins.

Male with vertex sparsely setose and frons moderately so. Antennal sockets separated by 2X socket diameter. Antenna short, just reaching ring 3 when manipulated backwards; relative length of antennomeres 2>(3,6)>(4,5), antennomere 6 widest. Col-

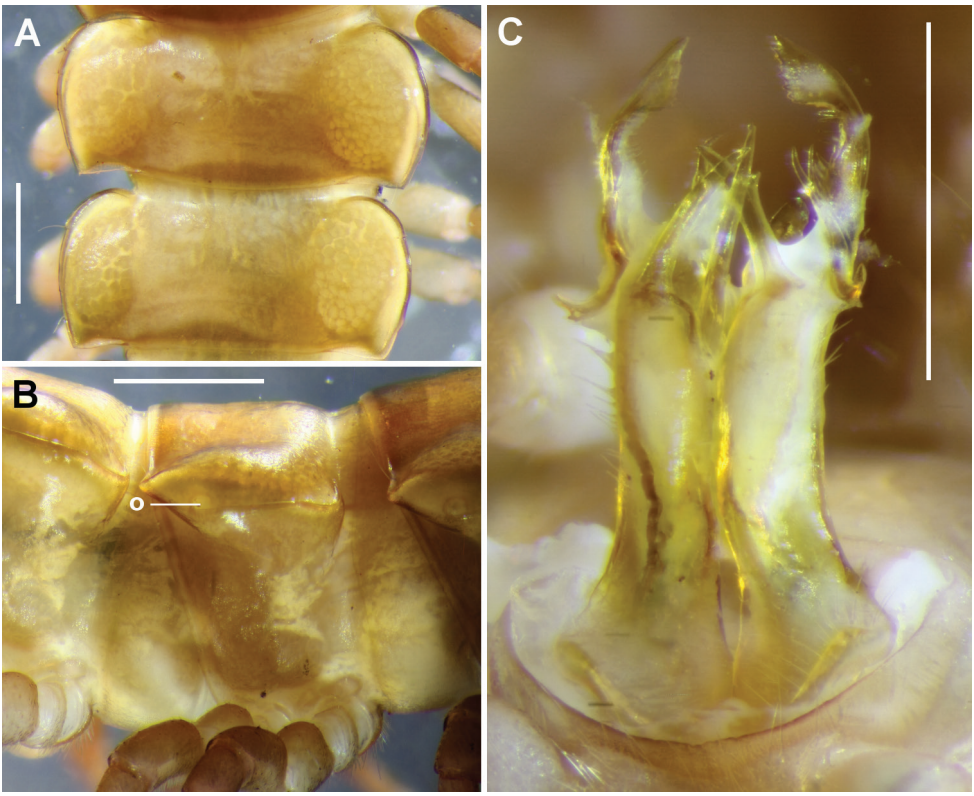

Figure 2. *Lissodesmus nivalis* sp. n., holotype male five days after killing and preserving, QVM 2018:23:0038. **A** Dorsal view of rings 10 and 11 **B** Right lateral view of rings 9–11; **o** = ozopore **C** Posterior view of gonopods in situ. Scale bars: 1.0 mm.

lum slightly narrower than head, slightly wider than tergite 2; anteriorly very slightly convex, laterally slightly convex; posterior edge medially a little emarginate; corners rounded. Tergite width increasing gradually from rings 2–6, then subequal, then decreasing 17–19. Waist (Fig. 2A, B) well-defined, with faint longitudinal striations. Prozonites and metazonites with faint cellular sculpturing; limbus composed of close-set flat tabs. Paranota (Fig. 2A, B) smooth, swollen, wide (ratio of overall width to prozonite width ca 1.4 on midbody ring); anterior shoulder tightly curved, projected anteriorly; lateral margin slightly convex, sometimes with small notches detectable, the first and last usually with 1 short seta on anterior corner of notch; posterior corner rounded, not extending past posterior metatergite margin on most rings, produced as rounded tooth on rings 17–19; posterior corner seta prominent, erect. Ozopore (Fig. 2B) small, opening dorsolaterally close to paranotal margin and anterior to posterior paranotal corner; pore formula 5, 7, 9, 10, 12, 13, 15–19. Spiracles with rims slightly raised above pleural surface; anterior spiracle on diplosegments larger, posterior spiracle about midway between leg bases. Sternites about as long as wide, with fine, short, sparse setae; transverse impression much deeper than longitudinal. Legs short; from legpair 3 prefemur greatly

swollen dorsally, femur somewhat swollen dorsally, gradually less so posteriorly; most legs with postfemur and tibia expanded ventrodistally; relative podomere lengths tars us>femur>prefemur>(postfemur, tibia) on midbody legs; tarsus straight. From legpair 3, sphaerotrichomes on prefemur, femur, postfemur, tibia and tarsus, densest on tibia and tarsus; each sphaerotrichome hemispherical with blunt-tipped, tapered setal shaft inclined distoventrally; dense brush setae on prefemur and femur, tapering with blunt tips; no sphaerotrichomes or brush setae on last 2 legpairs. Pre-anal ring with sparse, long setae; hypoproct paraboloid; epiproct extending a little past anal valves, sides slightly emarginate, tip truncate between 2 short, rounded, apical bumps; spinnerets in square array in shallow, low-walled cavity just ventral to epiproct tip.

Gonopore small, opening on rounded, mediodistal enlargement of leg 2 coxa. Gonopod telopodites extending to leg 5 bases when retracted; bases of legs 6 and 7 well-separated, coxae of legs 6 and 7 slightly swollen ventrally; sternite between legs 6 and 7 slightly excavate, with brushes of long, stiff setae on sternite just medial to coxae. Aperture ovoid but with anterior margin straight, wider than long, about 1/2 the width of ring 7 prozonite, rim slightly raised laterally.

Gonopods: gonocoxae truncate-conical, tapering distally, lightly joined medially, moderately setose on posterobasal surface. Telopodite (Figs 2C, 3) long, slender, gently curving anteriorly from base, with a band of long setae (Fig. 3C) on posterolateral surface from telopodite base almost to level of solenomere base. Telopodite base tapering from thickened basal rim. Cannula prominent, entering telopodite base in excavation lined with fine setae; prostatic groove running on anterior surface of telopodite before joining base of solenomere, opening at solenomere tip. Solenomere thin, rod-like, tapering to point, arising at ca 1/2 telopodite height on anteromedial surface, directed a little posterodistally before curving anterodistally. Tibiotarsus arising on posterior surface a little distal to level of solenomere base, thicker than solenomere, directed distomedially, apex bifurcated, the tips blunt. Femoral process arising on anterolateral surface distal to tibiotarsus origin, L-shaped; the longer portion of the "L" directed posterodistally with a forked tip; the shorter portion of the "L" directed posterobasally, also with forked tip but with distal portion of fork larger than basal portion. In distal 1/3 of telopodite, prefemoral process separated on posteromedial side from prominent, tab-like "shoulder" process with irregularly and bluntly toothed margin. Prefemoral process flattened anterolaterally, curving medially near obliquely truncate apex, with apical margin irregularly and bluntly toothed and with ca 15 discrete teeth forming comb on posterior margin.

Female closely resembling male but a little wider; legs not swollen. Genital aperture with posterior margin rounded-triangular medially; cyphopods not examined.

Name. Latin *nivalis*, of snow; adjective. This species spends several months each winter with its habitat covered in snow.

Distribution. So far known only from alpine moorland and shrubland at three localities on the Ben Lomond plateau in northeast Tasmania (Fig. 1A, B). Found in peaty material under prostrate and rock-hugging alpine shrubs (Fig. 1C).

Remarks. The gonopod telopodite of *L. nivalis* sp. n. shares several features with other Tasmanian *Lissodesmus* species. As in *L. anas* and *L. horridomontis*, for example,

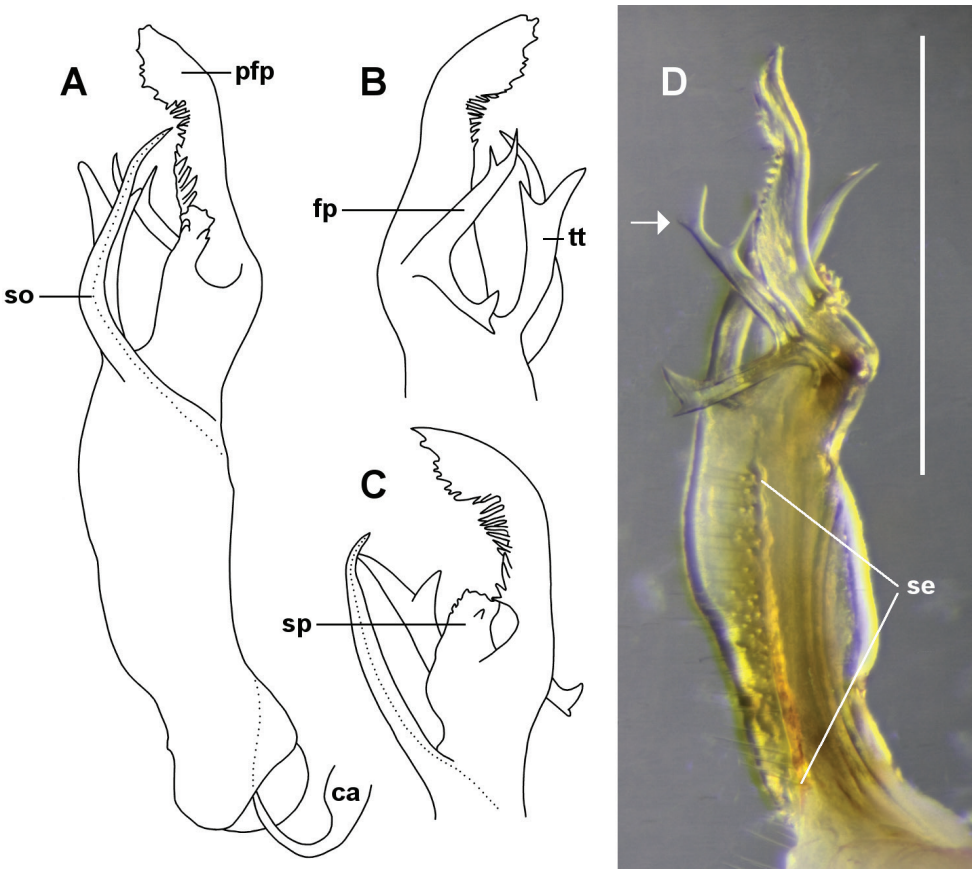

Figure 3. *Lissodesmus nivalis* sp. n., gonopod telopodites of paratype male ex QVM 2018:23:0039. Medial (**A**), posterolateral (**B**) and anteromedial (**C**) views of right telopodite; drawings not to scale and setation not shown **D** Lateral view of left telopodite; scale bar = 1.0 mm. **fp** = femoral process, **pfp** = prefemoral process, **se** = band of setae on posterolateral surface, **so** = solenomere, **sp** = "shoulder process", **tt** = tibiotarsus. Arrow in **D** indicates unusually forked tip of **fp**; dotted lines in **A** and **C** indicate course of prostatic groove.

the prefemoral process is offset laterally by the distal development of a roughened, tab-like "shoulder" process. The tibiotarsus has a bifurcated tip, as in *L. cornutus* and *L. montanus*, and the femoral process is L-shaped, as in *L. clivulus* and *L. latus*. However, the distinctive combination of telopodite characters in *L. nivalis* sp. n. makes it hard to judge from morphology what its nearest relation in the genus might be. It is quite unlike the five other *Lissodesmus* species found in the Ben Lomond area, namely *L. adrianae*, *L. cognatus*, *L. devexus*, *L. hamatus* and *L. plomleyi*.

The upright portion of the femoral process "L" is doubly forked on the left gonopod of the paratype male (Fig. 3D). There is no second bifurcation on the right gonopod of the paratype, or on the femoral processes of the holotype, so the double forking appears to be a developmental abnormality. (The third, non-type male is missing its femoral processes.)

The holotype and paratypes were collected by Tasmanian land snail specialist Kevin Bonham in company with the author. We searched the group of rocks shown in Fig. 1C and similar nearby habitats for more than an hour but found no more *L. nivalis* sp. n., although we saw scattered specimens of the common northeast Tasmanian dalodesmids *L. adrianae* and *Tasmaniosoma clarksonorum* Mesibov, 2010. My collecting in November 2017 was even less successful, yielding only one presumed juvenile of *L. nivalis* sp. n., despite my searching a larger area of apparently suitable shrub habitat for several hours. *L. nivalis* sp. n. may be naturally scarce in its alpine habitat.

The types were collected live and transported from the field in a collecting jar filled with peaty material. As often happens when dalodesmids are live-collected, the female and one of the males (the holotype) mated in the jar and were still *in copula* when killed by freezing several hours later. In Fig. 2C, white amorphous material (spermatic fluid?) can be seen adhering to the gonopod telopodites of the holotype.

Acknowledgements

Peter Decker and Sergei Golovatch are thanked for useful suggestions for improving the manuscript. I am again very grateful to Kevin Bonham (Hobart, Tasmania) for his diligent collecting, and the main reason I have not named *L. nivalis* sp. n. in his honour is that there are already three Tasmanian millipedes named *bonhami*, one of them in the *Lissodesmus* group of dalodesmid genera.

References

Attems C (1940) Myriapoda. 3. Polydesmoidea. III. Fam. Polydesmidae, Vanhoeffeniidae, Cryptodesmidae, Oniscodesmidae, Sphaerotrichopidae, Peridontodesmidae, Rhachidesmidae, Macellolophidae, Pandirodesmidae. Das Tierreich 70. Walter de Gruyter and Co., Berlin, 577 pp.

Carl J (1902) Exotische Polydesmiden. Revue Suisse de Zoologie 10(2): 563–679. [pls 10–12] https://biodiversitylibrary.org/page/9477493 https://doi.org/10.5962/bhl.part.13794

Chamberlin RV (1920) The Myriopoda of the Australian region. Bulletin of the Museum of Comparative Zoology 64(1): 1–269. http://biodiversitylibrary.org/page/30743608

Hoffman RL (1980) [1979] Classification of the Diplopoda. Muséum d'Histoire Naturelle, Geneva, 237 pp.

Jeekel CAW (1971) [1970] Nomenclator generum et familiarum Diplopodorum: a list of the genus and family-group names in the Class Diplopoda from the 10th edition of Linnaeus, 1758, to the end of 1957. Monografieën van de Nederlandse Entomologische Vereniging 5, 412 pp.

Jeekel CAW (1982) Millipedes from Australia, 4: A new genus and species of the family Dalodesmidae from Australia (Diplopoda, Polydesmida). Bulletin Zoölogisch Museum, Universiteit van Amsterdam 9(2): 9–15. http://www.repository.naturalis.nl/document/549072

Jeekel CAW (1983) Millipedes from Australia, 8: A new genus and species of the family Dalodesmidae from Victoria (Diplopoda, Polydesmida). Bulletin Zoölogisch Museum, Universiteit van Amsterdam 9(16): 145–151. http://www.repository.naturalis.nl/document/549000

Jeekel CAW (1984) Millipedes from Australia, 7: The identity of the genus *Lissodesmus* Chamberlin, with the description of four new species from Tasmania (Diplopoda, Polydesmida, Dalodesmidae). Papers and Proceedings of the Royal Society of Tasmania 118: 85–101. http://dx.doi.org/10.3853/j.0067-1975.36.1984.323

Jeekel CAW (1985) Millipedes from Australia, 9: A new polydesmoid millipede from Queensland (Diplopoda, Polydesmida: Dalodesmidae). Entomologische Berichten (Amsterdam) 45: 50–55.

Johns PM (1964) The Sphaerotrichopidae (Diplopoda) of New Zealand. 1. Introduction, revision of some known species and description of new species. Records of the Canterbury Museum 8(1): 1–49.

Mesibov R (2003) A new genus of Tasmanian millipedes (Diplopoda, Polydesmida, Dalodesmidae) with unusual spiracles and a mosaic distribution. Memoirs of Museum Victoria 60(2): 197–206. http://museumvictoria.com.au/pages/3984/60_2_Mesibov1.pdf https://doi.org/10.24199/j.mmv.2003.60.20

Mesibov R (2004) Redescription of *Tasmanodesmus hardyi* Chamberlin, 1920 (Diplopoda: Polydesmida: Dalodesmidae). Myriapodologica 8(3): 21–36. http://www.vmnh.net/content/uploads/PDF/Research_and_Collections/Myriapodologica/Myriapodologica_v8_n3.pdf

Mesibov R (2006) The millipede genus *Lissodesmus* Chamberlin, 1920 (Diplopoda: Polydesmida: Dalodesmidae) from Tasmania and Victoria, with descriptions of a new genus and 24 new species. Memoirs of Museum Victoria 62(2): 103–146. http://museumvictoria.com.au/pages/3905/62_Mesibov.pdf https://doi.org/10.24199/j.mmv.2005.62.4

Mesibov R (2006–2018) Millipedes of Australia. https://www.polydesmida.info/millipedesofaustralia/index.html [Accessed 5 April 2018]

Mesibov R (2008) The millipede genera *Gephyrodesmus* Jeekel, 1983 and *Orthorhachis* Jeekel, 1985 in southeastern Australia, a new *Lissodesmus* Chamberlin, 1920 from Victoria, and observations on male leg setae, spinnerets and metatergite sculpture (Diplopoda: Polydesmida: Dalodesmidae). Zootaxa 1790: 1–52.

Mesibov R (2009) A new millipede genus and a new species of *Asphalidesmus* Silvestri, 1910 (Diplopoda: Polydesmida: Dalodesmidea) from southern Tasmania, Australia. ZooKeys 7: 55–74. http://dx.doi.org/10.3897/zookeys.7.111

Mesibov R (2010) The millipede genus *Tasmaniosoma* Verhoeff, 1936 (Diplopoda: Polydesmida: Dalodesmidae) from Tasmania, Australia, with descriptions of 18 new species. ZooKeys 41: 31–80. http://dx.doi.org/10.3897/zookeys.41.420

Shelley RM, Sierwald P, Kiser SB, Golovatch SI (2000) Nomenclator generum et familiarum Diplopodorum II. A List of the Genus and Family-Group Names in the Class Diplopoda from 1958 through 1999. Pensoft, Sofia, 167 pp.

ZooKeys 754: 113–125 (2018)
doi: 10.3897/zookeys.754.23296
http://zookeys.pensoft.net

RESEARCH ARTICLE

A peer-reviewed open-access journal
ZooKeys
Launched to accelerate biodiversity research

Descriptions of two new species of *Platygaster* Latreille that attack gall midges (Diptera, Cecidomyiidae) with notes on their biology (Hymenoptera, Platygastridae)

Kazunori Matsuo[1], Tomohisa Fujii[2], Makoto Tokuda[3], Tomoko Ganaha-Kikumura[4], Junichi Yukawa[5], Kenzou Yamagishi[6]

1 *Biosystematics Laboratory, Faculty of Social and Cultural Studies, Kyushu University, Fukuoka 812–0395, Japan* **2** *NARO Kyushu Okinawa Agricultural Research Center, Kumamoto 861–1192, Japan* **3** *Laboratory of Systems Ecology, Faculty of Agriculture, Saga University, Saga 840–8502, Japan* **4** *Okinawa Prefectural Agricultural Research Center, Okinawa 901–0336, Japan* **5** *Entomological Laboratory, Faculty of Agriculture, Kyushu University, Fukuoka 812–8581, Japan* **6** *Entomological Laboratory, Faculty of Agriculture, Meijo University, Nagoya 468–8502, Japan*

Corresponding author: *Kazunori Matsuo* (matsuosudachi@scs.kyushu-u.ac.jp)

Academic editor: *N. Johnson* | Received 28 December 2017 | Accepted 3 April 2018 | Published 3 May 2018

http://zoobank.org/4956FE6C-9FA6-4D3F-A9B9-436EC90052F5

Citation: Matsuo K, Fujii T, Tokuda M, Ganaha-Kikumura T, Yukawa J, Yamagishi K (2018) Descriptions of two new species of *Platygaster* Latreille that attack gall midges (Diptera, Cecidomyiidae) with notes on their biology (Hymenoptera, Platygastridae). ZooKeys 754: 113–125. https://doi.org/10.3897/zookeys.754.23296

Abstract

Platygaster ingeniosus Matsuo & Yamagishi, **sp. n.** and *P. urniphila* Matsuo & Yamagishi, **sp. n.** (Hymenoptera: Platygastridae) are described from Japan. The former species is an egg-larval solitary parasitoid of *Masakimyia pustulae* Yukawa and Sunose (Diptera: Cecidomyiidae). The latter species is an egg-larval gregarious parasitoid of *Rhopalomyia longitubifex* (Shinji) (Diptera: Cecidomyiidae).

Keywords

Platygaster ingeniosus, *Platygaster urniphila*, platygastrids, taxonomy

Introduction

The genus *Platygaster* Latreille (Hymenoptera: Platygastridae) contains 601 species, of which approximately 300 species have been described from various biogeographic regions during the last two decades (e.g., Buhl 2004a, b, 2006a, b). Most *Platygaster* species share the following morphological characters: antenna with 10 antennomeres; scutoscutellar suture deep and usually forming a fovea; mesoscutellum rounded, usually without a distinct spine or tuft of hairs; fore and hind wings without venation; T1 without dense hairs. In addition, *Platygaster* includes some exceptional species that do not share all of the aforementioned characters (Buhl 1994a, b, 2001a, b, 2003a, b).

Today, nine species of *Platygaster* are known to occur in Japan, of which seven parasitize gall midge species (Diptera: Cecidomyiidae) (Ashmead 1904; Ishii 1953; Yoshida and Hirashima 1979; Yamagishi 1980; Buhl and Duso 2008; Vlug 1995). In addition to the nine known Japanese species, two unidentified species of *Platygaster* have been recognized to parasitize gall midge larvae (Sunose 1984; Ganaha et al. 2007). One species is an egg-larval parasitoid of *Masakimyia pustulae* Yukawa and Sunose (Diptera: Cecidomyiidae) that induces leaf galls on *Euonymus japonicus* (Celastraceae) (Yukawa and Sunose 1976; Sunose 1984). This *Platygaster* species avoids hyperparasitism by manipulating larvae of the host gall midge to make leaf galls thicker (Fujii et al. 2014). Another species parasitizes *Rhopalomyia longitubifex* (Shinji) (Diptera: Cecidomyiidae) that induces axillary bud galls on *Artemisia indica* var. *maximowiczii* (Asteraceae) (Yukawa and Masuda 1996; Ganaha et al. 2007).

As demonstrated by Askew (1975) for parasitoids of Cynipidae (Hymenoptera), Yukawa et al. (1981) also divided parasitoids of gall-inducing cecidomyiids (Diptera: Cecidomyiidae) into two groups, early and late attackers, according to their parasitic strategies. Early attackers (koinobionts) are host-specific endoparasitoids that oviposit into host eggs or younger host larvae before galls start to develop (Sunose 1984, 1985a; Tabuchi and Amano 2004). In contrast, late attackers (idiobionts) are polyphagous ectoparasitoids attacking final (third) instars or pupae. Species of *Platygaster* that are associated with gall-inducing cecidomyiids are known as typical early attackers (Askew 1975). Host specificity has been paid special attention in behavioral and ecological studies of *Platygaster*, particularly host–parasitoid interactions. For example, Stireman III et al. (2006) demonstrated host-associated genetic differentiation in *Platygaster variabilis* Fouts that attacks *Rhopalomyia solidaginis* (Loew) (Diptera: Cecidomyiidae). Yamagishi (1980) reported that larvae of *Rabdophaga rosaeformis* Kovalev (Diptera: Cecidomyiidae) parasitized by *Platygaster stimulator* Yamagishi mature in summer whereas unparasitized *R. rosaeformis* larvae pass through the summer as first instars. In terms of reproductive strategy, some species including *P. robiniae* Buhl and Duso are known to be gregarious parasitoids (Kim et al. 2011). In addition, polyembryony, the production of genetically identical embryos from a single egg through clonal division, has been found in several species of *Platygaster* such as *P. feltii* Fouts, and *P. vernalis* (Myers) (Leiby and Hill 1924; Segoli et al. 2010).

In order to contribute to further taxonomic and ecological studies of platygastrid parasitoids, we intend in this paper to identify the two undescribed species of *Platygaster* and to provide information on their host range and reproductive strategies.

Materials and methods

Galls of *Masakimyia pustulae* and *Rhopalomyia longitubifex* were collected from Kyushu, Japan, in 2007–2017 to rear sufficient numbers of adults of *Platygaster* species for taxonomic study. In rearing *Platygaster* species that attacks *Rhopalomyia longitubifex*, the number of males and females emerged from one host larva were recorded to confirm its gregarious parasitism.

For morphological observation, adult parasitoids were preserved in 70–75% ethanol and subsequently dried from ethanol using the method described in Matsuo and Yukawa (2009). Specimens were observed under a binocular microscope (LEICA S8APO). Several specimens were gold-coated for microphotography with a JEOL JSM-5600LV scanning electronic microscope. High-resolution bright field images were taken with LEICA S8APO and CANON EOS D600 (Matsuo et al. 2012).

To compare morphological characters between known and the two Japanese species, we referred to original descriptions, redescriptions or keys for 512 (85.2%) out of 601 known species (Suppl. material 1). Unfortunately, we could not obtain adequate morphological information on the remaining 89 species. In addition to literature survey, we examined high-resolution images of the type specimen of a Japanese species, *Platygaster gifuensis* (Ashmead) that has been kept in the Smithsonian National Museum of Natural History, Washington, DC, USA. Adult morphological terminology follows Masner and Huggert (1989), except for head and mesosoma, which follows Mikó et al. (2007).

Holotypes and paratypes of the new species are deposited in the collection of the Biosystematics Laboratory, Faculty of Social and Cultural Studies, Kyushu University, Fukuoka, Japan.

Taxonomy

Morphological comparison with some congeners revealed that the two unidentified species of *Platygaster* are distinct species and new to science. They are described below as *P. ingeniosus* and *P. urniphila*. The two new species share typical morphological characteristics of *Platygaster* and are distinctly different from the exceptional species mentioned in the Introduction.

Platygaster ingeniosus Matsuo & Yamagishi, sp. n.

http://zoobank.org/AEE14D9B-872E-446A-93C7-56270048F020

Etymology. The specific name is derived from its ingenious parasitoid strategy.

Type material. Holotype: Female, emerged on 16 March 2011 from a gall of *Masakimyia pustulae* on *Euonymus japonicus* collected by T. Fujii from Nijoshikaka, Itoshima, Fukuoka, Japan. Paratypes: 5 females and 5 males, same data as holotype.

Figure 1. Holotype female of *Platygaster ingeniosus*.

Description. FEMALE (Fig. 1). Body length 1.4–1.6 mm. Head, mesosoma, and metasoma black. A1 dark brown basally; A2–A4 dark brown to black; A5–A10 black. Fore wing slightly infuscate. All coxae black; all femora brown yellow to black; all tibiae brown yellow.

Head in dorsal view, 1.9–2.1 times as wide as long, 1.1–1.2 times as wide as mesosoma; occiput transversely striate; vertex between ocelli with transverse wrinkles, with reticulation between posterior ocelli (Fig. 2); POL: OOL: LOL = 2.5: 1.3: 1.0. Head in frontal view 1.3–1.4 times as wide as high; frons with transverse wrinkles (Fig. 3); gena smooth. A1 5.5–5.6 times as long as wide, 0.7–0.8 times as long as height of head; A2 2.4–2.6 times as long as wide; A3 1.2–1.3 times as long as wide; A4–A6 1.4–1.5 times as long as wide; A7–A9 1.4–1.5 times as long as wide; A10 1.7–1.8 times as long as wide (Fig. 4).

Mesosoma 1.3–1.4 times as long as wide, 1.1–1.2 times as high as wide; sides of pronotum reticulate, smooth along upper and posterior margins (Fig. 6); mesoscutum reticulate, smooth between notauli which are indicated in posterior half (Fig. 7); posterior margin of median lobe of mesoscutum overlapping base of mesoscutellum; posterior margin of lateral mesoscutal lobes hairy; scuto-scutellar groove smooth and bare; mesoscutellum evenly convex, smooth and covered with long hairs except median glabrous area (Fig. 8); mesopleuron with two setae anteriorly, with a coriaceous area

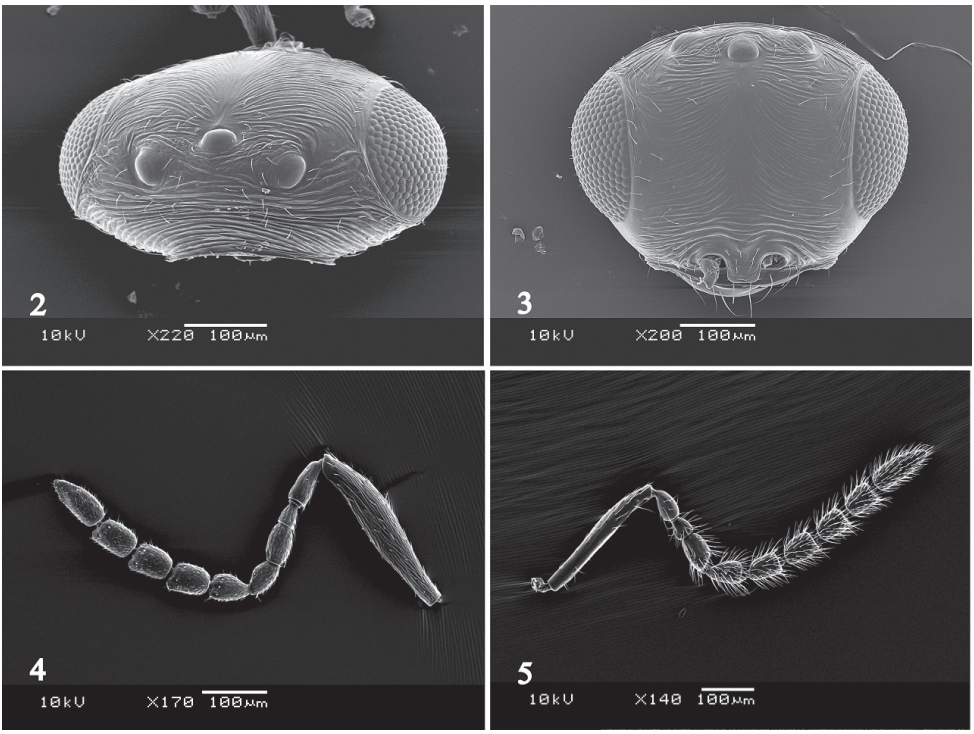

Figure 2–5. *Platygaster ingeniosus*. **2** female head, dorsal view **3** female head, frontal view **4** female antenna **5** male antenna.

below tegula; mesopleural carina absent; mesofurcal pit present; metapleuron completely pilose; propodeal carinae widely separated, parallel. Fore wing 2.3–2.4 times as long as wide; marginal cilia approximately 0.1 times as long as width of fore wing. Hind wing approximately 4.8 times as long as wide, with two hamuli; marginal cilia approximately 0.2 times as long as width of hind wing.

Metasoma as long as head and mesosoma combined; T1 evenly crenulated, 1.8–1.9 times as wide as long, 0.2–0.3 times as long as T2; T2–T5 with a band of shallow punctation along posterior margin; T2 weakly striated in basal half, with shorter striae medially (Fig. 9); T3 with a few setae; T4 with a row of setae which is broken medially; T5 with a complete setal row; T6 with a complete setal row, smooth.

MALE. Differs from the female as follows: Body length 1.5–1.6 mm. Antenna with erect setae; A4 distinctly widened (Fig. 5). Metasoma approximately 0.8 times as long as head and mesosoma combined, obtuse at apex.

Differential dagnosis. *Platygaster ingeniosus* is similar to the two Palearctic species, *P. rutilipes* Buhl and *P. yunnanensis* Buhl, because they share the following morphological characteristics: notaulus indicated in posterior half; mesopleuron with a coriaceous area below tegula; posterior margin of mesoscutum reaching base of mesoscutellum; hind wing approximately 4.8 times as long as wide. *Platygaster ingeniosus* can be distinguished from *P. rutilipes* by having the stouter fore wing that is 2.3–2.4 times as long

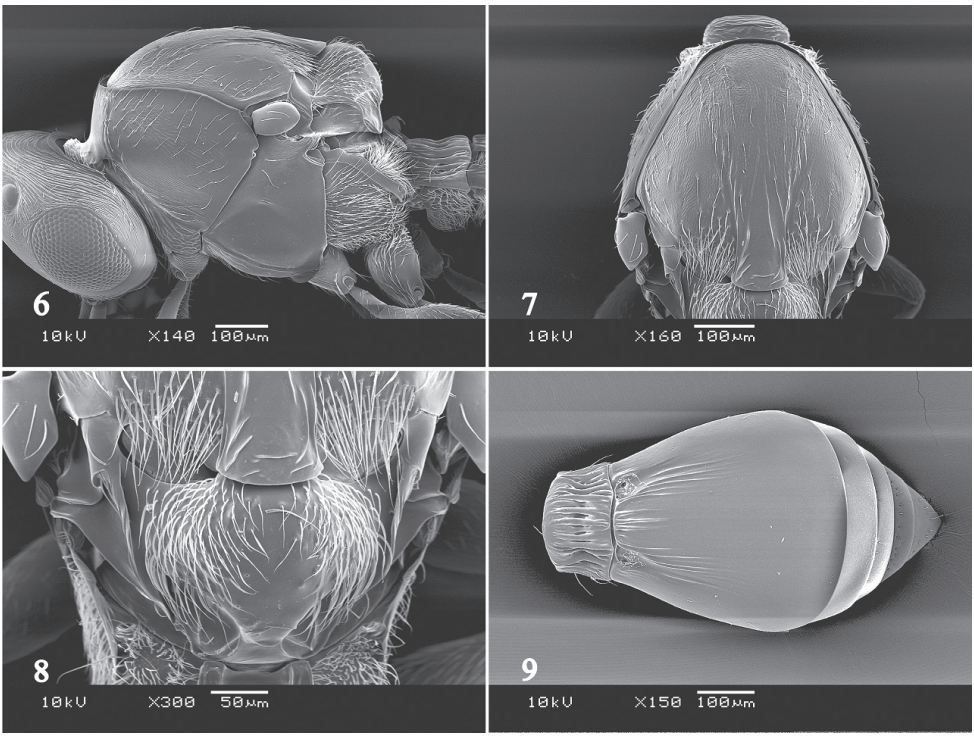

Figure 6–9. *Platygaster ingeniosus*. **6** female mesosoma, lateral view **7** female mesoscutum, dorsal view **8** female mesoscutellum, dorsal view **9** female metasoma, dorsal view.

as wide whereas *P. rutilipes* has elongated fore wing, approximately 2.8 times as long as wide. *Platygaster ingeniosus* could be distinguished from *P. yunnanensis* because sides of pronotum are finely reticulate whereas smooth in *P. yunnanensis*.

Biological notes. *Platygaster ingeniosus* is an egg-larval solitary parasitoid of *Masakimyia pustulae* in Japan (Yukawa and Sunose 1976; Sunose 1983, 1984; Fujii et al. 2014). Although *Masakimyia pustulae* induces dimorphic leaf galls, thick and thin types (Sunose 1983), *Platygaster ingeniosus* can attack gall midge larvae inhabiting both types of gall (Sunose 1984; Fujii et al. 2014). Because the genus *Masakimyia* is monotypic and its tribal position in the supertribe Lasiopteridi has not been determined (Gagné and Jaschhof 2017), the possible host range of *Platygaster ingeniosus* is restricted to *Masakimyia* alone at this moment.

Platygaster urniphila Matsuo & Yamagishi, sp. n.

http://zoobank.org/0F1C3380-1D61-4754-9B97-9C0EA75F16CD

Etymology. The specific name, *urniphila*, is derived from the jar-shaped gall of *Rhopalomyia longitubifex*.

Figure 10. Holotype female of *Platygaster urniphila*.

Type material. Holotype: Female, emerged on 2–4 April 2014 from a globular-jar shaped gall of *Rhopalomyia longitubifex* on *Artemisia indica* var. *maximowiczii* collected by K. Matsuo and Y. Matsuguma on 9 November 2013 from Chojabaru, Kokonoe, Oita, Japan. Paratypes: 1 female and 1 male, same data as holotype. 3 females, emerged on 31 March 2008 from a globular-jar shaped gall of *Rhopalomyia longitubifex* on *Artemisia indica* var. *maximowiczii* collected by K. Matsuo on 8 December 2007 from Jizoubaru, Kokonoe, Oita, Japan. 2 females, emerged on 8 April 2008 from a globular-jar shaped gall of *Rhopalomyia longitubifex* on *Artemisia indica* var. *maximowiczii* collected by K. Matsuo on 2 March 2008 from Chojabaru, Kokonoe, Oita, Japan. 2 females, emerged on 13 April 2008 from a globular-jar shaped gall of *Rhopalomyia longitubifex* on *Artemisia indica* var. *maximowiczii* collected by N. Wachi on 12 April 2008 from Kuju, Taketa, Oita, Japan. 5 males, emerged in April 2016 from a globular-jar shaped gall of *Rhopalomyia longitubifex* on *Artemisia indica* var. *maximowiczii* collected by K. Matsuo and Y. Matsuo on 24 March 2016 from Tano, Kokonoe, Oita, Japan.

Description. FEMALE (Fig. 10). Body length 1.1–1.3 mm. Head, mesosoma, and metasoma black. A1–A2 black; A3–A10 dark brown to black. Fore wing slightly infuscate. All legs dark brown to black.

Head in dorsal view, 1.7–1.8 times as wide as long, 1.0–1.1 times as wide as mesosoma; occiput with weak transverse striations; vertex between ocelli smooth (Fig. 11); POL: OOL: LOL = 2.4: 1.0: 1.0. Head in frontal view 1.2–1.3 times as wide as high; frons smooth medially (Fig. 12), sometimes with fine striations; gena reticulate. A1 5.7–5.9 times as long as wide, 0.7–0.8 times as long as height of head; A2 1.5–1.6 times

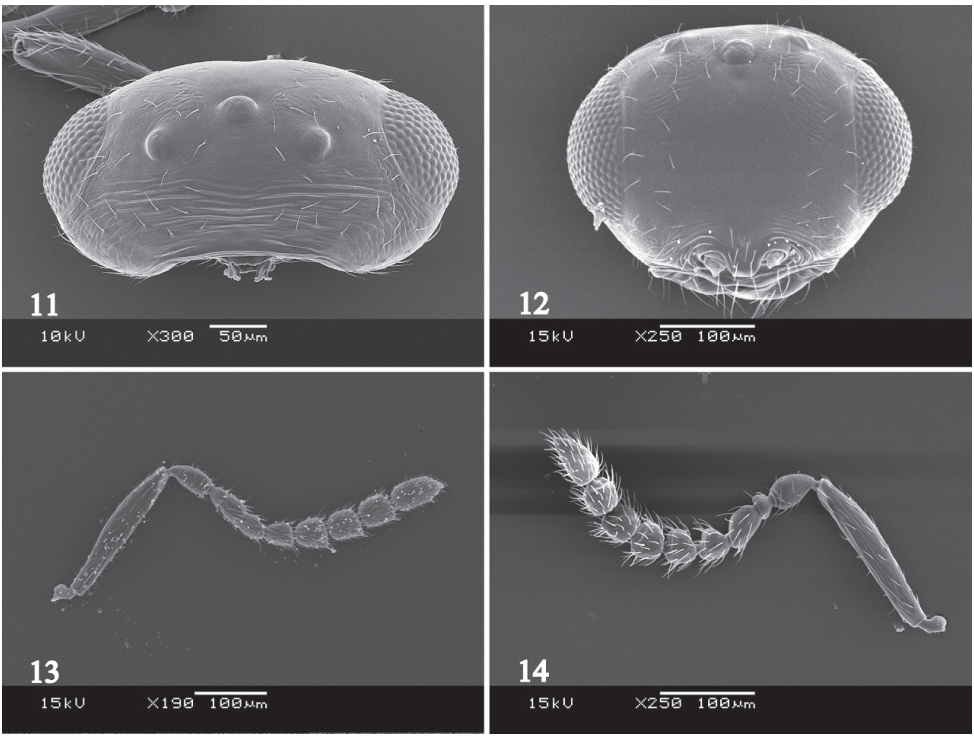

Figure 11–14. *Platygaster urniphila*. **11** female head, dorsal view **12** female head, frontal view **13** female antenna **14** male antenna. Scale bar 100 μm.

as long as wide; A3 quadrate; A4–A6 subquadrate, 1.1–1.2 times as long as wide; A7–A9 1.1–1.3 times as long as wide; A10 1.4–1.6 times as long as wide (Fig. 13).

Mesosoma as high as wide, 1.3–1.4 times as long as wide; sides of pronotum broadly smooth which is sometimes with extremely fine striae, smooth along posterior margin (Fig. 15); mesoscutum smooth in posterior half; notauli indicated in posterior half (Fig. 16); posterior margin of median lobe of mesoscutum not reaching base of mesoscutellum, with numerous long setae laterally; scuto-scutellar groove smooth and bare; mesoscutellum distinctly convex, smooth and covered with long hairs except median glabrous area (Fig. 17); mesopleuron with two setae anteriorly, with a coriaceous area below tegula; mesopleural carina absent; mesofurcal pit present; metapleuron pilose, sparse in dorsal one-third; propodeal carinae widely separated, parallel. Fore wing approximately 2.4 times as long as wide; marginal cilia approximately 0.1 times as long as width of fore wing. Hind wing approximately 5.3 times as long as wide, with two hamuli; marginal cilia approximately 0.2 times as long as width of hind wing.

Metasoma as long as head and mesosoma combined; T1 evenly crenulated, 1.7–1.8 times as wide as long, 0.2–0.3 times as long as T2; anterior margin of T2 weakly produced and overlapped T1; T2 weakly striated in basal half, with shorter striae medially (Fig. 18); T2–T5 with a band of shallow punctuation along posterior margin; T3–T5

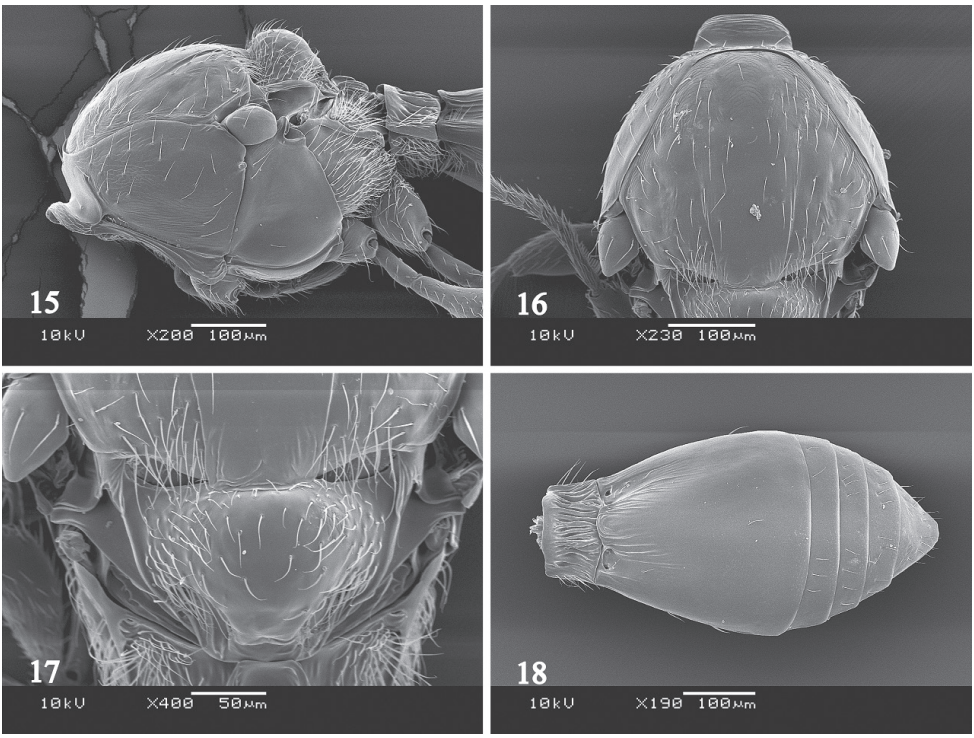

Figure 15–18. *Platygaster urniphila*. **15** female mesosoma, lateral view **16** female mesoscutum, dorsal view **17** female mesoscutellum, dorsal view **18** female metasoma, dorsal view.

with a row of setae which is broken medially; T6 with a setal row which is sometimes sparse medially, smooth.

MALE. Differs from the female as follows: Body length 1.1 mm. Antenna with erect setae; A4 distinctly widened; A5–A9 quadrate (Fig. 14). Metasoma approximately 0.8 times as long as head and mesosoma combined, obtuse at apex.

Differential diagnosis. *Platygaster urniphila* can be distinguished from *P. urnicola* Yamagishi, a Japanese species, based on the following characteristics: mesopleuron with a few setae anteriorly (glabrous in *P. urnicola*); posterior margin of median lobe of mesoscutum not reaching base of mesoscutellum (reaching base of mesoscutellum in *P. urnicola*). *Platygaster gifuensis* was described based on a single male from Japan, from which *P. urniphila* can be distinguished by having A5–A9 quadrate (approximately 1.5 times as long as wide in *P. gifuensis*). *Platygaster urniphila* is quite similar to *P. sublongicornis* Buhl because they share the following morphological characteristics: vertex between ocelli smooth; frons smooth medially; mesopleuron with a few setae anteriorly, with a coriaceous area below tegula; mesoscutellum distinctly convex; T2 weakly striated in basal half, with shorter striae medially. However, *Platygaster urniphila* can be distinguished from *P. sublongicornis* based on the following characters: A4–A5 subquadrate (distinctly elongate in *P. sublongicornis*); OOL as long as LOL (1.6 times as

Table 1. Reproduction by *Platygaster urniphila*: the number of adults emerged from a single larva of *Rhopalomyia longitubifex*.

Collecting date	Locality	Number of broods examined	Number of *P. tubiphila* emerged per larva (Mean ± SE)		
			Female	Male	Total (Female + Male)
8 December 2007	Jizoubaru, Kokonoe, Oita, Japan	1	29	0	29
2 March 2008	Chojabaru, Kokonoe, Oita, Japan	1	7	0	7
12 April 2008	Kuju, Taketa, Oita, Japan	1	8	0	8
9 November 2013	Chojabaru, Kokonoe, Oita, Japan	1	18	1	19
24 March 2016	Tano, Kokonoe, Oita, Japan	11	16.6 ± 1.4	2.7 ± 0.4	19.4 ± 1.6
18 March 2017	Machida, Kokonoe, Oita, Japan	23	11.4 ± 0.9	1.3 ± 0.3	12.7 ± 0.9

long as LOL in *P. sublongicornis*); sides of pronotum smooth along posterior margin (smooth along anterior and posterior margins in *P. sublongicornis*); hind wing approximately 5.3 times as long as wide (4.5 times in *P. sublongicornis*).

Biological notes. *Platygaster urniphila* is an egg-larval gregarious parasitoid of *Rhopalomyia longitubifex* that induces axillary bud galls on *Artemisia indica* var. *maximowiczii* in Japan (Yukawa and Masuda 1996; Ganaha et al. 2007). Gall polymorphism has been found in *R. longitubifex*: long jar-shaped, jar-shaped, and globular jar-shaped (see figures 1–5 of Ganaha et al. 2007). At present, *P. urniphila* has been reared only from globular jar-shaped galls. Various sorts of galls induced by *Rhopalomyia* spp. have been found on *Artemisia* spp. (e.g. Yukawa and Masuda 1996; Yukawa 2014; Gagné and Jaschhof 2017), but *P. urniphila* has been reared only from galls of *Rhopalomyia longitubifex* on *A. indica* var. *maximowiczii* in Japan. Future intensive studies are needed to confirm the host range of *P. urniphila.*

Leiby and Hill (1924) noted that *Platygaster vernalis*, a polyembryonic species, occasionally laid male and female eggs into a single host egg. Thus, *P. vernalis* has both polyembryonic and gregarious reproductive strategies. Our rearing experiments indicated that *P. urniphila* is a gregarious parasitoid because males and females were reared from a single host larva (Table 1). To confirm polyembryonic reproduction by *P. urniphila*, we need histological survey or MIG-seq analysis (Suyama and Matsuki 2015) that discriminate individuals originated from clonal division and sexual reproduction.

Acknowledgements

We wish to express our thanks to Dr E. Talamas for sending us high-resolution images of *Platygaster gifuensis*. We also thank Prof Y. Abe and Dr T. Ide for their support in taking SEM images, and Dr N. Wachi and Ms Y. Matsuo for their help in collecting galls of *Rhopalomyia longitubifex*. This study was supported partly by the Global COE Program (Center of excellence for Asian conservation ecology as a basis of human-nature

mutualism), Ministry of Education, Culture, Sports, Science and Technology, Japan to KM and the Academic Challenge 2010 from Robert T. Huang Entrepreneurship Center of Kyushu University, Japan to TF.

References

Ashmead WH (1904) Descriptions of new Hymenoptera from Japan – I. Journal of the New York Entomological Society 12: 65–84.

Askew RR (1975) The organization of chalcid-dominant parasitoid communities centred upon endophytic hosts. In: Price PW (Ed.) *Evolutionary Strategies of Parasitic Insects and Mites*. Plenum Press, New York, 130–153. https://doi.org/10.1007/978-1-4615-8732-3_7

Buhl PN (1994a) A extralinital species of the *Platygaster* complex (Hymenoptera: Platygastridae) from Denmark and England. Reichenbachia Staatliches Museum für Tierkunde Dresden 30: 163–165.

Buhl PN (1994b) Three new species of *Platygaster* Latreille, 1809, from Denmark (Hymenoptera, Platygastridae). Entomofauna 15: 77–84.

Buhl PN (2001a) Taxonomical notes on Platygastridae (Hymenoptera, Platygastroidea). Entomofauna 22: 17–40.

Buhl PN (2001b) Eleven new species of Platygastrinae (Hymenoptera: Platygastridae). Folia Entomologica Hungarica 62: 133–149.

Buhl PN (2003a) New or little known Palaearctic species of Platygastrinae (Hymenoptera: Platygastridae). Entomologica Fennica 14: 109–117.

Buhl PN (2003b) Three new species of Platygastrinae from Sri Lanka (Hymenoptera, Platygastridae). Entomofauna 24: 1–8.

Buhl PN (2004a) New African Platygastrinae (Hymenoptera: Platygastridae). Folia Entomologica Hungarica 65: 65–83.

Buhl PN (2004b) New Australasian Platygastrinae (Hymenoptera: Platygastridae). Folia Entomologica Hungarica 65: 85–105.

Buhl PN (2006a) Key to *Platygaster* (Hymenoptera: Platygastridae) from Denmark, with descriptions of new species. Steenstrupia 29: 127–167.

Buhl PN (2006b) New species of Platygastrinae from Canada (Hymenoptera: Platygastridae). Entomofauna 27: 193–205.

Buhl PN, Duso C (2008) *Platygaster robiniae* n. sp. (Hymenoptera: Platygastridae) parasitoid of *Obolodiplosis robiniae* (Diptera: Cecidomyiidae) in Europe. Annals of the Entomological Society of America 101: 297–300. https://doi.org/10.1603/0013-8746(2008)101[297:PRNSHP]2.0.CO;2

Fujii T, Matsuo K, Abe Y, Yukawa J, Tokuda M (2014) An endoparasitoid avoids hyperparasitism by manipulating immobile host herbivore to modify host plant morphology. PLOS ONE 9: e102508. https://doi.org/10.1371/journal.pone.0102508

Gagné RJ, Jaschhof M (2017) A catalog of the Cecidomyiidae (Diptera) of the world 4th (edn). https://www.ars.usda.gov/ARSUserFiles/80420580/Gagne_2017_World_Cat_4th_ed.pdf

Ganaha T, Nohara M, Sato S, Uechi N, Yamagishi K, Yamauchi S, Yukawa J (2007) Polymorphism of axillary bud galls induced by *Rhopalomyia longitubifex* (Diptera: Cecidomyiidae) on *Artemisia princeps* and *A. montana* (Asteraceae) in Japan and Korea, with designation of new synonyms. Entomological Science 10: 157–169. https://doi.org/10.1111/j.1479-8298.2007.00210.x

Ishii T (1953) A report of the studies of the parasitic wasps of injurious insects. Bulletin of the Faculty of Agriculture, Tokyo University of Agriculture and Technology 1: 1–10.

Kim IK, Parl JD, Shin SC, Park IK (2011) Prolonged embryonic stage and synchronized life-history of *Platygaster robiniae* (Hymenoptera: Platygastridae), a parasitoid of *Obolodiplosis robiniae* (Diptera: Cecidomyiidae). Biological Control 57: 24–30. https://doi.org/10.1016/j.biocontrol.2010.12.007

Leiby RW, Hill CC (1924) The polyembryonic development of *Platygaster vernalis*. Journal of Agricultural Research 28: 829–839.

Masner L, Huggert L (1989) World review and keys to genera of the subfamily Inostemmatinae with reassignment of the taxa to the Platygastrinae and Sceliotrachelinae. Memoirs of the Entomological Society of Canada 147: 1–214.

Matsuo K, Yang MM, Tung GS, Tokuda M, Yukawa J (2012) Description of a new and redescriptions of two known species of *Torymus* (Hymenoptera: Torymidae) in Taiwan with a key to Taiwanese species. Zootaxa 3409: 47–57.

Matsuo K, Yukawa J (2009) Two new species of *Torymus* Dalman, 1820 (Hymenoptera: Torymidae) parasitizing *Celticecis japonica* Yukawa & Tsuda, 1987 (Diptera: Cecidomyiidae) that induces leaf galls on *Celtis* species (Ulmaceae) in Japan. Entomological Science 12: 261–269. https://doi.org/10.1111/j.1479-8298.2009.00330.x

Mikó I, Vilhelmsen L, Johnson NF, Masner L, Pénzes Z (2007) Skeletomusculature of Scelionidae (Hymenoptera: Platygastroidea): head and mesosoma. Zootaxa 1571: 1–78.

Segoli M, Harari AR, Rosenheim JA, Bouskila A, Keasar T (2010) The evolution of polyembryony in parasitoid wasps. Journal of Evolutionary Biology 23: 1807–1819. https://doi.org/10.1111/j.1420-9101.2010.02049.x

Stireman III JO, Nason JD, Heard SB, Seehawer JM (2006) Cascading host-associated genetic differentiation in parasitoids of phytophagous insects. Proceedings of the Royal Society B 273: 523–530. https://doi.org/10.1098/rspb.2005.3363

Sunose T (1983) Studies on the population dynamics of the euonymus gall midge *Masakimyia pustulae* Yukawa et Sunose (Diptera: Cecidomyiidae) under different environmental conditions. Kontyû 51: 29–40.

Sunose T (1984) Parasitoid complex of the euonymus gall midge *Masakimyia pustulae* Yukawa et Sunose (Diptera: Cecidomyiidae) in Japan. Kontyû 52: 557–564.

Sunose T (1985) Population regulation of the euonymus gall midge *Masakimyia pustulae* Yukawa & Sunose (Diptera: Cecidomyiidae) by hymenopterous parasitoids. Researches on Population Ecology 27: 287–300. https://doi.org/10.1007/BF02515467

Suyama Y, Matsuki Y (2015) MIG-seq: an effective PCR-based method for genome-wide single-nucleotide polymorphism genotyping using the next-generation sequencing platform. Scientific Reports 5: 16963. https://doi.org/10.1038/srep16963

Tabuchi K, Amano H (2004) Impact of differential parasitoid attack on the number of chambers in multilocular galls of two closely related gall midges (Diptera: Cecidomyiidae). Evolutionary Ecology Research 6: 695–707.

Vlug HJ (1995) Catalogue of the Platygastridae (Platygastroidea) of the world. Hymenopterorum Catalogus 19: 1–168.

Yamagishi K (1980) Platygastrid parasites of willow gall midges in Japan. Esakia 15: 161–175.

Yoshida N, Hirashima Y (1979) Systematic studies on proctotrupoid and chalcidoid parasites of gall midges injurious to *Pinus* and *Cryptomeria* in Japan and Korea. Esakia 14: 113–133.

Yukawa J (2014) Family Cecidomyiidae. The Entomological Society of Japan. Catalogue of the Insects of Japan, Volume 8 Diptera, Part 1 Nematocera – Brachycera Aschiza. Touka Shobo, Fukuoka, 126–160.

Yukawa J, Masuda H (1996) Insect and Mite Galls of Japan in Colors. Zenkoku Nôson Kyôiku Kyôkai, Tokyo, 826 pp. https://doi.org/10.4241/kyubyochu.27.113 [In Japanese with English explanation for color plates]

Yukawa J, Ohsako S, Ikenaga H (1981) Parasite complex of the Japanese species of the genus *Asphondylia* (Diptera: Cecidomyiidae), including the soybean pod gall midge. Proceedings of the Association for Plant Protection of Kyushu 27: 113–115. [In Japanese with English summary]

Yukawa J, Sunose T (1976) Description of a new gall midge (Diptera, Cecidomyiidae) on *Euonymus*, with notes on its bionomics. Kontyû 44: 159–168.

Supplementary material 1

A list of papers that were used for morphological comparison

Authors: Kazunori Matsuo, Tomohisa Fujii, Makoto Tokuda, Tomoko Ganaha–Kikumura, Junichi Yukawa, Kenzou Yamagishi

Data type: bibliographic records

Link: https://doi.org/10.3897/zookeys.754.23296.suppl1

ZooKeys 754: 127–139 (2018)
doi: 10.3897/zookeys.754.23404
http://zookeys.pensoft.net

RESEARCH ARTICLE

A peer-reviewed open-access journal
ZooKeys
Launched to accelerate biodiversity research

Characterization of the complete mitochondrial DNA of *Theretra japonica* and its phylogenetic position within the Sphingidae (Lepidoptera, Sphingidae)

Jun Li[1], Rui-Rui Lin[1], Yao-Yao Zhang[1], Kun-Jie Hu[1], Ya-Qi Zhao[1], Yan Li[1], Zhuo-Ran Huang[1], Xu Zhang[1], Xue-Xia Geng[1], Jian-Hua Ding[1]

1 *School of Life Sciences, Huaibei Normal University, Huaibei, China*

Corresponding author: *Jian-Hua Ding* (59823039@qq.com)

Academic editor: *Rodolphe Rougerie* | Received 4 January 2018 | Accepted 3 April 2018 | Published 3 May 2018

http://zoobank.org/148A44C4-C211-4B84-97BC-4D22BBFF47F9

Citation: Li J, Lin R-R, Zhang Y-Y, Hu K-J, Zhao Y-Q, Li Y, Huang Z-R, Zhang X, Geng X-X, Ding J-H (2018) Characterization of the complete mitochondrial DNA of *Theretra japonica* and its phylogenetic position within the Sphingidae (Lepidoptera: Sphingidae). ZooKeys 754: 127–139. https://doi.org/10.3897/zookeys.754.23404

Abstract

In the present study, the complete mitogenome of *Theretra japonica* was sequenced and compared with other sequenced mitogenomes of Sphingidae species. The mitogenome of *T. japonica*, containing 37 genes (13 protein-coding genes, 22 tRNA genes, and two rRNA genes) and a region rich in adenine and thymine (AT-rich region), is a circular molecule with 15,399 base pairs (bp) in length. The order and orientation of the genes in the mitogenome are similar to those of other sequenced mitogenomes of Sphingidae species. All 13 protein-coding genes (PCGs) are initiated by ATN codons except for the cytochrome *C* oxidase subunit 1 gene (*cox1*) which is initiated by the codon CGA as observed in other lepidopteran insects. Cytochrome *C* oxidase subunit 2 gene (*cox2*) has the incomplete termination codon T and NADH dehydrogenase subunit 1 gene (*nad1*) terminates with TAG while the remainder terminates with TAA. Additionally, the codon distributions of the 13 PCGs revealed that Ile and Leu2 are the most frequently used codon families and codons CGG, CGC, CCG, CAG, and AGG are absent. The 431 bp AT-rich region includes the motif ATAGA followed by a 23 bp poly-T stretch, short tandem repeats (STRs) of TC and TA, two copies of a 28 bp repeat 'ATTAAATTAATAAATTAA TATATTAATA' and a poly-A element. Phylogenetic analyses within Sphingidae confirmed that *T. japonica* belongs to the Macroglossinae and showed that the phylogenetic relationship of *T. japonica* is closer to *Ampelophaga rubiginosa* than *Daphnis nerii*. Phylogenetic analyses within *Theretra* demonstrate that *T. japonica*, *T. jugurtha*, *T. suffusa*, and *T. capensis* are clustered into one clade.

Keywords
Lepidoptera, mitogenome, Sphingidae, *Theretra japonica*

Introduction

The Sphingidae (Lepidoptera) moths are commonly known as hawk moths, sphinx moths, or hornworms and include 1,463 species (Nieukerken et al. 2011). *Theretra japonica*, known as a pest, is widely distributed in Korea, Japan, Russia, and China. Its larva eats leaves and is harmful to many important ornamental plants, such as *Vitis vinifera*, *Saxifraga stolonifera*, *Hoya carnosa*, and *Cayratia japonica* etc. (Zhu and Wang 1997; Shirotsuka and Yano 2012).

Mitochondrial DNA sequences have been widely used to study the molecular evolution of insects due to protein-coding genes (PCGs) sequence conservatism, maternal inheritance, and rapid evolution (Cameron 2014). In Sphingidae, however, only the complete mitochondrial DNA sequences of *Notonagemia analis* (KU934302) (Kim et al. 2016), *Sphinx morio* (KC470083) (Kim et al. 2013), *Manduca sexta* (EU286785) (Cameron and Whiting 2008), *Ampelophaga rubiginosa* (KT153024) (Xin et al. 2017), *Agrius convolvuli* (https://doi.org/10.1139/gen-2016-0058) (Dai et al. 2017), and *Daphnis nerii* (https://doi.org/10.1371/journal.pone.0178773.s001) (Sun et al. 2017) have been reported up to now. Among these six species, *N. analis*, *S. morio, A. convolvuli,* and *M. sexta* belong to the subfamily Sphinginae, while *A. rubiginosa* and *D. nerii* belong to the Macroglossinae. More mitogenome sequences from Sphingidae will be helpful to discover the interfamilial phylogenetic relationships. *Theretra japonica* is taxonomically classified into the subfamily Macroglossinae according to its morphology (Zhu and Wang 1997), but its mitogenome has not yet been reported, nor a phylogenetic analysis based on this.

In this study polymerase chain reaction (PCR) amplification, DNA sequencing, and overlapped fragments assembling methods were used to determine the complete mitogenome of *T. japonica*. The characteristics of the mitogenome were also analyzed and a phylogeny was constructed. These will be helpful to understand the evolutionary position of *T. japonica* within Sphingidae.

Materials and methods

Specimens sampling and DNA extraction

The specimen was collected from Xiangshan mountain, Huaibei city, Anhui province, China (33°59.02'N, 116°48.57'E), and then was preserved in -20 °C refrigerator. Total genomic DNA was extracted from the abdomen of the moth (voucher number TJ20171011) using Ezup Column Animal Genomic DNA Purification Kit (Sangon Biotech, China) following the manufacturer's instructions. The extracted DNA sam-

ples were stored at -20°C. The specimen and the template DNA are respectively deposited in Specimens Room within the Human and Animal Genetics Laboratory, School of Life Sciences, Huaibei Normal University.

PCR amplification and DNA sequencing

The mitochondrial DNA fragments were amplified by PCR method and the total genomic DNAs were used as template. PCR primers were designed according to the conservative sequences of mitochondrial DNA of Lepidoptera insects and showed in Table 1. The overlapping fragments were amplified using PrimeSTAR® GXL DNA Polymerase (Takara, China) according to the manufacturer's instructions. PCR reaction mixture (25 μL in total) included 5 μL 5× PrimeSTAR GXL Buffer, 2 μL dNTP mixture (2.5 mM each), 2.5 μL primer (10 μM) each, 1 μL PrimeSTAR GXL DNA Polymerase, 1 μL template DNA (100 ng/μL) and 11 μL double distillated water. PCR reaction was performed in Eppendoff Mastercycler gradient PCR instrument under the following conditions: 30 sec at 98 °C; followed by 30 cycles of 15 sec at 98 °C, 15 sec at 40–55 °C and 2–8 min at 68 °C; and at last 10 min at 68 °C. PCR productions were confirmed by 1% (w/v) agarose gel electrophoresis and sequenced at least three times.

Sequences assembly, annotation and analysis

The overlapping fragments were assembled into a complete linear mitochondria DNA sequence using the DNAStar package (DNAStar Inc. Madison, WI, USA), and the mitogenome was annotated using MITOS2 (Bernt et al. 2013). The PCGs and ribosomal RNA (rRNA) genes were verified by NCBI BLAST. The transfer RNA (tRNA) genes were verified by tRNAscan-SE2.0 (Lowe and Chan 2016; Lowe and Eddy 1997). Barcoding analysis was performed in Bold Systems v4 using *cox1* as the marker following the recom-

Table 1. Details of the primers used to amplify the mitochondrial DNA of *T. japonica*.

Primer name	Orientation	Annealing position (bp)	Nucleotide sequence (5'-3')	PCR length
Q1F	F	1314-1336	AAACTAATAATCTTCAAAATTAT	
Q1R	R	6236-6213	AATATTAATGGAATTTAACCACTA	4923
Q2F	F	6193-6216	TAAGCTGCTAACTTAATTTTTAGT	
Q2R	R	9637-9617	GTTTCAATAATCCGAACTCAT	3445
Q3F	F	8601-8618	CGTCTATGCAATCGCTCA	
Q3R	R	12319-12302	GCATTACTTGGAGGGTTG	3719
Q4F	F	11600-11620	TCCCTATGTTATTACAGGACA	
Q4R	R	14809-14791	CCAGCAGTTGCGGTTATAC	3210
Q5F	F	14637-14659	TAATAGGGTATCTAATCCTAGTT	
Q5R	R	1400-1378	ATATAAAATTGCAAATTTTAAGG	2163

mendations of Botera-Castro et al (2016). The protein sequences were translated with the invertebrate mitochondrial genetic code. Nucleotides composition and codon usage were counted using MEGA 7.0. The bias of nucleotide composition was measured as AT skew (AT skew = (A-T)/(A+T)) and GC skew (GC skew = (G-C)/(G+C)) respectively.

Phylogenetic analyses

To clarify the phylogenetic position of *T. japonica* within the Sphingidae, all published complete mitogenomes of members of the Sphingidae were collected and their 13-protein amino acid (AA) sequences were incorporated together for alignment and phylogenetic tree construction. Sequences were aligned using ClustalX 2.1 (Larkin et al. 2007) and phylogenetic trees were constructed using the Neighbor-Joining (NJ) and Maximum likelihood analysis (ML) methods with bootstrap test of 1000 replications by MEGA 7.0 (Kumar et al. 2016). *Bombyx mori* (Bombycidae, AF149768) and *Antheraea pernyi* (Saturniidae, AY242996) were utilized as outgroups. The gaps or missing data subsets were completely deleted. Before constructing the ML phylogeny, Mega 7.0 was utilized to find the best model (mtREV + F + G). The NJ phylogeny was constructed using Poisson model and bootstrap for 1000 times. The parameter of Rates among Sites was set as Gamma distributed (G) and value as 13. The parameter for Pattern among Lineages was set as homogeneous.

The *cox1* barcodes (481 barcodes) were gathered for the genus *Theretra* in BOLD system v4 to construct phylogeny. Those barcodes without gaps or missing nucleotides (total 658 bp in size) were selected to construct ML phylogenetic tree, and finally 285 barcodes (41 species) were utilized. The *cox1* sequence of *B. mori* (AF149768) was used as outgroup. The best model was GTR + G + I. To infer nodal support, bootstrapping was conducted 1000 times.

Results and discussion

Genome organization and nucleotides composition

The complete mitogenome sequence of *T. japonica* (MG655620) is 15,399 base pairs (bp) in length, shorter than *M. sexta* but longer than the other 5 species of Sphingidae. It contains 13 PCGs, 22 tRNAs genes, two rRNAs genes, and an AT-rich region with a length of 431 bp (Fig. 1, Suppl. material 2). Among the 37 genes, 23 genes are encoded by the majority-coding strand (J-strand) and 14 genes are encoded by the minority-coding strand (N-strand). The gene order and orientation are consistent to the other Sphingidae species.

The nucleotide composition in J-strand of *T. japonica* mitogenome is as follows: 6,331 bp (41.11%) A, 6,043 bp (39.24%) T, 1,883 (12.23%) C, and 1,142 bp (7.42%) for G. A+T accounts for 80.36%, which is slightly higher than *D. nerii* (80.29%) but

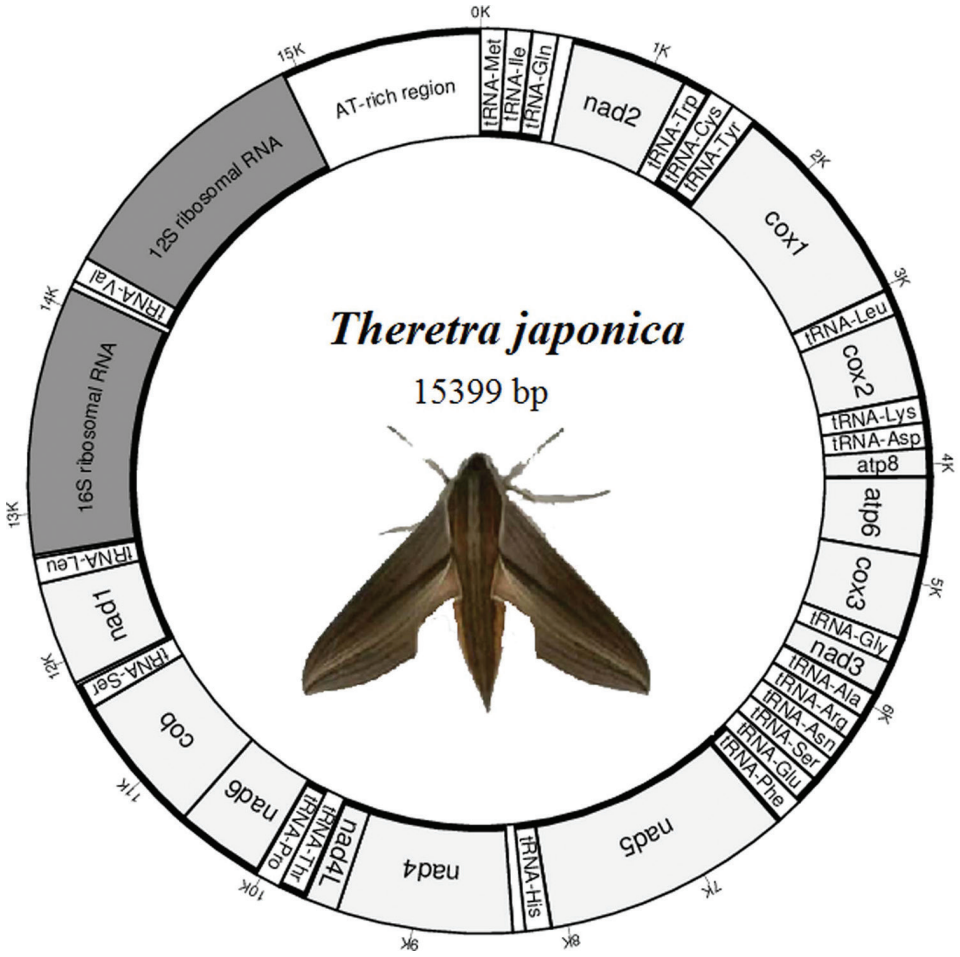

Figure 1. The schematic illustration for mitogenome of *T. japonica*. Gene order and positions are shown. *cox1*, *cox2,* and *cox3* refer to the cytochrome *c* oxidase subunits; *cob* refers to cytochrome *b*; *nad1-nad6* refers to NADH dehydrogenase components; *rrnL* and *rrnS* refer to ribosomal RNAs. The bold lines on outer or inner ring represent that the genes lie in the majority-coding strand (J-strand) or the minority-coding strand (N-strand).

lower than *M. sexta* (81.79%), *S. morio* (81.17%), *N. analis* (81.79%), *A. convolvuli* (81.49%), and *A. rubiginosa* (81.5%) (Sun et al. 2017; Xin et al. 2017; Dai et al. 2016). The AT skew and GC skew of *T. japonica* J-strand are 0.023 and -0.245 respectively (Table 2). The GC skews of the seven Sphingidae species are all negative and the AT skews are positive except for *M. sexta* (-0.005) and *A. convolvuli* (-0.001) (Sun et al. 2017; Xin et al. 2017; Dai et al. 2016).

In the mitogenome of *T. japonica*, there are 13 gene overlaps and 15 intergenic spacers (Suppl. material 2). The 13 gene overlaps range from 1 to 17 bp in size and the longest is present between *trnF* and *nad5*. The 15 intergenic spacers range from 1 to 88 bp in size, and the longest is present between *trnQ* and *nad2*, which is also founded

Table 2. Base composition of protein-coding, tRNA and rRNA genes, and A+T rich region of *T. japonica* mitogenome.

Genes or regions	Size (bp)	Base composition (%)				A+T (%)	AT skewness	GC skewness
		A	T	C	G			
nad2	1014	37.87	47.14	9.66	5.33	85.01	-0.109	-0.289
cox1	1536	32.42	38.61	15.63	13.35	71.03	-0.087	-0.079
cox2	685	37.96	39.27	13.14	9.64	77.23	-0.017	-0.154
atp8	165	44.85	44.24	9.09	1.82	89.09	0.007	-0.667
atp6	678	36.28	41.89	14.16	7.67	78.17	-0.072	-0.297
cox3	792	34.22	39.52	14.52	11.74	73.74	-0.072	-0.106
nad3	354	36.44	43.79	12.99	6.78	80.23	-0.092	-0.314
nad5	1758	32.82	48.81	5.92	12.46	81.63	-0.196	0.356
nad4	1332	33.63	48.42	6.38	11.56	82.06	-0.180	0.289
nad4L	291	30.93	52.58	3.78	12.71	83.06	-0.259	0.542
nad6	531	40.49	45.20	8.66	5.65	85.69	-0.056	-0.210
cob	1149	34.64	40.82	14.45	10.10	75.46	-0.082	-0.177
nad1	936	30.02	48.08	7.48	14.42	78.10	-0.231	0.317
Total	11221	34.50	44.38	10.53	10.59	78.88	-0.125	0.003
tRNA	1465	41.77	39.32	8.05	10.85	81.09	0.030	0.148
rRNA	2048	41.50	42.24	5.08	11.18	83.74	-0.009	0.375
AT-rich region	431	41.50	42.24	5.08	11.18	93.04	-0.007	-0.400
Complete mitogenome	15399	41.11	39.24	12.23	7.42	80.36	0.023	-0.245

in the other six Sphingidae species. However, the intergenic spacer between *trnQ* and *nad2* of *T. japonica* is longer than that of the other six species, which range from 51bp in *N. analis* to 56 bp in *A. rubiginosa*.

Protein-coding genes and codon usage

The *T. japonica* mitogenome contains 13 PCGs as expected with a total of 11,221 bp in size. All the PCGs are initiated with ATN codons, except for *cox1*, which uses CGA as the initiation codon. Most PCGs are terminated with TAA codon while *nad1* uses TGA as termination codon. And yet, *cox2* has an incomplete termination codon 'T'. The incomplete termination codon 'T' or 'TA' could become TAA by posttranscriptional polyadenylation (Ojala et al. 1981). In the 13 PCGs, only the AT skewness of *atp8* is positive (0.007) while the others are negative. The GC skewness of *nad1*, *nad4*, *nad4L,* and *nad5* are positive and all lie in the N-strand.

The amino acids (AAs) components and their codon usage in the PCGs of *T. japonica* mitogenome were also analyzed. The results reveal that two codon families (Ile and Leu2) are more than 100 codons per thousand codons (CDpT), six codon families (Asn, Gly, Met, Phe, Ser2, and Tyr) are between 50 CDpT and 100 CDpT, and the other fourteen codon families are less than 50 CDpT (Fig. 2). AAs codon usage is assessed by values of the relative synonymous codon usage (RSCU) and five codons

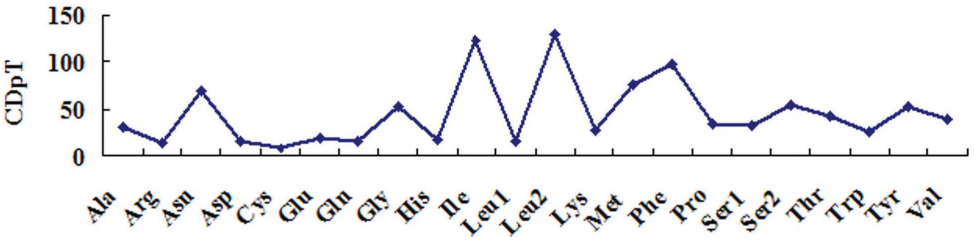

Figure 2. The amino acids usage in the mitogenome of *T. japonica*. CDpT = codons per thousand codons.

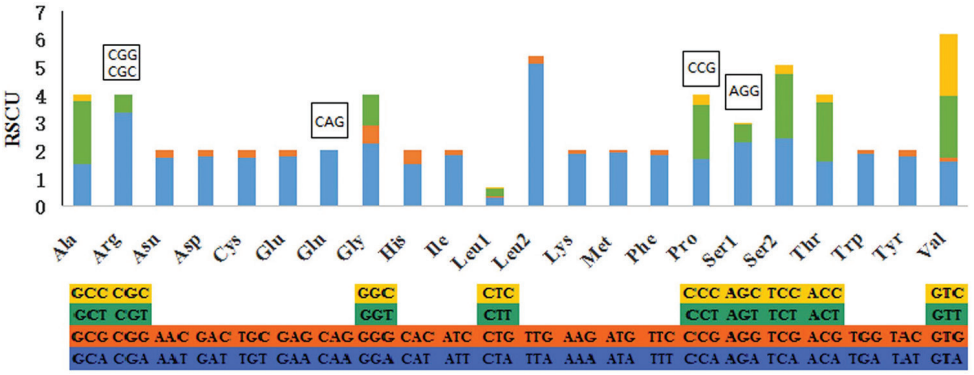

Figure 3. The relative synonymous codon usage (RSCU) in the mitogenome of *T. japonica*. The codons listed up the columns are absent in *T. japonica*.

(CGG, CGC, CCG, CAG, and AGG) are absent in the PCGs of *T. japonica* (Fig. 3). It is found that the codons with high G and C content are likely not to be favored in lepidopteran insects (Dai et al. 2016).

Ribosomal RNA genes and transfer RNA genes.

The 22 rRNA genes of *T. japonica* range from 64 bp to 71 bp in size and totally comprise 1,465 bp of the whole mitogenome. Of these genes, 14 are encoded in J-strand and 8 in N-strand just as other Sphingidae moths. The predicted secondary structures of the tRNAs are shown in Figure 4. All the tRNA genes except for *trnS1* could be folded into the typical cloverleaf secondary structure (Fig. 4). The A+T content of the 22 tRNAs is 83.74%, with a positive AT skew (0.030) and GC skew (0.148).

Just as the other Sphingidae species there are two rRNA genes in *T. japonica* with a total length of 2,048 bp. The large ribosomal gene (*rrnL*) locates between *trnL1* and *trnV,* with a length of 1,284 bp whereas the small ribosomal gene (*rrnS*) locates between *trnV* and the A+T-rich region with a length of 764 bp. The AT skew is slightly negative (–0.009), but the GC skew is strongly positive (0.375). The total A+T content of the rRNA genes (83.74%) is higher than that of total tRNA genes (81.09%) and total PCG genes (79.10%).

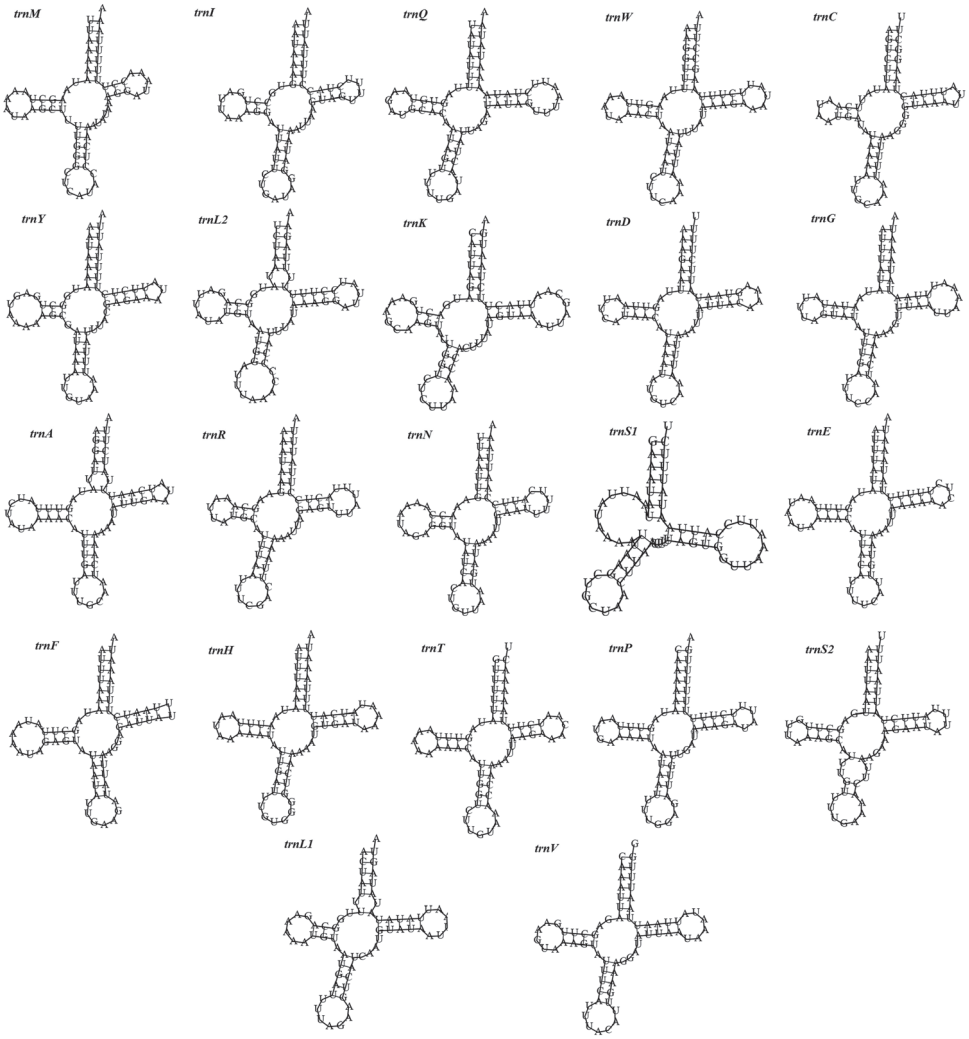

Figure 4. The cloverleaf secondary structure of transfer RNA of *T. japonica*.

A+T rich region

The A+T rich region locates between *rrnS* and *trnM* in *T. japonica* with 431 bp in length and serves as the initiation of mitochondrial replication in both vertebrates and invertebrates (Cameron 2014). This region contains the highest A+T content (93.04%) in the mitogenome of *T. japonica*. As the other lepidopteran mitogenomes, the A+T rich region of *T. japonica* has some conserved structures including the motif 'ATAGA' followed by a 23 bp poly-T stretch, a short tandem repeats (STRs) of TC and TA, two copies of a 28 bp repeat 'ATTAAATTAATAAATTAATATAT-

rrnS-AAAATTTATTTATTTGTAAAATTTTTCACATAGATTTTTTTTTTTTTTTTTTTTTTATA
TATAAATATTTAATATATAATAATTATATTAATTAATTAAAATTATTGTTATAAATTATTAAAC
AATTTATATTCTCTCTCTCTCTCTAACTAATATTAAATATAAATATAAAATTGCTATATAAA
ATTTCATAATTTAATAAATAATAATAAATATATGTAATTATTATTTATTTTTTTACATTAATTT
AATAAATTAATATATTAATAATAAATTAAAAATTTAATTTATTATTAATTAAAAAAATAAAT
TAAATTTTTAATATATATATATATATATACATGTGCATATAAATAAATTAAAGTTAAATAA
CTTAATTTTTTTCTATACCATTTGAAAAAAAATTTCATTAAATATAAAAAAAAAAA-*trnM*

Figure 5. Features of the A+T-rich region of *T. japonica*. The ATATG motif is shaded. The polyT stretch is underlined while the poly-A stretch is double underlined. The TA and GC repeats sequence are indicated by dotted underlining. The 28 bp repeats 'ATTAAATTAATAAATTAATATATTAATA' are labeled with wave underlining.

TAATA', and a poly-A element upstream of the *trnM* (Fig. 5). The poly-T element may be associated with mitochondrial transcription controlling and replication initiation.

Barcoding analysis and phylogenetic analysis

By using the identified *cox1* barcode and aligning it with the three barcodes of *T. japonica* deposited in Bold system v4 we found that the similarities are 100% with GBMIN88089-17 (KX440686, 541 bp) and SOWD617-06 (JN678612, 658 bp), and 99.85% with GBMIN88088-17 (KT988392, 658 bp) respectively. The only mutation of GBMIN88088-17 takes place at the third position nucleotide of a codon for Leucine which mutates from TTA to TTG, but the mutation is synonymous because it does not change its AA code (Fig. 6). SOWD617-06 was collected from Sichuan province, China (Wilson et al. 2011) and the positions where the two others were collected are unspecified.

Phylogenetic analyses were firstly based on the sequences of 13 PCGs of seven mitogenomes using NJ and ML Methods. The phylogenetic trees constructed by NJ and ML are consistent with high intermediate bootstrap values (Fig. 7). The Sphingidae includes three subfamilies, Sphinginae, Macroglossinae, and Smerinthinae, but no complete mitogenome from the Smerinthinae has been published so far. Among these species of Sphingidae, *T. japonica*, *A. rubiginosa* and *D. nerii* belong to Macroglossinae and the other four belong to Sphinginae. *T. japonica, D. nerii* and *A. rubiginosa* are clustered together into a monophyletic group and *T. japonica* is phylogenetically closer to *A. rubiginosa* than *D. nerii*. The phylogenetic tree of these seven species is ((*T. japonica* + *A. rubiginosa*) + *D. nerii*) + ((*N. analis* + *A. convolvuli*) + (*S. morio* + *M. sexta*)) which is also partly supported by Kawahara et al (2009). ML phylogenetic tree constructed for genus *Theretra* demonstrates that *T. japonica*, *T. jugurtha*, *T. suffusa*, and *T. capensis* are clustered into one clade (Suppl. material 1).

```
MG655620          ACTTCATTAAGATTACTAATTCGAGCAGAATTAGGA
SOWD617-06        ACTTCATTAAGATTACTAATTCGAGCAGAATTAGGA
GBMIN88088-17     ACTTCATTAAGATTGCTAATTCGAGCAGAATTAGGA
GBMIN88089-17     ..............TAATTCGAGCAGAATTAGGA
Consensus         acttcattaagatt*ctaattcgagcagaattagga
AA                S  L  S  L  L  I  R  A  E  L  G  T
```

Figure 6. Barcoding analysis of *T. japonica*.

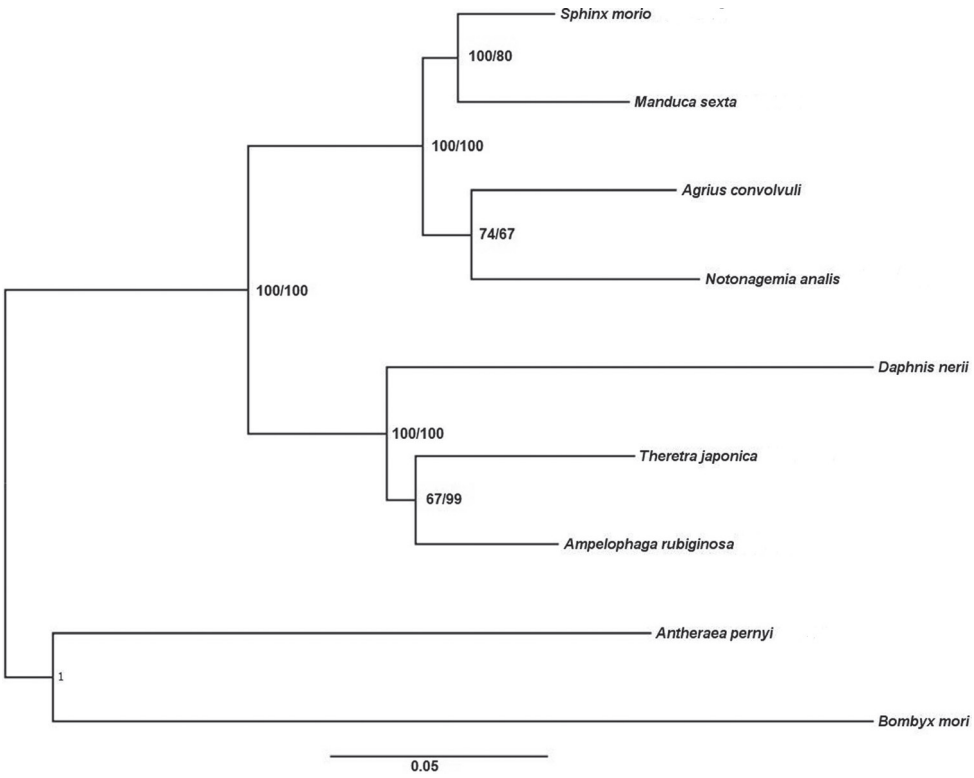

Figure 7. Phylogenetic analysis. Phylogenetic tree constructed using NJ and ML methods based on the amino acid sequences of 13 PCGs of 7 species with *Bombyx mori* (Lepidoptera: Bombycidae) and *Antheraea pernyi* (Lepidoptera: Saturniidae) as outgroups. The support values at the nodes represent bootstrap values for NJ and ML respectively.

References

Bernt M, Donath A, Juhling F, Externbrink F, Florentz C, Fritzsch G, Putz J, Middendorf M, Stadler PF (2013) MITOS: improved de novo metazoan mitochondrial genome annotation. Molecualr Phylogenetics Evolution 69: 313–319. https://doi.org/10.1016/j.ympev.2012.08.023

Botero-Castro F, Delsuc F, Douzery EJP (2016) Thrice better than once: quality control guidelines to validate new mitogenomes. Mitochondrial DNA. Part A, DNA mapping, sequencing, and analysis 27(1): 449–454. https://doi.org/10.3109/19401736.2014.900666

Cameron SL (2014) Insect mitochondrial genomics: implications for evolution and phylogeny. Annual Review of Entomology 59(1): 95–117. https://doi.org/10.1146/annurev-ento-011613-162007

Cameron SL, Whiting MF (2008) The complete mitochondrial genome of the tobacco hornworm, *Manduca sexta*, (Insecta: Lepidoptera: Sphingidae), and an examination of mitochondrial gene variability within butterflies and moths. Gene 408: 112–123. https://doi.org/10.1016/j.gene.2007.10.023

Dai LS, Li S, Yu HM, Wei GQ, Wang L, Qian C, Zhang CF, Li J, Sun Y, Zhao Y, Zhu BJ, Liu CL (2017) Mitochondrial genome of the sweet potato hornworm, *Agrius convolvuli* (Lepidoptera: Sphingidae), and comparison with other Lepidoptera species. Genome 60: 128–138. https://doi.org/10.1139/gen-2016-0058.

Kawahara AY, Mignault AA, Regier JC, Kitching IJ, Mitter C (2009) Phylogeny and biogeography of hawkmoths (Lepidoptera: Sphingidae): evidence from five nuclear genes. PLoS ONE 4(5): e5719. https://doi.org/10.1371/journal.pone.0005719

Kim MJ, Choi SW, Kim I (2013) Complete mitochondrial genome of the larch hawk moth, *Sphinx morio* (Lepidoptera: Sphingidae). Mitochondrial DNA 24: 622–624. https://doi.org/10.3109/19401736.2013.772155

Kim MJ, Kim JS, Kim I (2016) Complete mitochondrial genome of the hawkmoth *Notonagemia analis scribae* (Lepidoptera: Sphingidae). Mitochondrial DNA Part B 1: 416–418. https://doi.org/10.1080/23802359.2016.1176883

Kumar S, Stecher G, Tamura K (2016) MEGA7: Molecular Evolutionary Genetics Analysis Version 7.0 for Bigger Datasets. Molecular Biology & Evolution 33: 1870–1874. https://doi.org/10.1093/molbev/msw054

Larkin MA, Blackshields G, Brown NP, Chenna R, McGettigan PA, McWilliam H, Valentin F, Wallace IM, Wilm A, Lopez R, Thompson JD, Gibson TJ, Higgins DG (2007) Clustal W and Clustal X version 2.0. Bioinformatics 23: 2947–2948. https://doi.org/10.1093/bioinformatics/btm404

Lowe TM, Chan PP (2016) tRNAscan-SE On-line: integrating search and context for analysis of transfer RNA genes. Nucleic Acids Research 44: W54–57. https://doi.org/10.1093/nar/gkw413

Lowe TM, Eddy SR (1997) tRNAscan-SE: a program for improved detection of transfer RNA genes in genomic sequence. Nucleic Acids Research 25(5): 955–964. https://doi.org/10.1093/nar/25.5.955

Nieukerken LK, Kitching IJ, Kristensen NP, Lees DC, Minet J, Mitter C, Mutanen M, Regier JC, Simonsen TJ, Wahlberg N, Yen SH, Zahiri R, Adamski D, Baixeras J, Bartsch D, Bengtsson BA, Brown JW, Bucheli SR, Davis DR, Prins JD, Prins WD, Epstein ME, Patricia GP, Gielis Cees, Hättenschwiler P, Hausmann A, Holloway JD, Kallies A, Karsholt O, Kawahara AY, Koster S, Kozlov MV, Lafontaine D, Lamas G, Landry JF, Lee S, Nuss M, Park KT, Penz C, Rota J, Schintlmeister A, Schmidt BC, Sohn JC, Solis MA, Tarmann

GM, Warren AD, Weller S, Yakovlev RV, Zolotuhin VV, Zwick A (2011) Order Lepidoptera Linnaeus, 1758. In: Zhang Z-Q (Ed.) Animal biodiversity: An outline of higher-level classification and survey of taxonomic richness. Zootaxa 3148: 212–221.

Ojala D, Montoya J, Attardi G (1981) tRNA punctuation model of RNA processing in human mitochondria. Nature 290: 470–474. https://doi.org/10.1038/290470a0

Shirotsuka K, Yano S (2012) Coincidental intraguild predation by caterpillars on spider mites. Experimental & Applied Acarology 56(4): 355–364. https://doi.org/10.1007/s10493-012-9514-4

Sun Y, Chen C, Gao J, Abbas MN, Kausar S, Qian C, Wang L, Wei G, Zhu BJ, Liu CL (2017) Comparative mitochondrial genome analysis of *Daphnis nerii* and other lepidopteran insects reveals conserved mitochondrial genome organization and phylogenetic relationships. PLoS ONE 12(6): e0178773. https://doi.org/10.1371/journal.pone.0178773

Wilson JJ, Rougerie R, Schonfeld J, Janzen DH, Hallwachs W, Hajibabaei M, Kitching IJ, Haxaire J, Hebert PD (2011) When species matches are unavailable are DNA barcodes correctly assigned to higher taxa? An assessment using sphingid moths. BMC Ecology 11: 18. https://doi.org/10.1186/1472-6785-11-18

Xin ZZ, Yu L, Zhu XY, Wang Y, Zhang HB, Zhang DZ, Zhou CL, Tang BP, Liu QN (2017) Mitochondrial Genomes of Two Bombycoidea Insects and Implications for Their Phylogeny. Scientific Reports 7: 6544. https://doi.org/10.1038/s41598-017-06930-5

Zhu HF, Wang LY (1997) Fauna Sinica: Insecta. Vol. 11, Lepidoptera, Sphingidae. Science Press, Beijing, 359 pp.

Supplementary material 1

Phylogenetic analysis

Authors: Li J, Lin R-R, Zhang Y-Y, Hu K-J, Zhao Y-Q, Li Y, Huang Z-R, Zhang X, Geng X-X, Ding J-H

Data type: molecular data

Explanation note: ML tree constructed based on the *cox1* barcodes of genus *Theretra* using *B. mori* as outgroups. The asterisk represents the species researched presently.

Link: https://doi.org/10.3897/zookeys.754.23404.suppl1

Supplementary material 2

List of annotated mitochondrial genes of *T. japonica*

Authors: Li J, Lin R-R, Zhang Y-Y, Hu K-J, Zhao Y-Q, Li Y, Huang Z-R, Zhang X, Geng X-X, Ding J-H

Data type: molecular data

Link: https://doi.org/10.3897/zookeys.754.23404.suppl2

ZooKeys 754: 141–155 (2018)
doi: 10.3897/zookeys.754.23655
http://zookeys.pensoft.net

RESEARCH ARTICLE

A peer-reviewed open-access journal
ZooKeys
Launched to accelerate biodiversity research

A new *Notomastus* (Annelida, Capitellidae) species from Korean waters, with genetic comparison based on three gene markers

Man-Ki Jeong[1], Ho Young Soh[2], Jin Hee Wi[3], Hae-Lip Suh[4]

1 *The Fisheries Science Institute, Chonnam National University, Daehak-ro, Yeosu 59626, South Korea* **2** *Faculty of Marine Technology, Chonnam National University, Daehak-ro, Yeosu 59626, South Korea* **3** *School of Environmental Science and Engineering, Gwangju Institute of Science and Technology, Choemdangwagi-ro, Buk-gu, Gwangju 61005, South Korea* **4** *Department of Oceanography, Chonnam National University, Yongbong-ro, Buk-gu, Gwangju 61186, South Korea*

Corresponding authors: *Ho Young Soh* (hysoh@chonnam.ac.kr); *Hae-Lip Suh* (suhhl@chonnam.ac.kr)

Academic editor: *C. Glasby* | Received 31 January 2018 | Accepted 26 April 2018 | Published 4 May 2018

http://zoobank.org/99197F00-54A7-457D-92AC-4F6D5D2BF08E

Citation: Jeong M-K, Soh HY, Wi JH, Suh H-L (2018) A new *Notomastus* (Annelida, Capitellidae) species from Korean waters, with genetic comparison based on three gene markers. ZooKeys 754: 141–155. https://doi.org/10.3897/zookeys.754.23655

Abstract

Notomastus koreanus **sp. n.**, collected from the sublittoral muddy bottom of Korean waters, is described as a new species. The Korean new species closely resembles *N. torquatus* Hutchings & Rainer, 1979 in the chaetal arrangement and the details of abdominal segments, but differs in the position of genital pores and the absence of eyes. DNA sequences (mtCOI, 16S rRNA, and histone H3) of the new species were compared with all the available sequences of *Notomastus* species in the GenBank database. Three genes showed significant genetic differences between the new species and its congeners (COI: 51.2%, 16S: 38.1–47.3%, H3: 3.7–9.3%). This study also includes a comprehensive comparison of the new Korean *Notomastus* species with its most closely similar species, based on the morphological and genetic results.

Keywords

Polychaeta, *Notomastus koreanus* sp. n., morphology, DNA barcoding, COI, 16S rRNA, histone H3, South Korea

Introduction

Capitellid polychaetes build spiral burrows or U-shape tubes in bottom sediments, which increase the subsurface penetration of water and oxygen, thus improving the recruitment and growth of small benthic organisms (Fauchald and Jumars 1979, Scaps 2002). In particular, the genus *Notomastus* Sars, 1851 is one of the most common and species-rich genus in the Capitellidae Grube, 1862 and occurs from the intertidal to the deep sea in a variety of sediment types including fine, medium, and silty sand and mud (Dean 2001). It currently contains 43 valid species, which is the highest number of species among the capitellid genera (Gil and Bellan 2017). Despite their ecological success and high species diversity, the lack of good generic characters and the incorrect descriptions in several previous records have led to taxonomic confusion in the genus (Green 2002). For instance, the hooded hook dentition of *N. latericeus* Sars, 1851 has been described differently in the published records of the species, and the protruded lateral organs had been mistaken as the branchiae in the former records of *Notomastus* species from Japan and Vietnam (Day 1967, Fauvel 1927, Green 2002, Thomassin 1970).

The taxonomic boundary of the genus *Notomastus* has been continually modified over the last century. The genus was designated by Sars (1851) with the description of the type species, *N. latericeus*. Eisig (1887) divided *Notomastus* into two subgenera, *Tremomastus* and *Clistomastus*, by the presence/absence of genital pores in the abdomen and the development of hooded hooks. Fauvel (1927) suggested that the subgeneric name of *Notomastus* (*Notomastus*) should replace *Notomastus* (*Tremomastus*) and Hartman (1947) accepted this view. However, Day (1967) and Fauchald (1977) did not agree with these subgeneric categories in their diagnoses of the genus. Ewing (1982) placed three genera, *Dodecaseta* McCammon & Stull, 1978, *Paraleiocapitella* Thomassin, 1970, and *Rashgua* Wesenberg-Lund, 1949, within *Notomastus*. Green (2002) clarified that *Dodecaseta* and *Rashgua* differed from *Notomastus* in the chaetal distribution, which was regarded as a good generic character. Green (2002) also suggested the need for a review of the taxonomic boundary of *Notomastus* and its species. In this study, *Notomastus* is defined based on the characteristics of its 12 thoracic segments, which comprise an achaetigerous peristomium and 11 chaetigers, including a uniramous or biramous first chaetiger, subsequent chaetigers usually with only capillaries, and posterior thoracic chaetigers with capillaries and sometimes neuropodial hooks; abdominal segments have only hooks. Although this study provides detailed descriptions of the *Notomastus* species from Korean waters, the comparison with closely related species was limited due to the insufficient morphological information of many records. To overcome this difficulty, studies using a combination of morphological analysis and DNA barcoding have been conducted to distinguish closely related capitellid species and to improve species recognition between them (Jeong et al. 2017b, Silva et al. 2016). The aim of the present study is to clarify the taxonomic status of the undescribed *Notomastus* species of Korea by morphological and genetic analysis using three different partial genes (mtCOI, 16S rRNA, and H3) and to compare Korean species with their closest congeners.

Materials and methods

Morphological analysis. Samples were collected from seven stations in sublittoral areas of Korea using a 0.05 m^2 Van Veen grab (Fig. 1). The sediment samples were elutriated over a 0.5 mm sieve in a 30 l seawater container, and the organisms were transferred to a 1 l collecting jar with 7% $MgCl_2$ solution for anesthesia. The relaxed samples were fixed in a buffered solution of 10% formalin within 2 hours and finally preserved in 90% ethanol. In the laboratory, *Notomastus* specimens were sorted under a stereomicroscope (SMZ745T, Nikon). Line drawings were generated using a differential interference contrast microscope (Eclipse Ci-L, Nikon) and a digital pen display (Cintiq 22HD, Wacom). Methyl green staining patterns (MGSP) and scanning electron microscopy (SEM) analyses were described and photographed, as delineated by Jeong et al. (2017b). The examined type materials were deposited in the collections of the Marine Biodiversity Institute of Korea (MABIK) in Seocheon, Korea (Table 1). Two additional specimens (voucher numbers: NIBRIV0000634919 and NIBRIV0000634920) were deposited at the National Institute of Biological Resources (NIBR) in Incheon, Korea.

Molecular analysis. Genomic DNA was extracted from tissue obtained from partial dissection of the middle part of the abdomen of the ethanol-preserved specimens. To extract the genomic DNA, 1.5 mL centrifuge tubes each containing 90 μL of 10% Chelex suspension (Bio-Rad Laboratories Inc.), 10 μL of Proteinase K (10 mg/ml, iNtRON Biotechnology, Inc.) and dissected tissues (ca. 1/2 segment) were incubated at 56 °C for 3–12 hours.

The extracted genomic DNA was used as a template to amplify the target region. Polymerase chain reaction (PCR) was performed on a MasterCycler PCR thermal cycler (Eppendorf Co.). The primer pair for COI was LoboF1 and LoboR1 (Lobo et al. 2013), for 16S rRNA was 16SarL and 16SbrH (Palumbi 1996) and for histone H3 was H3F and H3R (Colgan et al. 1998). The PCR mixtures contained 16 μL of deionized water, 1 μL of each primer (10 μM), 2 μL of DNA template and PCR premix (BiONEER Co.). The temperature profile was as follows: 94 °C/180s–(94 °C/30s–48 °C/30s–72 °C/60s)*40 cycles–72 °C/420s for mtCOI, 94 °C/180s–(94 °C/45s–50 °C/60s–72 °C/60s)*35 cycles–72 °C/420s for 16S rRNA, and 94 °C/180s–(94 °C/45s–50 °C/60s–72 °C/60s)*35 cycles–72 °C/420s for histone H3. The results of the PCR amplification were confirmed on 1.0% agarose gels using ethidium bromide staining. Purification and sequencing of the obtained PCR products were performed at the Macrogen Inc. facilities (Seoul, Korea).

The forward and reverse sequences were compared and edited using Chromas software version 2.3 (Technelysium Pty. Ltd.). The partial sequences of the COI, 16S rRNA and H3 genes were aligned with the sequences of available *Notomastus* species obtained from GenBank (https://www.ncbi.nlm.nih.gov/genbank/) using the Molecular Evolutionary Genetics Analysis (MEGA) software version 7.0 (Kumar et al. 2016). Table 1 summarizes information for all sequences used in the analyses. The aligned sequences were used as data sets to generate the genetic distance using Kimura's two-

Table 1. A list of sampling localities, species names, sample types, voucher numbers, Genbank accession numbers, and references.

Location		Latitude / Longitude (DDM)	Species name	Type	Voucher number	Accession number of Genbank			References
						mtCOI	16SrRNA	histone H3	
South Korea	Yeosu	34°39.03'N, 127°40.86'E	*N. koreanus* sp. n.	Paratype	NA00146048	MG437146	MG748697	MG748700	This study
				Paratype	NA00146049	MG437147	MG748698	MG748701	
	Busan	35°5.83'N, 129°2.42'E		Paratype	NA00066329	MG437148		MG748699	
		35°6.33'N, 129°3.31'E		Holotype	NA00066337				
	Hwaseong	37°8.95'N, 126°35.39'E			NA00066302		MG748696		
	Geoje	34°54.17'N, 128°36.98'E		Paratype	NA00066311				
	Pohang	36°1.31'N, 129°25.16'E		Paratype	NA00066396				
Portugal	Sado estuary	38°29.22'N, 8°53.1'W	*N. profondus*		RR132	KR916897			Lobo et al. (2016)
Canada	Bamfield		*N. hemipodus*				HM746714	HM746759	Paul et al. (2010)
Sweden	Bohuslän		*N. latericeus*		SMNH75827		AY340469	DQ779747	Rousset et al. (2007)
Australia			*N. torquatus*		AMW23426			AF185258	Brown et al. (1999)
China	Bohai Sea	38°21.12'N, 120°7.92'E	*Notomastus* sp.		BIOUG03550-A09				BOLD Systems (2017)

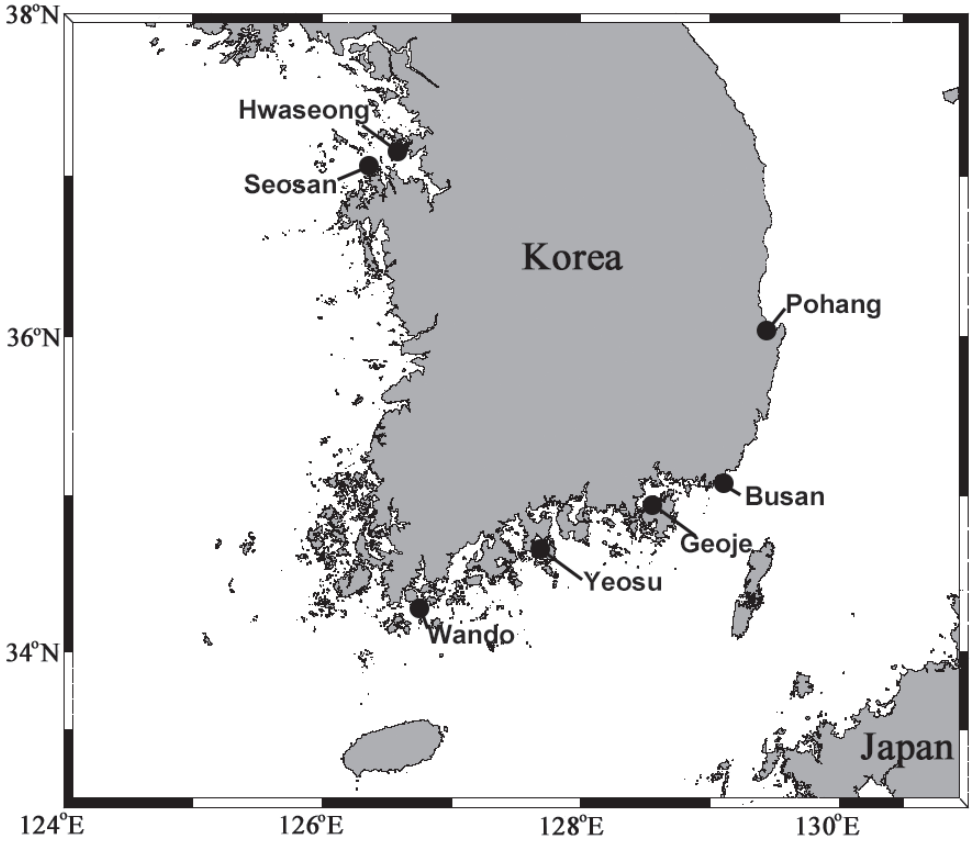

Figure 1. Map of study area with main collecting locations.

parameter (K2P) model (Kimura 1980). Based on the K2P distances, we calculated the intraspecific genetic differences within the Korean specimens and the interspecific genetic differences among the closest taxa.

Results

Systematics
Family Capitellidae Grube, 1862

Genus *Notomastus* Sars, 1851

Type species. *Notomastus latericeus* Sars, 1851

Type locality. Komagfjord, Norway

Generic diagnosis (modified after Green 2002). Thorax with 12 segments including an achaetous peristomium and 11 chaetigers with capillary chaetae. Last three

thoracic chaetigers may have capillary chaetae in both rami or may be transitional with capillary chaetae in notopodia and hooded hooks in neuropodia. Remaining chaetigers with hooded hooks only. Hooded hooks with one or more rows of teeth above main fang; more than two teeth in basal row. Branchiae may be present or absent.

Remarks. According to the former generic diagnosis by Green (2002), *Notomastus* may or may not have a transitional chaetiger with capillary notochaetae and neurohooks in the last part of thorax. However, *N. precocis* Hartman, 1960 and *N. teres* Hartman, 1965 have three and two transitional chaetigers in the posterior thoracic region, respectively (Gil and Bellan 2017, Hartman 1960, 1965). Therefore, the generic diagnosis was amended including the expanded range of the thoracic chaetal arrangement.

***Notomastus koreanus* sp. n.**
http://zoobank.org/18FE9853-2A6B-45B4-9C79-E3E7569C9E3B
Figs 2A–D, 3A–G

Materials examined. Holotype: MABIKNA00066337, sex uncertain, Busan, 35°6.33'N, 129°3.31'E (DDM), subtidal, sandy mud bottom, 16 m depth, October 2011, collected by Byoung-Mi Choi. Paratypes: MABIKNA00146048, MABIKNA00146049, sex uncertain, Yeosu, 34°39.03'N, 127°40.86'E, subtidal, sandy mud bottom, 20 m depth, October 2017, collected by Man-Ki Jeong; MABIKNA00066329, sex uncertain, Busan, 35°5.83'N, 129°2.42'E subtidal, sandy mud bottom, 15 m depth, October 2011, collected by Byoung-Mi Choi; MABIKNA00066396, sex uncertain, Pohang, 36°3.09'N, 129°23.55'E, subtidal, sandy mud bottom, 12 m depth, January 2012, collected by Byoung-Mi Choi; MABIKNA00066311, sex uncertain, Geoje, 34°54.17'N, 128°36.98'E, subtidal, sandy mud bottom, 10 m depth, January 2012, collected by Byoung-Mi Choi.

Additional materials examined. MABIKNA00115263, sex uncertain, Busan, 35°4.7'N, 128°55.4'E, subtidal, sandy mud bottom, 14 m depth, January 2012, collected by Byoung-Mi Choi; MABIKNA00066302, sex uncertain, Hwaseong, 37°8.95'N, 126°35.39'E, subtidal, sandy mud bottom, 20 m depth, September 2011, collected by Byoung-Mi Choi; MABIKNA00066303, MABIKNA00115303, sex uncertain, Seosan, 37°2.03'N, 126°23.94'E subtidal, sandy mud bottom, 15 m depth, September 2011, collected by Byoung-Mi Choi; MABIKNA00066385, sex uncertain, Pohang, 36°1.31'N, 129°25.16'E subtidal, sandy mud bottom, 12 m depth, November 2010, collected by Byoung-Mi Choi; MABIKNA00115314, sex uncertain, Wando, 34°22.12'N, 127°0.79'E, subtidal, sandy mud bottom, 10 m depth, September 2011, collected by Byoung-Mi Choi. Additional 3 specimens from type locality on SEM stub.

Diagnosis. Thorax with achaetigerous peristomium and 11 chaetigers. Anterior 5 thoracic segments tessellated. First chaetiger without neuropodia. Chaetigers 1–11 with capillary chaetae only. Abdominal chaetigers with hooded hooks only. Lateral organs not protruded above surface, narrow and oval shape, present along body. Genital pores present in intersegmental furrows between chaetigers 7–8, 8–9, 9–10, and 10–11. Parapo-

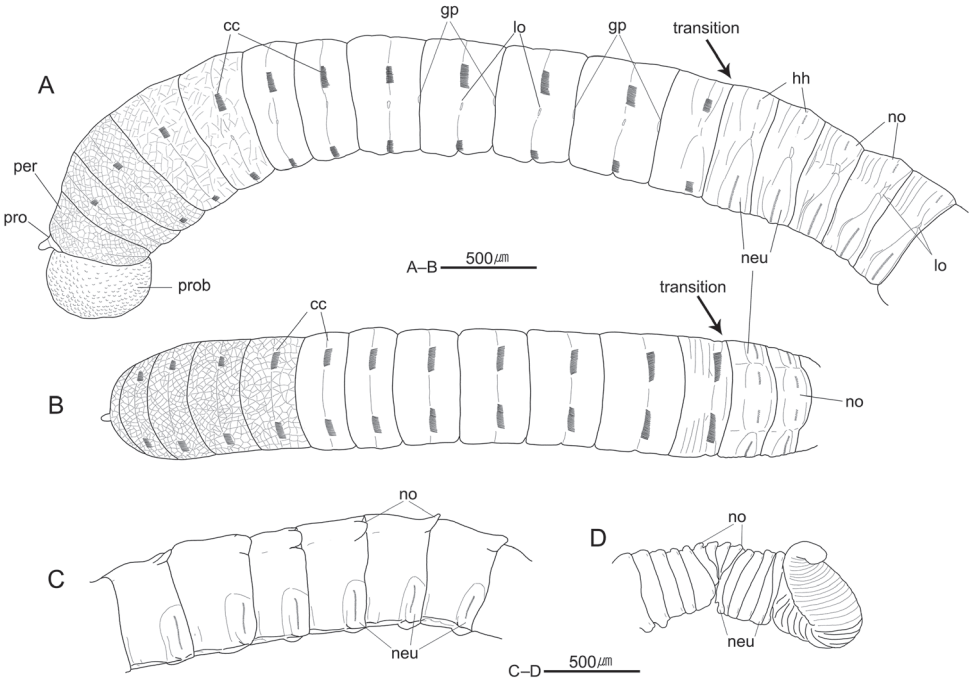

Figure 2. *Notomastus koreanus* sp. n. **A** anterior end, left lateral view (MABIKNA00146048) **B** same, dorsal view (MABIKNA00146048) **C** posterior abdominal segments, left lateral view (Holotype, MABIKNA00066337) **D** posterior end, left lateral view (Holotype, MABIKNA00066337). Abbreviations: cc, capillary chaetae; gp, genital pore; hh, hooded hooks; lo, lateral organ; neu, neuropodium; no, notopodium; pro, prostomium; prob, proboscis; per, peristomium; transition, transition between thorax and abdomen.

dial lobes in anterior to moderate abdominal region not protruded. Posteriorly extended parapodial lobes present on posterior abdominal segments. Pygidium without anal cirri.

Description. Holotype entire, about 80 mm long, 1.2 mm wide for 280 chaetigers. Paratype material ranges from 31–87 mm in length, 0.7–1.3 mm width with 30–270 chaetigers. Body elongate, rounded dorsally, flattened ventrally, widest in anterior thoracic chaetigers, with ventral white line in abdominal region. Color in alcohol whitish yellow.

Prostomium conical, with short and rounded palpode; nuchal organs not seen, eyespots absent (Figs 2A, 3A, D). Proboscis everted, with numerous hemispherical papillae (Figs 2A, 3D). Peristomium achaetous, weakly biannulated, slightly longer than first chaetiger (Figs 2A, 3D).

Thorax with 12 segments including achaetous peristomium and 11 chaetigers (Figs 2A–B, 3B). Thoracic segments biannulated with intra- and inter-segmental furrows (Figs 2A–B, 3A). Anterior thoracic segments tessellated; peristomium and chaetigers 1–2 tessellated, chaetigers 3–4 slightly tessellated; remaining segments smooth (Figs 2A–B, 3D). First chaetiger with only notopodia having 12 capillaries per fascicle; remaining thoracic chaetigers with 40–60 bilimbate capillaries per fascicle in both parapodia (Figs 2A–B, 3D–E). Thoracic parapodia reduced, located in intra-segmental furrows (Figs 2A–B, 3D);

notopodia dorso-laterally on first chaetiger and middorsally on following chaetigers (Fig. 2B); neuropodia ventrolaterally on whole chaetigers. (Figs 2A, 3A–B). Lateral organs not protruded above surface, narrow and oval shape, present along body, situated in furrow between notopodia and neuropodia, less distinct in posterior abdominal region (Figs 2A–B, 3A–D); position of lateral organs slightly nearer to neuropodium in chaetigers 1–3, nearer to notopodium in following chaetigers (Figs 2A, 3A, D). Genital pores present in intersegmental furrows of between chaetigers 7–8, 8–9, 9–10, and 10–11 (Figs 2A, 3A–B).

Transition between thorax and abdomen distinguished by changes in shape of chaeta and segment (Figs 2A–B, 3A–B); last thoracic chaetiger bi-annulated, with capillaries only, slightly thinner than first abdominal chaetiger; anterior abdominal segments multi-annulated, with better developed neuropodial lobes than thoracic ones, having hooded hooks only (Figs 2A–B, 3B). Parapodia in anterior to mid abdominal region not protruded, well separated (Figs 2A–B, 3A–B). Notopodial lobes not protruded in anterior abdomen, middorsal on anterior few segments, becoming dorsolateral in following abdominal region, with 6–15 hooded hooks only per fascicle, having posteriorly extended and semicircular lamella from chaetiger 160 to end of body (Figs 2A–C, 3A–C). Neuropodial lobes having 15–30 hooded hooks per fascicle, well separated and weakly protruded in anterior abdomen, more protruded and almost fused ventrally in posterior abdomen, partially fused to notopodial lobes in posterior end (Figs 2A, C, 3A–C); dorsal tips of neuropodial lobes do not protruded above surface, extended below lateral organs in anterior to mid abdominal region (Figs 2A, C, 3B).

Hooded hooks with main fang extending slightly beyond hoods; hood slightly flared. Main fang of hooded hooks with 3 rows of small teeth; 5 in basal row, 6–8 in second row, and at least 6 in superior row (Fig. 3F–G).

Digitiform branchiae not observed in abdomen; each notopodial lobe with posteriorly extended semicircular lamella in posterior abdomen (Figs 2C, 3C). Pygidium simple, without anal cirri (Fig. 2D).

Methyl green staining pattern. Anterior thoracic segments (peristomium and chaetigers 1–6) not stained. Posterior thoracic segments (chaetigers 7–10 or 11) stained (Fig. 3A); chaetiger 10 and dorsum of chaetiger 7 more deeply stained with blue (Fig. 3A). Anterior few abdominal chaetigers temporary stained with green; fading within 10 minutes (Fig. 3A). Ventral side of abdominal segments having pair of longitudinal green bands. Individual-specific variations observed; sometimes chaetigers 5–6 and chaetiger 11 weakly stained with blue, posterior edge of each abdominal segment stained with blue in large specimens (Fig. 3C).

Etymology. The new species is named for its wide distribution in coastal waters of Korea.

Distribution. The subtidal areas (10–20 m) near Korea (Fig. 1). The subtidal habitat (ca. 20 m) of Bohai Sea, China (see details in Discussion).

Ecology. *Notomastus koreanus* sp. n. was sampled from soft sediments throughout the year. Most well-developed individuals (having over 250 segments) were obtained between October and January. The sediment of the collecting stations was mainly composed of sandy mud with shell fragments. *Leiochrides yokjidoensis* Jeong, Wi & Suh, 2017 and an undescribed *Heteromastus* Eisig, 1887 species co-occurred in southern stations of this study.

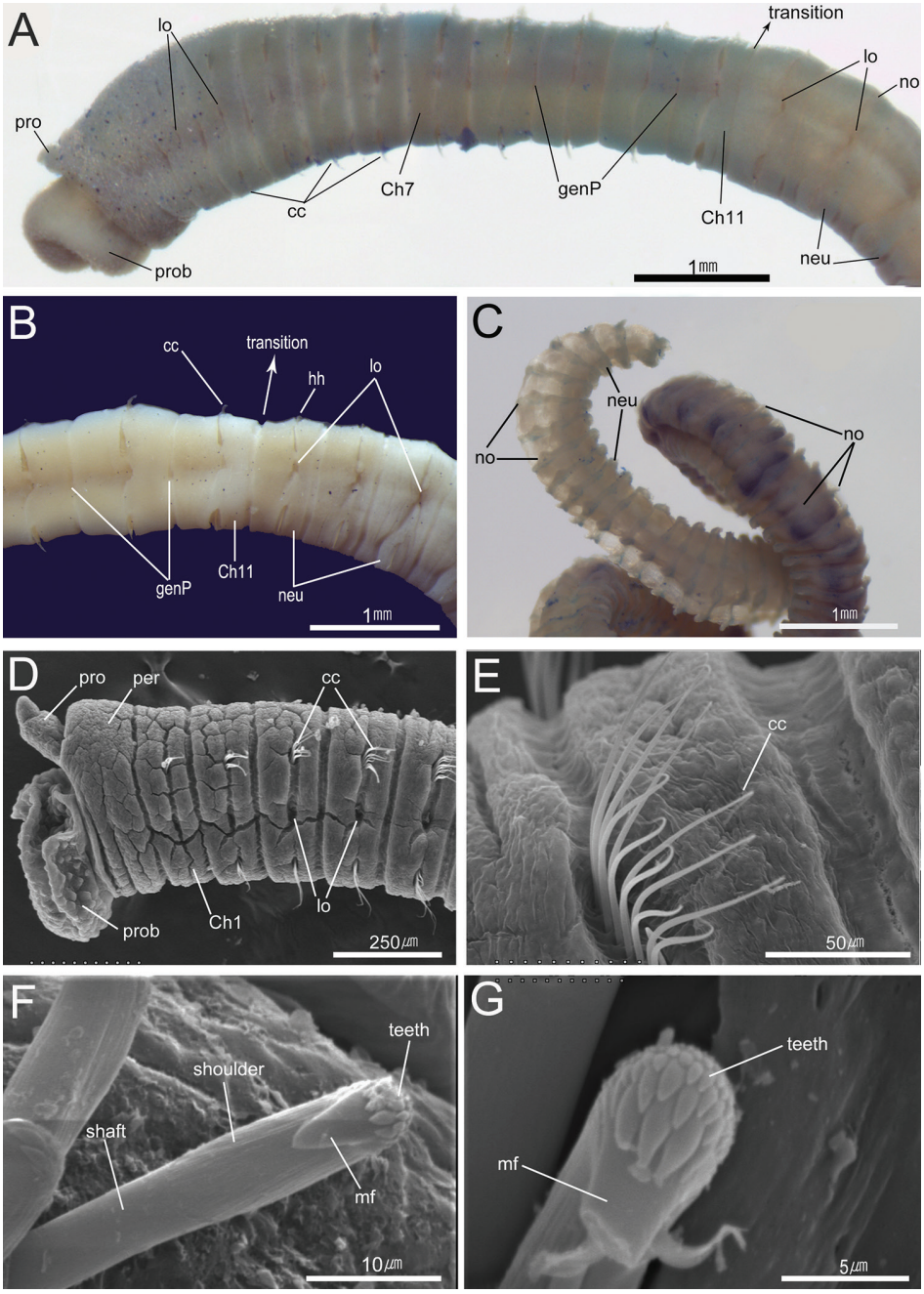

Figure 3. *Notomastus koreanus* sp. n. **A–C** photomicrographs **A** anterior end in left lateral view (showing methyl green staining reaction, MABIKNA00066311) **B** chaetigers 9–15 in left lateral view (MABIKNA00066396) **C** posterior end (MABIKNA00066396) **D–G** scanning electron micrographs (using additional specimens from type locality) **D** anterior 6 thoracic segments in left lateral view **E** capillary chaetae of chaetiger 4 **F–G** abdominal hooded hooks in frontal view. Abbreviations: cc, capillary chaetae; Ch, chaetiger; genP, genital pore; hh, hooded hooks; lo, lateral organ; mf, main fang; neu, neuropodium; no, notopodium; per, peristomium; pro, prostomium; prob, proboscis; transition, transition between thorax and abdomen.

Remarks. *Notomastus koreanus* sp. n. is distinguished from other species of the genus by the morphological combination of absence of distinct eyes and first neuropodia, last thoracic chaetigers with only capillary chaetae, presence of genital pores between chaetigers 7–11, non-protruded lateral organs and neuropodial lobes in anterior abdomen, and posteriorly extended parapodial lobes in posterior abdomen. The new Korean *Notomastus* species closely resembles *N. torquatus* Hutchings & Rainer, 1979 in the chaetal arrangement, the absence of developed neuropodial lobes in anterior abdomen, and the presence of posteriorly extended parapodial lobes in the posterior abdomen (Table 2). However, they differ in the presence of eyes on posterior prostomium (eyespots vs. absence) and the location of genital pores (between chaetigers 3 or 5–10 vs. 7–11, Table 2). Additionally, *N. torquatus* is regarded as an endemic species of Australia and has a much wider thorax (4 mm vs. 1.3 mm) than comparable specimens of *N. koreanus* sp. n., which have 280 segments when fully developed (Doyle 1991, Hutchings and Rainer 1979). *Notomastus hemipodus* Hartman, 1945 and *N. tenuis* Moore, 1909 are also similar to *N. koreanus* sp. n. in the chaetal arrangement and the absence of protruded neuropodial lobes in anterior abdomen, but clearly differ in the details of the eyes, the genital/lateral organs, and the MGSP (Table 2). Moreover, they have the unique features of the indistinct palpode and the bilobed notopodial lobes, respectively.

Genetic comparison with the published sequences of *Notomastus* species. To confirm the genetic distances among the new species and its closely related species, we used the partial sequences of mitochondrial (mtCOI and 16S rRNA) and nuclear (histone H3) genes. In all genetic comparisons, the intraspecific differences among the Korean specimens were negligible (0–0.1%, Table 3). The mean interspecific differences for mitochondrial COI (50.9%) and 16S rRNA (43.2%) genes were much higher than the mean interspecific difference for the nuclear histone H3 gene (7.6%). In the mtCOI gene comparison, the mean genetic difference between *N. koreanus* sp. n. and *N. profondus* (Eisig, 1887) of Portugal (KR916899) was substantial (51.2%, Table 3). In the interspecific comparison for the 16S rRNA gene, *N. koreanus* sp. n. was well distinguished from *N. hemipodus* (38.1%, HM746714) of Canada and *N. latericeus* (47.3%, AY340469) of Sweden (Table 3). In the histone H3 gene comparison, *N. koreanus* sp. n. genetically differed from *N. torquatus* (3.7%, AF185258) of Australia, *N. latericeus* (7.0%, DQ779747) of Sweden, and *N. hemipodus* (9.3%, HM746759) of Canada (Table 3). Previously known genetic difference of the mtCOI and the 16S rRNA genes among the capitellid species is generally about 18–20% (Jeong et al. 2017b, Silva et al. 2016). In contrast, the histone H3 gene difference between cryptic nereidid polychaetes is around 2–9% (Glasby et al. 2013). Thus, the genetic differences between *N. koreanus* sp. n. and its closely related species (COI: 51.2%, 16S: 38.1–47.3%, H3: 3.7–9.3%) is significant at the species level revealing the speciation among them. On the other hand, the mtCOI gene sequence of the Chinese specimen (BIOUG03550-A09, Table 1) is genetically matched with *N. koreanus* sp. n. (0.007 in K2P distance, Table 3), although it has been reported as *N. latericeus* on BOLD (www.barcodinglife.org) database (BOLD Systems 2017). *Notomastus latericeus* was originally described from Norwegian waters, and it is easily discriminated from our new species in terms of morphology (Table 2). The published histone H3 and 16S rRNA sequences of *N. latericeus*

Table 2. Morphological comparison between Korean *Notomastus* species and its closely similar species. A: absent; P: present; Ch: chaetiger; NM: not mentioned; abd: abdomen; th: thorax; uni: uniramous; bi: biramous.

Species	First Ch	Eyes	Distinct palpode	Lateral organs	Genital pores	Dental structure of hooks	Parapodial lobes in posterior abdomen	Methyl green staining patterns	Habitat (locality)	References
N. koreanus sp. n.	uni	A	P	not protrude	between Ch 7–11	>17 teeth in 3 rows (5/6–8/>6)	parapodial lobes posteriorly extended	dorsum of Ch 7 and Ch 8–10 stained blue, Ch 5–6 and 11 sometimes stained, abd with 2 ventral blue lines	subtidal, 10–20 m, sandy mud with shell fragments (Korea)	This study
N. latericeus	bi	P	P	not protrude	between Ch 7–20	3 rows (5/?/?)	not extended	NM	intertidal to abyssal, sand, mud (cosmopolitan)	Day 1967
N. hemipodus	uni	P (single pair)	P	protrude on anterior abd	between Ch 8–12	16–24 teeth in 3 rows (4–6/6–8/6–8)	bilobed notopodial lobes posteriorly extended	Ch 1–6 green, Ch 7–10 blue, dorsum of abd green, abd with 2 ventral blue lines	intertidal to shelf depths, 0.5–426 m (America)	García-Garza et al. 2012, Green 2002
N. tenuis	uni	P (eyespots)	A	protrude on anterior abd	between Ch 5–10	many teeth (NM) in 4–5 rows	notopodial lobes posteriorly extended	Whole segments stained with light green	intertidal to shallow subtidal (America)	García-Garza et al. 2012
N. torquatus	uni	P (eyespots)	P	NM	between Ch 3 or 5– 10	16–24 teeth in 3 rows (4–6/6–8/6–8)	parapodial lobes posteriorly extended	NM	sea grass beds on muddy sand (Australia)	Hutchings and Rainer 1979

Table 3. Mean genetic distances between examined *Notomastus* species based on K2P distance. Bold numbers represent the mean intraspecific K2P distance of Korean specimens.

mtCOI	1	2	3
1. *N. koreanus* n. sp. (Korea)	**0.001**		
2. *Notomastus* sp. (China)	0.007	–	
3. *N. profondus* (Portugal)	0.512	0.506	–
16S rRNA	1	2	3
1. *N. koreanus* n. sp. (Korea)	**0.000**		
2. *N. hemipodus* (Canada)	0.381	–	
3. *N. latericeus* (Sweden)	0.473	0.441	–
histone H3	1	2	3
1. *N. koreanus* n. sp. (Korea)	**0.000**		
2. *N. torquatus* (Australia)	0.037	–	
3. *N. latericeus* (Sweden)	0.070	0.088	–
4. *N. hemipodus* (Canada)	0.093	0.092	0.075

from Swedish waters are clearly distinguished from the sequences of *N. koreanus* sp. n. by the significant genetic difference (Table 3). Thus, the mtCOI sequence of the Chinese specimen on the BOLD database is regarded as a misidentification at the species level and confirms the additional occurrence of our new species in the Bohai Sea of northeastern China.

Key to species of *Notomastus* closely similar to the Korean new species.

1 First chaetiger biramous; dorsally protruded neuropodial lobes present in anterior abdomen; genital pores present between chaetigers 7–20..... .....***N. latericeus*** **Sars, 1851**

– First chaetiger uniramous; dorsally protruded neuropodial lobes absent in anterior abdomen; posteriorly extended notopodial lobes present in posterior abdomen.....**2**

2 Lateral organs protruded above surface in anterior abdominal region.....**3**

– Lateral organs not protruded above surface in anterior abdominal region **4**

3 Palpode indistinct; posterior abdominal region with unilobed notopodial lobes; genital pores present between chaetigers 5–10; all segments stain green in MGSP .....***N. tenuis*** **Moor, 1909**

– Distinct palpode present; posterior abdominal region with bi-lobed notopodial lobes; genital pores present between chaetigers 8–12; chaetigers 1–6 and dorsum of abdomen stain green, chaetigers 7–10 stain blue in MGSP..... ..... ***N. hemipodus*** **Hartman, 1945**

4 Eyespots present on posterior prostomium; genital pores present between chaetigers 3 or 5–10.....***N. torquatus*** **Hutchings & Rainer, 1979**

– Eyespots absent on prostomium; genital pores present between chaetigers 7–11; dorsum of chaetiger 7 and chaetiger 8–10 stain blue in MGSP..... .....***N. koreanus*** **n. sp.**

Acknowledgements

We would like to acknowledge and thank Dr. Hutchings and Dr. Glasby who made constructive and invaluable suggestions and useful comments. We also thank the captain and crew of the R/V *Cheong-Gyeong-Ho* for their support at sea. This work was supported by a grant from the National Institute of Biological Resources (NIBR), funded by the Ministry of Environment (MOE) of the Republic of Korea (NIBR201601201). This study was supported by National Marine Biodiversity Institute Research Program (2018M01200), funded by National Marine Biodiversity Institute of Korea (MABIK). This study was a part of the project titled "Long-term change of structure and function in marine ecosystems of Korea", funded by the Ministry of Oceans and Fisheries, Korea.

References

BOLD Systems (2017) Chinese *Notomastus* specimen. Accessed through: Barcode of life data systems. http://www.boldsystems.org/index.php/Public_RecordView?processid=HZPLY104-12 [Accessed 28 December 2017]

Brown S, Rouse G, Hutchings P, Colgan D (1999) Assessing the usefulness of histone H3, U2 snRNA and 28S rDNA in analyses of polychaete relationships. Australian Journal of Zoology 47: 499–516. https://doi.org/10.1071/zo99026

Colgan D, McLauchlan A, Wilson G, Livingston S, Edgecombe G, Macaranas J, Cassis G, Gray M (1998) Histone H3 and U2 snRNA DNA sequences and arthropod molecular evolution. Australian Journal of Zoology 46: 419–437. https://doi.org/10.1071/zo98048

Day JH (1967) A monograph on the Polychaeta of Southern Africa. Part II. British Museum (Natural History), London, 450 pp. https://doi.org/10.5962/bhl.title.8596

Dean HK (2001) Capitellidae (Annelida: Polychaeta) from the Pacific Coast of Costa Rica. Revista De Biologia Tropical 49: 69–84.

Doyle S (1991) Setal type and distribution in two Australian species of *Scyphoproctus* (Polychaeta, Capitellidae) and three other capitellids, with a description of *Scyphoproctus towraiensis* sp. n. Zoologica Scripta 20: 263–275. https://doi.org/10.1111/j.1463-6409.1991.tb00290.x

Eisig H (1887) Monographie der Capitelliden des Golfes von Neapel. Fauna und Flora des Golfes von Neapel 16:1–906. https://doi.org/10.5962/bhl.title.11542

Ewing R (1982) A partial revision of the genus *Notomastus* (Polychaeta: Capitellidae) with a description of a new species from the Gulf of Mexico. Proceedings of the Biological Society of Washington 95: 232–237.

Fauchald K (1977) The polychaete worms: definitions and keys to the orders, families and genera. Natural History Museum of Los Angeles County, Los Angeles, 188 pp.

Fauchald K, Jumars PA (1979) The diet of worms: a study of polychaete feeding guilds. Oceanography and Marine Biology Annual Review 17: 193–284. https://doi.org/10.1146/annurev-marine-010814-020007

Fauvel P (1927) Polychètes Sendentaires. Faune De France. Lechevalier, Paris, 494 pp.

Gil J, Bellan G (2017) *Notomastus* Sars, 1851. In: Read G, Fauchald K (Eds) World Polychaeta database. Accessed through: World Register of Marine Species. http://marinespecies.org/aphia.php?p=taxdetails&id=129220 [Accessed 28 December 2017]

Glasby CJ, Wei NWV, Gibb KS (2013) Cryptic species of Nereididae (Annelida: Polychaeta) on Australian coral reefs. Invertebrate Systematics 27: 245–264. https://doi.org/10.1071/IS12031

Green K (2002) Capitellidae (Polychaeta) from the Andaman Sea. Phuket Marine Biological Center Special Publication 24: 249–343.

Grube AE (1862) Noch ein Wort über die *Capitellen* und ihre Stelle im Systeme der Anneliden. Archiv für naturgeschichte 28: 366–378.

Hartman O (1945) The marine annelids of North Carolina. Duke University Marine Station Bulletin 2: 1–54. https://doi.org/10.1086/395019

Hartman O (1947) Polychaetous annelids. Part VII. Capitellidae. Allan Hancock Pacific Expeditions 10: 391–481.

Hartman O (1960) Systematic account of some marine invertebrate animals from the deep basins off southern California. Allan Hancock Pacific Expeditions 22: 69–216.

Hartman O (1965) Deep-water benthic polychaetous annelids off New England to Bermuda and other North Atlantic areas. Allan Hancock Occasional Papers 28: 1–378.

Hutchings P, Rainer S (1979) The polychaete fauna of Careel Bay, Pittwater, New South Wales, Australia. Journal of Natural History 13: 745–796. https://doi.org/10.1080/00222937900770561

Jeong MK, Wi JH, Suh HL (2017a) A new species of *Leiochrides* from the Korean subtidal waters with notes on the taxonomic status of the genus *Pseudomastus* (Annelida, Capitellidae). Zookeys 685: 91–103. https://doi.org/10.3897/zookeys.685.12700

Jeong MK, Wi JH, Suh HL (2017b) A reassessment of *Capitella* species (Polychaeta: Capitellidae) from Korean coastal waters, with morphological and molecular evidence. Marine Biodiversity: 1–10. https://doi.org/10.1007/s12526-017-0707-2

Kimura M (1980) A simple method for estimating evolutionary rates of base substitutions through comparative studies of nucleotide sequences. Journal of molecular evolution 16: 111–120. https://doi.org/10.1007/bf01731581

Kumar S, Stecher G, Tamura K (2016) MEGA7: Molecular Evolutionary Genetics Analysis version 7.0 for bigger datasets. Molecular biology and evolution 33: 1870–1874. https://doi.org/10.1093/molbev/msw054

Lobo J, Costa PM, Teixeira MA, Ferreira MS, Costa MH, Costa FO (2013) Enhanced primers for amplification of DNA barcodes from a broad range of marine metazoans. BMC ecology 13: 34. https://doi.org/10.1186/1472-6785-13-34

Lobo J, Teixeira MA, Borges L, Ferreira MS, Hollatz C, Gomes PT, Sousa R, Ravara A, Costa MH, Costa FO (2016) Starting a DNA barcode reference library for shallow water polychaetes from the southern European Atlantic coast. Molecular ecology resources 16: 298–313. https://doi.org/10.1111/1755-0998.12441

McCammon JA, Stull JK (1978) A new genus and species of Capitellidae (Polychaeta) from California. Bulletin of the Southern California Academy of Sciences 77: 40–43.

Moore JP (1909) Polychaetous annelids from Monterey Bay and San Diego, California. Proceedings of the Academy of Natural Sciences of Philadelphia 61: 235–295.

Palumbi SR (1996) Nucleic acids II: the polymerase chain reaction. Molecular systematics 2: 205–247.

Paul C, Halanych KM, Tiedemann R, Bleidorn C (2010) Molecules reject an opheliid affinity for *Travisia* (Annelida). Systematics and Biodiversity 8: 507–512. https://doi.org/10.1080/14772000.2010.517810

Rousset V, Pleijel F, Rouse GW, Erséus C, Siddall ME (2007) A molecular phylogeny of annelids. Cladistics 23: 41–63. https://doi.org/10.1111/j.1096-0031.2006.00128.x

Sars M (1851) Beretning om en i Sommeren 1849 foretagen zoologisk Reise i Lofoten og Finmarken. Nyt Magazin for Naturvidenskaberne, Oslo, 211 pp.

Scaps P (2002) A review of the biology, ecology and potential use of the common ragworm *Hediste diversicolor* (O.F. Muller) (Annelida: Polychaeta). Hydrobiologia 470: 203–218. https://doi.org/10.1023/A:1015681605656

Silva CF, Shimabukuro M, Alfaro-Lucas JM, Fujiwara Y, Sumida PY, Amaral AC (2016) A new *Capitella* polychaete worm (Annelida: Capitellidae) living inside whale bones in the abyssal South Atlantic. Deep Sea Research Part I: Oceanographic Research Papers 108: 23–31. https://doi.org/10.1016/j.dsr.2015.12.004

Thomassin B (1970) Contribution à l'etude des Polychètes de la région de Tuléar (SW de Madagascar). III. Sur les Capitellidae des sables coralliens. Recueil des Travaux de la Station Marine d'Endoume 10: 71–101.

Wesenberg-Lund E (1949) Polychaetes of the Iranian Gulf. Danish Scientific Investigations in Iran 4: 247–400.